

AD-A277 305

3



NAVAL POSTGRADUATE SCHOOL
Monterey, California

2

S DTIC
ELECTE
MAR 28 1994
F **D**



THESIS

AIR-SEA INTERACTION PATTERNS
IN THE EQUATORIAL PACIFIC

by

John E. Kent

December, 1993

Thesis Advisor:
Co-Advisor:

James Thomas Murphree
Peter C. Chu

Approved for public release; distribution is unlimited.

1971/94-08975



DTIC QUALITY INSPECTED 1

9 4 3 25 092

REPORT DOCUMENTATION PAGE			Form Approved OMB No. 0704	
Public reporting burden for this collection of information is estimated to average 1 hour per response, including the time for reviewing instruction, searching existing data sources, gathering and maintaining the data needed, and completing and reviewing the collection of information. Send comments regarding this burden estimate or any other aspect of this collection of information, including suggestions for reducing this burden, to Washington Headquarters Services, Directorate for Information Operations and Reports, 1215 Jefferson Davis Highway, Suite 1204, Arlington, VA 22202-4302, and to the Office of Management and Budget, Paperwork Reduction Project (0704-0188) Washington DC 20503.				
1. AGENCY USE ONLY (Leave blank)	2. REPORT DATE 21 Dec. 1993.	3. REPORT TYPE AND DATES COVERED Master's Thesis		
4. TITLE AND SUBTITLE AIR-SEA INTERACTION PATTERNS IN THE EQUATORIAL PACIFIC		5. FUNDING NUMBERS		
6. AUTHOR(S) John Eliot Kent				
7. PERFORMING ORGANIZATION NAME(S) AND ADDRESS(ES) Naval Postgraduate School Monterey CA 93943-5000		8. PERFORMING ORGANIZATION REPORT NUMBER		
9. SPONSORING/MONITORING AGENCY NAME(S) AND ADDRESS(ES)		10. SPONSORING/MONITORING AGENCY REPORT NUMBER		
11. SUPPLEMENTARY NOTES The views expressed in this thesis are those of the author and do not reflect the official policy or position of the Department of Defense or the U.S. Government.				
12a. DISTRIBUTION/AVAILABILITY STATEMENT Approved for public release; distribution is unlimited.		12b. DISTRIBUTION CODE *A		
13. ABSTRACT (maximum 200 words) We have investigated air-sea interaction patterns in the equatorial Pacific during the 1991-1992 El Niño/Southern Oscillation (ENSO) event. Our study focused on the identification of spatial and temporal relationships between sea surface temperatures, subsurface temperatures, and winds. These relationships were examined using time series and statistical analyses of atmosphere and ocean data from the moored buoys of the Tropical Oceans-Global Atmosphere (TOGA) program. Our results strongly suggest that the heat content of the ocean mixed layer greatly affected air-sea interactions. In almost all regions, mixed layer warming was followed within one week by increased winds. In most cases, the mixed layer warming before wind events was accompanied by a thickening of the mixed layer, suggesting that internal waves were strongly influencing air-sea interactions. Increased winds tended to precede surface cooling and subsurface warming by a few days. There were strong correlations between warming (cooling) thermocline temperature and increased (decreased) zonal winds at the central and eastern equatorial Pacific buoys. In the central Pacific, thermocline warming (cooling) was associated with westerlies (easterlies). This suggested that equatorially trapped Kelvin waves warmed and thickened the mixed layer, resulting in increased zonal winds. In the central Pacific, these local zonal winds then reinforced the Kelvin waves through downwelling and upwelling. Ocean temperature inversions were found throughout the Pacific. Such inversions were most pronounced in the central Pacific. The inversions in this region were associated with a relatively thick and warm mixed layer, and with relatively strong westerly winds and deep atmospheric convection. One particularly strong and persistent equatorial inversion event at 155°W apparently resulted from weak wind induced surface cooling combined with strong Kelvin wave induced subsurface warming. The westerly winds during this inversion were part of a tropical cyclone that formed just north of the equator. The air-sea relationships during this case study were consistent with those identified by the basin wide statistical analyses. Taken together, these results suggest the following remote feedback cycle. (1) Tropical cyclones in the west Pacific generate equatorially trapped Kelvin waves. (2) These waves propagate into the central and eastern Pacific, warming and thickening the mixed layer. (3) The warmer ocean generates wind events. (4) The wind events, coupled with the warmer ocean temperatures, create conditions favorable for tropical cyclone formation. (5) Tropical cyclones develop, and propagate westward into the west Pacific.				
14. SUBJECT TERMS MIXED LAYER, KELVIN WAVES, TURBULENT KINETIC ENERGY, BOUYANCY DAMPING, TROPICAL CYCLONE, EL NINO, ENSO, HEAT CONTENT, THERMOCLINE, AIR-SEA INTERACTION, EQUATORIAL PACIFIC, OCEAN TEMPERATURE INVERSIONS, TOGA, BARRIER-LAYER.		15. NUMBER OF PAGES 202		16. PRICE CODE
17. SECURITY CLASSIFICATION OF REPORT Unclassified	18. SECURITY CLASSIFICATION OF THIS PAGE Unclassified	19. SECURITY CLASSIFICATION OF ABSTRACT Unclassified	20. LIMITATION OF ABSTRACT UL	

Approved for public release; distribution is unlimited.

Air-Sea Interaction Patterns
in the Equatorial Pacific

by

John E. Kent
Lieutenant Commander, United States Navy
B.S., University of California, Los Angeles, 1978
M.S., University of Southern Mississippi, 1991

Submitted in partial fulfillment
of the requirements for the degrees of

MASTER OF SCIENCE IN METEOROLOGY, and
MASTER OF SCIENCE IN PHYSICAL OCEANOGRAPHY

from the

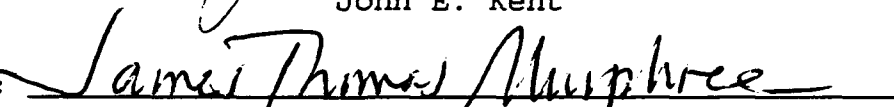
NAVAL POSTGRADUATE SCHOOL
December 1993

Author:

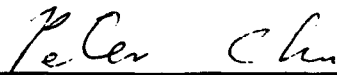


John E. Kent

Approved by:



James Thomas Murphree, Thesis Advisor



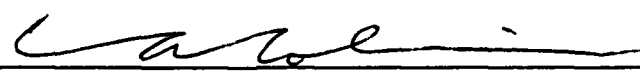
Peter C. Chu, Co-Advisor

Peter C. Chu, Co-Advisor



Robert L. Haney, Chairman

Department of Meteorology



Curtis A. Collins, Chairman

Department of Oceanography

ABSTRACT

We have investigated air-sea interaction patterns in the equatorial Pacific during the 1991-1992 El Niño/Southern Oscillation (ENSO) event. Our study focused on the identification of spatial and temporal relationships between sea surface temperatures, subsurface temperatures, and winds. These relationships were examined using time series and statistical analyses of atmosphere and ocean data from the moored buoys of the Tropical Oceans-Global Atmosphere (TOGA) program.

Our results strongly suggest that the heat content of the ocean mixed layer greatly affected air-sea interactions. In almost all regions, mixed layer warming was followed within one week by increased winds. In most cases, the mixed layer warming before wind events was accompanied by a thickening of the mixed layer, suggesting that internal waves were strongly influencing air-sea interactions. Increased winds tended to precede surface cooling and subsurface warming by a few days.

There were strong correlations between warming (cooling) thermocline temperature and increased (decreased) zonal winds at the central and eastern equatorial Pacific buoys. In the central Pacific, thermocline warming (cooling) was associated with westerlies (easterlies). This suggested that equatorially trapped Kelvin waves warmed and thickened the mixed layer, resulting in increased zonal winds. In the central Pacific, these local zonal winds then reinforced the Kelvin waves through downwelling and upwelling.

Ocean temperature inversions were found throughout the Pacific. Such inversions were most pronounced in the central Pacific. The inversions in this region were

associated with a relatively thick and warm mixed layer, and with relatively strong westerly winds and deep atmospheric convection.

One particularly strong and persistent equatorial inversion event at 155°W apparently resulted from weak wind induced surface cooling combined with strong Kelvin wave induced subsurface warming. The westerly winds during this inversion were part of a tropical cyclone that formed just north of the equator. The air-sea relationships during this case study were consistent with those identified by the basin wide statistical analyses.

Taken together, these results suggest the following remote feedback cycle. (1) Tropical cyclones in the west Pacific generate equatorially trapped Kelvin waves. (2) These waves propagate into the central and eastern Pacific, warming and thickening the mixed layer. (3) The warmer ocean generates wind events. (4) The wind events, coupled with the warmer ocean temperatures, create conditions favorable for tropical cyclone formation. (5) Tropical cyclones develop, and propagate westward into the west Pacific.

Accession For		1
NTIS	CRA&I	<input checked="" type="checkbox"/>
DTIC	TAB	<input type="checkbox"/>
Unannounced		<input type="checkbox"/>
Justification		
By		
Distribution /		
Availability Codes		
Dist	Avail and/or Special	
A-1		

LIST OF ABBREVIATIONS

AT	air temperature
CTD	conductivity-temperature-depth
dT	air-sea temperature difference ($dT = SST - AT$)
E	easterlies
ENSO	El Niño/Southern Oscillation
IR	infrared
M	horizontal wind speed
N	northerlies
OLR	outgoing longwave radiation
OTIS	Optimal Thermal Interpolation System
S	southerlies
SEC	South Equatorial Current
SST	sea surface temperature
TAO	Thermal Array for the Ocean
TASITA	Towed Air-Sea Interface Analyzer
TG	temperature gradient = $(SST - \text{Temp. at depth}) / \text{depth}$
TKE	turbulent kinetic energy
Tmax	ocean temperature with the greatest fluctuations
TOGA	Tropical Ocean-Global Atmosphere
TOPS	Thermal Ocean Prediction System
Tup	ocean temperature just above the thermocline
XBT	expendable bathythermograph

WEPOCS	Western Equatorial Pacific Ocean Circulation Study
U	zonal wind speed
V	meridional wind speed
W	westerlies

TABLE OF CONTENTS

I. INTRODUCTION	1
A. PREVIOUS WORK	1
B. HYPOTHESES	5
C. UNRESOLVED PROBLEMS	7
D. OVERVIEW OF THESIS	8
II. DATA AND METHODS	9
A. DATA	9
B. STATISTICAL METHODS	10
1. WIND FORCING REGIONS	11
2. SEQUENTIAL SCATTERPLOTS	12
3. DETRENDING	12
4. CROSS CORRELATIONS	13
5. INVESTIGATED RELATIONS	16
III. ANALYSES AND RESULTS	20
A. CLIMATOLOGICAL BACKGROUND	20
B. TIME SERIES RESULTS	21

C.	SEQUENTIAL SCATTERPLOT RESULTS	22
D.	ESTIMATED CROSS-CORRELATION RESULTS	29
1.	SST/U	33
2.	SST/V	35
3.	SST/M	37
4.	Summary of SST/Wind Correlations	38
5.	Tup/U	40
6.	Tup/V	41
7.	Tup/M	42
8.	Summary of Tup/Wind Correlations	43
10.	TG/U	44
10.	TG/V	49
11.	TG/M	52
12.	Summary of TG/Wind Correlations	54
13.	Tmax/U	56
14.	Tmax/V	59
15.	Tmax/M	60
16.	Summary of Tmax/Wind Correlations	62
17.	SST/Tup	63
18.	SST/Tmax	64
19.	SST/AT	65
20.	TG/AT	65

21. AT/M	66
22. dT/M	68
23. Summary of Cross-Correlation Results	70
E. TEMPERATURE INVERSIONS	77
IV. CONCLUSIONS AND RECOMMENDATIONS	82
A. CONCLUSIONS	82
B. RECOMMENDATIONS	86
LIST OF REFERENCES	88
TABLES	90
FIGURES	105
APPENDIX A 2°S 165°W TIME SERIES	158
APPENDIX B EQ 169°W TIME SERIES	165
APPENDIX C 5°S 155°W TIME SERIES	171
APPENDIX D 2°N 110°W TIME SERIES	177
APPENDIX E EQ 155°W TIME SERIES	183
INITIAL DISTRIBUTION LIST	190

I. INTRODUCTION

This study investigates air-sea interaction patterns in the tropical Pacific using equatorial Pacific buoy data. Two principal questions are addressed in this work.

1. What are the observed relationships between sea surface temperature (SST), subsurface ocean temperatures, air temperature, and wind; and how do these relationships vary spatially?

2. What evidence is there of ocean temperature inversion regions, and, if found, how are these inversions related to specific air-sea interaction processes?

These issues have been studied using time series and statistical analyses of observational atmosphere and ocean data from the moored buoys of the Tropical Ocean Global Atmosphere (TOGA) program during the 1991-1992 El Niño/Southern Oscillation (ENSO).

A. PREVIOUS WORK

Meyers et al. (1986) compared observed mixed layer heat storage, in the equatorial western Pacific during 1979-1983, with local heat budget processes, including various surface fluxes and mixing. They found correlations between the heat storage rate and the total surface flux estimated from surface observations. They concluded that evaporation due to anomalous meridional winds was the major factor in the ocean surface cooling observed during the 1982-1983 ENSO.

Lindstrom et al. (1987) showed that precipitation may significantly alter the temperature, salinity, and density structure of the tropical upper ocean. The downward flux of freshwater may lower salinities, increase stability, and reduce mixing, which may lead to an increase in SST. The net result may be a surface lens of relatively fresh, stable, and warm water (Webster and Lukas 1992).

McPhaden et al. (1990) studied the 1986-1987 ENSO event using data from three buoys at 165°E, 2°N, 0°, and 2°S. They found that, typically, zonal ocean currents in the upper 100 meters responded to westerly wind anomalies within a week, in some cases with speeds exceeding 100 cm s^{-1} . They concluded that wind driven zonal currents at the equator were important in the mass and heat balance of the western Pacific during the 1986-1987 ENSO. They also found that the meridional wind stress and meridional current velocity energy levels at periods longer than 100 days on the equator were 5-10 times weaker than in the zonal direction, and consequently less important to the development of the ENSO.

McPhaden et al. (1990) also found that the depth of the thermocline was poorly correlated with SST. They therefore concluded that cold water entrained from the thermocline was not a dominant process affecting SST in the western Pacific. They suspected this was because the thermocline is on average deep and the surface layer thick in the western Pacific. Thus, surface temperatures are buffered by the large thermal capacity of the warm pool and entrainment mixing has relatively little effect on SST variations.

McPhaden and Hayes (1991), in a study of TOGA buoy data along 165°E, concluded that: (a) evaporative cooling accounted for a significant fraction of SST and heat content variability; (b) wind forced entrainment, and horizontal and vertical advection, were not as important as evaporative cooling; and (c) a large fraction of SST and surface layer heat content variability could not be accounted for by wind fluctuations alone. They suggested that much of the variability may have been due to variations in shortwave radiative fluxes at the air-sea interface.

Lukas and Lindstrom (1991) analyzed conductivity-temperature-depth (CTD) profiles from the Western Equatorial Pacific Ocean Circulation Study (WEPOCS). They found that in the western equatorial Pacific, the mixed layer, based on salinity gradients, was about 30 m deep while the thermocline was about 65 m deep. They attributed the difference to salinity stratification. They concluded that this stratification may limit deep turbulent mixing to periods of strong winds. Thus they suggested that, in the western Pacific warm pool, periods in which SST is strongly impacted by vertical entrainment may be infrequent. Fig. 1, from Lukas and Lindstrom (1991), shows examples of salinity, density, and temperature profiles for a well mixed upper ocean and for an upper ocean with a freshwater lens (low salinity layer) at the surface.

In addition, Lukas and Lindstrom (1991) proposed that advection and subduction may also form freshwater lenses in the western Pacific. In this process, the relatively high precipitation and low evaporation in the western tropical Pacific may produce relatively low surface salinities. Thus, as more saline water from the central Pacific is

advected to the west by the South Equatorial Current (SEC), it is subducted under the fresher western Pacific waters, forming freshwater lenses.

Ravier-Hay and Godfrey (1993) took fine scale boundary layer measurements during Sep. 90 at 4°S 149°E, using an air-sea profiling device, the Towed Air Sea Interface Analyzer (TASITA). They found a strong relationship between the diurnal variation of SST, solar radiation (cloud cover) and wind speed. They also noted that heavy rainfall caused a reduction of incoming solar radiation to near zero, and a drop in SST of around 0.5°C.

Cechet (1993), commenting on the same TASITA results, noted that diurnal warming was confined to a relatively shallow layer. Cechet noted that the temperature within one centimeter of the surface, the "skin" temperature, responded rapidly to solar heating and had a range of over 3°C. According to Cechet, diurnal heating resulted in increased evaporative and sensible heat fluxes. This caused enhanced atmospheric convection which led to a negative feedback through increased cloudiness, increased wind induced mixing, and increased precipitation which formed *cool* freshwater lenses on the sea surface.

Cechet also found that, under low wind speed conditions (< 3 m/s), solar heating significantly warmed and stabilized the ocean surface layer. He noted that the absorption of solar radiation produced a positive buoyancy flux which suppressed wind induced turbulent mixing. Under these conditions, the skin temperature could be up to a few degrees warmer than the temperature tens of centimeters below the surface. Cechet

concluded that this ocean skin temperature could play a dominant role in air-sea interactions.

B. HYPOTHESES

These and other previous studies have shown that the wind affects the local SST in several ways. Three major ways are: 1) altering the surface fluxes of latent and sensible heat; 2) driving currents which advect waters with different temperatures; and 3) generating turbulent mixing between waters of different temperatures (McPhaden et al. 1990, McPhaden and Hayes 1991, Webster and Lukas 1992).

For a wind speed of M , these three processes are proportional to M , M^2 , and M^3 , respectively (McPhaden and Hayes 1991, Webster and Lukas 1992). All of these processes are inversely proportional to the mixed layer depth. The smaller this depth, the greater the rate at which SST tends to vary (McPhaden and Hayes 1991, Webster and Lukas 1992). This dependence on mixed layer depth provides one example of how the ability of the wind to change the SST is affected by pre-existing mixed layer conditions.

Of course, the state of the mixed layer (e.g., its thickness and heat content) is strongly influenced by the preceding winds and surface fluxes. So air-sea relationships, especially cause-effect relationships, can be very difficult to clearly establish.

A conceptual model of the ocean that has been useful in interpreting air-sea interactions is a two layer model in which temperature changes are interpreted in terms of vertical turbulent mixing and buoyancy fluxes (Niiler and Kraus 1977). Wind forcing may lead to upper ocean turbulence and the mixing of warmer surface waters with cooler

waters from below, causing surface cooling of the surface and warming at subsurface depths (Fig. 2a). Buoyancy fluxes resulting from heat and mass fluxes may lead to convection or to a more stable stratification. In situations where surface heating and precipitation are high, buoyancy fluxes may stabilize the upper ocean and limit the depth to which turbulent mixing penetrates (Fig. 2b). This is probably a common situation in much of the equatorial western Pacific (Webster and Lukas 1992). If so, then this may help explain why several studies have found that SST cooling in the equatorial western Pacific was primarily due to evaporation rather than entrainment (e.g., Lukas and Lindstrom 1991, McPhaden and Hayes 1991). However, strong buoyancy damping is probably much less common in the equatorial central and eastern Pacific, where, in general, precipitation is lower, winds are more consistent, and the thermocline is shallower than in the equatorial western Pacific. Thus, one might expect to find some regional differences in equatorial air-sea interaction patterns.

The simple two layer model also illustrates how pre-existing mixed layer conditions (e.g., depth, temperature, stratification) affect subsequent air-sea interactions. One important process that may significantly modify the equatorial mixed layer is the propagation of internal waves. In particular, equatorial Kelvin waves may produce large intraseasonal variations in mixed layer depth and temperature (cf. McPhaden et al. 1990, Cooper 1992). Thus, air-sea relationships may be strongly affected in situations where Kelvin waves have a pronounced near surface impact (e.g., in the equatorial central and eastern Pacific). For example, wind induced entrainment may have a relatively small impact on SST if it occurs during the downwelling phase of a Kelvin wave.

Another important process that may modify the mixed layer and alter air-sea interactions is the development of regions of relatively low salinity water or "freshwater lenses". Some freshwater layers may be associated with negative near surface vertical temperature gradients, or temperature inversions (Cechet 1993). Such layers and inversions would be most likely to form under strong wind conditions, and in the presence of a deep, warm, salty mixed layer (cf. Lukas and Lindstrom 1991, Cechet 1993). Air-sea relationships in such inversion situations should, of course, be distinctly different from those found in positive vertical temperature gradient situations. Thus, the identification of inversions may be useful in clarifying spatial and temporal variations in equatorial air-sea interactions.

C. UNRESOLVED PROBLEMS

The previous studies discussed in Sec. A have clarified many aspects of equatorial Pacific air-sea interactions, but many questions remain unanswered. Many of these questions fit into the two main problem areas of this study.

1. Wind and Ocean Temperature Relationships. What are the dominant temporal relationships between wind, SST, and sub-surface temperatures? How do these relationships vary across the Pacific? In what situations is entrainment cooling of the surface comparable to evaporative cooling? What is the importance of the meridional wind in SST and subsurface temperature variations? What are the major feedbacks by which winds alter the mixed layer and, thereby, influence subsequent interactions between the wind and ocean? How are these relationships influenced by ENSO phenomena?

2. Temperature Inversions. How common are inversions and under what conditions do they tend to form? How are inversions influenced by the wind and ocean dynamics? How do inversions affect air-sea relationships?

D. OVERVIEW OF THESIS

This study investigates air-sea interaction patterns in the tropical Pacific using equatorial Pacific buoy data. To address some of the outstanding problems listed above, we focus on two specific questions:

1. What are the observed relationships between SST, subsurface temperatures, air temperature, and wind, and how do these relationships vary regionally?
2. What evidence is there of temperature inversions; and, if found, how are these inversions related to specific air-sea interaction processes?

These issues will be studied using time series and statistical analyses of observational atmosphere and ocean data from the moored buoys of the Tropical Oceans-Global Atmosphere (TOGA) program during the 1991-1992 ENSO.

Chapter (Chap.) II describes the data sources, methods, and statistical procedures. Results are presented in Chap. III. Conclusions are given in Chap. IV.

II. DATA AND METHODS

A. DATA

The data for this study came from the Tropical Ocean-Global Atmosphere - Thermal Array for the Ocean (TOGA-TAO) moored buoys in the equatorial Pacific. These buoys include Autonomous Temperature Line Acquisition System (ATLAS) buoys and Equatorial Pacific Ocean Climate Studies (EPOCS) buoys. The ATLAS buoys used in this study are located at longitudes 156°E, 165°E, 170°W, 169°W, 155°W, 140°W, 125°W, 110°W. The EPOCS buoys used in this study are located on the equator at 165°E, 140°W, and 110°W. Fig. 3, from Cooper (1992), shows the locations of these buoys.

The ATLAS buoys measure zonal and meridional surface wind components, air temperature (AT), sea surface temperature (SST), and subsurface temperatures. The EPOCS buoys measure surface wind, AT, SST, and currents. For both types of buoys, wind measurements are made 4 m above the surface. Air temperature (AT) is measured 3 m above the surface, and sea surface temperature is measured 1 m below the surface. The ATLAS buoys measure subsurface temperatures at ten depths to a maximum depth of 500 m (McPhaden et al. 1990). Neither the ATLAS or EPOCS buoys provide salinity data.

Buoy data are telemetered to shore via Service ARGOS as 2-hour or in some cases 1-hour averages. Normally, five unique data transmissions are received each day. The time series used in this study were constructed from the daily averages of these data. The

data were obtained from the National Oceanic Atmospheric Administration's (NOAA) Pacific Marine Environmental Laboratory (PMEL) in Seattle, WA

According to Linda Mangum of PMEL, the accuracies of the various measured fields are:

winds	+/- 0.1 m/s
wind direction	+/- 10°
SST and subsurface temps.	+/- 0.01 °C
air temp.	+/- 0.5 °C

The data used in this study covered a 183 day period from 01 October 1991 to 31 March 1992. As a result of equipment failures, losses in transmission, or vandalism of the buoys, most of the time series had gaps in the data. For this study period, relatively little current data was available. So we restricted our analyses to the air temperature, wind, and ocean temperature time series. Table 1, from Cooper (1992), shows the record lengths of useable data for each of the buoys, where dashes indicate the presence and gaps indicate the absence of data.

B. STATISTICAL METHODS

Air-sea relationships were analyzed in terms of: (1) specific events within the time series; and (2) cross correlations of the time series based on the entire 183 day study period. To study regional variations in air-sea relationships, each buoy location was categorized as belonging to one of several distinct wind regions. These wind regions were defined according to the characteristics of the mean winds at each buoy location.

For each location, various cross-correlations were calculated. Regional average cross-correlations were then calculated for each wind region in order to identify characteristic spatial patterns in the correlations.

1. WIND FORCING REGIONS

After plotting time series of the data from each individual buoy, the buoys were grouped into three different regions based on their predominant zonal wind, or U, components, (Fig. 4). The U and V statistics used to define the different wind regions are shown in Table 2. These **zonal wind regions** are: 1) The **westerly** region - four buoys at 2°N 156°E, 2°S 156°E, EQ 165°E, and 2°S, 165°E, where U was predominantly westerly; 2) the **transition** region - three buoys at 2°N 165°E, EQ 170°W, and EQ 169°W, where U was both easterly and westerly; 3) the **easterly** region - thirteen buoys at 5°N 155°W, 2°N 155°W, EQ 155°W, 5°S 155°W, 2°N 140°W, EQ 140°W, 2°S 140°W, 2°N 125°W, EQ 125°W, 2°S 125°W, 2°N 110°W, EQ 110°W, 2°S 110°W, where U was predominantly easterly.

After further examination of the time series, the thirteen buoys in the easterly wind forcing region were subdivided into three **sub-regions** based on the variation of the meridional wind, or V, component and on the presence of ocean temperature inversions (Fig. 5). The V statistics used to define the different wind subregions are shown in Table 2. These subregions are: 1) The **steady V** region - three buoys with steady southerly V wind components at 2°N 110°W, EQ 110°W, and 2°S 110°W; 2) the **varying V** region - ten buoys with varying V wind components at 5°N 155°W, 2°N 155°W, EQ 155°W, 5°S 155°W, 2°N 140°W, EQ 140°W, 2°S 140°W, 2°N 125°W, EQ 125°W, and 2°S 125°W; 3)

the **inversion** region - with four buoys within the varying V region, and with pronounced ocean temperature inversions, at 5°N 155°W, 2°N 155°W, EQ 155°W, and 2°N 140°W.

2. SEQUENTIAL SCATTERPLOTS

Sequential scatterplots are simply conventional scatterplots, but with the addition of line segments that connect the points of the scatterplot in chronological order. These plots are used in this study to investigate air-sea relationships associated with specific wind and SST events.

3. DETRENDING

Prior to calculating the cross-correlations, the data was linearly detrended after Makridakis and Wheelright (1987):

$$e_t = X_t - X_t^{(1)} \quad (1a)$$

$$S_t = S_{t-1} + T_{t-1} + h_1 e_t \quad (1b)$$

$$T_t = T_{t-1} + h_2 e_t \quad (1c)$$

$$X_t^{(m)} = S_t + mT_t \quad (1d)$$

where X_t is the observed value of the series in period t ; $X_t^{(m)}$ is the forecast made at the end of t for m steps ahead; e_t is the forecast error in t ; S_t is the mean of the series at the end of t ; T_t is the trend at the end of t ; and h_i is the smoothing parameter for the level of the series.

4. CROSS CORRELATIONS

The estimated cross correlations were calculated using the following formula from Box and Jenkins (1976):

$$r_{xy} = \frac{c_{xy}(k)}{S_x S_y} \quad k = 0, \pm 1, \pm 2, \dots \quad (2)$$

where the estimated cross covariance coefficient at lag k is:

$$c_{xy}(k) = \begin{cases} \frac{1}{n} \sum_{i=1}^{n-k} (x_i - \bar{x})(y_{i+k} - \bar{y}) & k = 0, 1, 2, \dots \\ \frac{1}{n} \sum_{i=1}^{n+k} (x_i - \bar{x})(y_{i-k} - \bar{y}) & k = 0, 1, 2, \dots \end{cases} \quad (3)$$

and where:

$$S_x = \sqrt{C_{xx}(0)}, \quad S_y = \sqrt{C_{yy}(0)} \quad (4)$$

r^2 is referred to as the sample coefficient of determination. It expresses the proportion of the total variation in the values of variable Y that can be explained by a linear relationship with the values of variable X. For example, if $r = 0.3$, then 0.09 or 9% of the total variation of the values of sample Y is accounted for by a linear relationship with values of sample X.

Ideally, both of the time series used in calculating a cross correlation would have a complete record of 183 days of data. However, one or both of the series usually had gaps. When this occurred, cross-correlations were calculated only for those consecutive days when both series had data. If one series had a large gap in the middle,

then two separate cross-correlations were calculated for the periods when both series had data. The final cross-correlation for the buoy was the weighted average of the two correlations, where the weighting was based on the number of observations used to calculate the separate correlations. Thus, the buoy was treated as two separate buoys with shorter record lengths. Because of such gaps in the time series, we limited the correlation leads and lag ranges to 24 days.

The 95% significance limits for the average cross correlations were calculated after Spiegel (1991) as:

$$z = \frac{1}{2} \ln \left(\frac{1+r}{1-r} \right) \quad (5)$$

which is approximately normally distributed with a mean:

$$\mu_z = \frac{1}{2} \ln \left(\frac{1+\rho}{1-\rho} \right) \quad (6)$$

and a variance:

$$\sigma_z^2 = \frac{1}{n-3} \quad (7)$$

where ρ is the true (population) correlation coefficient; and n is the number of independent observations.

The regional average correlations were found by calculating, at each lag, the weighted average of the correlation coefficients from all the buoys in a region. The weighting was based on the number of observations used to calculate the individual

correlations. To calculate the significance limits for these average correlations, n was calculated as in Trenberth (1987):

$$n = N \frac{\Delta t}{T_o} \quad (8)$$

where N is the total number of observations used in calculating the correlation; Δt is the time between observations (one day, for this study); and T_o is the time between effectively independent observations:

$$T_o = 1 + 2 \sum_{L=1}^N \left(1 - \frac{L}{N}\right) r_{L_a} r_{L_b} \quad (9)$$

Here, L is the lag (in days); and r_{L_a} and r_{L_b} are the lagged autocorrelation coefficients for the two time series, a and b , that are being correlated. Trenberth (1987) describes n calculated in this way as the effective number of independent observations. Table 3 shows values of n calculated for zero lag cross-correlations between SST and U .

Of course, cross-correlation results must be used with considerable care. It is important to realize that a zero value for r does not mean that there is no association between two variables. It only means that there is not a linear relationship between the two. Two variables could have a strong quadratic relationship but have zero correlation. It is also important to note that the existence of a correlation does not imply a causal relationship (Walpole and Myers 1978; Wallis & Roberts 1956, p.79). Thus, the correlations obtained in this study are used simply to identify significant relationships and as a basis for suggesting some plausible physical mechanisms for these relationships.

5. INVESTIGATED RELATIONS

The time series used to analyze air-sea relationships were the:

- 1) zonal wind component, U
- 2) meridional wind component, V
- 3) horizontal wind speed, M
- 4) air temperature, AT
- 5) sea surface temperature, SST
- 6) temperature just above the thermocline, T_{up}
- 7) temperature at the depth with maximum temperature variation, T_{max}
- 8) vertical temperature gradient in the mixed layer, TG
- 9) sea-air temperature difference, dT.

Series 1, 2, 4, and 5 came directly from the TOGA-TAO data set. M was calculated as:

$$M = \sqrt{U^2 + V^2} \quad (14)$$

T_{up} and T_{max} were determined by analyzing the subsurface temperature time series. TG and dT were calculated using the differences, SST- T_{up} and SST-AT, respectively. These time series are discussed in more detail in the remainder of this section.

The thermocline was assumed to be indicated by those temperatures which experienced the maximum temperature variation. T_{max} was defined as the ocean temperature at the depth which had this maximum variation during most of the 183 day study period. For most buoys, this was at 140 m or 150 m, although for some it was as

deep as 180 m. These large temperature variations, particularly in the central and eastern Pacific, have been attributed to the passage of Kelvin waves (e.g., Cooper 1992).

Tup was defined as the ocean temperature at the depth which appeared to be just above the thermocline during most of the 183 day study period. For most buoys, this was at 80 m, although for some buoys it was as deep as 140 m. Thus, variations in **Tup** and the depth at which **Tup** occurs may be used to infer possible variations in the uniform upper layer.

TG was defined as the temperature gradient between the surface and the **Tup** level. For example, if **Tup** was at 80 m, then the temperature gradient would be:

$$TG = \frac{T_{sst} - T_{up}}{79 \text{ m}} \quad (15)$$

The difference is divided by 79 m instead of 80 m, because SST was measured at 1 m below the surface. **TG** variations may be used to infer possible variations in the stratification of the mixed layer.

The air-sea temperature difference was defined as:

$$dT = SST - AT \quad (16)$$

Variations in **dT** may be used to infer possible variations in air-sea heat fluxes.

Cross-correlations were used to analyze many of the relationships between the nine different time series. In this study, the correlation between two time series, **a** and **b**, is symbolically represented as **a/b**.

Relationships between the wind and SST were examined using the SST/U, SST/V, and SST/M correlations. Note that correlations involving U or V are affected by the wind direction. For example, if strong easterly winds resulted in SST decreases, then the SST/U correlation would be positive. And if strong westerly winds resulted in SST decreases, then SST/U would be negative.

The relationships between the U and V were investigated in order to help interpret other correlations.

The relationships between subsurface temperatures and wind were examined using the following correlations: T_{up}/U , T_{up}/V , T_{up}/M , TG/U , TG/V , TG/M , T_{max}/U , T_{max}/V , and T_{max}/M .

SST/ T_{up} and SST/ T_{max} were examined to study interactions between the surface and subsurface temperatures. SST/AT relations were examined to see how the ocean and air temperatures affect each other.

The relationships between the upper-ocean stratification and air temperature, TG/AT ; air temperature and wind, AT/M ; and wind and air-sea temperature difference, dT/M (an important quantity in electro-optics); were also studied.

It is important to recognize that these various correlations do not indicate that certain physical processes were operating. However, the correlation values, and their leads and lags, may be combined with knowledge of such quantities as the mean values of the fields being correlated to identify processes that are consistent with the correlations. Thus, in the following chapter, where correlation results are presented, we offer some possible physical explanations. By identifying such possible explanations, we hope to

stimulate future studies that might clarify the dominant air-sea interaction mechanisms in the equatorial Pacific.

III. ANALYSES AND RESULTS

A. CLIMATOLOGICAL BACKGROUND

During the study period, Oct. 1991 through Mar. 1992, an El Niño event evolved from its initial stage to its mature stage (Kousky 1991a-1992c). As described by Kousky (1991a-1992c), this evolution was characterized by anomalously weak easterly winds in the central and eastern Pacific. This weakening of the easterlies, which was very evident in Sep. 1991, initiated an eastward propagating Kelvin wave (Kousky 1991a). One effect of this wave was to increase the thermocline depth in the eastern Pacific and decrease the thermocline depth in the western Pacific. Associated with this Kelvin wave was the slow migration of the warmest equatorial waters ($SST > 30^{\circ}\text{C}$) from the dateline to a position near 160°W . Anomalously low outgoing longwave radiation (OLR) was also found in the central Pacific (Kousky 1991a-1992c). Low OLR anomalies are used as a proxy for deep convection. The lowest OLR anomalies (strongest convection) coincided with the warmest SST anomalies. The largest westerly wind anomalies (including actual westerlies and weak easterlies) were associated with the areas of greatest convection.

Figs. 6 through 9 (Kousky 1991a, 1992c), depict the evolution of the El Niño in terms of several key fields for Oct. 1991 (initial stage) and for Mar. 1992 (mature stage). Fig. 6 compares the equatorial depth-longitude sections of ocean temperatures for these two months. The deepening of the thermocline, roughly indicated by the depth of the 20°C isotherm, in the central and eastern Pacific is clearly evident. Fig. 7 compares SST

anomalies and shows the easterly migration and intensification of the warm SST anomaly. Fig. 8 compares anomalous 850 mb winds for the two months. Note that the anomalous westerlies became stronger in the central Pacific during the mature phase (Mar. 1992). Fig. 9 compares anomalous OLR. Note that Figs 5 through 9 show that during the mature phase, Mar. 1992, the largest anomalous westerly winds, the strongest convection (lowest OLR), and the highest SST anomalies were all coincident along the equator at approximately 160°W.

B. TIME SERIES RESULTS

The time series for representative buoys from each region are contained in appendices A through E. The buoys shown there were chosen based on the completeness of their data records. Each appendix displays the time series of: a) U, b) V, c) M, d) detrended U, e) detrended V, f) detrended M, g) SST, h) AT, i) dT, j) detrended SST, k) detrended AT, l) detrended dT, m) upper-layer ocean temps., n) temperature gradient TG, and o) multi-depth ocean temps. The representative buoys are:

BUOY	REGION REPRESENTED	APPENDIX
2°S 165°E	Westerly wind	A
EQ 169°W	Transition	B
5°S 155°W	Easterly & Varying V	C
2°N 110°W	Steady V	D
EQ 155°W	Inversion	E

The buoy at 169°W 0° was missing air temperature data. So, at this location, four time series involving AT are missing: AT, detrended AT, dT, and detrended dT.

Table 2 contains the summary statistics for each region. Notice that the easterly wind region had the lowest variance in wind speed and direction. This low variance is probably related to the region's lack of convection, as well as the deep equatorial penetration of the tradewinds. Notice also that the easterly wind region had the largest variance in both SST and AT. Within the easterly region, the ocean temperature inversion region had the highest wind variance. Table 2 shows that the transition region had the highest zonal wind variance and the lowest variance in SST. These preliminary statistics suggest that there may be an inverse relationship between wind variability and the SST and AT response to the winds.

C. SEQUENTIAL SCATTERPLOT RESULTS

We initially used scatterplots to identify relationships between individual wind events and SST variations. We found that these plots could be made much more useful by indicating the chronological order of the individual points in the scatterplots. We call this chronological scatterplot a **sequential scatterplot**. Fig. 10 is a sequential scatterplot of raw SST versus raw M for 2°N 156°E. The line segments connect the points in chronological order. The points, each representing a one day average, are labeled first with capital letters then with small letters. This gives 52 characters to represent 183 days, so each character is used to represent four consecutive days. The first four days are labeled A, A, A, A, the next four B, B, B, B, and so on until Z, Z, Z, Z. Then the

sequence starts over using small letters a, a, a, a, continuing until all 183 data points are labeled. If days were missing data, the letters for those days were omitted from the sequence.

The sequential scatterplots in this study (Figs. 10-12 are representative) generally consist of complex patterns of clustered points and lines. The clusters of points around one wind speed and temperature indicate periods when the forces driving both SST and wind are in equilibrium. Interpretation of the lines is more complex. This interpretation is made easier by using a sequential scatterplot key, Fig. 13, which groups the plot lines into sixteen event categories. This key is for the SST and M wind component. By adding and interpreting negative wind speed values for easterly and northerly winds, similar keys could also be developed for U and V. When referring to Fig. 13, letter pairs refer to line segments. For example, AO refers to the vector from point A to point O. The event categories in Fig. 13 are:

AE - Vertical line straight down (could be located anywhere, not just at 0 m/s). Indicates decreasing SST, constant M. Suggests wind induced cooling through increased: mixing, evaporation, and/or surface heat fluxes. Could also be due to advection of cooler water and/or upwelling near the equator.

EA - Vertical line straight up (could be located at any windspeed). Indicates increasing SST, constant M. Suggests wind induced cooling was significantly overpowered by other factors.

OB - Upward sloping diagonal from left to right. Indicates increasing wind speed, increasing SST. Suggests wind induced cooling was overpowered by other factors.

BO - Downward sloping diagonal from right to left. Indicates decreasing wind speed, decreasing SST. Suggests buoyancy damping is being overpowered by other factors.

OC - Horizontal line from left to right. Indicates constant SST, increasing wind speed. Suggests that the wind is having an insignificant effect on SST. It may mean that wind induced cooling is being offset by other factors.

CO - Horizontal line from right to left. Indicates constant SST, decreasing wind speed. Suggests that the wind had an insignificant effect on the SST. It may mean that buoyancy damping was offset by other factors.

OD - Downward sloping diagonal from left to right. Indicates decreasing SST, increasing wind speed. Suggests wind induced cooling overpowered buoyancy damping. Could also be due to advection of cooler water.

DO - Upward sloping diagonal from right to left. Indicates weakening wind speed, increasing SST. Suggests buoyancy damping, or decreased cold advection.

Fig. 10, the sequential scatterplot of raw SST and M at 2°N 156°E, contains large numbers of parallel diagonal lines sloping from upper left to lower right (OD and DO in Fig. 13). The fact that many of the diagonals have similar slopes suggests that the changes in wind speed and changes in SST had a consistent linear relation. Thus, we

would expect to find a strong correlation between the wind magnitude M and SST in the westerly wind region. As will be shown in the discussion of cross-correlation results, Chap. III, Sec. D, the strongest correlations between wind and SST variations did occur in the westerly wind region.

Fig. 10 contains other interesting events. Notice the point labeled O at 10.8 m/s and 28.85°C, which corresponds to 26 Nov. 1991. Fig. 12 shows that during the previous two days the wind increased by about 5.5 m/s, but the SST decreased by less than about 0.05°C. Notice that the wind burst began on 24 Nov. but the slight SST cooling does not begin until 25 Nov. Fig. 10 also shows that the wind relaxed by 3.7 m/s from the 26 to 27 Nov. but the SST continued to drop by another 0.05°C. This suggests that there was a time lag involved in the cooling process. This lag may have been a result of the ocean's "thermal inertia". For example, there may have been a measurable time lag between the wind changes and the initiation of the entrainment and the resulting surface cooling. Then there may have been an additional lag between the slackening of the winds and the cessation of the entrainment cooling. As will be shown in Chap. III, Sec. D, Cross-Correlation Results, there was a clear one day lag between increasing wind and decreasing SSTs, and between decreasing wind and increasing SSTs across the entire equatorial Pacific.

Fig. 10 also shows a descending and nearly vertical line, WXXXX, representing 31 Dec. 1991 - 04 Jan. 1992. In this case, the wind holds fairly steady at approximately 7 m/s for 5 days and the SST drops .6°C.

These two events suggest that the duration and magnitude of wind events may be important factors affecting SST response. The quick increase in winds to 10.5 m/s, followed by a sudden relaxation around 26 Nov. 1991 had much less effect on SST than did the 7 m/s wind which held steady for five days from 31 Dec. 1991 - 4 Jan. 1992.

Wind variability (e.g., the duration and magnitude of the wind events) is just one of many possible explanations for variable SST responses to wind events. Another possible explanation is the varying thickness of the mixed layer. Consider again the 26 Nov. 1991 wind event. The time series for this event (Fig. 14a) shows that the 10.8 m/s wind burst in M on 26 Nov. 1991 came after three sustained westerly wind bursts in Oct. and Nov., each of which lasted at least twelve days. Notice also that during most of this westerly wind period, the SST and temperature at 75 m were relatively similar (Fig. 14d). This indicates that the mixed layer was relatively thick and warm during this period. This thick, warm mixed layer may well have resulted from warm water advection and downwelling resulting from the preceding six weeks of westerly winds. The presence of this thick mixed layer may explain why the large wind variations during 24-27 Nov. 1991 had relatively little impact on the SST. These results are consistent with the hypothesis that a wind burst will have less effect on a thick warm mixed layer (large h) than a thin one (see Chap. I, Sec. B, Hypotheses). The sustained 7 m/s wind event during 31 Dec. 1991 - 04 Jan. 1992 was in the middle of a westerly wind burst with a southerly component (Fig. 14a,b,c). The SST was about the same as in the 24-27 Nov. 1991 event, but the 75 m temperature was about 3°C cooler (Fig. 14d). This indicates that the mixed layer was much thinner and cooler during 31 Dec. 1991 - 4 Jan.

1992. The greater SST cooling during the 31 Dec. 1991 - 4 Jan. 1992 wind event may have been related to the presence of this thinner and cooler mixed layer. Notice also that during this event there was a slight warming at 50 m and 75 m. This suggests that the westerly winds during this event may have induced warming through warm water advection and through mixing and downwelling of relatively warm surface waters. The sequential scatterplots of raw SST and M at EQ 170 W, in the transition region, and at 2°N 110°W, in the easterly region, are shown in Figs. 11 and 12. These show that there was considerable variability in SST and M relationships across the Pacific. In each plot, there are times when both the wind speed and SST increased or when both decreased.

Consider for example, the sequence of points in Fig. 11 starting at point f, at approximately 3.5 m/s, 29.0°C (representing 05 Feb. 1992), and ending at point g, at approximately 2 m/s, 28.6°C (representing 07 Feb. 1992). During this period, the wind speed *decreased* by 1.5 m/s, but the SST *dropped* 0.4°C. The sequence continues from the g at 2 m/s, 28.6°C to the g at 3.5 m/s, 29.3°C (representing 09 Feb. 1992). During this two day period, the wind *increased* by 1.5 m/s but the SST *increased* by 0.8°C. Thus, during this five day period, the relationships between SST and wind were exactly the opposite of what mixing, evaporation, and buoyancy forcing would suggest. The time series of the raw data for this buoy (Fig. 15a) show two westerly wind bursts during the twenty-one days prior to 07 Feb. 1992. On 05, 06, and 07 Feb., the wind was easterly at about 2 m/s. On 08, 10, and 11 Feb. 1992, the wind was weakly westerly. Then, after this period, there was an easterly wind burst lasting approximately 10 days. The subsurface temperature time series at EQ 170°W (Fig. 15f) shows that the westerly wind

events in mid-Jan. and early Feb. were associated with a thick warm mixed layer (extending to about 150 m in mid-Jan. 1992) and that the easterly wind events in mid and late Feb. were associated with a much thinner mixed layer (less than about 100 m in mid Feb. 1992). Thus, the SST and wind speed variations during early Feb. (Fig. 11) were associated with a transition from westerly to easterly winds and from a warm thick mixed layer to a cool thin mixed layer.

These transitions suggest an association between wind direction and mixed layer thickness and temperature. The westerlies along the equator may have produced downwelling that warmed and deepened the mixed layer, while the easterlies may have produced upwelling that shoaled the mixed layer.

The sequential scatterplot of raw SST and M at 2°N 110°W (Fig. 12) shows the effects of the 1991-1992 El Niño on SST in the eastern Pacific. This figure shows a long term increase in SST and decrease in winds throughout the 183 day record. On a short time scale, the local winds appear to have played a relatively minor role in the SST variations. Thus, in some cases, such as this one, other processes that affect SST may overwhelm the effects of the local winds. The major SST variations at this location (see App. D, panel g) were likely due to advection, internal wave activity, and other large scale El Niño processes (Cooper 1992).

The sequential scatterplot results provide a number of useful insights into SST/wind relationships. Their complexity reveals that many competing forces drive SST, and highlights some of the difficulties in identifying equatorial air-sea interaction patterns. The sequential scatterplots show that there is an inherent lag between the wind and SST

changes, and that wind variability may play an important role in determining SST responses to the wind. The sequential scatterplots also suggest that the temperature and depth of the mixed layer, as evidenced by temperatures at deeper depths, is very important in determining SST responses to the wind, and that SST/wind relationships may be complicated by the environmental history from the preceding week or two. It is therefore essential to study the history of preceding winds, currents, surface fluxes, etc. to determine how they have preconditioned the mixed layer.

D. ESTIMATED CROSS-CORRELATION RESULTS

Average air-sea interaction patterns were analyzed using cross-correlations. All correlations shown in this study are based on linearly detrended time series, unless otherwise stated.

According to McPhaden and Hayes (1991), turbulent air-sea heat exchange is proportional to zonal wind speed, $|U|$, the magnitude of the Ekman pumping at the equator is proportional to $|U|U$, and wind work (TKE) is proportional to $|U|^3$. To investigate these relations, correlations of SST/ $|U|$, SST/ $|U|U$, and SST/ $|U|^3$ using raw data were made for a representative buoy from each region. Fig. 16 shows that the correlations of SST with wind speed, Ekman pumping, and wind work at 2°S 165°E were essentially the same: a very slight positive correlation when SST leads U and a moderately strong negative correlation when SST lags U, with the correlations involving wind speed slightly larger than the other two. These correlations suggest that SST warmed (cooled) approximately two weeks prior to an increase (decrease) in U, then SST

cooled (warmed) approximately one to three days after an increase (decrease) in U that lasted for at least two weeks. These results are consistent with those obtained by McPhaden and Hayes (1991). Similar results were found for all the other regions (not shown).

Cross-correlations of linearly detrended data for nineteen relations were calculated for each of the twenty buoys for each of the six regions. As discussed in Chap. II, Sec. B5, these relations were: SST/U, SST/V, SST/M, U/V, Tup/U, Tup/V, Tup/M, TG/U, TG/V, TG/M, Tmax/U, Tmax/V, Tmax/M, SST/Tup, SST/Tmax, SST/AT, TG/AT, AT/M, and dT/M.

To summarize the results and identify any regional dependence of the air-sea relationships, the cross correlations were weighted averaged for each of the three zonal wind regions described in Chap. II, Sec. B1. The weighting was based on the number of data days used to calculate the correlations. The three regions are: westerly, transition, and easterly. The easterly region was further subdivided into the varying V, steady V, and ocean temperature inversion regions. Comparisons of the correlations for the individual buoys with their regional averages showed that the averaged correlations were good approximations for all the buoys in each region.

Figs. 17 through 24 depict the averaged cross-correlations for the nineteen relationships for each of the six wind regions. Cross-correlation significance limits were dependent on the number of data points used. These varied from buoy to buoy and from region to region and consequently could not be displayed on the plots. Table 3 gives the 95% significance limits for SST/U in each of the regions. Other relationships may have

slightly different limits due to gaps in the data. If a correlation is within the limits, the null hypothesis of $r = 0$ cannot be rejected. The peak significant values for all the correlations and regions are shown on Tables 4 and 5.

As shown in Table 2, the average and mode (the most frequently occurring) zonal winds are positive in the westerly and negative in the easterly wind regions. Thus, in general, a strengthening of the wind in the westerly region means the zonal wind is becoming more positive, while a strengthening of the wind in the easterly region means the zonal wind is becoming more negative. For all regions, the term "wind event" is used to refer to a strengthening of the prevailing winds (e.g., stronger westerlies in the westerly region and stronger easterlies in the easterly wind region). If we assume that stronger winds result in greater mixing and evaporation, and that mixing and evaporation are major factors controlling SST, then we would expect that strengthening winds (a wind event) would result in SST cooling. Similarly, weakening winds would result in SST warming. These assumptions and this line of reasoning would also lead us to expect negative SST/U correlations in the westerly wind region and positive SST/U correlations in the easterly wind region. Similarly, if we assume that a strengthening (weakening) wind results in a weaker (stronger) TG (vertical upper ocean temperature gradient), then we would expect negative TG/U correlations in the westerly region and positive TG/U correlations in the easterly wind region.

Tables 4 and 5 summarize the correlation plots by giving the maximum and minimum significant cross-correlations for each of the fourteen relationships. Table 4 gives the correlations for the zonal wind regions: westerly, transition, and easterly. Table

5 gives the correlations for the easterly wind sub-regions: varying V, steady V, and ocean temperature inversion (inversion) regions. Those relationships for which the null hypothesis, $r = 0$, could not be rejected at the 95% confidence are labeled not significant.

In Tables 4 and 5 and the cross-correlation plots (Figs. 17-24), a negative lag means that the variations in the first term in the relation (for example, SST in SST/U) lag or come after the variations in the second term. A positive lag means the variations in the first term lead or come before the second. A positive lag is also referred to as a lead. In the discussions of the correlations that follow, the numbers in parentheses refer to the maximum or minimum correlation and the corresponding lag. The first number is the correlation, and the second number is the lag, in days.

For example, from Table 4 we see that in the westerly region, the strongest lag correlation was (-.37/-5) in the SST/U correlation. This means that the largest correlation was -.37 and it occurred at a lag of five days. This implies that a U wind maximum (minimum) at time zero tended to be followed by an SST minimum (maximum), with the minimum (maximum) SST occurring five days after the maximum (minimum) zonal wind.

Each relationship in Tables 4 and 5 generally has two entries. The first is normally the strongest significant lag correlation, if one exists, and the second is generally the strongest significant lead correlation, if one exists. Some entries have only one or no correlations because the strongest lag and lead correlations were not significant. Some entries have a third correlation which is an additional significant correlation of interest at the indicated lag or lead.

Before discussing the cross-correlation results, three points need to be emphasized. First, the existence of a correlation does not mean that one event causes another; hence the frequent use of terms such as "implies" and "suggests" in the discussions. Second, the absence of a correlation does not mean that events are not related; it only implies the absence of a linear relationship between the two. Third, the difference between the size of the correlations between regions may be due to the averaging process and may not have any physical meaning. Generally, those regions with a large number of buoys and data points (e.g., easterly and varying V) will have smaller correlation peaks than regions with fewer buoys simply due to the smoothing effect of averaging. In the sub-sections which follow, the correlations shown in Figs. 17-24 are discussed. In general, the discussions address only the significant correlations.

1. SST/U

a. Zonal Wind Regions Lead Correlations.

Fig 17a shows that the lead correlations in the easterly wind region were negative. The peak lead correlation (where variations in SST led variations in U) in the easterly region was $-.10$ at a lead of four days (Table 4). The strongest correlations were when SST led U by three to nine days. This suggests that increased (decreased) SST resulted in increased (decreased) easterlies about one week later.

In the interest of brevity, this and future descriptions of the correlations will be shortened to: [peak ($-.10/4$), range (3 to 9)], where the range indicates the approximate lag or lead range, in days, of the strongest correlations. These correlations indicate that in the easterly region, SST tended to increase (decrease) from a few days to

a week prior to an increase (decrease) in the prevailing zonal winds. An increase in the zonal winds means that the westerlies increased in the westerly wind region or the easterlies increased in the easterly wind region, as discussed in Chap. III, Sec. C1. The peak correlation values for the zonal wind regions and the easterly wind sub-regions are listed in Tables 4 and 5 respectively.

b. Zonal Wind Regions Lag Correlations.

Fig. 17a shows that the SST/U lag correlations in the westerly region were negative [peak (-.37/-5), range (-1 to -7)]. These correlations indicate that the SST decreased (increased) from one day to one week after the zonal wind increased (decreased).

It is useful to note that a strong zonal wind may cause: (1) SST cooling due to mixing and evaporation; (2) downwelling (for westerlies) or upwelling (for easterlies); and (3) advection associated with zonal currents. The downwelling will tend to cause SST warming, while the upwelling will tend to cause SST cooling. Advection from the west (east) will tend to cause warming (cooling), given the observed SST gradient (Kousky 1991a-1992c). Thus, the effects associated with easterly winds will tend to cause cooling and a positive SST/U correlation at some lag. The effects of a westerly wind will be in conflict. The mixing and evaporation will cause cooling and a negative SST/U correlation, while the advection and downwelling will cause warming and a positive SST/U correlation. These warming effects will be most obvious after the mixing and evaporative cooling, since advection and downwelling have longer time scales than mixing and evaporation.

c. Easterly Wind Sub-Regions Lead Correlations.

Fig. 17d shows that the SST/U lead correlations were negative in the varying V region [peak (-.23/3), range (2 to 9)]. These indicate that SST increased (decreased) about two days to one week prior to an increase (decrease) in the easterlies. This suggests that a warming (cooling) of the oceans surface was associated with a subsequent increase (decrease) in the easterlies.

d. Easterly Wind Sub-Regions Lag Correlations.

Fig. 17d shows that the SST/U lag correlations were positive in the steady V regions [peak (.32/-4), range (-12 to 6)]. These correlations suggest that easterly (westerly) wind events resulted in SST decreases (increases) one to two weeks later. The broad curve associated with the steady V region lag suggests that cooling after an easterly wind event is due to evaporation and mixing immediately after the event, and advection and/or upwelling and downwelling two to three weeks later.

2. SST/V

a. Zonal Wind Regions Lead Correlations.

The SST/V lead correlations in the westerly region were positive [peak (.23/11), range (9 to 21)] (Fig. 17b). According to Table 2, the average meridional wind is weakly northerly (negative) in the westerly region. Thus, the correlations in the westerly region suggest that SST increases (decreases) were associated with increased (decreased) southerlies about one to three weeks later.

b. Zonal Wind Regions Lag Correlations.

Fig. 17b shows that the SST/V lag correlations were negative in the easterly [peak (-.11/-13), range (-9 to -20)] region. Table 2 shows that the average meridional winds were southerly in the easterly region. Thus, these correlations suggest that in the easterly region, increased (decreased) southerly winds were associated with decreased (increased) SST about nine to 20 days later. In the easterly wind region, the relatively long lag period between increases (decreases) in the southerly wind and decreases (increases) in SST suggest that advection and upwelling effects may have been more important than mixing and evaporation.

c. Easterly Wind Sub-Regions Lead Correlations.

Fig. 17e shows that the SST/V lead correlations were positive in the varying V region [peak (.16/12), range (9-14)]. The average meridional wind is southerly (positive) in this region (Table 2). Thus, these correlations indicate that the SST increased (decreased) from one to two weeks prior to an increase (decrease) in the southerly wind component.

d. Easterly Wind Sub-Regions Lag Correlations.

Fig. 17e shows that SST/V lag correlations were negative in the varying V region [peak (-.16/-12), range (-11 to -18)]. According to Table 2, the average meridional wind is southerly (positive) in this region. Thus, these correlations indicate that SSTs decreased (increased) two to three weeks after the southerly winds increased (decreased). These long lags suggest that upwelling and advection effects may be more

important than mixing and evaporation when considering the V component of the wind.

3. SST/M

a. Zonal Wind Regions Lead Correlations.

Fig. 17c shows that the SST/M lead correlations were positive in the easterly region [peak (.10/3), range (2 to 12)]. These correlations indicate that the SST increased (decreased) two days to two weeks prior to increased (decreased) horizontal winds, M. It is possible that increased winds were associated with increased atmospheric convection which was due to increased SST.

b. Zonal Wind Regions Lag Correlations.

Fig. 17c shows that the SST/M lag correlations were strongly negative in the westerly [peak (-.47/1), range (0 to -3)], moderately negative in the transition [peak (-.23/-1), range (0 to -9)], and weakly negative in the easterly [peak (-.15/-1), range (0 to -21)] regions. These correlations suggest that the SST decreased (increased) within a few days after the wind speed increased (decreased) in all three zonal wind regions. These associations are consistent with cooling due to wind induced evaporation and mixing, and warming due to buoyancy damping. The strongest correlation occurred in the westerly wind region (-.47/-1). In all three regions, the strongest correlation occurred at a lag of one day.

Fig. 17c shows that the easterly wind region had a second negative peak at longer lags [peak (-.17/-17), range (-15 to -18)]. This suggests that wind events resulted in SST cooling two to three weeks later. The long lags suggest that the cooling may have been due to advection and/or upwelling. In its entirety, the easterly wind lag

correlation curve suggests that wind events result in cooling first through evaporation and turbulent mixing, then, at longer lags, through advection and upwelling.

c. Easterly Wind Sub-Regions Lead Correlations.

Fig. 17f shows that the SST/M lead correlations in the varying V region were positive [peak (.20/4), range (2 to 10)]. This suggests that the SST increased (decreased) a couple of days to two weeks prior to an increase (decrease) in the wind speed.

d. Easterly Wind Sub-Regions Lag Correlations.

Fig. 17f shows that the SST/M lag correlations were negative in the varying V [peak (-.20/-17), range (-1 and -12 to -19)] and the steady V [peak (-.27/-14), range (-1 to -22)] regions. These correlations suggest that in all these sub-regions, the SST decreased (increased) within a few days after the wind speed increased (decreased). The results indicate that in the varying and steady V regions, stronger (weaker) easterly winds resulted in cooler (warmer) SSTs approximately one day later, due to evaporation and mixing, followed by additional cooling, due to advection and upwelling at longer lags.

4. Summary of SST/Wind Correlations

At this point, it is useful to summarize the SST/wind results. Basically, the SST/wind correlations have suggested that: (1) increased (decreased) SST was followed by increased (decreased) winds, suggesting that the winds were driven by heat fluxes from the ocean; and (2) increased (decreased) winds were followed by decreased (increased)

SST within a few days, suggesting that the ocean was cooled (warmed) by evaporative cooling, and turbulent mixing (buoyancy damping).

Tables 6-11 summarize all the cross-correlation results. To aid in this and all other correlation summaries, we need to explain how to read the tables. Consider the following typical entry:

SST ↑ (9 to 21) S ↑

Positive (negative) numbers in the parenthesis indicate lead (lag) in days. Up (down) arrows indicate positive (negative) change in the indicated variable. Thus, two (one) arrows in the same direction indicate the variables were positively (negatively) correlated. The wind variables have been expressed in terms of direction: W = westerlies, E = easterlies, S = southerlies, N = northerlies, M = horizontal wind speed. Thus, the above example means that SST increased 9 to 21 days before southerly winds increased.

Tables 6 and 7 show that, generally, SST warming (cooling) was followed from one to three weeks later by increased (decreased) southerlies in the westerly wind region, and by increased (decreased) easterlies, southerlies, and horizontal wind speed in the varying V region. This suggests that the winds were driven by heat fluxes from the ocean. The leads show that wind events followed warming sooner in the easterly (0 to 12 days) than the westerly region (6 to 24 days). The one exception to the above results was found in the steady V region, where increased (decreased) SST was followed within a week by decreased (increased) easterlies.

Tables 8 and 9 show that, generally, increased (decreased) winds resulted one day later in decreased (increased) SST in all regions, suggesting cooling (warming) due to

increased evaporation and turbulent mixing (buoyancy damping). The tables also show that SST changes following a wind event tended to occur over a longer range of lags in the easterly wind region (0 to 21 days) than in the westerly (0 to 3 days) or transition (0 to 9 days) regions. This may be associated with larger SST impacts in the easterly region from wind induced advection and/or upwelling.

5. Tup/U

a. Zonal Wind Regions Lead Correlations.

Fig. 19a shows that Tup/U lead correlations were negative in the easterly region [peak (-.17/3), range (0 to 7)]. This implies that Tup increased (decreased) about a week before increased (decreased) easterlies.

b. Zonal Wind Regions Lag Correlations.

There were no significant Tup/U lag correlations in the zonal wind regions.

c. Easterly Wind Sub-Regions Lead Correlations.

Fig. 19d shows that the Tup/U lead correlations negative in the varying V [peak (-.24/2), range (-12 to 9)] and steady V [peak (-.26/0), range (-6 to 9)] regions. These both imply that Tup increased (decreased) within about one week prior to increased (decreased) easterlies.

d. Easterly Wind Sub-Regions Lag Correlations.

Fig. 19d shows that the Tup/U lag correlations in both the varying V and steady V regions were negative. These correlations imply that Tup warmed (cooled) from one day to one week after the easterlies increased (decreased). If upwelling or

downwelling had been important, we would expect positive lag correlations in the varying V and steady V sub-regions. Since the correlations are negative, it appears that the predominantly easterly winds in this region influenced Tup primarily through turbulent mixing.

6. Tup/V

a. Zonal Wind Regions Lead Correlations.

Fig. 19b shows that Tup/V lead correlations in the westerly region were positive [peak (.24/3), range (3 to 15)]. The average meridional winds were weakly northerly (negative) in the westerly wind region (Table 2). Thus, these correlations imply that Tup increased (decreased) from a few days to two weeks prior to increased (decreased) southerly winds. This suggests that increased (decreased) mixed layer heat content was followed a few days to two weeks later by increased (decreased) southerlies.

b. Zonal Wind Regions Lag Correlations.

Fig 19b. shows that Tup/V lag correlations were positive in the westerly region [peak (.19/-1), range (0 to -2)]. Table 2 shows that the average meridional wind was weakly northerly in the westerly region. Thus, the positive lag correlations in the westerly region imply increased (decreased) southerlies were followed zero to four days later by increased (decreased) Tup. This suggests Tup warmed (cooled) due to turbulent mixing (buoyancy damping). The negative lag correlations in the transition region imply that increased (decreased) southerlies were followed about nine days later by decreased (increased) Tup.

c. Easterly Wind Sub-Regions Lead Correlations.

The Tup/V lead correlations were not significant in any of the easterly wind sub-regions.

d. Easterly Wind Sub-Regions Lag Correlations.

The Tup/V lag correlations were not significant in the easterly wind sub-regions.

7. Tup/M

a. Zonal Wind Regions Lead Correlations.

Fig. 19c shows that Tup/M lead correlations were positive in the easterly region [peak (.19/5), range (0 to 9)]. These correlations suggest that Tup warmed (cooled) from one day to one week prior to an increase (decrease) in the wind.

b. Zonal Wind Regions Lag Correlations.

The Tup/M correlations were not significant in the zonal wind regions.

c. Easterly Wind Sub-Regions Lead Correlations.

Fig. 19f shows that Tup/M lead correlations were positive in the varying V region [peak (.29/5), range (0 to 8)]. This suggests that in the varying V region, Tup warmed (cooled) from one day to one week prior to a horizontal wind speed increase (decrease). Note that in the varying V region, we also had indications that SST warmed (cooled) from one day to two weeks prior to increased (decreased) horizontal wind speeds (Fig 17f). Together, these results suggest that in the varying V region the entire mixed layer warmed (cooled) one day to two weeks prior to increased (decreased) winds.

d. Easterly Wind Sub-Regions Lag Correlations.

The Tup/M lag correlations were not significant in the easterly wind sub-regions.

8. Summary of Tup/Wind Correlations

Tup was the temperature just above the thermocline. The Tup/wind correlations suggest that: (1) Tup increased (decreased) within the week prior to increased (decreased) winds suggesting that the heat content of the mixed layer affected wind generation; and (2) Tup warmed (cooled) within the week after increased (decreased) winds, suggesting that turbulent mixing (buoyancy damping) warmed (cooled) Tup. The correlations suggesting Tup warming (cooling) prior to increased (decreased) winds were much smaller than the correlations suggesting Tup warming (cooling) after increased (decreased) winds.

Table 6 shows that increased (decreased) Tup was followed by increased (decreased) southerlies in the westerly wind region, and increased (decreased) easterlies and horizontal wind in the easterly wind region. Table 7 shows that increased Tup was followed by increased easterlies and horizontal wind in the varying V region and increased easterlies in the steady V region. As seen in the SST/wind results, the lag between Tup changes and wind changes was shorter in the easterly wind region (0 to 9 days) than the westerly wind region (3 to 15 days).

Table 8 shows that in the westerly wind region, increased (decreased) southerlies were followed within three days by increased (decreased) Tup. Table 9 also shows that in the easterly wind region, increased (decreased) easterlies, southerlies, and

horizontal wind speed were followed within 10 days by increased (decreased) T_{up} . These correlations suggest that T_{up} warmed as a result of turbulent mixing.

9. TG/U

As discussed in Chap. II, Sec. B5, TG represents the upper ocean temperature gradient. TG is the difference between SST and the temperature just above the thermocline, divided by the difference in the depths of the two temperatures. See Chap. II, Sec. B5 for an explanation of how the temperature just above the thermocline, T_{up} , was chosen. Note that a larger (smaller) TG indicates stronger (weaker) stratification of the upper ocean. The interpretation of the correlations between TG and the wind is complicated because there are three different ways TG can change: 1) SST changes, 2) T_{up} changes, or 3) both SST and T_{up} change.

For example, a decrease in TG means that the difference between the surface and deeper temperatures has decreased. This suggests that either the SST has cooled and/or T_{up} has increased. A TG decrease could be caused by several factors including: wind induced evaporation and/or entrainment, downwelling, or advection of cooler water at the surface, and/or warmer water at the T_{up} depth. A TG increase means that the SST- T_{up} difference is increasing. This could be due to SST warming and/or T_{up} cooling. A TG increase could be caused by many factors, including: buoyancy damping, upwelling, advection of warmer water at the surface, and/or advection of cooler water at depth.

a. Zonal Wind Regions Lead Correlations.

Fig. 20a shows that the TG/U lead correlations in the easterly wind region were positive [peak (.15/0), range (0 to 3)]. The positive correlations suggest that TG increased (decreased) a few days before a decrease (increase) in the easterlies. An increased (decreased) TG implies that the mixed layer was more (less) stratified. Thus the positive correlations at short leads imply that increased (decreased) stratification preceded decreased (increased) easterlies by one day to one week. These results suggest that either SST increased and/or T_{up} decreased prior to a decrease in the easterly winds. The latter process was dominant, according to Figs. 17a and 19a.

Fig. 17a shows that in the easterly wind region, SST decreased (increased) a few days before the easterlies decreased (increased). Fig. 19a shows that T_{up} decreased (increased) one day to one week prior to a decrease (increase) in the easterlies. Thus, the combined correlations indicate that in the easterly wind region, the subsurface temperature, T_{up} , cooled (warmed), leading to a stronger (weaker) stratification. This was followed, one day to one week later by a decrease (increase) in the easterlies. This suggests that an increase (decrease) in the heat content of the mixed layer resulted in an increase (decrease) in the zonal winds (easterlies) approximately one week later.

In summary, the easterly region TG/U lead correlations, along with previous results, suggest that a strongly (weakly) stratified upper ocean was associated with decreased (increased) easterlies one week later. The one week lead correlations indicate that the easterlies in this region were responding to changes in the upper ocean

stratification. This suggests that in this area, the stratification tended to significantly affect heat fluxes to the atmosphere and, thus, influenced the winds.

b. Zonal Wind Regions Lag Correlations.

Fig. 20a shows that the TG/U lag correlations in the westerly region were negative several days after a wind event [peak (-.22/-2), range (1 to -7)]. The negative correlations imply that TG decreased (increased) several days after an increase (decrease) in the westerlies.

We have seen that in the westerly wind region, an increase (decrease) in the westerlies was followed by decreased (increased) SST one to three days later (Fig. 17a), with no significant increase (decrease) of T_{up} at those lags (Fig. 19a). Thus, the decrease in TG a few days after an increase in westerlies was most likely due to shallow cooling of the surface.

Fig. 20a shows that the TG/U lag correlations in the easterly region were positive [peak (.15/-10), range (0 to -12)]. These correlations imply that TG decreased (increased) within one to two weeks after the easterly wind increased (decreased). Fig. 17a shows that SST decreased (increased) within the three weeks following increased (decreased) easterly winds. Fig. 19a shows that T_{up} slightly increased (decreased) within one to two weeks following increased (decreased) easterlies with the maximum T_{up} increase occurring at zero to three days lag. Combined, these correlations imply that the weakened (strengthened) stratification in the easterly region within one to two weeks following increased (decreased) easterlies was due both to decreased (increased) SST and increased (decreased) T_{up} . The T_{up} warming was strongest within a few days of the

easterly wind event, suggesting turbulent mixing, while the SST cooling was strongest approximately three weeks after the easterly wind event suggesting longer term processes such as advection, upwelling or downwelling. Thus the easterly region's broad correlation peak between about -18 days and 7 days (Fig. 20a) suggests that both shorter term processes (e.g., turbulent mixing, evaporative cooling) and longer term processes (e.g., advection, upwelling and downwelling) were involved in linking TG and U.

c. Easterly Wind Sub-Regions Lead Correlations.

Fig. 20d shows the TG/U correlations were positive in the varying V [peak (.23/0), range (-3 to 3)] and steady V [peak (.24/0), range (-3 to 3)] regions. The positive correlations at short leads in both the varying V and steady V region suggests that TG increased (decreased) zero days to one week before the easterly wind decreased (increased).

The only way for TG to increase is for SST to increase and/or T_{up} to decrease. Fig. 17d shows that in the varying V region SST decreased (increased) three days to a week before the easterly wind decreased (increased). Fig 19d shows that in the varying V region T_{up} decreased (increased) zero days to one week before the easterly wind decreased (increased). This implies that the decrease (increase) in T_{up} was much greater than the decrease (increase) in SST prior to a decrease (increase) in the easterlies in the varying V region.

Now consider the steady V region. Fig. 17d shows that SST increased from zero days to two weeks before the easterly wind decreased (increased). Fig. 19d shows that T_{up} decreased (increased) zero days to one week before the easterly wind

decreased (increased). Thus, the stratification changes in the upper ocean prior to a decrease (increase) in the easterlies in the steady V region were caused by an increase (decrease) in SST and a decrease (increase) in T_{up} . However, in the varying V region these stratification changes were caused by T_{up} decreasing (increasing) more than SST increased (decreased).

In summary, the TG/U lead correlations for the varying V region imply that strengthening (weakening) of the upper ocean stratification was followed, zero days to one week later, by a decrease (increase) in the easterlies. This was the same implication from the easterly wind region TG/U lead correlations. Thus, we conclude that the easterly region's TG/U lead correlations are primarily due to the varying V region buoys. In addition, we infer that the upper ocean stratification in the varying V region had a significant impact on the winds. This impact may have been exerted through the control exerted by the stratification on heat fluxes to the atmosphere.

d. Easterly Wind Sub-Regions Lag Correlations.

Fig. 20d shows that TG/U lag correlations were positive in the varying V region [peak (.25/-11), range (3 to -15)]. This implies that TG decreased (increased) three days to three weeks after the easterly wind increased (decreased). Fig. 17d shows that SST cooled (warmed) about two to three weeks after increased (decreased) easterlies in the varying V region. Fig. 19d shows that T_{up} increased (decreased) within the two weeks after the easterly wind increased (decreased). Thus, the weakened (strengthened) stratification in the varying V region within the three weeks after increased (decreased) easterlies was due both to increased T_{up} and decreased SST. Similar to the easterly

region, these correlations suggest that the maximum T_{up} warming occurred within a few days after an easterly wind event suggesting turbulent mixing, while the maximum decrease in SST occurred approximately three weeks after an easterly wind event suggesting advection, upwelling and downwelling processes.

Thus the short lag portion of the TG/U lag correlation curves imply that evaporative cooling, turbulent mixing, and/or buoyancy damping were responsible for the mixed layer temperature changes. The longer lag portion of the curves (greater than a few days) suggests that advection, upwelling and/or downwelling effects came into play. For example, an easterly wind burst might have initially lowered TG through evaporative cooling and turbulent mixing cooling SST and warming T_{up} . Then, several days later, cooler water from the east may have arrived cooling SST, having been advected from the east and/or upwelled. This hypothesis is supported by our previous discussions of Figs. 17d and 19d.

10. TG/V

a. Zonal Wind Regions Lead Correlations.

Fig. 20b shows that TG/V lead correlations were negative in the westerly [peak (-.21/4), range (-3 to 12)] and transition [peak (-.22/1), range (-3 to 7)] regions. According to Table 2, the average V component of the wind is weakly negative (northerly) in both regions. Thus, a negative correlation implies that TG decreased (increased) within about two weeks prior to increased (decreased) southerlies.

A TG decrease means that SST decreased and/or T_{up} increased. Fig. 17b shows that in the westerly wind region SST increased (decreased) within the three weeks

prior to increased (decreased) southerlies. Fig. 19b shows that in the westerly wind region T_{up} increased (decreased) within the three weeks prior to increased (decreased) southerly winds. Thus, we conclude that T_{up} increased more than SST increased. Or in other words, the subsurface temperatures experienced greater variations than did the surface ocean temperatures prior to wind events in the westerly region. Furthermore, these correlations imply that the mixed layer heat content increased (decreased) followed from zero days two weeks later by increased (decreased) southerlies with the peak correlation occurring at zero days lag. This conclusion probably holds true for the transition region as well since it had a very similar TG/V curve even though neither its SST/V lead nor T_{up}/V lead correlations were significant.

b. Zonal Wind Regions Lag Correlations.

According to Fig. 20b, the TG/V lag correlations were negative in the westerly wind region [peak (-.19/-2), range (-3 to 12)]. The average V is weakly negative (northerly) in the westerly region (Table 2). Thus, the negative correlations imply that southerlies increased (decreased) followed zero to four days later by decreased (increased) TG.

If TG decreased shortly after the southerly wind increased, then either SST decreased or T_{up} increased within the week following increased southerlies. Fig. 17b shows that in the westerly region, SST did decrease a few days after the southerlies increased. Fig. 19b shows that in the westerly region, T_{up} increased a few days after the southerlies increased. Thus, in the westerly wind region, TG decreased (increased) within the week following increased (decreased) southerlies because both SST decreased

(increased) and T_{up} increased (decreased), with the peak correlation occurring near zero days. This suggests that in the westerly region, increased (decreased) southerlies resulted in decreased (increased) SST and increased (decreased) T_{up} from zero to four days later, probably as a result of increased evaporation and turbulent mixing (buoyancy damping).

The easterly wind region TG/V lag correlations were slightly negative [peak (-.08/-11), range (-10 to -13)]. Table 2 shows that in the easterly wind region, the average meridional wind was southerly (positive). Thus, these correlations imply that TG decreased (increased) approximately one to two weeks after the southerly wind increased (decreased). A TG decrease implies that SST decreased and/or T_{up} increased. Fig. 17b shows that SST decreased (increased) after the southerly winds increased (decreased). Fig. 19b. shows no correlation between T_{up} and V in the easterly wind region. Thus, we conclude that the negative TG/V correlation in the easterly wind region was probably because SST decreased (increased) about two weeks after the southerly wind increased (decreased).

c. Easterly Wind Sub-Regions Lead Correlations.

The TG/V lead correlations were not significant in the easterly wind sub-regions.

d. Easterly Wind Sub-Regions Lag Correlations.

The TG/V lag correlations were not significant in the easterly wind sub-regions.

11. TG/M

a. Zonal Wind Regions Lead Correlations.

Fig. 20c shows that TG/M lead correlations were negative in the easterly [peak (-.25/-1), range (-3 to 8)] region. This suggests that TG decreased (increased) within the week prior to a wind event. This implies that SST decreased and/or T_{up} increased within the week prior to a wind event. Since we have already seen that SST increased within the week prior to a wind event in the easterly region (Fig. 17c), this implies that T_{up} must have increased more than SST. Fig. 19c. indicates T_{up} warmed prior to wind events in the easterly region. This suggests that in the easterly region, the mixed layer warmed and thickened within approximately a week prior to a wind event.

b. Zonal Wind Regions Lag Correlations.

Fig. 20c shows that TG/M lag correlations were negative in the westerly [peak (-.29/-2), range (-1 to -5)], and easterly [peak (-.27/-1), range (-12 to 9)] regions. This implies that TG decreased within a few days after a wind event. This suggests that SST dropped and/or the temperature at T_{up} increased. Examination of Figs. 17c and 19c indicate that both occurred. This suggests that wind events in both the easterly and westerly wind regions were associated with surface cooling and subsurface warming a few days later.

The shorter lags in the westerly wind region suggest that evaporative cooling and turbulent mixing were dominant, while the larger range of the negative lags for the transition and easterly wind regions suggest that advection and/or upwelling and downwelling were also important.

c. Easterly Wind Sub-Regions Lead Correlations.

Fig. 20f shows that TG/M lead correlations were negative in the varying V [peak (-.36/0), range (-2 to 2)], and inversion [peak (-.16/-1), range (1 to -2)] regions. This implies that TG decreased a couple of days prior to a wind event. Fig 17f shows that SST increased prior to a wind event in the varying V and inversion regions. Fig. 19f shows that Tup increased prior to a wind event in both regions. Thus, we conclude that Tup increased (decreased) more than SST increased (decreased) before a wind event in the varying V and inversion regions. Further, since Tup increased (decreased) prior to a wind event, we conclude that the mixed layer warmed and thickened a few days prior to a wind event. This suggests that the increased heat content of the ocean may have led to increased atmospheric convection which led to increased wind speeds.

d. Easterly Wind Sub-Regions Lag Correlations.

Fig. 20f shows that the TG/M lag correlations in the varying V region were negative [peak (-.36/0), range (-2 to 2)]. Fig. 20f shows that TG/M correlations in the ocean temperature inversion region were negative at short lags [peak (-.16/-1), range (-2 to 0)] and at longer lags [peak (-.15/-9), range (-7 to -11)].

Consider first the negative correlations at short lags found in the varying V and inversion regions. These imply that TG decreased (increased) within a few days after the horizontal wind increased (decreased). This means that either SST decreased and/or Tup temperatures increased a few days after a wind event (most likely an increase in the easterly winds). Fig. 17f shows that SST decreased (increased) approximately one day after the wind increased in both regions. Fig. 19f shows that Tup

increased (decreased) within a few days after the horizontal wind increased (decreased) in both regions. Thus, we conclude that the negative TG/M correlation at short lags in the varying V and inversion sub-regions was due to both decreased (increased) SST and increased (decreased) T_{up} within a few days after a horizontal wind event. This is consistent with turbulent mixing cooling SST and warming T_{up} as previously described in our simple two layer model (Chap I, Sec. B).

The negative TG/M lag correlation at longer lags in the inversion region suggests that TG decreased from one to two weeks after a wind event. TG decreases could be due to decreased SST and/or increased T_{up} . Fig. 17f shows that SST decreased at long lags in the inversion region. Fig. 19f shows that T_{up} increased in the inversion region at longer lags after a wind event. Thus, the negative TG/M lag correlations at longer lags in inversion region is due both to decreased (increased) SST and increased (decreased) T_{up} two to three weeks after increased (decreased) M.

12. Summary of TG/Wind Correlations

The TG/wind correlations suggest that: (1) mixed layer warming (cooling) was followed within one week by increased (decreased) winds, suggesting that the winds were driven by heat fluxes from the ocean; (2) increased (decreased) winds were followed within a few days by cooler (warmer) SST and warmer (cooler) T_{up} , suggesting that evaporation, turbulent mixing, and buoyancy damping were primarily responsible for the SST, T_{up} , and TG changes; and (3) the mixed layer heating prior to wind events was primarily not due to surface heating.

To elaborate, consider first the lead correlations shown in Table 6 and 7. They show that TG decreased prior to increased southerlies in the westerly and transition regions and that TG decreased prior to increased easterlies and horizontal winds in the easterly region. Table 7 shows that TG decreased prior to increased easterlies and horizontal wind speeds in the varying V region, that TG decreased prior to increased easterlies in the steady V region, and that TG decreased prior to increased horizontal wind speed in the inversion region. In general, particularly in the easterly regions, when TG decreased prior to increased winds, it was because T_{up} increased more than SST increased. Thus, the TG decreases in the lead correlations indicate that T_{up} increased more than SST increased. T_{up} increases suggest that the mixed layer warmed and thickened prior to wind events. Thus when TG changes precede the winds, TG decreases (increases) were associated with a warming and thickening (cooling and thinning) of the mixed layer.

This is different than the buoyancy damping effect discussed in the hypotheses section (Chap. I, Sec. B). The buoyancy damping effect involves heating at the ocean's surface which results in a warming and shoaling of the mixed layer. The fact that in this study the mixed layer tended to warm and thicken suggests that the mixed layer warming was not primarily due to surface heating. For the Oct. 1991-Mar. 1992 period addressed in this study, the most likely cause of this mixed layer warming and thickening was series of equatorially trapped Kelvin waves (Cooper 1992). The process is discussed further in the inversion section (Chap. III, Sec. E)

The relationship between TG variations and mixed layer variations (see above) may be used to infer relationships between the mixed layer and winds. From the TG/wind relations in Table 6, we infer that the mixed layer warmed and thickened (cooled and shoaled) from zero to 12 days prior to increased (decreased) southerlies in the westerly region. The TG/V and TG/M relations in Table 6 also suggest that the mixed layer warmed and thickened (cooled and shoaled) from zero to 9 days prior to increased (decreased) southerlies and horizontal wind speeds in the transition region. These tables also suggest that the mixed layer warmed and thickened (cooled and shoaled) zero to eight days prior to increased (decreased) easterlies, and horizontal wind speeds in the easterly region. In the easterly wind sub-regions, these mixed layer changes generally led the wind changes by just a few days (Table 7).

Next, consider the lag portions of the TG/wind correlations. Tables 8 and 9 show that wind events resulted in decreased TG in all regions. TG decreases are caused by SST decreases and/or T_{up} increases. While not shown in the tables, analyses of the correlations reveals that decreased TG in the westerly, transition, and easterly wind regions was due to both decreased SST and increased T_{up} , suggesting turbulent mixing.

13. T_{max}/U

As discussed in Chap. II, Sec. B5, T_{max} was the ocean temperature time series with the greatest variability. T_{max} was interpreted to be the temperature at the approximate depth of the thermocline.

a. Zonal Wind Regions Lead Correlations.

There were no significant Tmax/U lead correlations in the zonal wind regions.

b. Zonal Wind Regions Lag Correlations.

Fig. 21a shows that the Tmax/U lag correlations in the transition region were strongly positive [peak (.47/-6), range (-10 to 3)]. These lag correlations are part of a broad positive correlation peak that includes both lag and lead correlations. The prominent peak at a lag of six days suggests that, overall, the zonal wind leads Tmax in this region. That is, that Tmax increased (decreased) approximately one week after the westerly wind (increased).

Figs. 25c, 26c, and 27c show that, at all three transition buoys, westerly (easterly) winds were associated with warming (cooling) Tmax. Further, Figs. 25d, 25e, and 25f show that the transition region's strong positive correlations (Fig. 21a) were largely due to the strong correlations found at the two equatorial buoys (EQ 170°W and EQ 169°W). This raises the question of whether or not strong Tmax/U correlations are found at all equatorial buoys.

The only other equatorial buoys in this study that measured Tmax were at EQ 155°W and EQ 125°W. Fig. 28a shows a very strong positive Tmax/U correlation with a peak at a lag of three days at EQ 155°W. Fig 28b shows that EQ 125°W has a strong negative Tmax/U correlation with a peak at a lead of three days. Because of gaps in the time series, this last correlation was based on only 48 data days.

In the inversion section to follow (Chap. III, Sec. E) we will find that despite the fact that the winds were predominantly easterly at EQ 155°W, there were periods when relatively strong westerlies were associated with strongly increased T_{max} , which is probably what the positive T_{max}/U correlation is reflecting. Fig. 28c. shows that during the 48 day period upon which the T_{max}/U correlation was based, easterly winds were associated with warming T_{max} . Thus, we conclude that a strong T_{max}/U correlation was characteristic of all equatorial buoys. However, in the central Pacific, thermocline warming (cooling) was associated with westerlies (easterlies), while in the eastern Pacific, thermocline warming (cooling) was associated with easterlies (westerlies).

Frequent periods of strong and sustained zonal winds occurred at all the equatorial buoys (cf. Figs. 8b, 25, 26, 27, 28). This, and the fact that they are all located on the equator, suggests that these strong T_{max}/U correlations may have been due to: 1) equatorial upwelling, downwelling and/or warm water advection from the west (cf. Kousky 1991a-1992c), and/or 2) equatorially trapped Kelvin waves.

Cooper (1992) showed that the largest of these T_{max} variations was associated with Kelvin waves forced by wind events in the general vicinity of 165°E. Thus, the local zonal winds on the equator in the central Pacific probably acted to reinforce pre-existing waves rather than generate them. The waves may have, in turn, influenced the winds, as indicated by the strong positive T_{max}/U correlations at zero to five days lead (Fig. 21a, transition region curve). The large T_{max} variations associated with the Kelvin waves may have led to an increased surface heat flux to the air and subsequent increase in the winds.

c. Easterly Wind Sub-Regions Lead Correlations.

Fig. 21d shows that T_{max}/U lead correlations were negative in the varying V region [peak (-.23/4), range (3 to 7)]. This implies that T_{max} increased (decreased) one to two weeks prior to increased (decreased) easterly winds. This suggests that the mixed layer warmed and thickened in the varying V region before a zonal wind event.

d. Easterly Wind Sub-Regions Lag Correlations.

There were no significant T_{max}/U lag correlations in the easterly wind sub-regions.

14. T_{max}/V

a. Zonal Wind Regions Lead Correlations.

Fig. 21b shows that T_{max}/V lead correlations were negative in the easterly wind region [peak (-.13/1), range (-6 to 5)]. Table 2 shows that the meridional winds were southerly (positive) in the easterly wind region. Thus a negative correlation suggests that T_{max} increased (decreased) within the week prior to decreased (increased) southerly winds.

b. Zonal Wind Regions Lag Correlations.

Fig. 21b shows that T_{max}/V lag correlations were negative in the transition region [peak (-.20/-5), range (0 to -9)]. Since the average V in the inversion region is weakly northerly (negative), these correlations suggest that increased (decreased) southerlies were followed one to two weeks later by decreased (increased) T_{max} .

Fig 21b shows that in the easterly wind region the Tmax/V lag correlations were negative [peak (-.13/1), range (-6 to 5)]. This suggests that Tmax decreased (increased) zero days to one week after increased (decreased) southerly winds. The positive correlations at longer lags suggests that Tmax increased (decreased) two to three weeks after increased (decreased) southerly wind.

c. Easterly Wind Sub-Regions Lead Correlations.

Fig. 21e shows that Tmax/V lead correlations in the ocean temperature inversion region were negative [peak (-.14/11), range (9 to 15)]. This suggests that Tmax decreased (increased) one to two weeks prior to increased (decreased) southerlies.

d. Easterly Wind Sub-Regions Lag Correlations.

Fig. 21e shows that Tmax/V lag correlations were negative in the varying V [peak (-.24/4), range (-7 to 5)]. This suggests that Tmax decreased (increased) within the week following increased (decreased) southerlies.

Fig. 21e shows that Tmax/V lag correlations were positive in the inversion region [peak (.14/-20), range (-20 to -22)]. This implies that Tmax increased (decreased) about three weeks after increased (decreased) southerlies.

15. Tmax/M

a. Zonal Wind Regions Lead Correlations.

Fig. 21c shows that the Tmax/M lead correlations were positive in the easterly wind region [peak (.18/6), range (5 to 14)]. This implies that Tmax increased (decreased) a few days to two weeks prior to increased (decreased) wind. This suggests

that the mixed layer warmed and thickened a few days to two weeks prior to increased horizontal winds.

b. Zonal Wind Regions Lag Correlations.

Fig. 21c shows that Tmax/M lag correlations in the westerly wind region were negative [peak (-.19/-8), range (-11 to -4)]. This suggests that Tmax decreased (increased) one to two weeks after the wind increased (decreased). The average winds were west-northwesterly in the westerly wind region (Table 2). Thus, one might have expected that increases in M in this region would have generally produced downwelling and warming of Tmax, leading to positive Tmax/M lag correlations. The unexpected negative correlations may be due to the large Tmax depth and possible surface barrier layers in the westerly region (see Tmax/U section, above).

c. Easterly Wind Sub-Regions Lead Correlations.

Fig. 21f shows that Tmax/M correlations were positive in the varying V [peak (.27/7), range (6 to 12)] and inversion [peak (.17/13), range (12 to 15)] regions. This suggests that Tmax warmed (cooled) one to two weeks prior to an increase in the horizontal wind. This suggests that the mixed layer warmed and thickened in the varying V and inversion regions one to two weeks prior to horizontal wind events.

d. Easterly Wind Sub-Regions Lag Correlations.

Tmax/M lag correlations were not significant in the easterly wind sub-regions.

16. Summary of Tmax/Wind Correlations

As discussed in Chap. II, Sec. B5, Tmax was the ocean temperature time series with the greatest variability. Tmax was interpreted to be the temperature at the approximate depth of the thermocline.

The Tmax/wind correlations were not nearly as consistent or clear as the previous ocean/wind correlations, perhaps due to the greater depths. However, in general, they suggested that: (1) increased (decreased) Tmax was followed one to two weeks later by increased (decreased) winds; and (2) increased (decreased) winds were followed by decreased (increased) Tmax in the westerly and easterly regions and by increased (decreased) Tmax in the transition region.

Tables 6 shows that increased (decreased) Tmax led increased (decreased) westerlies by zero to three days in the transition region and increased horizontal winds by five to fourteen days in the easterly wind region. Table 7 shows that increased Tmax led increased easterlies and horizontal winds in the varying V region by about three to 12 days and that increased Tmax led increased horizontal wind speed in the inversion region by 12 to 15 days.

There were exceptions to these general patterns, all involving the meridional wind. Tmax warming (cooling) led decreased (increased) southerlies in the easterly region; specifically, in the varying V and inversion regions where the lead was zero to 15 days (Tables 6 and 7).

The most interesting correlations were found in the transition region. The Tmax/U correlations were very strong ($r = .47$) at a lag of six days. Closer inspection

revealed that this correlation was especially strong and clear at all the equatorial buoys: EQ 170°W, EQ 169°W, EQ 155°W, and EQ 125°W. At the central Pacific buoys (EQ 170°W, EQ 169°W, EQ 155°W), the correlations suggested that increased (decreased) Tmax was associated with westerlies (easterlies). Cooper (1992) determined that the large Tmax variations at these locations were due to the passage of Kelvin waves. Thus, conclusion: (3) the Tmax/U correlations were strongest on the equator and suggested that internal Kelvin waves through their impacts on the temperature and thickness of the mixed layer, influenced the local zonal winds. In the central Pacific, these locally generated zonal winds in turn resulted in downwelling (due to westerlies) or upwelling (due to easterlies) which probably reinforced the Kelvin wave.

17. SST/Tup

a Zonal Wind Regions Lead Correlations.

Fig. 22a shows that SST/Tup lead correlations were positive in the westerly [peak (.22/-3), range (-.24 to 8)], and easterly region [peak (.26/7), range (3 to 9)]. This suggests that SST increased (decreased) within about a week prior to increased (decreased) Tup. The correlations suggest that in the easterly region SST leads Tup by approximately one week.

b. Zonal Wind Regions Lag Correlations.

Fig. 22a shows that SST/Tup lag correlations in the westerly wind region were positive [peak (.22/-3), range (-.24 to 8)]. Thus, in the westerly region, SST increased (decreased) after Tup increased (decreased). In its entirety, the lead and lag

portions of the SST/Tup correlation suggest that SST and Tup variations were in phase and mutually reinforced each other.

c. Easterly Wind Sub-Regions Lead Correlations.

Fig. 22c shows that SST/Tup lead correlations were strongly positive in the varying V [peak (.30/8), range (3 to 12)] and ocean temperature inversion [peak (.50/1), range (-9 to 9)] regions. Thus, in the varying V region, SST variations led Tup variations by a few days to two weeks. In the inversion region, SST and Tup were in phase.

d. Easterly Wind Sub-Regions Lag Correlations.

Fig. 22c shows that SST/Tup lag correlations in the ocean temperature inversion region were strongly positive [peak (.50/1), range (-9 to 9)]. This suggests that SST increased (decreased) within two weeks after Tup increased.

Together, the lead and lag portions of the SST/Tup correlations for the ocean temperature inversion region (Fig. 22c) show that SST and Tup were generally in phase, with a tendency for SST to lead Tup slightly. Overall, SST and Tup seem to have mutually reinforced each other.

18. SST/Tmax

As discussed in Chap. II, Sec. B5, Tmax was the ocean temperature time series with the greatest variability. Tmax was interpreted to be the temperature at the approximate depth of the thermocline.

There were no significant SST/Tmax correlations at any lead or lag in any region.

19. SST/AT

Figs. 23a and 23c show that the SST/AT correlations were strongly positive, with peaks at approximately zero lag in all regions. This suggests that in all regions SST and AT variations were in phase and were mutually reinforcing.

20. TG/AT

a. Zonal Wind Regions Lead Correlations.

There were no significant TG/AT lead correlations in the zonal wind regions.

b. Zonal Wind Regions Lag Correlations.

Fig. 23b shows that TG/AT lag correlations were negative in the transition [peak (-.24/-12), range (-9 to -16)] and easterly wind [peak (-.19/-12), range (-9 to -14)] regions. This suggests that TG decreased approximately two weeks after AT increased (decreased). This implies that the upper ocean became less (more) stratified two weeks after AT increased (decreased).

c. Easterly Wind Sub-Regions Lead Correlations.

Fig. 23c shows that TG/AT lead correlations in the varying V region were positive [peak (.17/14), range (8 to 15)]. This suggests that TG increased (decreased) one to two weeks prior to increased (decreased) AT. This suggests that the ocean became more (less) stratified one to two weeks prior to increased (decreased) AT. There were strong correlations between warming (cooling) thermocline temperature and

increased (decreased) zonal winds at the central and eastern equatorial Pacific buoys. In the central Pacific, thermocline warming (cooling) was associated with westerlies (easterlies). This suggested that equatorially trapped Kelvin waves warmed and thickened the mixed layer, resulting in increased zonal winds. In the central Pacific, these local zonal winds then reinforced the Kelvin waves through downwelling and upwelling.

d. Easterly Wind Sub-Regions Lag Correlations.

Fig. 23d shows that TG/AT lag correlations were negative in the varying V region [peak (-.25/-11), range (-9 to -13)]. These correlations suggest that TG decreased (increased) one to two weeks after AT increased (decreased). This implies that the ocean became less (more) stratified one to two weeks after AT increased (decreased).

21. AT/M

a. Zonal Wind Regions Lead Correlations.

Fig. 24a. shows that AT/M lead correlations in the easterly wind region were strongly positive [peak (.34/0), range (-1 to 1)]. The sharp positive peak at zero lag suggests that in the easterly wind region, increased (decreased) AT was associated with increased (decreased) wind speed. This suggests that the local wind and air temperature were strongly coupled. In addition, since SST and AT had a strong positive correlation at zero lag in the easterly region (Fig. 23a), the AT/M results suggest that the local air-sea heat exchange was strongly coupled with the wind. We have found that the air is generally colder than the sea, thus when the wind comes up the air probably warms due to increased heat fluxes.

b. Zonal Wind Regions Lag Correlations.

Fig. 24a shows that AT/M lag correlations in the easterly region were positive at short lags [peak (.34/0), range (-1 to 1)] and negative at longer lags [peak (-.11/-21), range (-20 to -23)]. The negative AT/M correlations at longer lags suggests that AT decreased (increased) from one to three weeks after the horizontal wind increased (decreased). The AT/M lag correlations in the transition region were also negative but at shorter lags [peak (-.28/-6), range (-3 to -5)]. This suggests that AT decreased (increased) within a week after the horizontal wind increased (decreased) in the easterly and transition regions. This suggests that wind induced cooling (warming) of the sea surface may have also led to a cooling (warming) of the air, perhaps by persistent horizontal advection of heat in the atmosphere.

c. Easterly Wind Sub-Regions Lead Correlations.

Fig. 24c shows that AT/M in the varying V region was positively correlated at zero lag [peak (.41/0), range (-1 to 1)] and at longer leads [peak (.13/16), range (15 to 18)]. Fig. 24c shows that AT/M was positively correlated in the steady V [peak (.25/0), range (-1 to 1)], and ocean temperature inversion [peak (.31/0), range (-1 to 1)] regions. These results are similar to those for the easterly region (Fig. 24a) and indicate that increased (decreased) AT was associated with increased (decreased) wind at zero lag in all three sub-regions. The positive correlations at longer lags in the varying V region suggest that AT increased (decreased) about two weeks before the horizontal wind increased (decreased).

d. Easterly Wind Sub-Regions Lag Correlations.

Fig. 24c shows that AT/M lag correlations were positive at short lags in all three subregions: varying V [peak (.41/0), range (-1 to 1)], steady V [peak (.25/0), range (-1 to 1)], and ocean temperature inversion [peak (.31/0), range (-1 to 1)] regions. This suggests that in the easterly wind sub-regions increased (decreased) horizontal wind speeds were associated with increased (decreased) AT. One possibility is that increased (decreased) winds were associated with nearly simultaneous increases (decreases) in heating (e.g., latent heating) of the atmosphere.

At longer lags, the AT/M correlations were negative in the steady V [peak (-.26/-4), range (-2 to -6) and also peak (-.23/-22), range (-19 to -23)] and ocean temperature inversion [peak (-.16/-14), range (-13 to -15)] regions. These results suggest that AT decreased (increased) from two days to three weeks after increased (decreased) winds in the easterly wind sub-regions, with the shortest lags occurring in the steady V region. Thus, the overall implication from Fig. 24c is that stronger (weaker) winds were associated with almost simultaneous warming (cooling) of the air which was followed one to three weeks later by cooling (warming) of the air.

22. dT/M

As discussed in Chap. II, Sec. B5, dT describes the sea-air temperature difference (SST-AT).

a. Zonal Wind Regions Lead Correlations.

Fig. 24b shows that dT/M lead correlations in the westerly wind region were positive [peak (.15/4), range (3 to 6)]. This suggests that dT increased (decreased)

within a week prior to increased (decreased) horizontal wind. Since in general SST was greater than AT (Table 2), this could be due to increased SST and/or decreased AT a week prior to increased M. Fig. 17c suggests that in the westerly wind region, SST increased (decreased) prior to a wind event. Fig. 24a suggests that within the westerly wind region AT also increased within the week prior to a wind event. Thus, we conclude that the SST increased more than the AT increased a week prior to a wind event in the westerly wind region. In addition, the SST/Tup correlations (Fig. 22a) indicate that the entire upper ocean tended to warm about a week before the wind increased.

Fig. 24b shows that dT/M lead correlations in the easterly wind region were strongly negative [peak (-.42/0), range (-1 to 1)]. This suggests that decreased (increased) air-sea temperature differences were associated with nearly simultaneous increased (decreased) horizontal wind speeds. Fig. 17c shows that SST decreased within one day of increased wind in the easterly wind region. Fig. 24a shows that AT increased within one day of increased wind. Thus we conclude that in the easterly wind region, the negative dT/M correlation at zero lag was due to decreased (increased) SST and increased (decreased) AT associated with increased (decreased) wind speed at zero lag. One possible explanation of these short lag correlations is that increased (decreased) horizontal winds in the easterly wind region led to: (1) decreased (increased) SST via turbulent mixing and evaporation; and (2) increased (decreased) AT via sensible heat gain of the atmosphere at the expense of the ocean.

c. Easterly Wind Sub-Regions.

Because the dT/M correlation peak is so sharp and centered at zero lag for all the easterly regions (Fig. 24d), the lead and lag correlations are discussed together.

Fig 24d shows that the dT/M correlations in the sub-regions were very similar to the easterly wind region correlations just discussed. However, the dT/M lag correlation was negative at longer lags in the steady V region [peak (-.23/-14), range (-12 to -15)] and positive at longer lags in the inversion region [peak (.15/-13), range (-12 to -15)].

The negative correlation at longer lags in the steady V region suggests that dT decreased (increased) about two weeks after the horizontal wind increased (decreased). Comparison of Figs. 17f and 24c suggests that this decrease in dT in the steady V region was because SST decreased more than AT decreased two weeks after wind events.

The positive correlation in the inversion region suggests that dT increased (decreased) about two weeks after the horizontal wind increased (decreased). Comparison of Figs. 17f and 24c suggest that the increase in dT in the inversion region was due to decreased AT two weeks after a wind event.

23. Summary of Cross-Correlation Results

Tables 6-11 summarize all the cross-correlation results. To aid in this and all other correlation summaries, we need to explain how to read the tables. Consider the following typical entry:

SST ↑ (9 to 21) S ↑

Positive (negative) numbers in the parenthesis indicate lead (lag) in days. Up (down) arrows indicate positive (negative) change in the indicated variable. Thus, two (one) arrows in the same direction indicate the variables were positively (negatively) correlated. The wind variables have been expressed in terms of direction: W = westerlies, E = easterlies, S = southerlies, N = northerlies, M = horizontal wind speed. Thus, the above example means that SST increased 9 to 21 days before southerly winds increased.

From the SST/wind correlations came two main conclusions: (1) increased (decreased) SST was followed by increased (decreased) winds, suggesting that the winds were driven by heat fluxes from the ocean; and (2) increased (decreased) winds were followed by decreased (increased) SST within a few days, suggesting that the ocean was cooled (warmed) by evaporative cooling, and turbulent mixing (buoyancy damping).

Tables 6 and 7 show that, generally, SST warming (cooling) was followed from one to three weeks later by increased (decreased) southerlies in the westerly wind region, and by increased (decreased) easterlies, southerlies, and horizontal wind speed in the varying V region. This suggests that the winds were driven by heat fluxes from the ocean. The leads show that wind events followed warming sooner in the easterly (0 to 12 days) than the westerly region (6 to 24 days). The one exception to the above results was found in the steady V region, where increased (decreased) SST was followed within a week by decreased (increased) easterlies.

Tables 8 and 9 show that, generally, increased (decreased) winds resulted one day later in decreased (increased) SST in all regions, suggesting cooling (warming) due to increased evaporation and turbulent mixing (buoyancy damping). The tables also show

that SST changes following a wind event tended to occur over a longer range of lags in the easterly wind region (0 to 21 days) than in the westerly (0 to 3 days) or transition (0 to 9 days) regions. This may be associated with larger SST impacts in the easterly region from wind induced advection and/or upwelling.

Tup was the temperature just above the thermocline. The Tup/wind correlations led to two main conclusions: (1) Tup increased (decreased) within the week prior to increased (decreased) winds suggesting that the heat content of the mixed layer affected wind generation; this warming or cooling may have been due to Kelvin wave passage, and (2) Tup warmed (cooled) within the week after increased (decreased) winds, suggesting that turbulent mixing (buoyancy damping) warmed (cooled) Tup. The correlations suggesting warming (cooling) prior to increased (decreased) winds were much smaller than the correlations suggesting Tup warming (cooling) after increased (decreased) winds.

Table 6 shows that increased (decreased) Tup was followed by increased (decreased) southerlies in the westerly wind region, and increased (decreased) easterlies and horizontal wind in the easterly wind region. Table 7 shows that increased Tup was followed by increased easterlies and horizontal wind in the varying V region and increased easterlies in the steady V region. As seen in the SST/wind results, the lag between Tup changes and wind changes was shorter in the easterly wind region (0 to 9 days) than the westerly wind region (3 to 15 days).

Table 8 shows that in the westerly wind region, increased (decreased) southerlies were followed within three days by increased (decreased) Tup. Table 9 also

shows that in the easterly wind region, increased (decreased) easterlies, southerlies, and horizontal wind speed were followed within 10 days by increased (decreased) T_{up} . These correlations suggest that T_{up} warmed as a result of turbulent mixing.

The TG/wind correlations led to four main conclusions: (1) mixed layer warming (cooling) was followed within one week by increased (decreased) winds, suggesting that the winds were driven by heat fluxes from the ocean; (2) increased (decreased) winds were followed within a few days by cooler (warmer) SST and warmer (cooler) T_{up} , suggesting that evaporation, turbulent mixing, and buoyancy damping were primarily responsible for the SST, T_{up} , and TG changes; and (3) the mixed layer heating prior to wind events was primarily not due to surface heating.

To elaborate, consider first the lead correlations shown in Table 6 and 7. They show that TG decreased prior to increased southerlies in the westerly and transition regions and that TG decreased prior to increased easterlies and horizontal winds in the easterly region. Table 7 shows that TG decreased prior to increased easterlies and horizontal wind speeds in the varying V region, that TG decreased prior to increased easterlies in the steady V region, and that TG decreased prior to increased horizontal wind speed in the inversion region. In general, particularly in the easterly regions, when TG decreased prior to increased winds, it was because T_{up} increased more than SST increased. Thus, the TG decreases in the lead correlations indicate that T_{up} increased more than SST increased. T_{up} increases suggest that the mixed layer warmed and thickened prior to wind events. Thus, in general, TG decreases (increases) were associated with a warming and thickening (cooling and thinning) of the mixed layer.

This is different than the buoyancy damping effect discussed in the hypotheses section (Chap. I, Sec. B). The buoyancy damping effect involves heating at the ocean's surface which results in a warming and shoaling of the mixed layer. The fact that in this study the mixed layer tended to warm and thicken suggests that the mixed layer warming was not primarily due to surface heating. For the Oct. 1991-Mar. 1992 period addressed in this study, the most likely cause of this mixed layer warming and thickening was series of equatorially trapped Kelvin waves (Cooper 1992). The process is discussed further in the inversion section (Chap. III, Sec. E)

The relationship between TG variations and mixed layer variations (see above) may be used to infer relationships between the mixed layer and winds. From the TG/wind relations in Tables 6, we infer that the mixed layer warmed and thickened (cooled and shoaled) from zero to 12 days prior to increased (decreased) southerlies in the westerly region. The TG/V and TG/M relations in Table 6 also suggest that the mixed layer warmed and thickened (cooled and shoaled) from zero to 9 days prior to increased (decreased) southerlies and horizontal wind speeds in the transition region. These tables also suggest that the mixed layer warmed and thickened (cooled and shoaled) zero to eight days prior to increased (decreased) easterlies, and horizontal wind speeds in the easterly region. In the easterly wind sub-regions, these mixed layer changes generally led the wind changes by just a few days (Table 7).

Next, consider the lag portions of the TG/wind correlations. Tables 8 and 9 show that wind events resulted in decreased TG in all regions. TG decreases are caused by SST decreases and/or T_{up} increases. While not shown in the tables, analyses of the

correlations reveals that decreased TG in the westerly, transition, and easterly wind regions was due to both decreased SST and increased T_{up} , suggesting turbulent mixing.

As discussed in Chap. II, Sec. B5, T_{max} was the ocean temperature time series with the greatest variability. T_{max} was interpreted to be the temperature at the approximate depth of the thermocline.

The T_{max} /wind correlations were not nearly as consistent or clear as the previous ocean/wind correlations, perhaps due to the greater depths. However, in general, they suggested that: (1) increased (decreased) T_{max} was followed one to two weeks later by increased (decreased) winds; and (2) increased (decreased) winds were followed by decreased (increased) T_{max} in the westerly and easterly regions and by increased (decreased) T_{max} in the transition region.

Tables 6 shows that increased (decreased) T_{max} led increased (decreased) westerlies by zero to three days in the transition region and increased horizontal winds by five to fourteen days in the easterly wind region. Table 7 shows that increased T_{max} led increased easterlies and horizontal winds in the varying V region by about three to 12 days and that increased T_{max} led increased horizontal wind speed in the inversion region by 12 to 15 days.

There were exceptions to these general patterns, all involving the meridional wind. T_{max} warming (cooling) led decreased (increased) southerlies in the easterly region; specifically, in the varying V and inversion regions where the lead was zero to 15 days (Tables 6 and 7).

The most interesting correlations were found in the transition region. The T_{max}/U correlations were very strong ($r = .47$) at a lag of six days. Closer inspection revealed that this correlation was especially strong and clear at all the equatorial buoys: EQ 170°W, EQ 169°W, EQ 155°W, and EQ 125°W. At the central Pacific buoys (EQ 170°W, EQ 169°W, EQ 155°W), the correlations suggested that increased (decreased) T_{max} was associated with westerlies (easterlies). Cooper (1992) determined that the large T_{max} variations at these locations were due to the passage of Kelvin waves. Thus, conclusion: (3) the T_{max}/U correlations were strongest on the equator and suggested that internal Kelvin waves through their impacts on the temperature and thickness of the mixed layer, influenced the local zonal winds. In the central Pacific, these locally generated zonal winds in turn resulted in downwelling (due to westerlies) or upwelling (due to easterlies) which probably reinforced the Kelvin wave.

SST and T_{up} was strongly positively correlated in the ocean temperature inversion region.

There were no clear correlations between SST and T_{max} (Tables 10 and 11).

SST and AT were strongly positively correlated at zero lag in all regions (Tables 10 and 11).

In the easterly region, increased (decreased) air temperature (AT) was followed by decreased (increased) TG nine to 16 days later (Table 11).

AT and M were strongly positively correlated at zero lag in the easterly wind region (Tables 10 and 11).

The air-sea temperature difference and the wind were strongly negatively correlated at zero lag in the easterly wind region (Table 10 and 11). This means that small (large) air-sea temperature differences (SST-AT) were associated with strong (weak) winds.

E. TEMPERATURE INVERSIONS

Episodic temperature inversions were detected across the entire Pacific from 156°E to 110°W. Fig. 29 is a vertical time series depicting a typical SST inversion in Oct. 1991 at 2°S 110°W. It depicts the difference between SST and deeper depth temperatures, with only negative values being shown in order to highlight the inversions. Fig. 29 shows that the SST was cooler than the temperature at: a) 20 m for 30 days; b) 40 m for 16 days; and c) 60 m for three days.

Four buoys had persistent temperature inversions lasting more than a month: 5°N 155°W, 2°N 155°W, EQ 155°W, and 2°N 140°W. These buoys were in the ocean temperature inversion region described in Chap. II, Sec. B1. The monthly wind and OLR anomalies for much of the study period (e.g., Figs. 8, 9) show that these buoys were under a region of westerly wind and low OLR anomalies. This suggests that the inversion subregion may have had anomalously strong atmospheric convection, surface wind stress, and precipitation. In addition, the summary statistics for the inversion region (Table 2) show that the winds in the inversion region were not much less than the winds in the other regions.

In Table 5, note that despite averaging over only four buoys, the SST/wind, T_{up} /wind, TG/wind, and T_{max} /wind correlations in the inversion region were smaller than the varying V and steady V regions. It is tempting to attribute these smaller correlations to the presence of a low density barrier layer in the inversion region. However, another possible explanation is that the cross-correlations show reduced association between the ocean temperatures and the wind because, at most of the inversion buoys, high winds were associated with a deep mixed layer.

To test this second hypothesis, we examined an individual inversion event. Fig. 30 depicts the difference between SST and the temperature at various depths at EQ 155°W. From Fig. 30c we see that the inversion based on the temperature at 60 m lasted essentially the entire study period. This large and persistent difference, combined with the very small differences between SST and the temperatures at 20 and 40 m (Figs. 30a and b), suggest that there was a rapid drop in temperature between 40 and 60 m. There was a prominent period of about 25 days centered around 31 Jan. 1992 when SST was as much as 0.5°C cooler than the water between 60 m and 140 m (Figs. 30c-g).

Fig. 31 shows several cross-correlations based on the entire 183 days of raw data at EQ 155°W. These correlations, SST/M, T60/M, and (SST-T60)/M suggest that: 1) there was only a very weak correlation between SST and M; 2) T60 and M were positively correlated at 0 lag; 3) inversions (indicated by SST-T60) were associated with westerly wind events (i.e., stronger westerlies or weaker easterlies); and 4) the inversions strengthened (weakened) one day after the wind increased (decreased).

Inversions may form as a result of surface cooling and/or subsurface warming. To determine if either was the case for this inversion event, we examined the time series of SST, temperature at 140 m, zonal wind, and SST - 140 m temperature difference (Fig. 32).

Fig. 32a shows that the inversion centered near 31 Jan. 1992 was due to both a very slight drop in SST and a dramatic rise of 10°C in the temperature at 140 m. Had the SST not dropped during this period, or had the 140 m temperature not risen so much, the inversion would have been weaker or absent. Fig. 32b confirms the cross-correlation results (Fig. 31b), showing that the winds were relatively strong during this period. Thus, this pronounced inversion event was associated with increased winds, and not with weaker winds.

Cooper (1992) attributed the sharp rise in the 140 m temperature during Jan. 1992 to the passage of the downwelling phase of an equatorial Kelvin wave. He tracked the propagation of this Kelvin wave across the equatorial Pacific, from 170°W on about 19 Jan. 92 to 110°W on about 22 Feb. 92. Thus, it is unlikely that the westerly winds at or near EQ 155°W caused this deep warming. It seems more likely that deep warming due to the Kelvin wave passage resulted in increased heat flux to the atmosphere at EQ 155°W. This in turn led to enhanced convection which resulted in stronger westerly winds. The westerly winds may have reinforced the deep warming through downwelling (see the discussion in Chap. III, Sec. D, on T_{max}/U).

Despite the relatively high winds during this inversion period, the changes in SST were very small. This may have been due to a near balance between the heat lost at the

surface to the air and the heat gained at the surface from the thick underlying layer of warm water. The small SST drop that did occur led to an inversion that was sustained by the high heat content of the thick, warm mixed layer. The small SST decrease and the relatively strong winds during this inversion period indicate that the heat flux from the ocean remained relatively constant and high throughout the inversion period.

Thus, there seem to have been two key factors involved in producing this pronounced inversion: 1) warming and thickening of the mixed layer associated with the downwelling phase of an equatorial Kelvin wave; and 2) slight surface cooling associated with strong westerly winds.

The development of the westerlies may be tied to the Kelvin wave, as discussed in the TG/wind and Tmax/wind sections of Chap. III. Thus, this inversion event may be linked in part to the westerly winds in the western Pacific which initiated the Kelvin wave (cf. Cooper 1992).

According to Elsberry et al. (1987), two primary climatological criteria for tropical cyclone formation are: 1) warm SSTs coupled with a deep ocean mixed layer; and 2) significant positive values of absolute vorticity in the lower troposphere.

Fig. 32a shows that the first criterion was satisfied during this inversion period. The SST was consistently above 29.2°C. In addition, the mixed layer was very warm and thick, as indicated by the 140 m temperature (Fig. 32).

The second criterion was satisfied by the strong westerly winds at the equator and weaker westerlies or easterlies north of the equator. As seen in the time series of raw zonal wind at EQ 155°W (Fig. 29), the period of strong westerlies at EQ 155°W around

29 Jan. 92, corresponded to weak westerlies or easterlies at 5°N EQ 155°W. This wind shear created a region of positive vorticity just north of the equator. (Note: App. C1 shows strong westerlies south of the equator at this time at 5°S 155°W).

In fact, a tropical cyclone did form over this inversion at about 4°N 154°W. The development of this tropical cyclone is shown in infrared (IR) satellite images from 25, 27, and 30 Jan. 1992 (Figs. 33-35). Note that on 27 Jan. 1993 there were high clouds, indicating deep convection and heavy precipitation near EQ 155°W, with cyclonic features just to the north. The average surface winds on 27 Jan. 1993 (Fig. 32b) were about 9.3 m/s, the strongest measured at this buoy during the six month study period. An animated sequence of IR images for the end of Jan. and beginning of Feb. 1992 (not shown) shows that the intense convection and cyclonic system shown in Figs. 33-35 near 155°W were the initial stages of hurricane Ekeka. The first warning on this storm was issued on 28 Jan. 1992 at 06 UTC, with the center located at 4.5°N, 157°W. This storm tracked westward to 6.5°N 150°E on 08 Feb. 1992.

Thus, the strong heat fluxes in part made possible by this inversion appear to have contributed to the development of a tropical cyclone north of the equator. This storm may therefore be linked to the equatorial Kelvin wave and the pronounced subsurface heat content in the western Pacific maintained by the wave (cf. Cooper 1992).

IV. CONCLUSIONS AND RECOMMENDATIONS

A. CONCLUSIONS

This study investigated air-sea interaction patterns in the tropical Pacific using equatorial Pacific buoy data. It addressed two principal questions:

- 1) What are the observed relationships among sea surface temperature (SST), subsurface ocean temperatures, air temperature, and wind, and how do these relationships vary regionally?
- 2) What evidence is there of ocean temperature inversion regions, and, if found, how are these inversions related to specific air-sea interaction processes? These issues were studied using time series and statistical analyses of observational atmosphere and ocean data from the moored buoys of the Tropical Oceans-Global Atmosphere (TOGA) program during the 1991-1992 ENSO.

The chief techniques used were sequential scatterplots, to study specific wind/ocean interaction events, and cross-correlations, to study average interaction patterns. The buoys were grouped into six regions based on predominant wind directions and the individual buoy correlations were averaged for each of these region. Regional averaging helped bring out strong patterns that were widespread over certain regions. However, it may also have obscured some patterns, since the grouping of buoys was not necessarily optimal for all relationships.

The 18 main relationships or patterns suggested were:

From sequential scatterplots:

1. The heat content of the mixed layer strongly affected how the SST responded to wind forcing. Consequently, to determine the SST response to the wind, it may be necessary to know how the mixed layer evolved prior to a wind event. This, in turn, requires knowing the recent history of air-sea interactions and how they have preconditioned the depth and temperature of the mixed layer.

From cross-correlations:

2. In most regions, increased (decreased) SST was followed within a week by increased (decreased) detrended winds, suggesting that the wind variations were driven by variations in heat fluxes from the ocean. Additionally, we found that both T_{up} , the temperature at the base of the mixed layer, and T_{max} , the temperature at the thermocline, increased (decreased) within the week prior to increased winds suggesting that the heat content of the mixed layer affected wind generation.

3. In all regions, increased (decreased) winds were followed by decreased (increased) SST within a few days, suggesting evaporative cooling and turbulent mixing (buoyancy damping) forced the cooling (warming).

These last two points suggest the following negative feedback cycle: SST warming generated a wind event, which led, about a day later, to SST cooling.

4. Points 2 and 3 exhibited strong regional dependence. Typically, wind events followed warming sooner in the easterly region (0 to 12 days) than the westerly region (6 to 24 days). In the easterly region, SST cooling following wind events typically

lasted over a larger range of lags (0 to 21 days). The correlations suggested that the longer range in the easterly region may be due to advection.

5. Typically, T_{up} warmed (cooled) within the week after increased (decreased) winds, suggesting that turbulent mixing (buoyancy damping) warmed (cooled) T_{up} .

6. In most regions, an increase (decrease) in SST prior to wind events was associated with increased (decreased) T_{up} and T_{max} suggesting a thickening and warming of the mixed layer and suggesting that ocean warming or cooling was due to internal waves. If the ocean warming had been due to surface fluxes (buoyancy damping) we would have expected to see a shoaling of the mixed layer.

7. In general, increased (decreased) winds were followed by decreased (increased) T_{max} in the westerly and easterly regions.

8. T_{max}/U correlations were strongest on the equator and suggested that equatorially trapped Kelvin waves caused a warming and thickening (cooling thinning) of the mixed layer which was followed by increased (decreased) zonal winds. In the central Pacific, these locally generated zonal winds in turn resulted in downwelling or upwelling which reinforced the Kelvin wave.

9. SST and T_{up} were strongly positively correlated in the ocean temperature inversion region.

10. There were no clear correlations between SST and T_{max} (the thermocline temperature).

11. SST and air temperature (AT) were strongly positively correlated at zero lag in all regions. SST was almost always warmer than AT.

12. AT and wind speed (M) were strongly positively correlated at zero lag in the easterly wind region.

13. The sea-air temperature difference and the wind were strongly negatively correlated at zero lag in the easterly wind region. This means that a small sea-air temperature difference (SST-AT) was associated with increased winds, due to increased fluxes.

14. In the easterly region, increased (decreased) AT was followed by decreased (increased) TG about one to two weeks later.

From studying inversions:

15. Short duration ocean temperature inversions were found across the entire equatorial Pacific.

16. An area of strong and persistent ocean temperature inversions was identified in the central equatorial Pacific. It was associated with relatively strong winds, a thick warm mixed layer, and deep atmospheric convection.

17. The ocean temperature/wind correlations were generally weaker in the persistent inversion areas than elsewhere. We suspect that these weak ocean temperature/wind correlations were not due to a "barrier layer" effect, as suggested by Lukas and Webster (1992), but rather, that the high heat content of the deep mixed layer prevented the wind from strongly affecting ocean temperatures.

18. In studying one pronounced inversion event in detail, we noted that intense atmospheric convection was associated with a thick warm mixed layer, which itself was associated with the passage of the downwelling phase of a Kelvin wave. This incident

suggested a hypothetical remote forcing feedback process depicted in Fig. 37. In this process, tropical cyclones in the west Pacific generate equatorial Kelvin waves which travel slowly eastward across the Pacific (e.g., Cooper 1992). These waves warm and thicken the mixed layer, and thus contribute to the generation of equatorial winds. These winds, and the thick warm mixed layer, create conditions favorable for tropical cyclone formation. Tropical cyclones form just north or south of the inversion area and travel back to the west Pacific, influencing the ocean along the way.

B. RECOMMENDATIONS

This study could be improved through the use of longer and more complete data sets. Gaps in the data complicated the analyses, and the short record length limited our confidence in the correlations. The analysis of non-El Niño periods and periods when equatorial Kelvin waves were less active would be especially useful in testing the conclusions of this study.

The complex relationships identified in this work highlighted the need for using additional fields, such as currents, radiation, and salinity, when studying tropical air-sea interactions.

Our results indicate that the heat content of the mixed layer, and not just SST, is critical to understanding air-sea interactions. Mixed layer heat content was inferred in this study by examining the difference between SST and deeper depth temperatures. This study could be improved by explicitly calculating the mixed layer heat content and calculating diagnostic quantities from it.

Sequential scatterplots were introduced and found to be a useful analysis tool. The technique could be enhanced through automation. Programs could be written to automatically assign SST/wind or other relationships into categories based on event characteristics. Histograms of the category frequencies could be made. Automation would also allow a way to quantify the sequences of categories, enabling a study of the history of the processes which precondition the mixed layer.

Ocean temperature inversions require more research. This study focused on one strong and intriguing event. Future studies should examine more cases, especially cases occurring during non-El Niño periods.

The remote feedback mechanism proposed in this thesis between Kelvin waves and tropical cyclones should be investigated further. How often and in what regions does it apply? A preliminary investigation has shown that several tropical cyclones during the study period might have been associated with Kelvin wave induced thickening and warming of the mixed layer. Could the identification of equatorially trapped Kelvin waves be used to help predict tropical cyclone formation? More generally, could more careful and regular analyses of mixed layer heat content be useful in forecasting the development and evolution of tropical cyclones?

Finally, the results of this thesis may be useful in improving and verifying the Navy's upper ocean analysis system [Optimum Thermal Interpolation System, (OTIS)] and prediction model [Thermal Ocean Prediction System, (TOPS)].

LIST OF REFERENCES

Box, G.E.P., and G.M. Jenkins, 1976: *Time Series Analysis, Forecasting and Control*, revised edition. Holden-Day, 575 pp.

Cechet, R.P., 1993: Diurnal SST cycle in the western equatorial Pacific: measurements made aboard the R/V Franklin during TOGA-COARE and pre-COARE cruises. *Proceedings of Fourth International Conference on Southern Hemisphere Meteorology and Oceanography*, Hobart, Australia, March 1993, 267 pp.

Cooper, G. A., 1992: *An Observational Study of the Local and Remote Response of the Equatorial Pacific to Westerly Wind Events During the 1991-92 El Niño*. Masters of Science Thesis, Naval Postgraduate School, Monterey, CA 93943, 103 pp.

Elsberry, R. L., W. Frank, G. Holland, J. Jarrell, and R. Southern, 1987: *A Global View of Tropical Cyclones*, ONR, 185 pp.

Kousky, V.E., 1991a: *Climate Diagnostics Bulletin* (October). Climate Analysis Center, U.S. Department of Commerce, Washington, D.C., No.91/10.

-----, 1991b: *Climate Diagnostics Bulletin* (November). Climate Analysis Center, U.S. Department of Commerce, Washington, D.C., No.91/11.

-----, 1991c: *Climate Diagnostics Bulletin* (December). Climate Analysis Center, U.S. Department of Commerce, Washington, D.C., No.91/12.

-----, 1992a: *Climate Diagnostics Bulletin* (January). Climate Analysis Center, U.S. Department of Commerce, Washington, D.C., No.92/1.

-----, 1992b: *Climate Diagnostics Bulletin* (February). Climate Analysis Center, U.S. Department of Commerce, Washington, D.C., No.92/2.

-----, 1992c: *Climate Diagnostics Bulletin* (March). Climate Analysis Center, U.S. Department of Commerce, Washington, D.C., No.92/3.

Lindstrom, E., R. Lukas, R. Fine, E. Firing, S. Godfrey, G. Meyers, and M. Tsuchiya, 1987: The western equatorial Pacific ocean circulation study. *Nature*, **330**, 533-537.

Lukas, R. and E. Lindstrom, 1991: The mixed layer of the western equatorial Pacific ocean. *J. Geophys. Res.*, **6**, supplement, 3343-3357.

Lukas, R. and P. Webster, 1992: TOGA COARE the coupled ocean-atmosphere response experiment. *Bull. Amer. Meteor. Soc.*, **73**, 1377-1416.

Makridakis, S. and S. Wheelwright, 1987: *The Handbook of Forecasting: A Manager's Guide*. Wiley, New York, 638 pp.

McPhaden, M., S. Hayes, 1991: On the variability of winds, sea surface temperature, and surface layer heat in the western Equatorial Pacific. *J. Geophys. Res.*, **6**, supplement, 3331-3342.

McPhaden, M., S. Hayes, L. Mangum, and J. Toole, 1990: Variability in the western equatorial Pacific during the 1986-87 El Niño/Southern Oscillation event. *J. Phys. Oceanogr.*, **20**, 190-208.

Meyers, G. J. Donguy, and R. Reed, 1986: Evaporative cooling of the western equatorial Pacific Ocean by anomalous winds. *Nature*, **323**, 523-526.

Niller, P., E. Kraus, 1977: One dimensional models of the upper ocean. *Modelling and Prediction of the Upper Layers of the Ocean*. E. Kraus editor, 143-172, Pergamon, New York.

Ravier-Hay, P., and J. Godfrey, 1993: A model of diurnal changes in sea surface temperature for the western equatorial Pacific. *TOGA Notes*, **11**, 5-8.

Spiegel, M.R. 1991: *Schaum's Outline of Theory and Problems of Probability and Statistics*, McGraw Hill, 372 pp.

Trenberth, K.E. 1984: Some effects of finite sample size and persistence on meteorological statistics. Part I: Autocorrelations. *Mon. Weath. Rev.*, **112**, 2359-2368.

Walpole, R.E., and R. Meyers, 1985: *Probability and Statistics for Engineers and Scientists*. MacMillan, 639 pp.

Webster, P.J., and R. Lukas, 1992: TOGA COARE: the coupled ocean atmosphere experiment. *Bull. Amer. Meteor. Soc.*, **73**, 1377-1416.

TABLES

Table 1. Data record lengths for each buoy. Dashes indicate the presence of data. Blanks represent gaps in the data (from Cooper 1992).

	OCT	NOV	DEC	JAN	FEB	MAR
ATLAS 2N156E						
U-wind	-----	-----	-----	-----	-----	-----
V-wind	-----	-----	-----	-----	-----	-----
SST	-----	-----	-----	-----	-----	-----
T100m	-----	-----	-----	-----	-----	-----
T150m	-----	-----	-----	-----	-----	-----
ATLAS 2S156E						
U-wind	-----	-----	-----	-----	-----	-----
V-wind	-----	-----	-----	-----	-----	-----
SST	-----	-----	-----	-----	-----	-----
T100m	-----	-----	-----	-----	-----	-----
T150m	-----	-----	-----	-----	-----	-----
ATLAS 2N165E						
U-wind	-----	-----	-----	-----	-----	-----
V-wind	-----	-----	-----	-----	-----	-----
SST	-----	-----	-----	-----	-----	-----
T100m	-----	-----	-----	-----	-----	-----
T150m	-----	-----	-----	-----	-----	-----
EPOCS 00165E						
U-wind	-----	-----	-----	-----	-----	-----
V-wind	-----	-----	-----	-----	-----	-----
SST	-----	-----	-----	-----	-----	-----
U-Current	-----	-----	-----	-----	-----	-----
ATLAS 2S165E						
U-wind	-----	-----	-----	-----	-----	-----
V-wind	-----	-----	-----	-----	-----	-----
SST	-----	-----	-----	-----	-----	-----
T100m	-----	-----	-----	-----	-----	-----
T150m	-----	-----	-----	-----	-----	-----

Table 1. (Continued).

	OCT	NOV	DEC	JAN	FEB	MAR
ATLAS 00169W						
U-wind	-----	-----	-----	-----	-----	-----
V-wind	-----	-----	-----	-----	-----	-----
SST	-----	-----	-----	-----	-----	-----
T100m	-----	-----	-----	-----	-----	-----
T150m	-----	-----	-----	-----	-----	-----
ATLAS 00170W						
U-wind				-----	-----	-----
V-wind				-----	-----	-----
SST				-----	-----	-----
T100m				-----	-----	-----
T150m				-----	-----	-----
ATLAS 00155W						
U-wind	-----	-----	-----	-----	-----	-----
V-wind	-----	-----	-----	-----	-----	-----
SST	-----	-----	-----	-----	-----	-----
T100m	-----	-----	-----	-----	-----	-----
T140m	-----	-----	-----	-----	-----	-----
ATLAS 2N140W						
U-wind	-----	-----	-----	-----	-----	-----
V-wind	-----	-----	-----	-----	-----	-----
SST	-----	-----	-----	-----	-----	-----
T100m	-----	-----	-----	-----	-----	-----
T140m	-----	-----	-----	-----	-----	-----
EPOCS 00140W						
U-wind	-----	-----	-----	-----	-----	-----
V-wind	-----	-----	-----	-----	-----	-----
SST	-----	-----	-----	-----	-----	-----
U-current	-----	-----	-----	-----	-----	-----

Table 1. (Continued).

	OCT	NOV	DEC	JAN	FEB	MAR
ATLAS 2S140W						
U-wind	-----		-----	-----	-----	-----
V-wind	-----		-----	-----	-----	-----
SST	-----		-----	-----	-----	-----
T100m	-----		-----	-----	-----	-----
T140m	-----		-----	-----	-----	-----
ATLAS 00124W						
U-wind	-----	-----	-----	-----	-----	-----
V-wind	-----	-----	-----	-----	-----	-----
SST			-----	-----	-----	-----
T100m			-----	-----	-----	-----
T140m			-----	-----	-----	-----
ATLAS 2N110W						
U-wind		-----	-----	-----	-----	-----
V-wind		-----	-----	-----	-----	-----
SST		-----	-----	-----	-----	-----
T100m		-----	-----	-----	-----	-----
T140m		-----	-----	-----	-----	-----
EPOCS 00110W						
U-wind	-----	-----	-----	-----	-----	-----
V-wind	-----	-----	-----	-----	-----	-----
SST	-----	-----	-----	-----	-----	-----
U-current	-----	-----	-----	-----	-----	-----
ATLAS 2S110W						
U-wind	-----	-----	-----	-----	-----	-----
V-wind	-----	-----	-----	-----	-----	-----
SST	-----	-----	-----	-----	-----	-----
T100m	-----	-----	-----	-----	-----	-----
T140m	-----	-----	-----	-----	-----	-----

Table 2. Summary statistics for each of the six wind regions: a) westerly, b) transition, c) easterly, d) varying V, e) steady V, c) ocean temperature inversion. Westerly and southerly winds are positive

a

WESTERLY WIND REGION					
Statistic	U m/s	V m/s	M m/s	SST °C	AT °C
Average	2.3	-0.8	4.6	29.3	27.7
Mode	1.6	-1.3	2.4	29.3	28.0
Variance	10.5	10.5	5.4	0.2	0.3
Minimum	-4.2	-7.5	0.5	28.5	26
Maximum	10.4	8.2	11.4	30.2	28.8

b

TRANSITION REGION					
Statistic	U m/s	V m/s	M m/s	SST °C	AT °C
Average	-0.3	-0.9	4.4	29.2	28.6
Mode	0.1	-1.3	1.8	29.0	28.6
Variance	12.6	9.9	4.1	0.1	0.4
Minimum	-7.0	-6.8	0.3	28.4	25.0
Maximum	7.2	6.5	8.9	30.0	29.8

c

EASTERLY WIND REGION					
Statistic	U m/s	V m/s	M m/s	SST °C	AT °C
Average	-4.2	0.7	5.4	27.6	26.9
Mode	-4.6	0.9	5.3	27.6	27.0
Variance	5.1	5.4	2.7	0.6	0.6
Minimum	-8.2	-5.5	0.8	26.2	24.9
Maximum	3.4	5.8	9.0	29.2	28.5

Table 2. (Continued).

d

VARYING MERIDIONAL WIND (V) REGION					
Statistic	U m/s	V m/s	M m/s	SST °C	AT °C
Average	-4.4	0.1	5.4	27.8	27.1
Mode	-5.0	0.5	5.2	28.1	27.3
Variance	5.5	4.9	2.5	0.3	0.5
Minimum	-8.1	-6.0	0.9	26.6	25.2
Maximum	3.9	5.1	8.9	29.3	28.6

e

STEADY MERIDIONAL WIND (V) REGION					
Statistic	U m/s	V m/s	M m/s	SST °C	AT °C
Average	-4.4	3.0	5.7	25.7	25.4
Mode	-4.6	3.3	6.1	25.3	25.3
Variance	2.1	3.0	1.6	1.5	1.2
Minimum	-7.3	-2.6	0.9	23.4	23.3
Maximum	1.0	6.6	8.2	28.3	27.6

f

OCEAN TEMPERATURE INVERSION REGION					
Statistic	U m/s	V m/s	M m/s	SST °C	AT °C
Average	-3.8	-0.5	5.2	28.7	27.8
Mode	-3.93	-0.23	5.0	28.6	27.8
Variance	6.6	7.8	3.8	0.2	0.4
Minimum	-8.9	-6.9	0.7	27.8	25.7
Maximum	4.5	6.3	9.7	29.7	29.1

Table 3. 95% significance limits for regional average SST/U cross-correlations. If a correlation falls within the limits, the null hypothesis $r = 0$ cannot be rejected. Total Data days are the total number of days upon which the correlations were based. Because sequential days in each time series were not independent, the number of effectively independent days, n , was calculated according to Trenberth (1984). The n values were then used to find the significance limits.

95% SIGNIFICANCE LIMITS FOR SST/U CROSS-CORRELATIONS			
Wind Region	Total Data Days	n	Limits at Lag = 0
westerly	583	125	+/- .18
transition	293	72	+/- .23
easterly	1,832	539	+/- .08
varying V	773	183	+/- .15
steady V	406	149	+/- .16
inversion	653	207	+/- .14

Table 4. Summary of largest lag and lead cross-correlations for lags up to 24 days for the three zonal wind regions. Results are displayed as correlation/lag. Lags are in days. A negative lag means that variations in the first term (e.g., SST in SST/U) came after variations in the second. A positive lag (lead) means that variations in the first term came before variations in the second. Normally, each table entry consists of the strongest lead and lag value. Entries with fewer than two correlations are due to insignificant correlations. Some entries have a third significant correlation of interest, not necessarily a maximum or minimum. All values listed are non-zero at 95% significance. Dashes indicate no significant correlation found.

Relation	Westerly	Transition	Easterly
SST/U	-.37/-5	-	-.10/4
SST/V	.23/11	-	-.11/-13
SST/M	-.47/-1	-.23/-1	-.17/-17 -.15/-1 .10/3
U/V	.36/1	-.22/-3 -.2/7	-.11/7
Tup/U	-	-	-.17/3
Tup/V	.19/-1 .24/3	-	-
Tup/M	-	-	.19/5
TG/U	-.22/-2	-	.15/-10 .15/0
TG/V	-.19/-2 -.21/4	-.22/1	-.08/-11
TG/M	-.29/-2	-	-.25/-1
Tmax/U	-	.47/-6	-
Tmax/V	-	-.20/-5	-.13/1
Tmax/M	-.19/-8	-	.18/6
SST/Tup	.22/-3	-	.26/7
SST/Tmax	-	-	-
SST/AT	.28/-1	.41/-1	.43/0
TG/AT	-	-.24/-12	-.19/-12
AT/M	-	-	-.11/-21 .34/0
dT/M	-.19/-2 .15/4	-	-.42/0

Table 5. Same as Table 4 except for the three sub-regions of the easterly wind region.

Relation	Vary. V	Steady V.	T. Inversion
SST/U	-.23/3	.32/-4	-
SST/V	-.16/-12 .16/12	-	-
SST/M	-.20/-17 -.15/-1 .20/4	-.21/-2 -.27/-14	-
U/V	-.16/5	-.26/-16 .24/0	.13/-9 -.15/7
Tup/U	-.24/2	-.26/0	-
Tup/V	-	-	-
Tup/M	.29/5	-	-
TG/U	.25/-11 .23/0	.24/0	-
TG/V	-	-	-
TG/M	-.36/0	-	-.15/-9 -.16/-1
Tmax/U	-.23/4	-	-
Tmax/V	-.24/-4	-	.14/-20 -.14/11
Tmax/M	.27/7	-	.17/13
SST/Tup	.30/8	-	.50/1
SST/Tmax	-	-	-
SST/AT	.36/0	.56/0	.43/0
TG/AT	-.25/-11 .17/14	-	-
AT/M	.41/0 .13/16	-.23/-22 -.26/-4 .25/0	-.16/-14 .31/0
dT/M	-.44/0	-.23/-14 -.41/0	.15/-13 -.41/0

Table 6. Summary of cross-correlation leads for ocean temperature/wind relations in the zonal wind regions. Positive (negative) numbers in parentheses indicate lead (lag) in days. Up (down) arrows indicate positive (negative) change in indicated variable. Thus, two (one) arrows in the same direction indicate the correlated variables were positively (negatively) correlated. Dashes indicate no significant correlation found. The wind variables have been expressed in terms of directions: W = westerlies, E = easterlies, S = southerly, N = northerly, M = horizontal wind speed. Example, the SST/V entry in the westerly column indicates SST increased 9 to 21 days before southerly winds increased. (See Chap. III, Sec. D, for more information.)

Relation	Westerly	Transition	Easterly
SST/U	-	-	SST ↑ (3 to 9) E ↑
SST/V	SST ↑ (9 to 21) S ↑	-	-
SST/M	-	-	SST ↑ (2 to 12) M ↑
Tup/U	-	-	Tup ↑ (0 to 7) E ↑
Tup/V	Tup ↑ (3 to 15) S ↑	-	-
Tup/M	-	-	Tup ↑ (0 to 9) M ↑
TG/U	-	-	TG ↑ (0 to 3) E ↓
TG/V	TG ↑ (-3 to 12) S ↓	TG ↑ (-3 to 7) S ↓	-
TG/M	-	-	TG ↑ (-3 to 8) M ↓
Tmax/U	-	Tmax ↑ (-10 to 3) W ↑	-
Tmax/V	-	-	Tmax ↑ (-6 to 5) S ↓
Tmax/M	-	-	Tmax ↑ (5 to 14) M ↑

Table 7. Summary of cross-correlation leads for ocean temperature/wind relations in the easterly wind sub-regions; otherwise, the same as Table 6.

Relation	Varying V	Steady V	Inversion
SST/U	SST ↑ (2 to 9) E ↑	SST ↑ (0 to 6) E ↓	-
SST/V	SST ↑ (9 to 14) S ↑	-	-
SST/M	SST ↑ (2 to 10) M ↑	-	-
Tup/U	Tup ↑ (-12 to 9) E ↑	Tup ↑ (-6 to 9) E ↑	-
Tup/V	-	-	-
Tup/M	Tup ↑ (0 to 8) M ↑	-	-
TG/U	TG ↑ (-3 to 3) E ↓	TG ↑ (-3 to 3) E ↓	-
TG/V	-	-	-
TG/M	TG ↑ (-2 to 2) M ↓	-	TG ↑ (1 to -2) M ↓
Tmax/U	Tmax ↑ (3 to 7) E ↑	-	-
Tmax/V	Tmax ↑ (-7 to 5) S ↓	-	Tmax ↑ (9 to 15) S ↓
Tmax/M	Tmax ↑ (6 to 12) M ↑	-	Tmax ↑ (12 to 15) M ↑

Table 8. Summary of cross-correlation lags for ocean temperature/wind relations in the zonal wind regions, otherwise; the same as Table 6.

Relation	Westerly	Transition	Easterly
SST/U	W ↑ (-1 to -7) SST ↓	-	-
SST/V	-	-	S ↑ (-9 to -20) SST ↓
SST/M	M ↑ (0 to -3) SST ↓	M ↑ (0 to -9) SST ↓	M ↑ (0 to -21) SST ↓ M ↑ (-15 to -18) SST ↓
Tup/U	-	-	-
Tup/V	S ↑ (0 to -3) Tup ↑	-	-
Tup/M	-	-	-
TG/U	W ↑ (-1 to -7) TG ↓	-	E ↑ (0 to -12) TG ↓
TG/V	S ↑ (-3 to 12) TG ↓	S ↑ (-3 to 7) TG ↓	S ↑ (-10 to -13) TG ↓
TG/M	M ↑ (-1 to -5) TG ↓	-	M ↑ (-3 to 7) TG ↓
Tmax/U	-	W ↑ (-10 to 3) Tmax ↑	-
Tmax/V	-	S ↑ (0 to -9) Tmax ↓	S ↑ (-6 to 5) Tmax ↓
Tmax/M	M ↑ (-11 to 4) Tmax ↓	-	-

Table 9. Summary of cross-correlation lags for ocean temperature/wind relations in the easterly wind sub-regions, otherwise; the same as Table 6.

Relation	Varying V	Steady V	Inversion
SST/U	E ↑ (-9 to -21) SST ↓	E ↑ (6 to -12) SST ↓	-
SST/V	S ↑ (-11 to -18) SST ↓	S ↑ (12 to -24) SST ↓	-
SST/M	M ↑ (-1 to -19) SST ↓	M ↑ (-1 to -22) SST ↓	M ↑ (0 to -3) SST ↓
Tup/U	E ↑ (9 to -12) Tup ↑	E ↑ (9 to -6) Tup ↑	-
Tup/V	-	S ↑ (-8 to -24) Tup ↑	-
Tup/M	M ↑ (0 to -5) Tup ↑	-	M ↑ (-8 to -10) Tup ↑
TG/U	E ↑ (3 to -15) TG ↓	E ↑ (3 to -15) TG ↓	-
TG/V	-	S ↑ (-12 to -24) TG ↓	-
TG/M	M ↑ (2 to -2) TG ↓	M ↑ (0 to 2) TG ↓	M ↑ (0 to -2) TG ↓ M ↑ (-7 to -11) TG ↓
Tmax/U	-	E ↑ (-8 to -10) Tmax ↓	-
Tmax/V	S ↑ (5 to -7) Tmax ↓	-	S ↑ (-20 to -22) Tmax ↓
Tmax/M	-	-	-

Table 10. Summary of a) zonal wind region's and b) easterly wind sub-region's lead cross-correlations for the remainder of the investigated relations; otherwise, the same as Table 6.

a

Relation	Westerly	Transition	Easterly
SST/Tup	SST ↑ (-24 to 8) Tup ↑	-	SST ↑ (3 to 9) Tup ↑
SST/Tmax	-	-	-
SST/AT	SST ↑ (-1 to 1) AT ↑	SST ↑ (-1 to 1) AT ↑	SST ↑ (-1 to 1) AT ↑
TG/AT	-	-	-
AT/M	-	-	AT ↑ (-1 to 1) M ↑
dT/M	dT ↑ (3 to 6) M ↑	-	dT ↑ (-1 to 1) M ↓

b

Relation	Varying V	Steady V	Inversion
SST/Tup	SST ↑ (3 to 12) Tup ↑	-	SST ↑ (-9 to 9) Tup ↑
SST/Tmax	-	-	-
SST/AT	SST ↑ (-1 to 1) AT ↑	SST ↑ (-1 to 1) AT ↑	SST ↑ (-1 to 1) AT ↑
TG/AT	TG ↑ (8 to 15) AT ↑	-	-
AT/M	AT ↑ (-1 to 1) M ↑ AT ↑ (15 to 18) M ↑	AT ↑ (-1 to 1) M ↑	AT ↑ (-1 to 1) M ↑
dT/M	dT ↑ (-1 to 1) M ↓	dT ↑ (-1 to 1) M ↓	dT ↑ (-1 to 1) M ↓

Table 11. Summary of a) zonal wind region's and b) easterly wind sub-region's lag cross-correlations for the remainder of the investigated relations; otherwise, the same as Table 6.

a

Relation	Westerly	Transition	Easterly
SST/Tup	Tup ↑ (-24 to 8) SST ↑	-	-
SST/Tmax	-	-	-
SST/AT	AT ↑ (-1 to 1) SST ↑	AT ↑ (-1 to 1) SST ↑	AT ↑ (-1 to 1) SST ↑
TG/AT	-	AT ↑ (-9 to -16) TG ↓	AT ↑ (-9 to -14) TG ↓
AT/M	-	-	M ↑ (-1 to 1) AT ↑ M ↑ (-20 to -23) AT ↓
dT/M	-	-	M ↑ (-1 to 1) dT ↓

b

Relation	Varying V	Steady V	Inversi:
SST/Tup	-	-	Tup ↑ (9 to -9) SST ↑
SST/Tmax	-	-	-
SST/AT	AT ↑ (1 to -1) SST ↑	AT ↑ (1 to -1) SST ↑	AT ↑ (1 to -1) SST ↑
TG/AT	AT ↑ (-9 to -13) TG ↓	-	AT ↑ (-6 to -12) TG ↓
AT/M	M ↑ (1 to -1) AT ↑	M ↑ (1 to -1) AT ↑ M ↑ (-2 to -6) AT ↓ M ↑ (-19 to -23) AT ↓	M ↑ (1 to -1) AT ↑ M ↑ (-13 to -15) AT ↓
dT/M	M ↑ (1 to -1) dT ↓	M ↑ (1 to -1) dT ↓ M ↑ (-12 to -15) dT ↓	M ↑ (1 to -1) dT ↓ M ↑ (-12 to -15) dT ↑

FIGURES

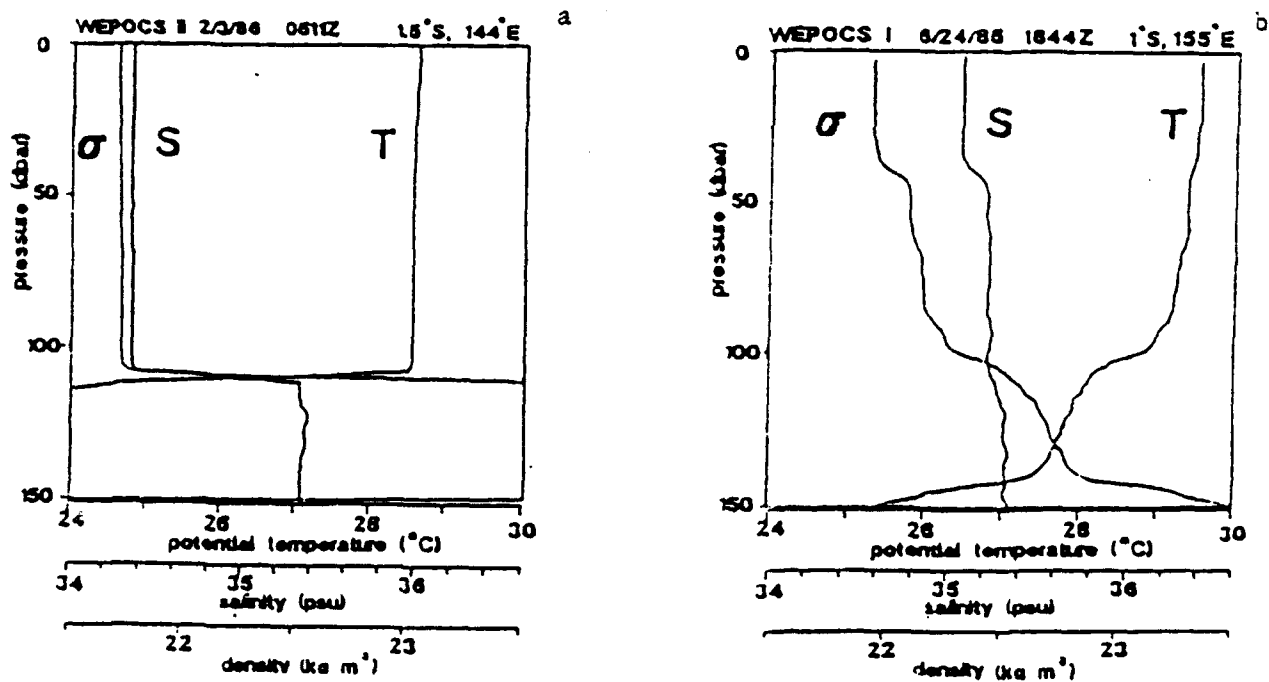


Fig. 1. Examples of temperature, salinity, and density profiles for: a) a well mixed upper ocean, b) an upper ocean with a freshwater lens (from Lukas and Lindstrom 1991).

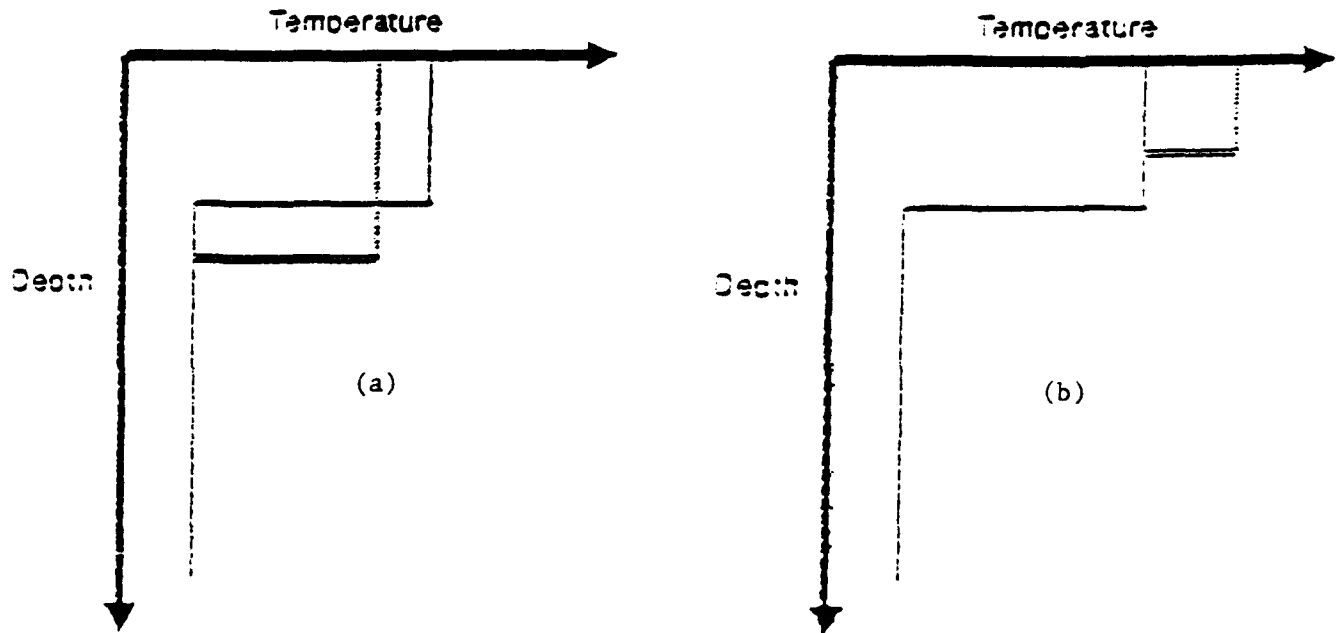


Fig. 2. Schematic temperature-depth profiles showing the effects of: a) turbulent mixing, and b) buoyancy damping. As shown in panel a, turbulent mixing will tend to drive the profile from solid to the dashed line. The net effect will be to cool and deepen the mixed layer. Buoyancy damping is one possible effect of buoyancy fluxes. As shown in panel b, damping will tend to drive the profile from the solid to the dashed line, warming and shallowing the mixed layer.

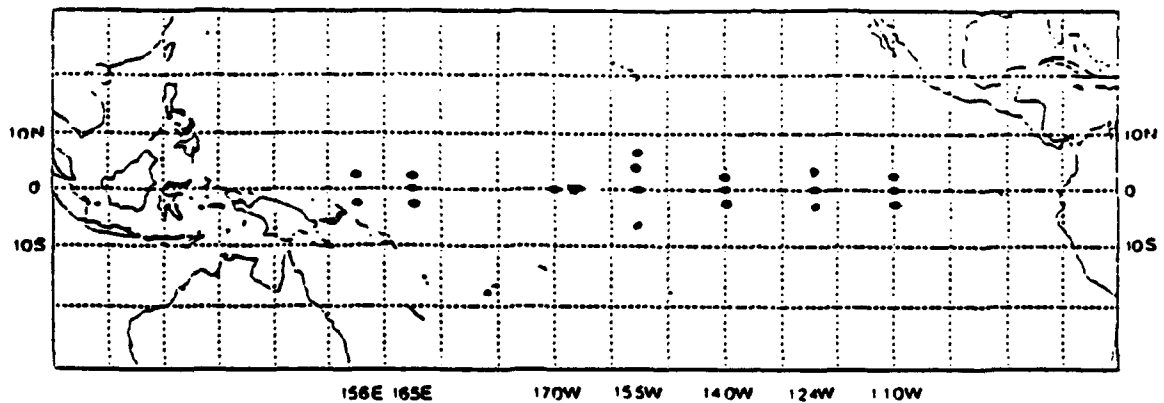


Fig. 3. Location of ATLAS and EPOCS buoys used in this study (from Cooper 1992).

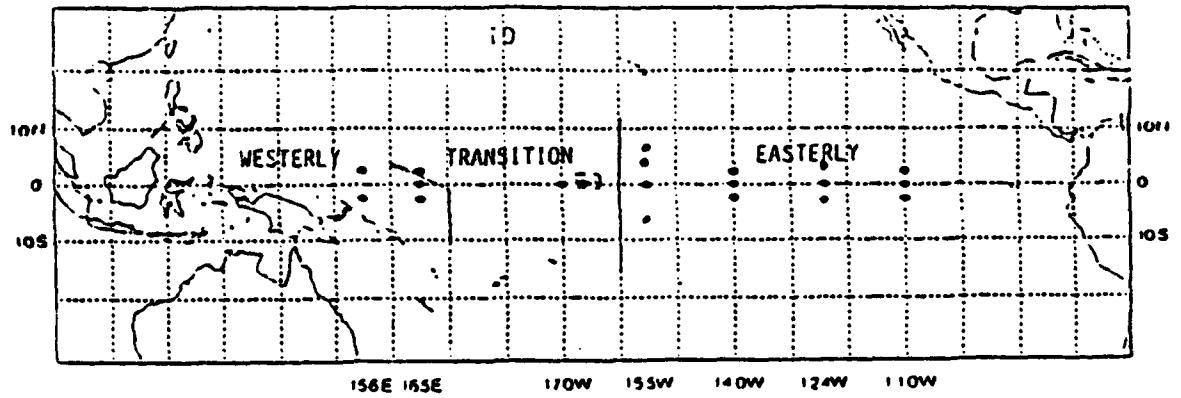


Fig. 4. Zonal wind regions: westerly, transition, and easterly.

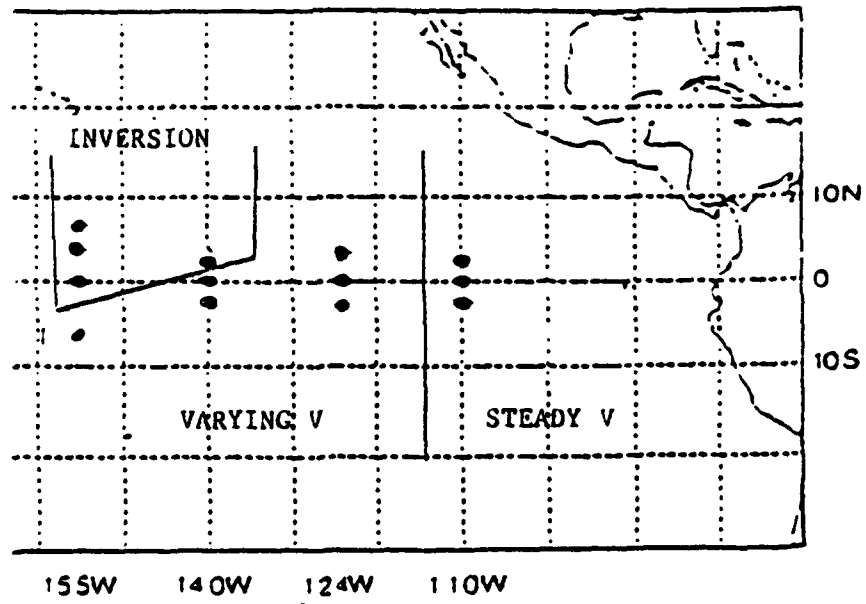


Fig. 5. Easterly wind sub-regions: varying V, steady V, and ocean temperature inversion regions.

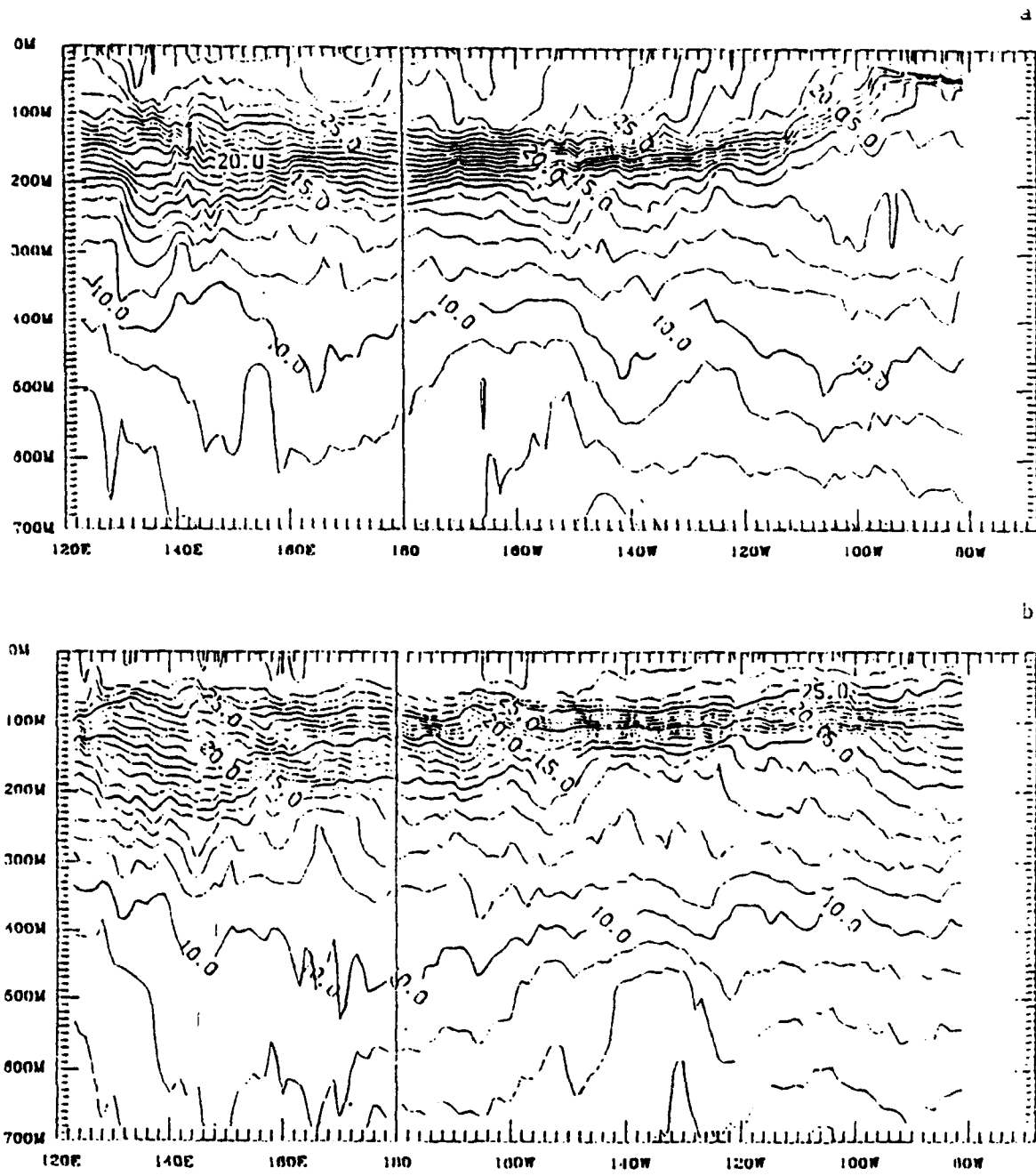


Fig. 6. Equatorial depth-longitude section of ocean temperature for: a) Oct. 91, b) Mar. 92 (from Kousky 1991a, 1992c)

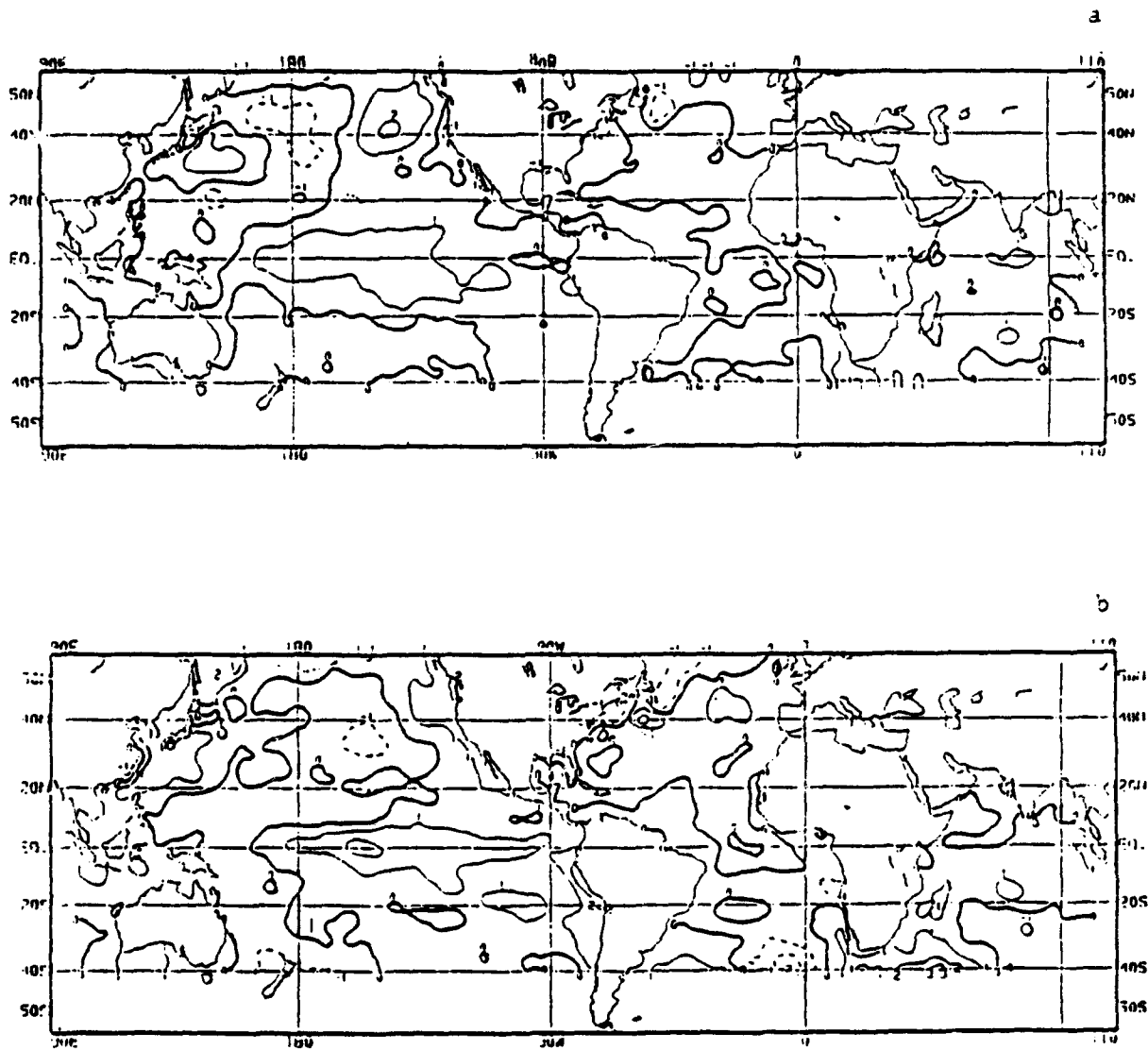


Fig. 7. Anomalous sea surface temperature for: a) Oct. 91, b) Mar. 92. Anomaly contour interval is 1°C with negative anomalies dashed (from Kousky 1991a, 1992c).

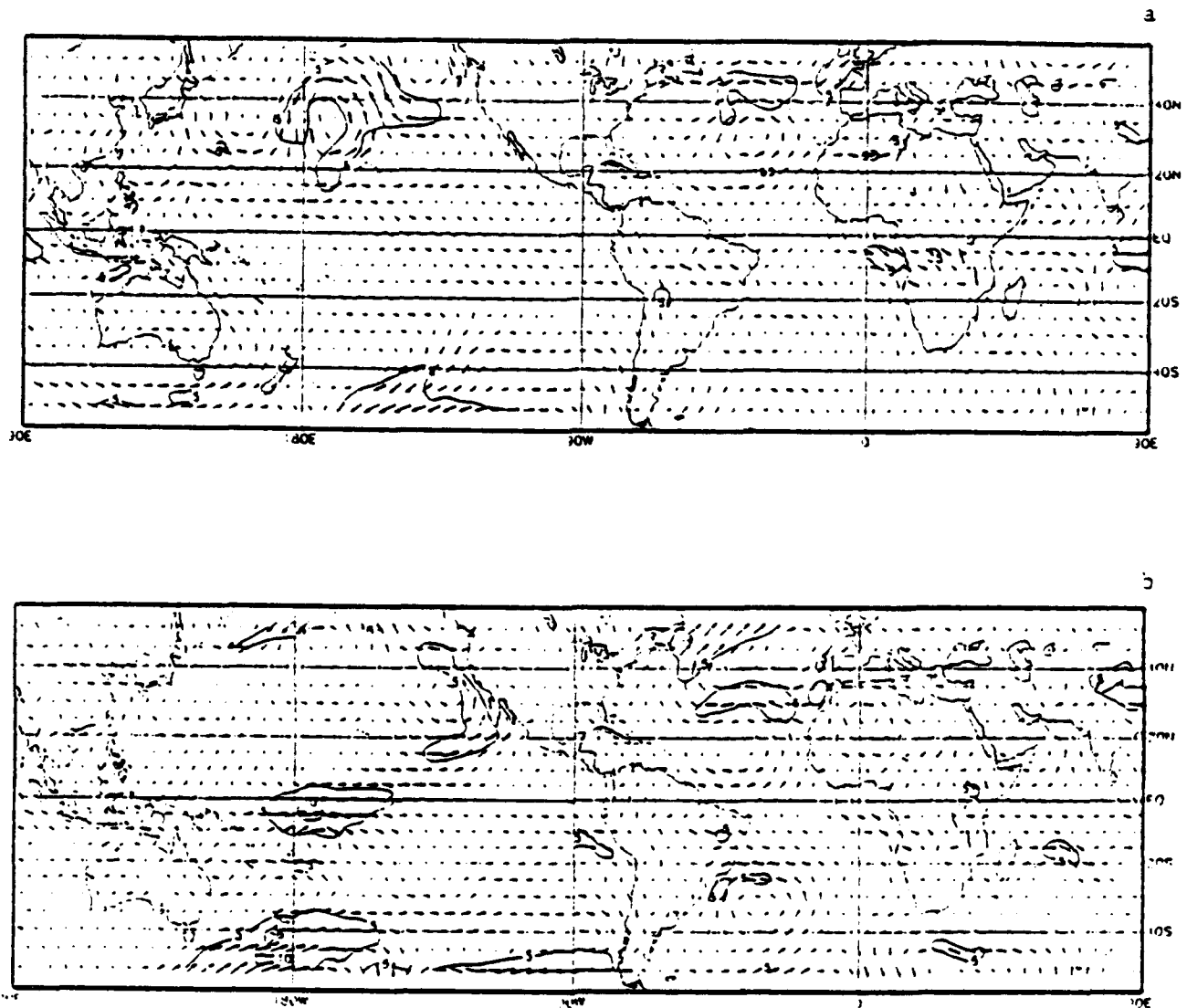


Fig. 8. Anomalous 850 mb vector wind on: a) Oct. 91, b) Mar. 92. Anomaly is departure from the 1979-1988 monthly means. Contour interval for isotachs is 5ms^{-1} (from Kousky 1991a, 1992c).

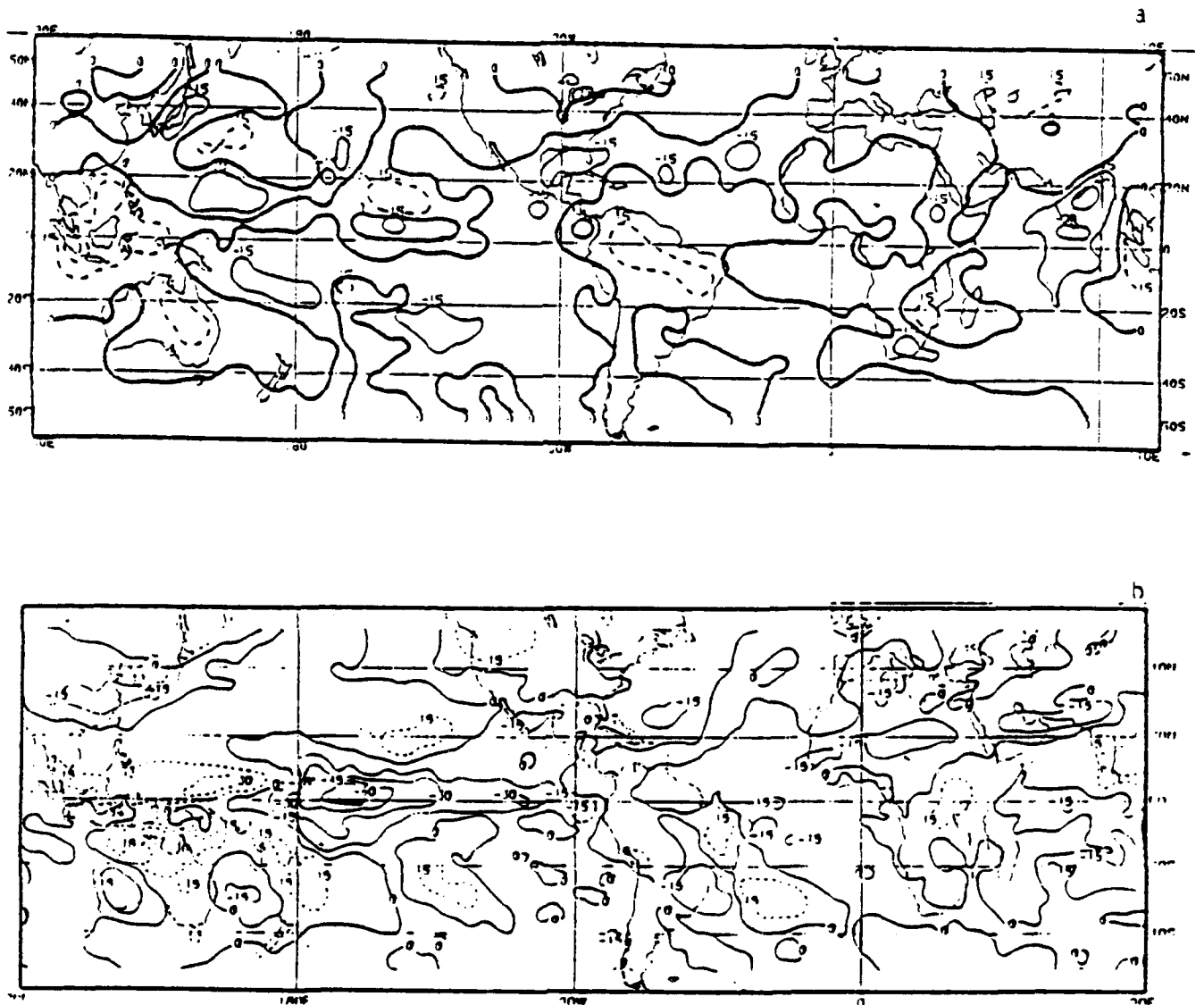


Fig. 9. Anomalous OLR for: a) Oct. 91, b) Mar 92. Anomalies are computed as departures from the 1979-1988 mean. Anomaly contour interval 15 Wm^{-2} (from Kousky 1991a, 1992c).

Sequential Scatterplot 2N 156E

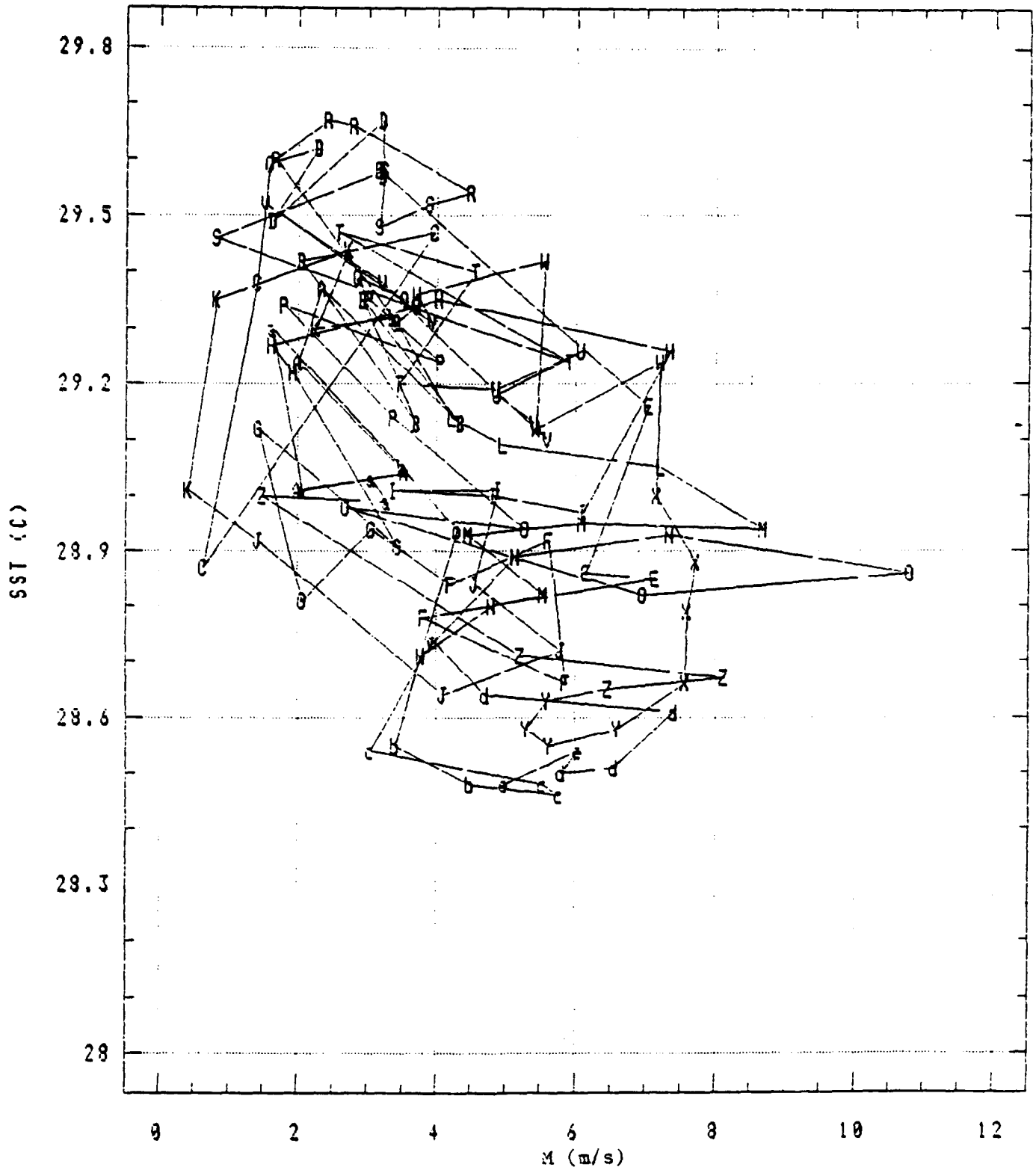


Fig. 10. Sequential scatterplot of raw SST/M at 2°N 156°E.

Sequential Scatterplot EQ 170W Raw

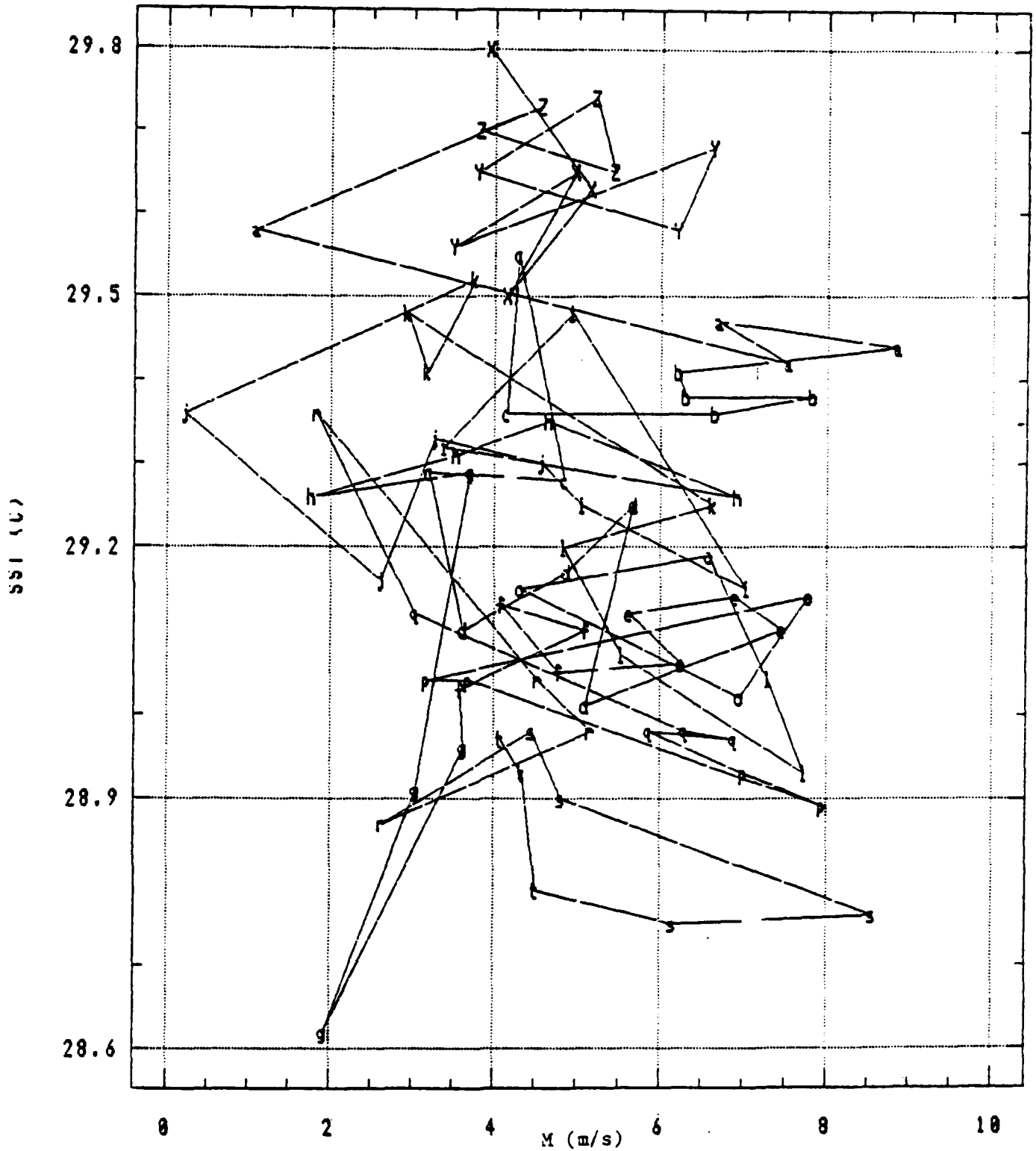


Fig. 11. Sequential scatterplot of raw SST/M at EQ 170°W.

Sequential Scatterplot 2N 110W

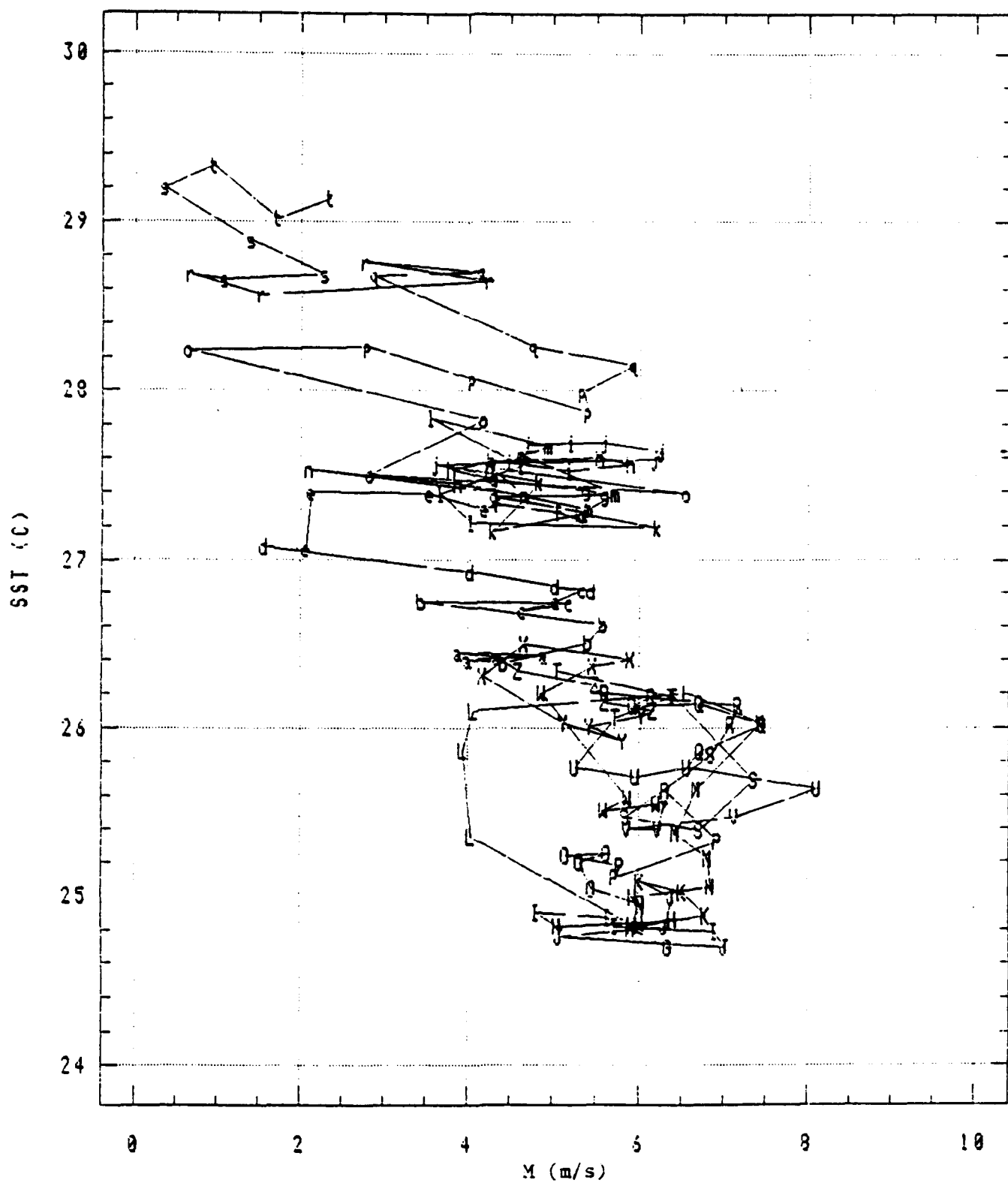


Fig. 12. Sequential scatterplot of raw SST/M at 2°N 110°W.

SEQUENTIAL SCATTERPLOT KEY

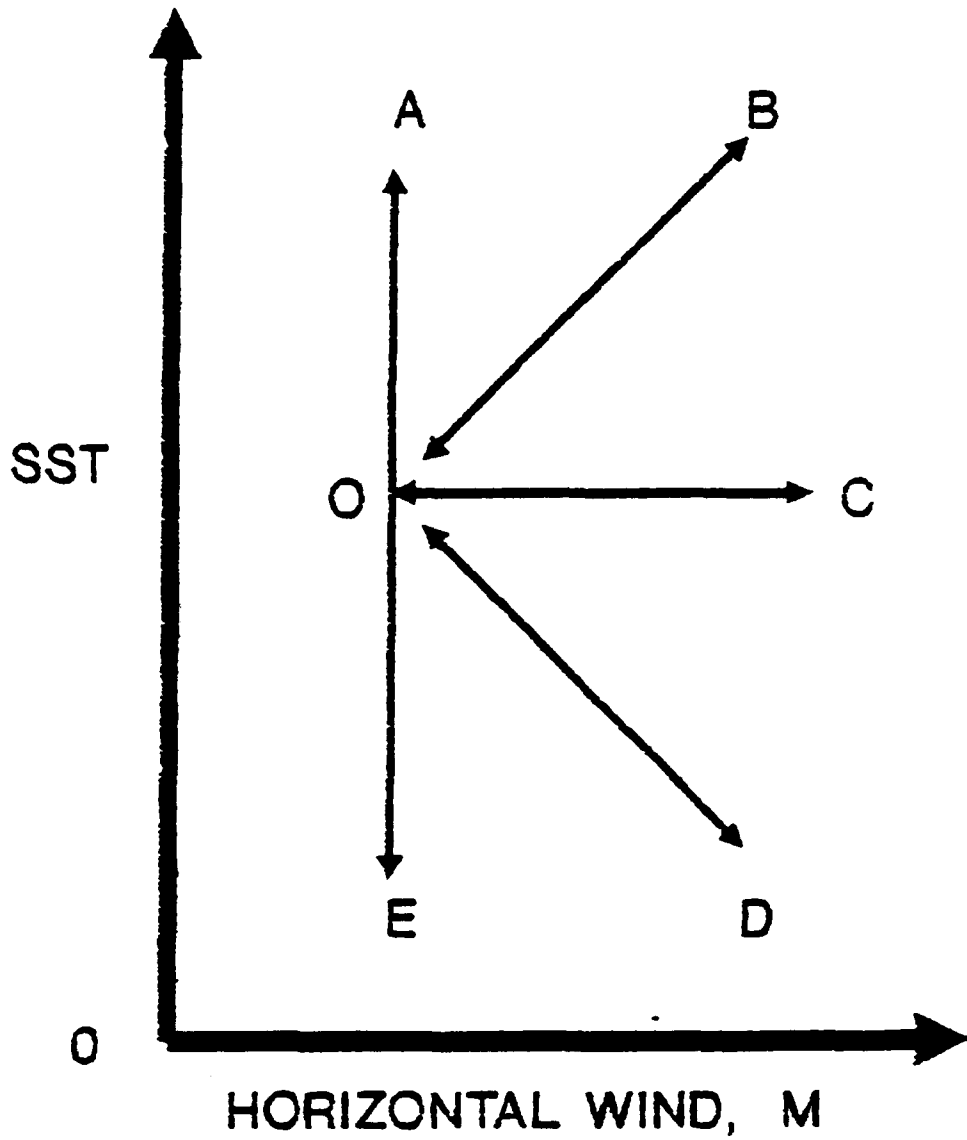


Fig. 13. Sequential scatterplot key for SST and M relations.

(Intentionally Blank)

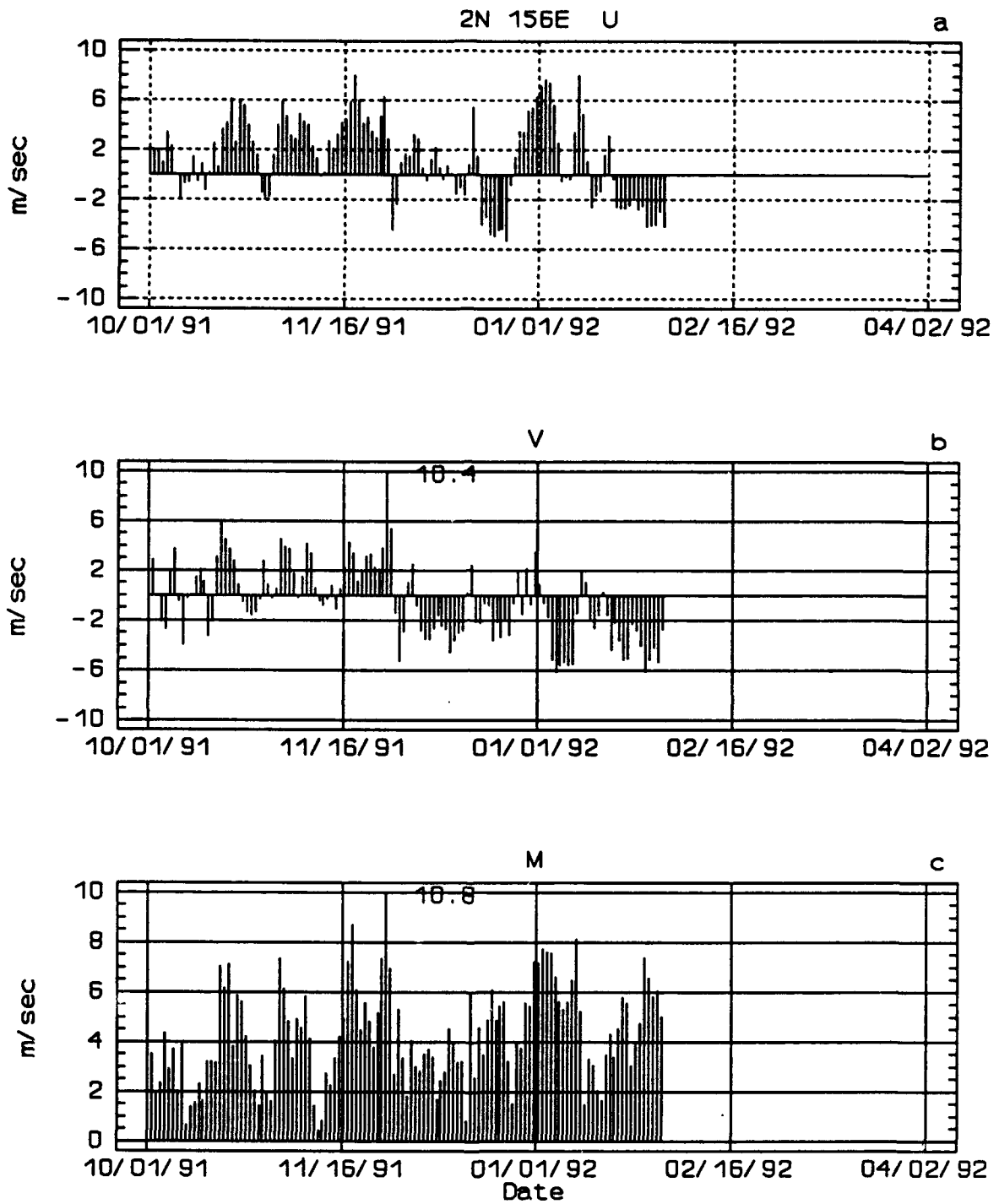


Fig. 14. Time series of linearly detrended: a) zonal wind (U), b) meridional wind (V), and c) wind magnitude (M) for 2°N 156°E.

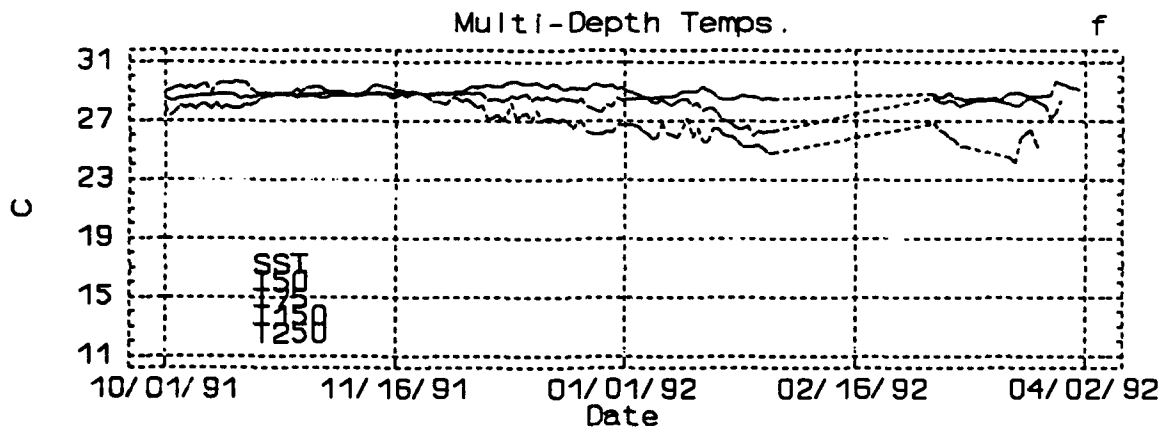
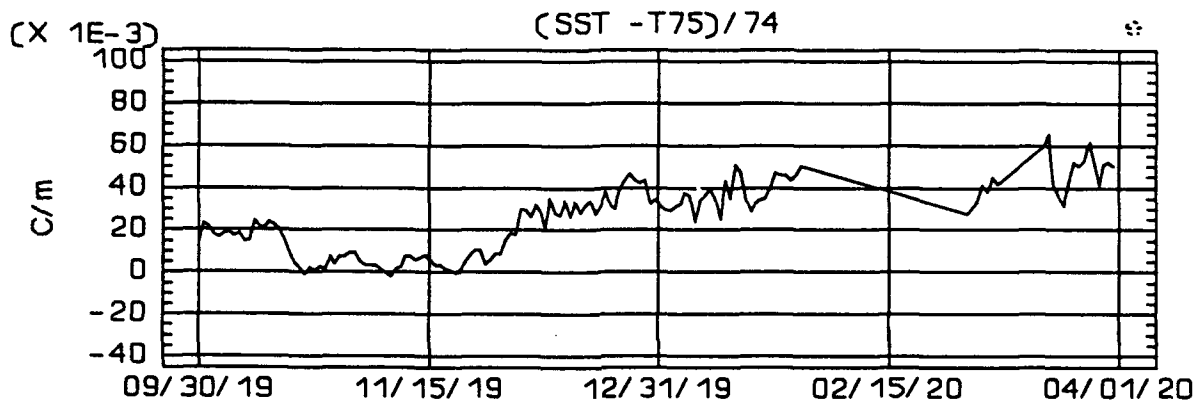
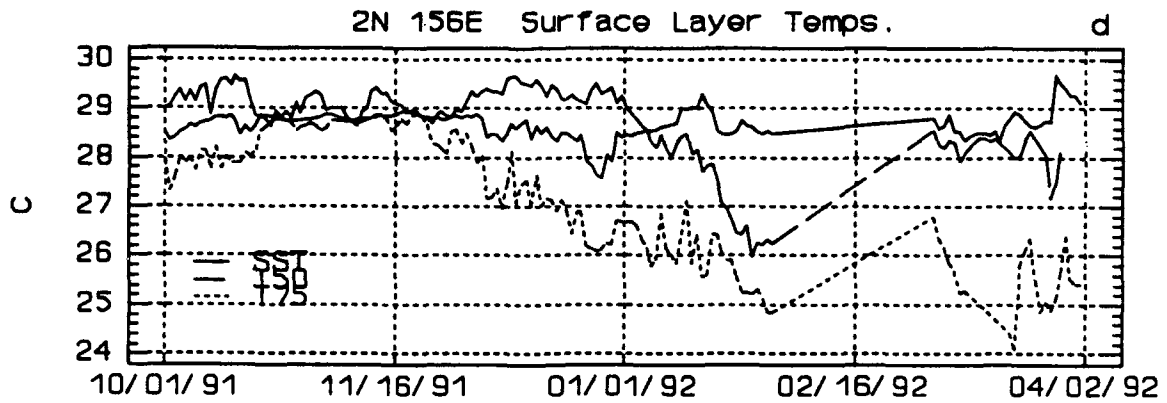


Fig. 14. (Continued) Time series of raw: a) surface layer temps., b) temperature gradient (TG), and c) multi-depth temperatures for 2°N 156°E.

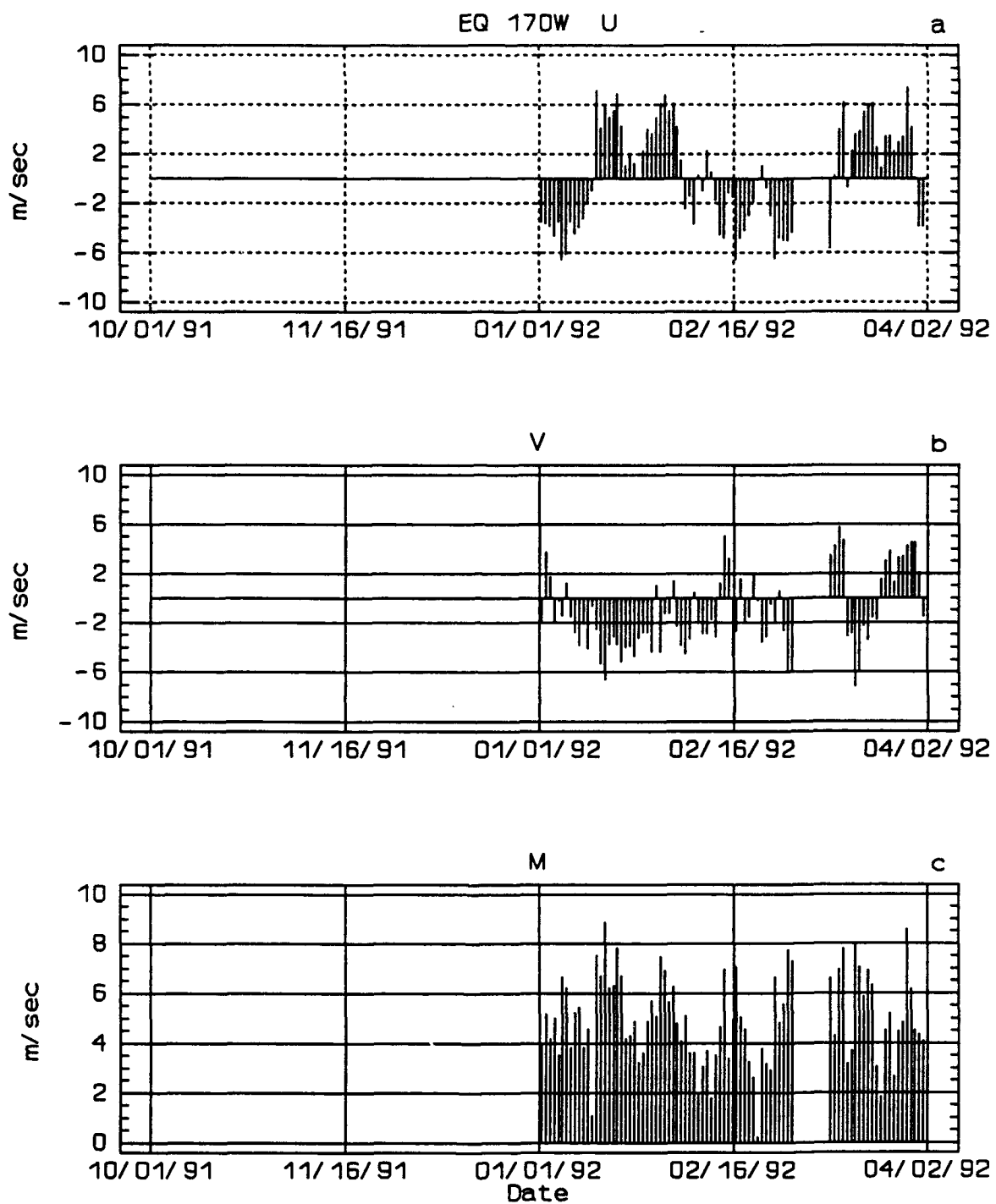


Fig. 15. Time series of linearly detrended: a) zonal wind (U), b) meridional wind (V), and c) wind magnitude (M) for EQ 170°W.

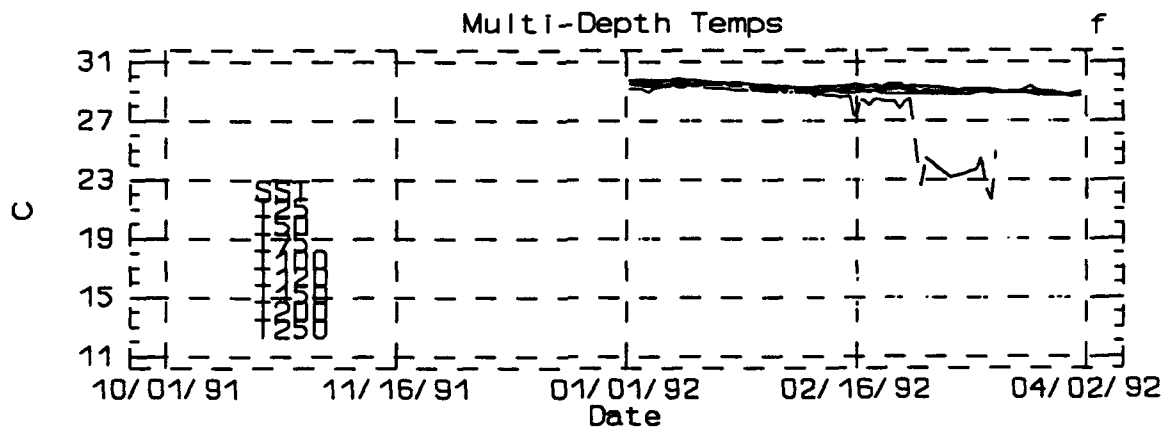
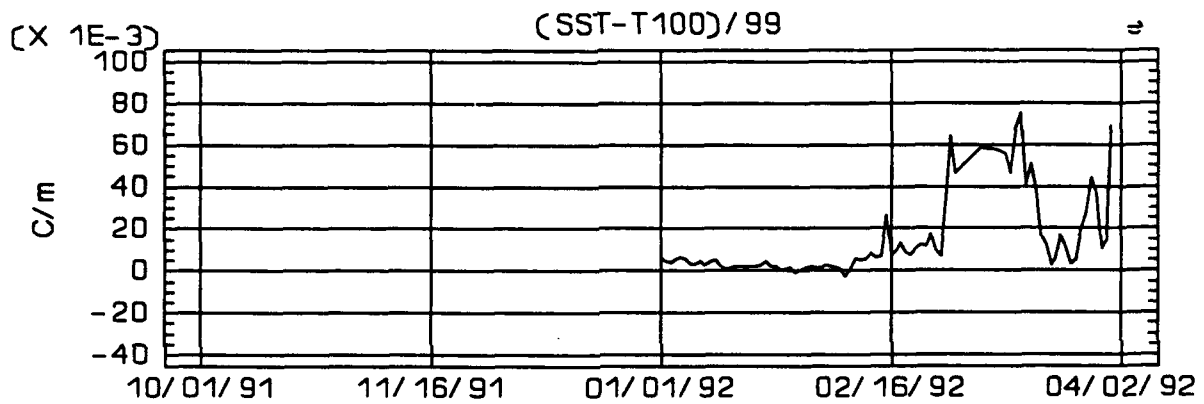
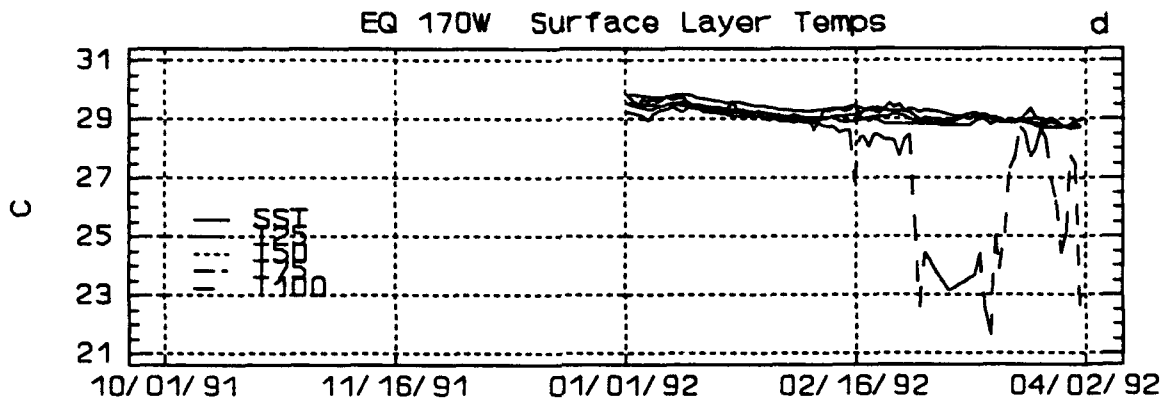


Fig. 15. (Continued) Time series of raw: d) surface layer temps., e) temperature gradient (TG), and f) multi-depth temps. for EQ 170°W.

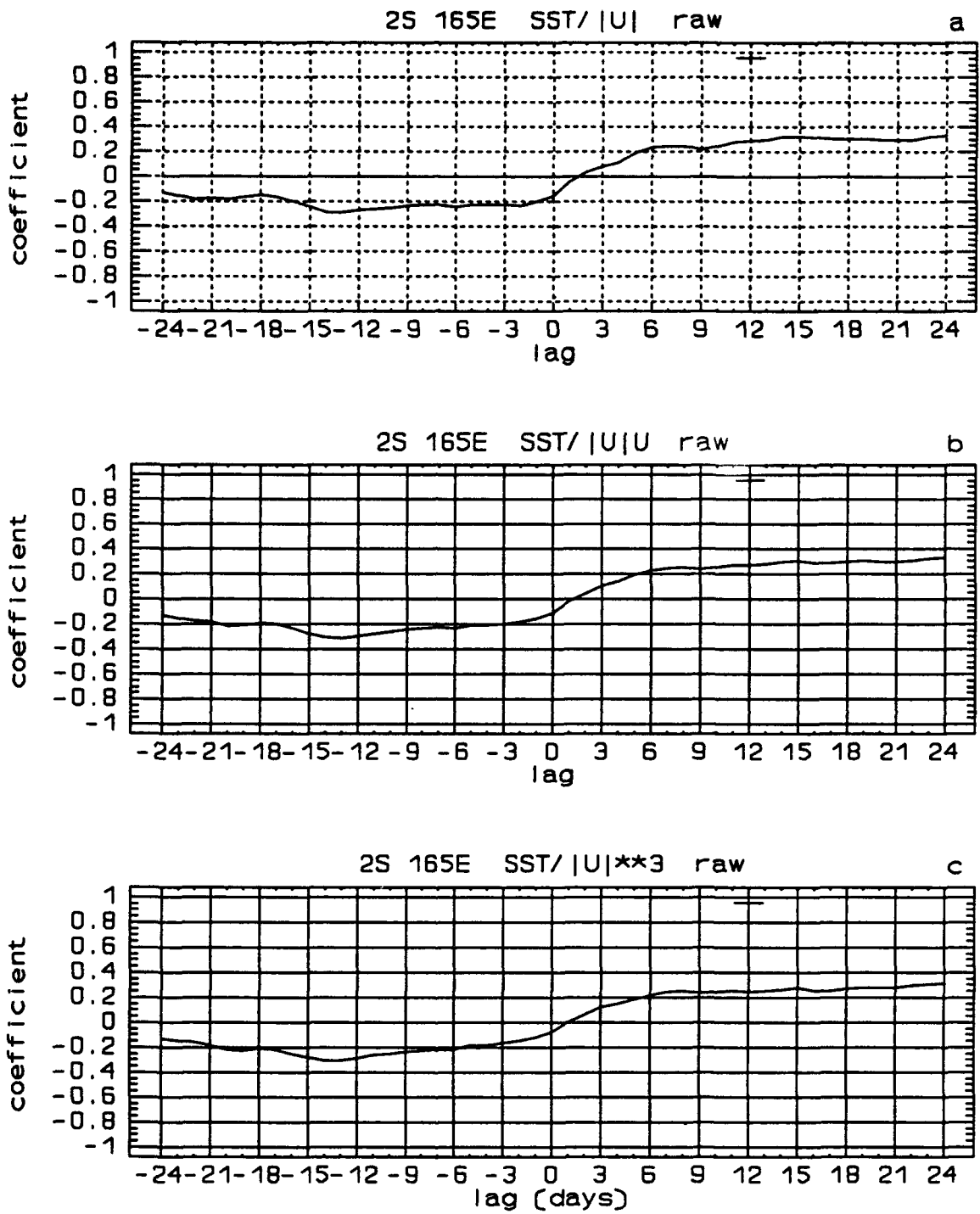


Fig. 16. Cross-correlations of SST and: a) $|U|$ (turbulent heat exchange), b) $|U|U$ (Ekman pumping), c) $|U|^3$ (Turbulent Kinetic Energy).

(Intentionally Blank)

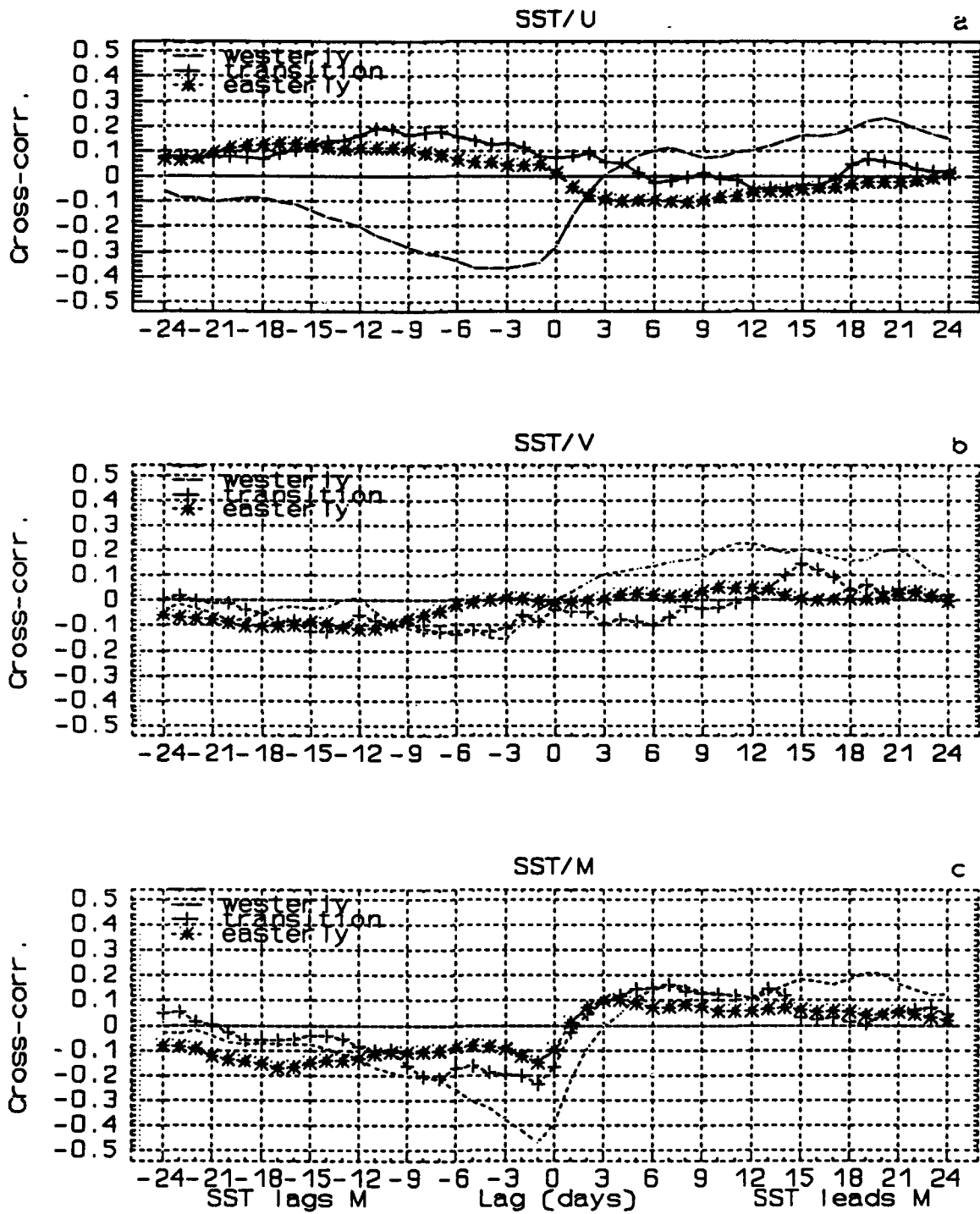


Fig. 17. Zonal wind regions averaged cross-correlations of: a) SST/U, b) SST/V, and c) SST/M. Each plot depicts the westerly, transition, and easterly wind regions.

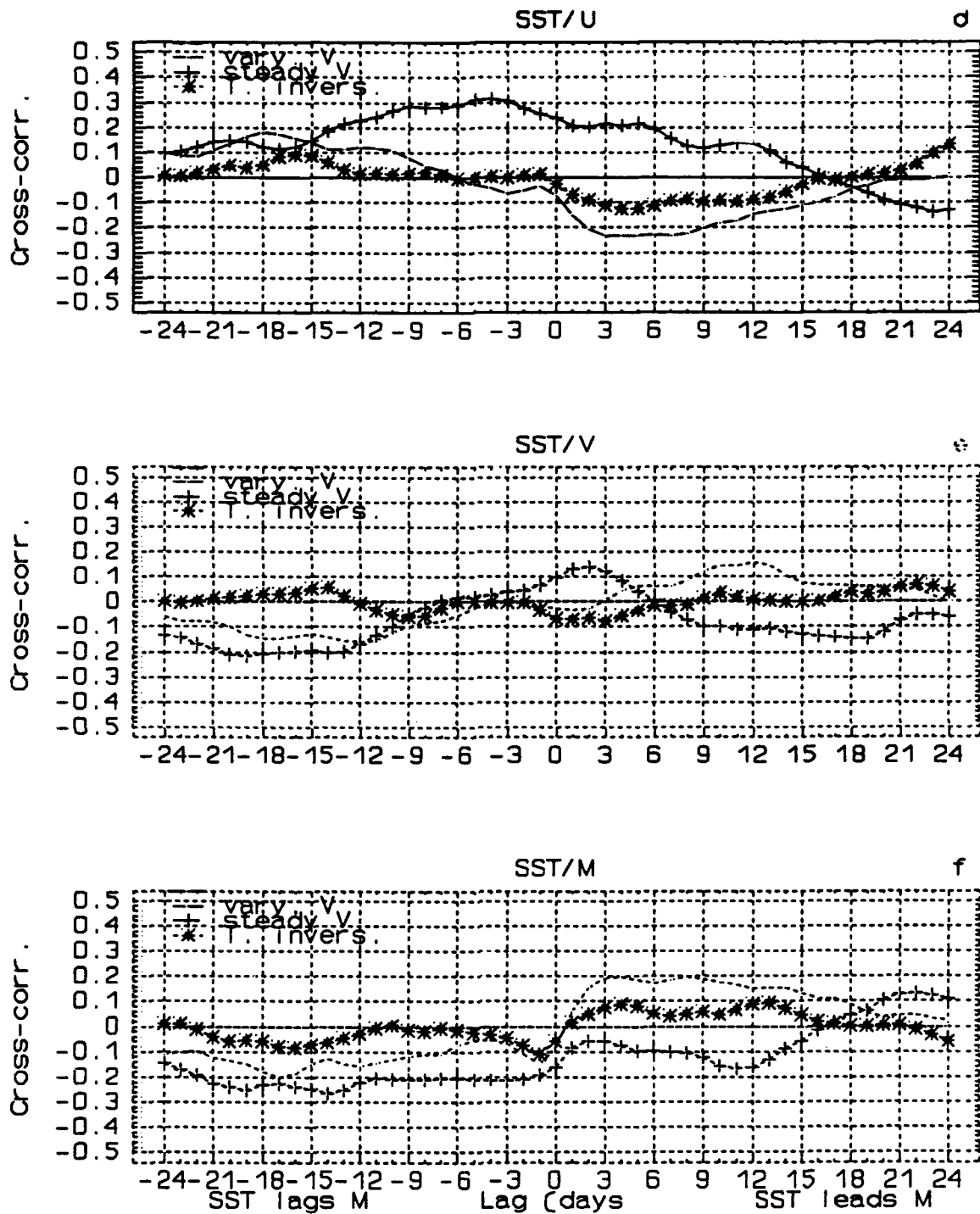


Fig. 17. (Continued) Easterly wind sub-regions cross-correlations of: a) SST/U, b) SST/V, and c) SST/M. Each plot depicts the varying V, steady V, and ocean temperature inversion regions.

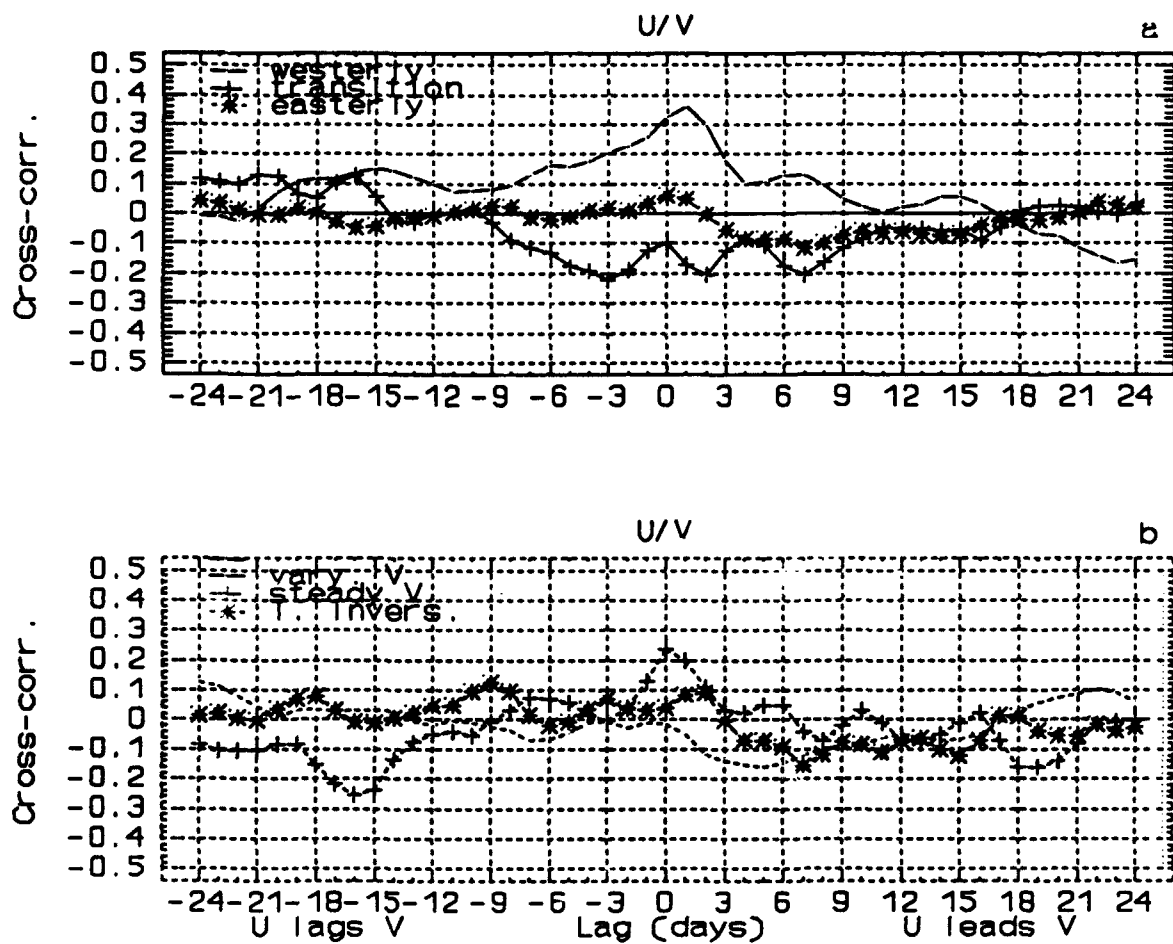


Fig. 18. Averaged estimated cross-correlations of U/V in the: a) zonal wind regions, and b) easterly wind sub-regions.

(Intentionally Blank)

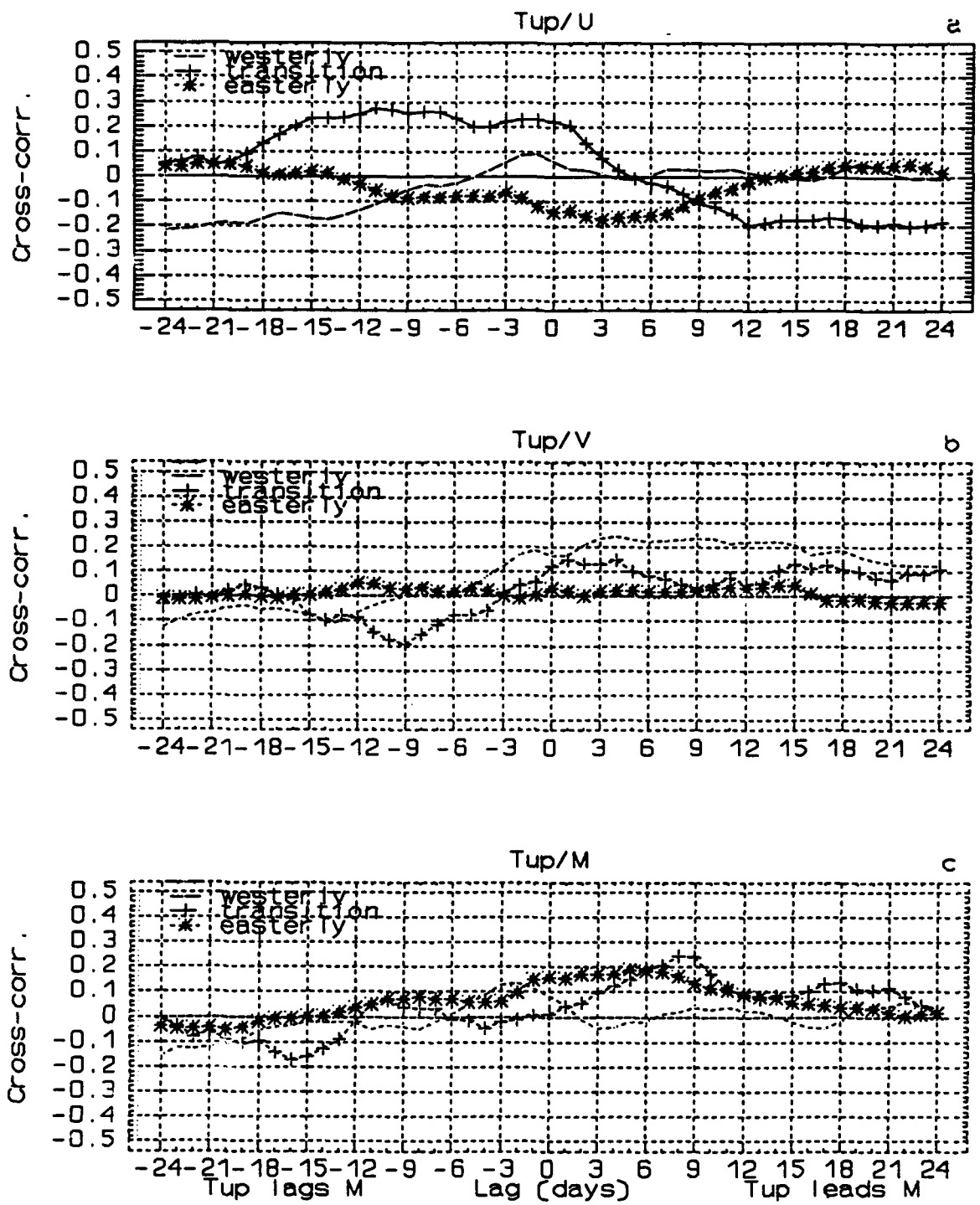


Fig. 19. Zonal wind regions estimated cross-correlations of: a) Tup/U , b) Tup/V , and c) Tup/M . Each plot depicts the westerly, transition, and easterly wind regions.

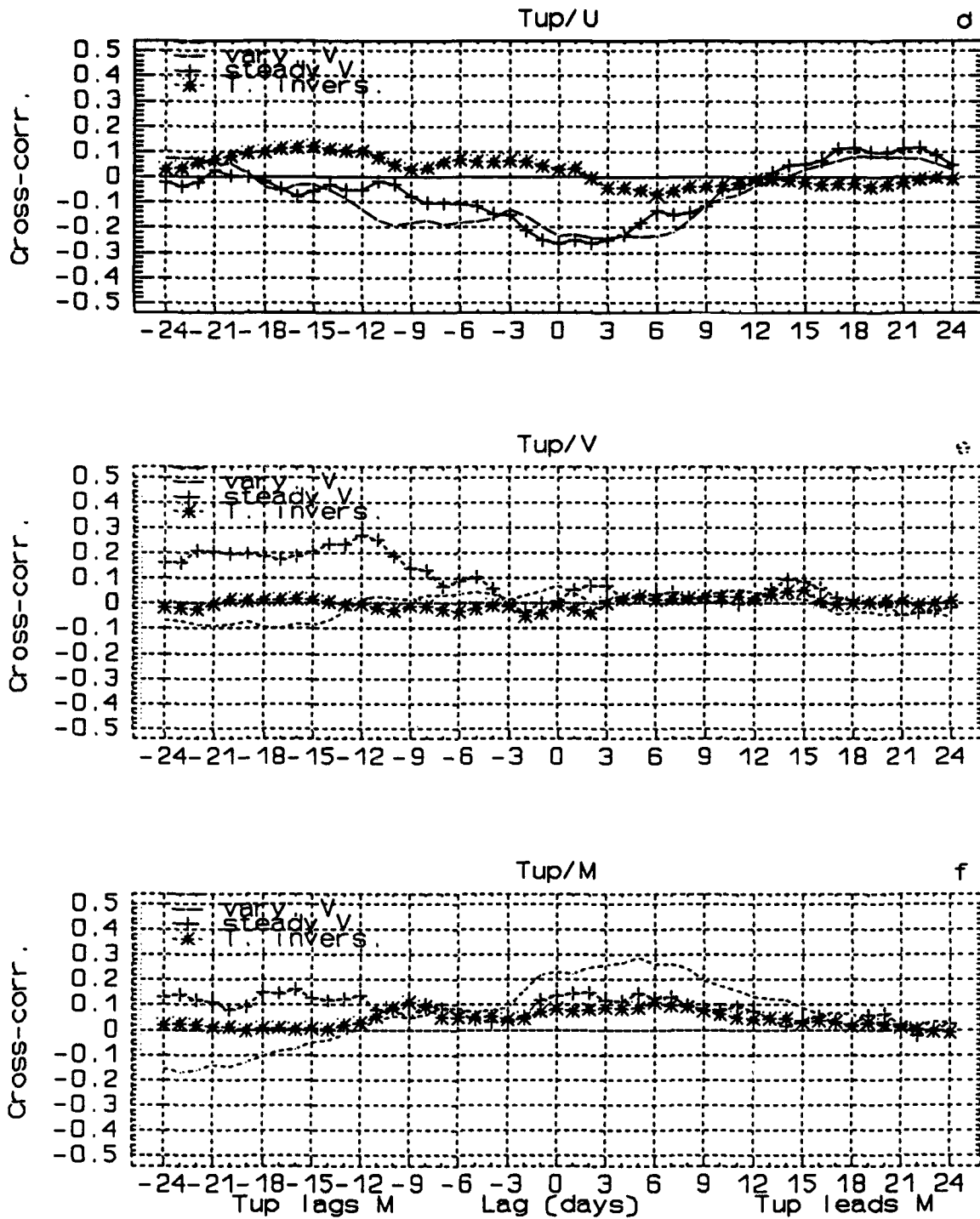


Fig. 19. (Continued) Easterly wind sub-regions cross-correlations of: a) Tup/U, b) Tup/V, and c) Tup/M. Each plot depicts the varying V, steady V, and ocean temperature inversion regions.

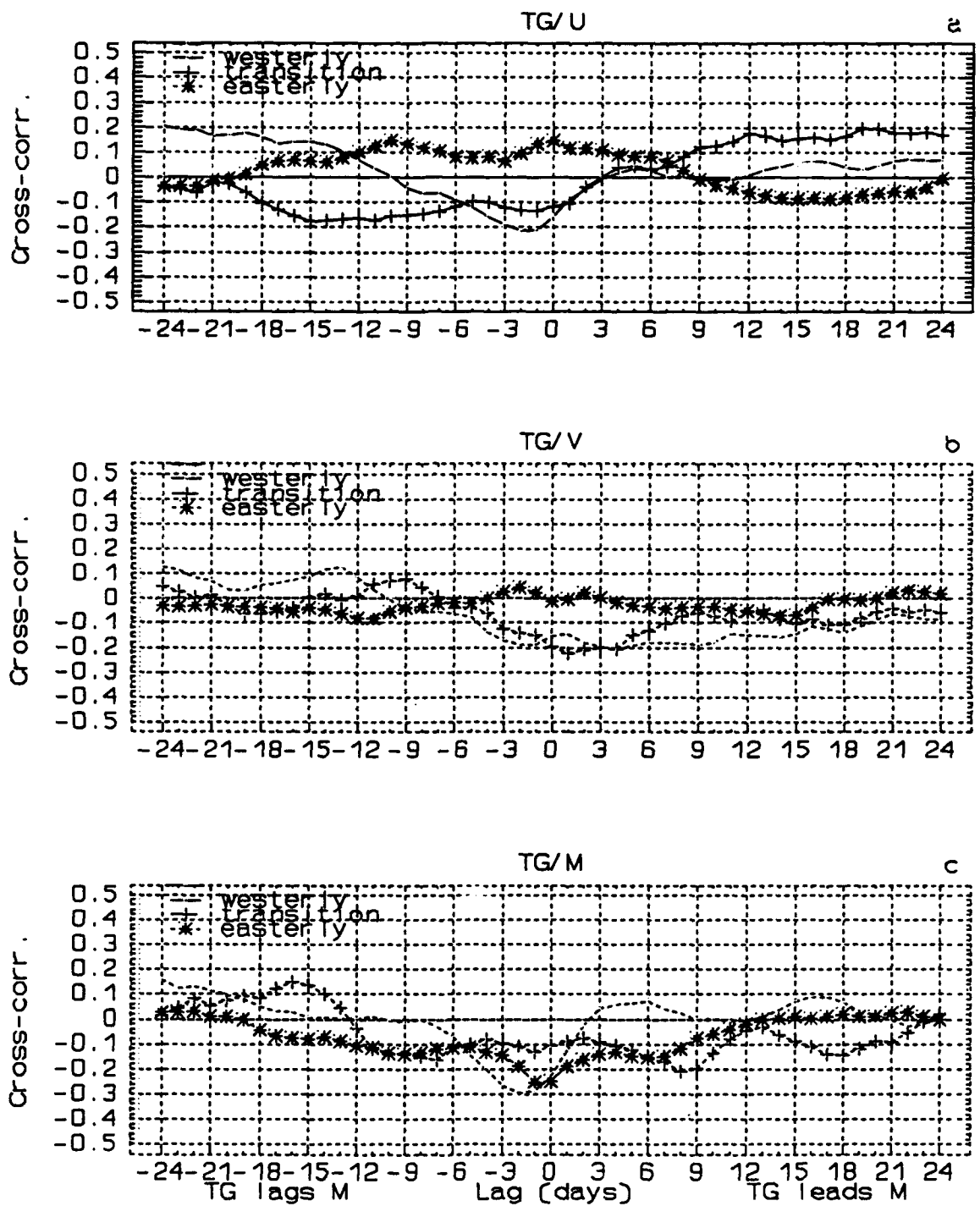


Fig. 20. Zonal wind regions averaged estimated cross-correlations of: a) TG/U, b) TG/V, and c) TG/M. Each plot depicts the westerly, transition, and easterly wind regions.

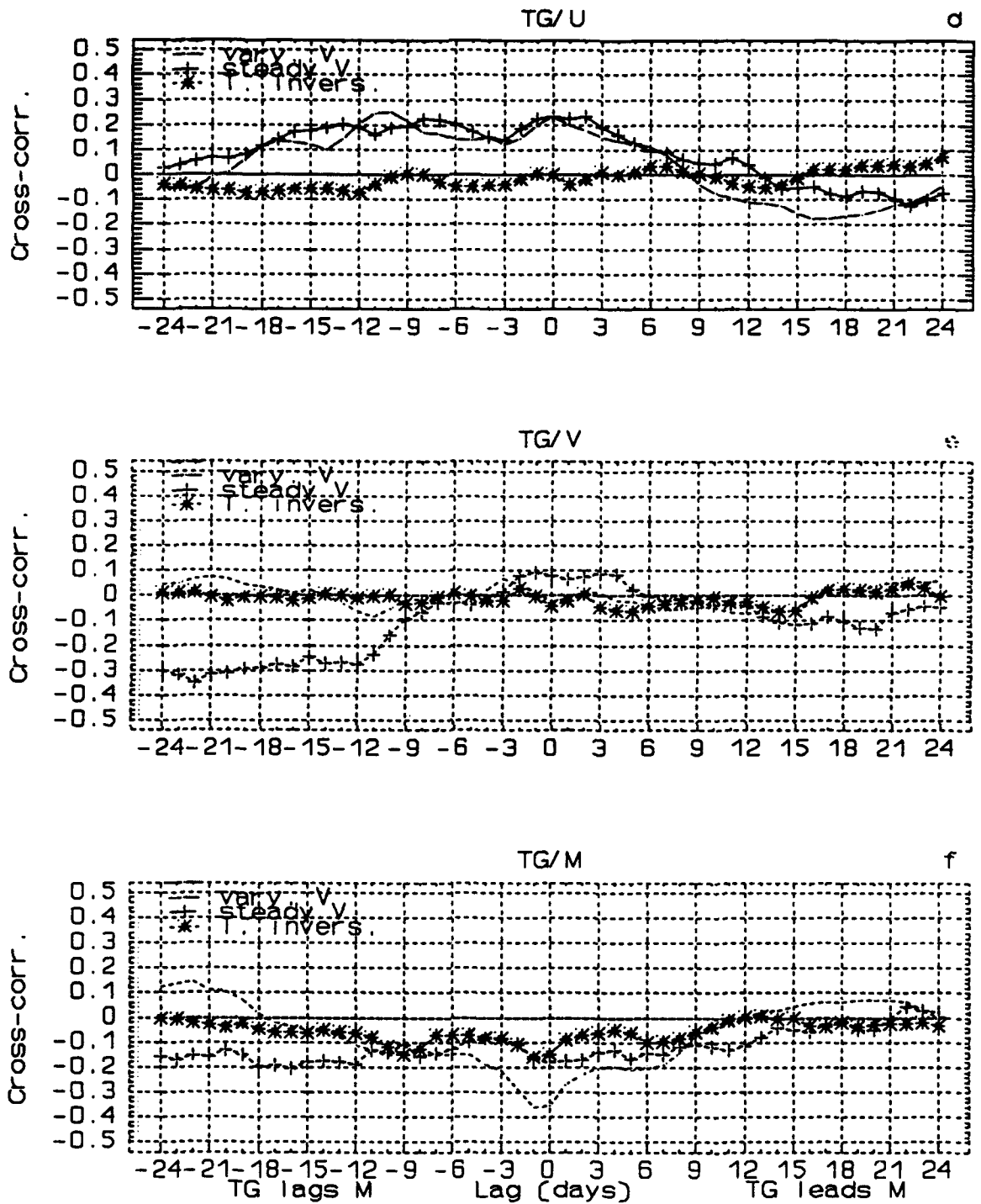


Fig. 20. (Continued) Easterly wind sub-regions cross-correlations of: a) TG/U, b) TG/V, and c) TG/M. Each plot depicts the varying V, steady V, and ocean temperature inversion regions.

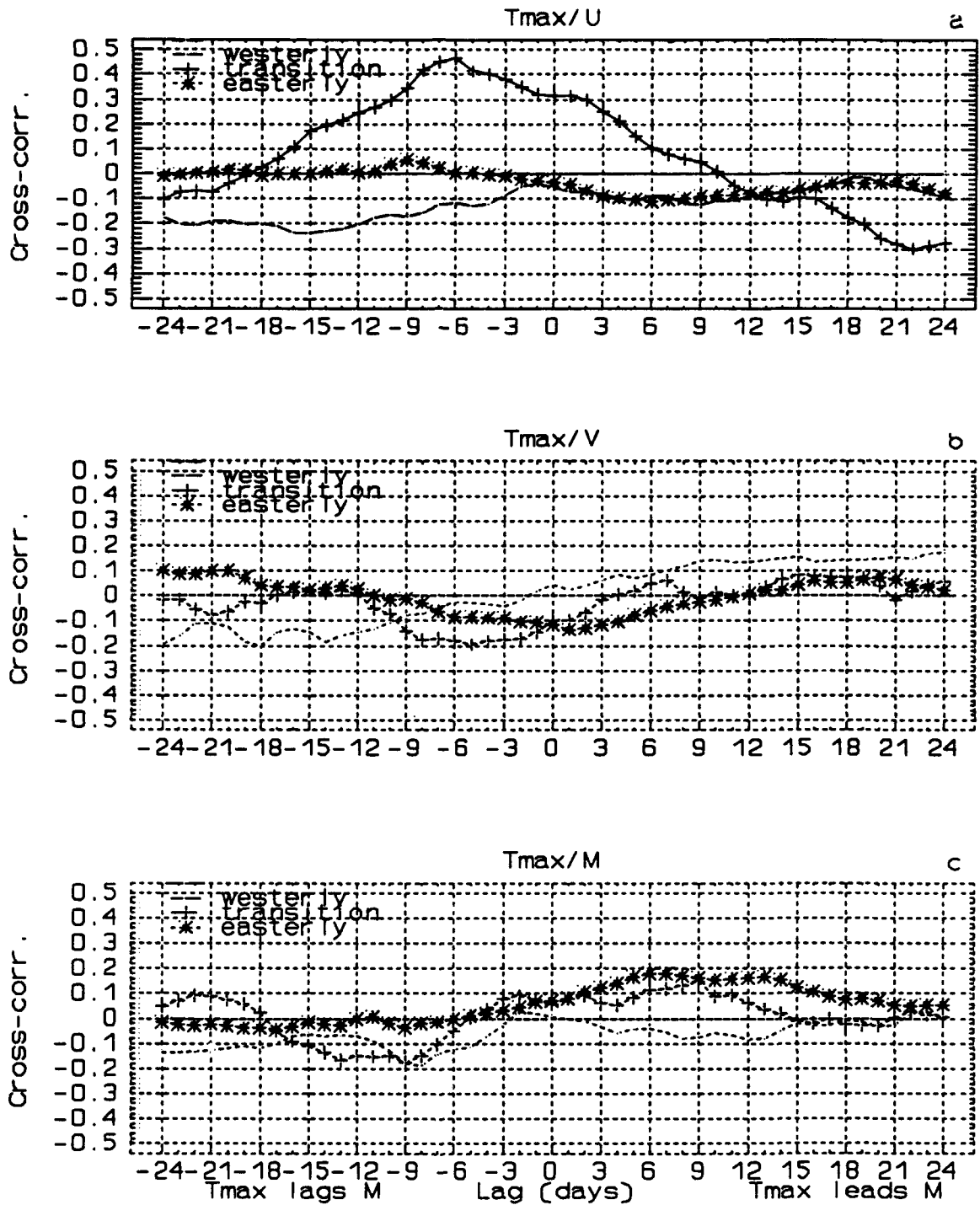


Fig. 21. Zonal wind regions averaged estimated cross-correlations of: a) T_{max}/U , b) T_{max}/V , and c) T_{max}/M . Each plot depicts the westerly, transition, and easterly wind regions.

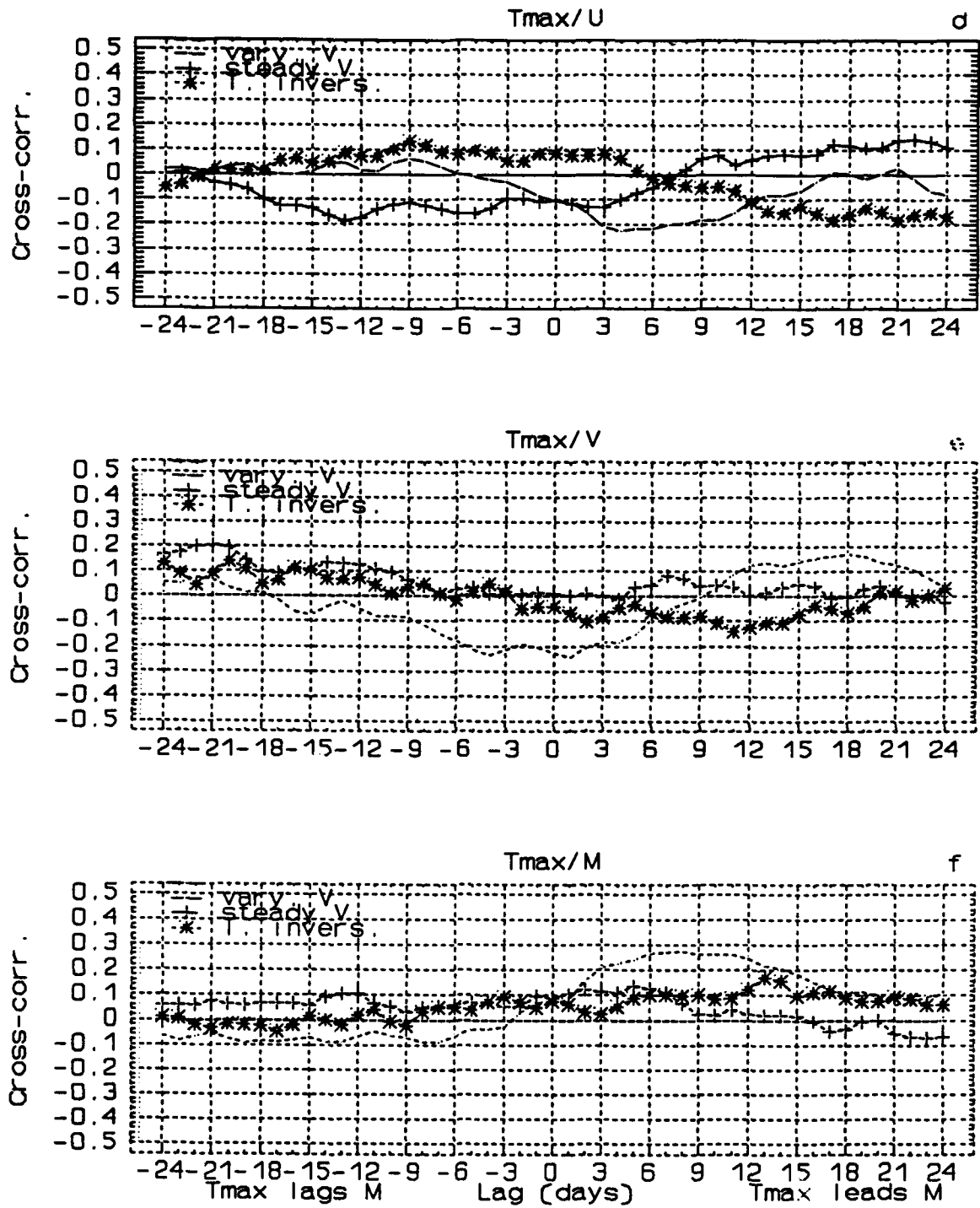


Fig. 21. (Continued) Easterly wind sub-regions cross-correlations of: a) T_{max}/U , b) T_{max}/V , and c) T_{max}/M . Each plot depicts the varying V, steady V, and ocean temperature inversion regions.

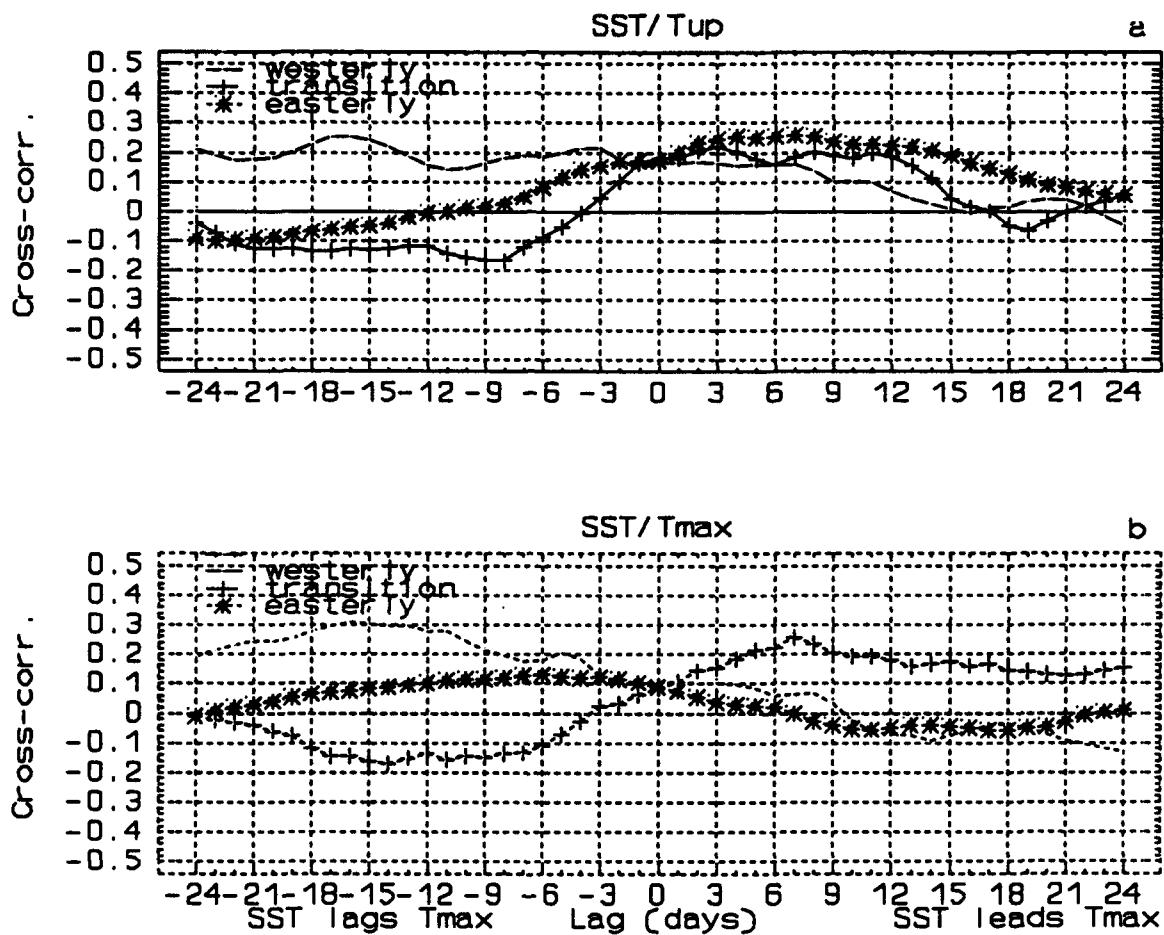


Fig. 22. Zonal wind regions averaged estimated cross-correlations of: a) SST/Tup, b) SST/Tmax. Each plot depicts the westerly, transition, and easterly wind regions.

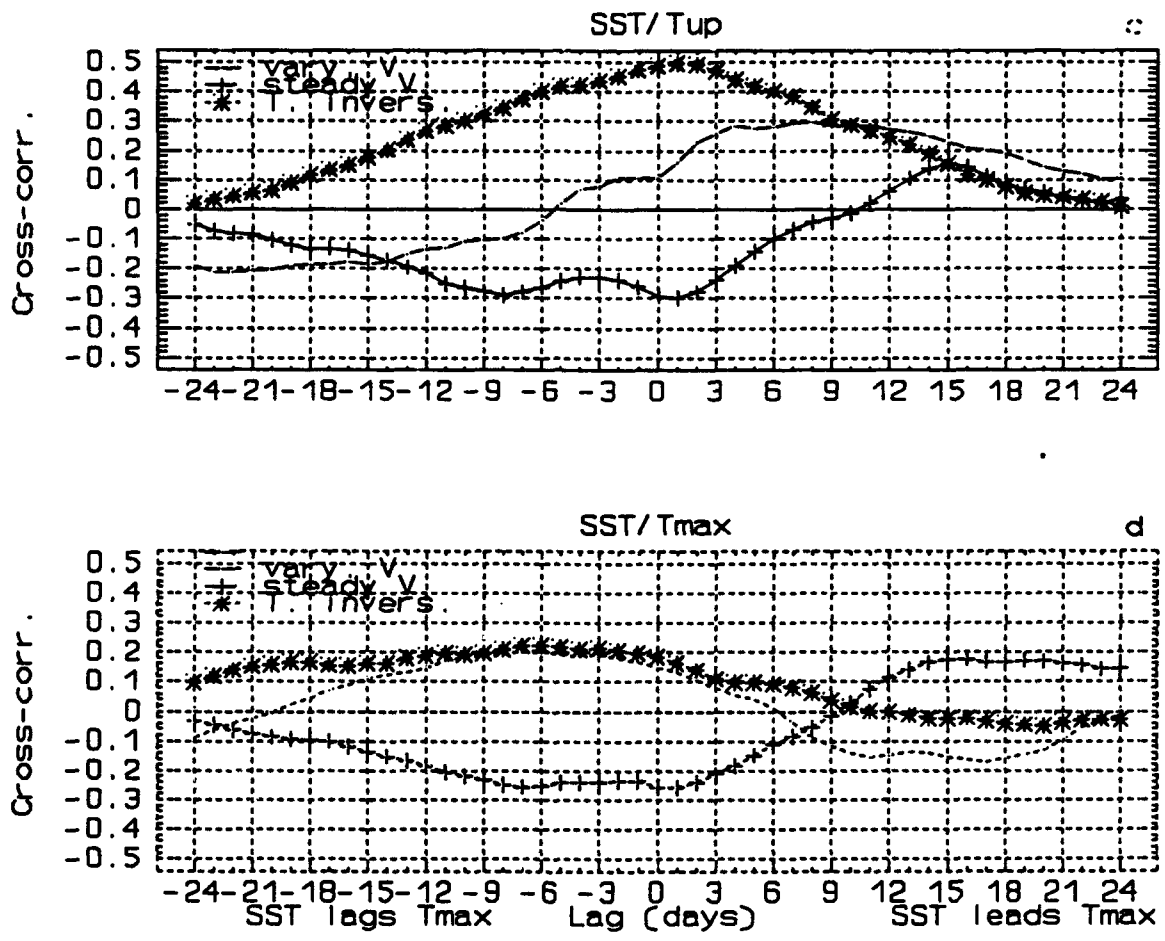


Fig. 22. (Continued) Easterly wind sub-regions cross-correlations of: a) SST/Tup, and b) SST/Tmax. Each plot depicts the varying V, steady V, and ocean temperature inversion regions.

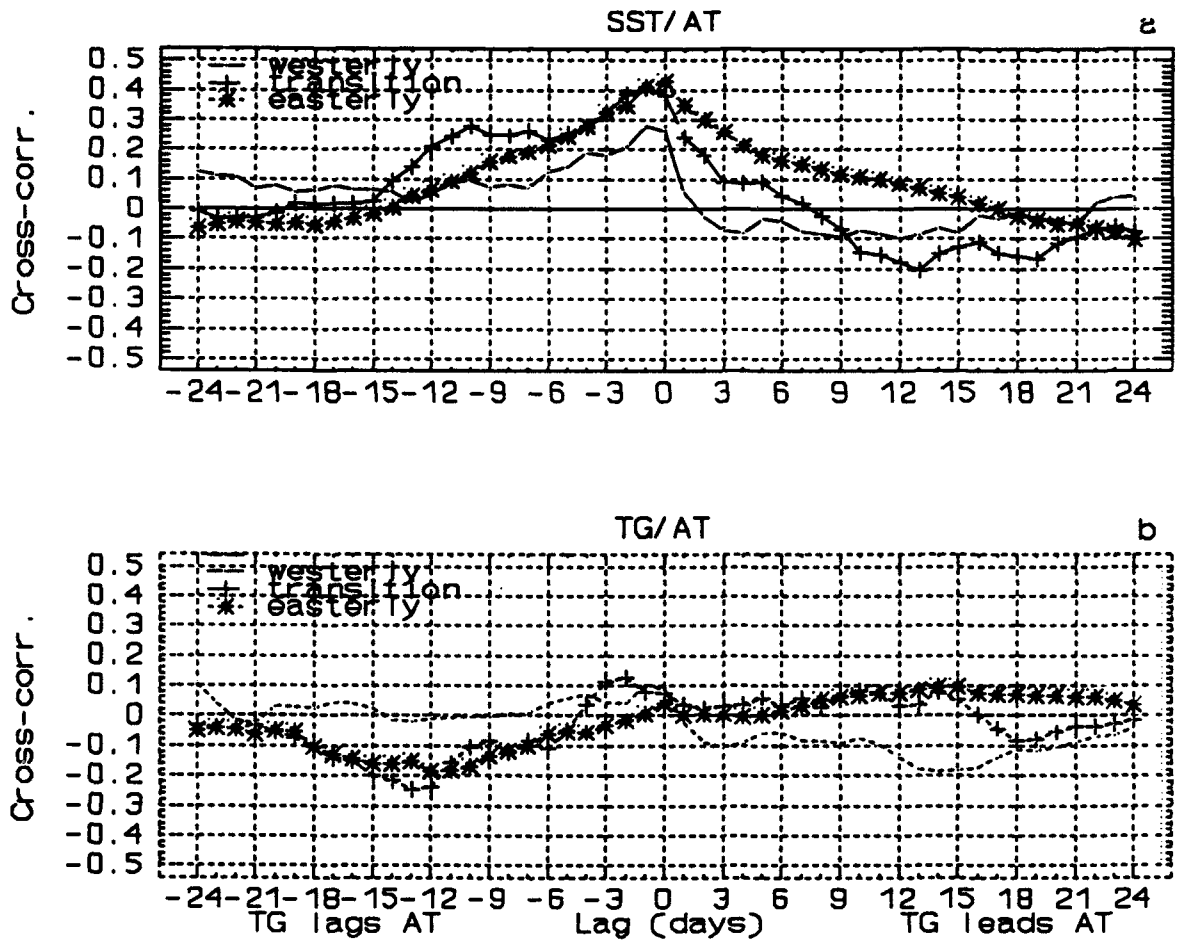


Fig. 23. Zonal wind regions averaged estimated cross-correlations of: a) SST/AT, b) TG/AT. Each plot depicts the westerly, transition, and easterly wind regions.

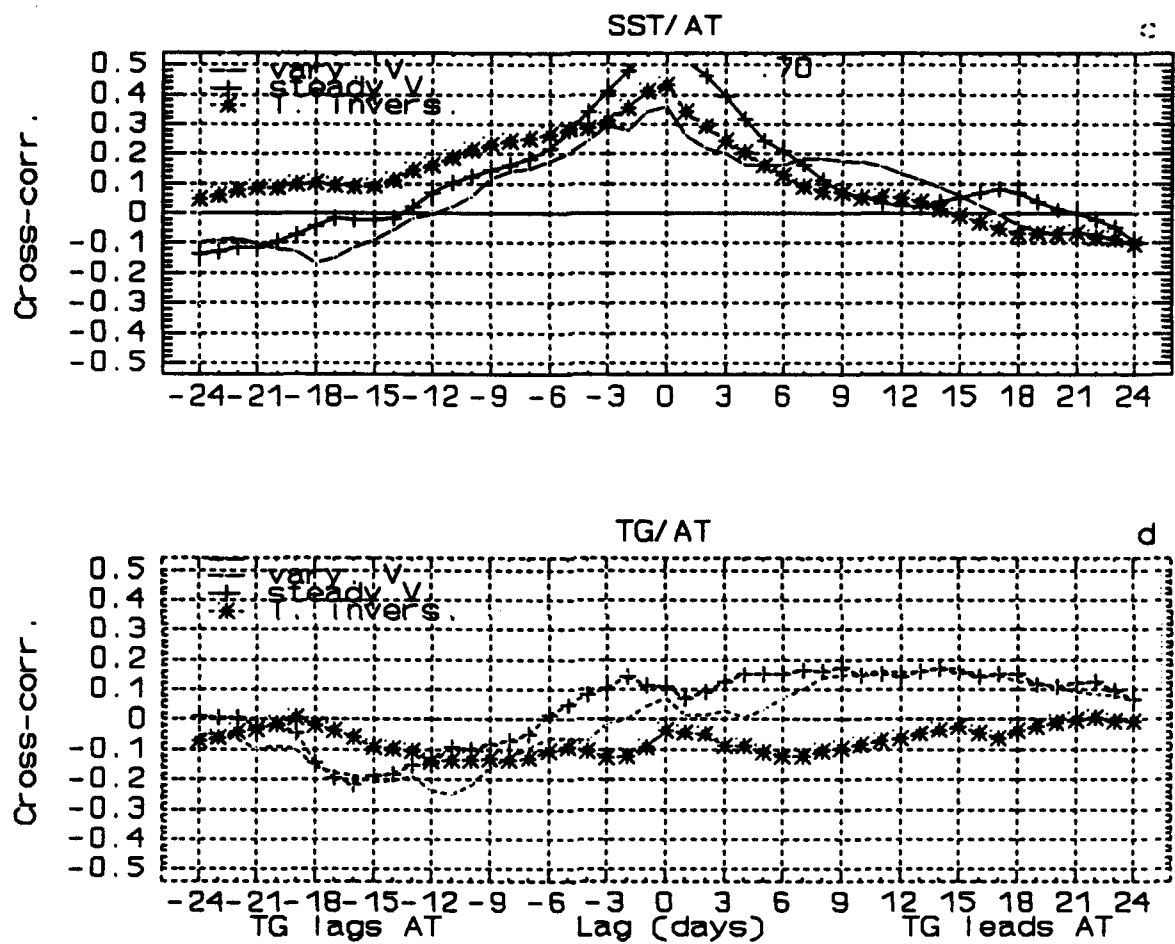


Fig. 23. (Continued) Easterly wind sub-regions cross-correlations of: a) SST/AT, and b) TG/AT. Each plot depicts the varying V, steady V, and ocean temperature inversion regions.

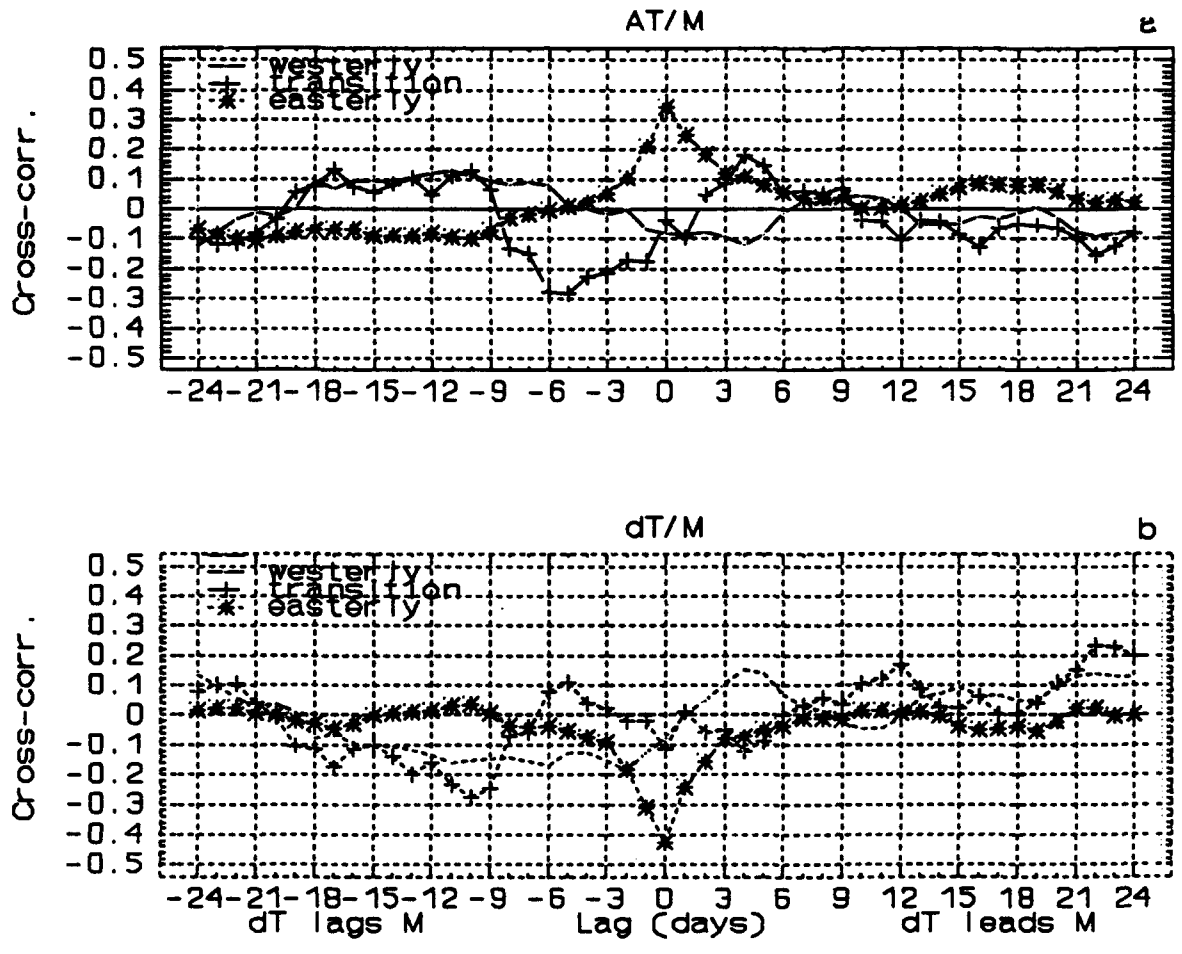


Fig. 24. Zonal wind regions averaged estimated cross-correlations of: a) AT/M, and b) dT/M. Each plot depicts the westerly, transition, and easterly wind regions.

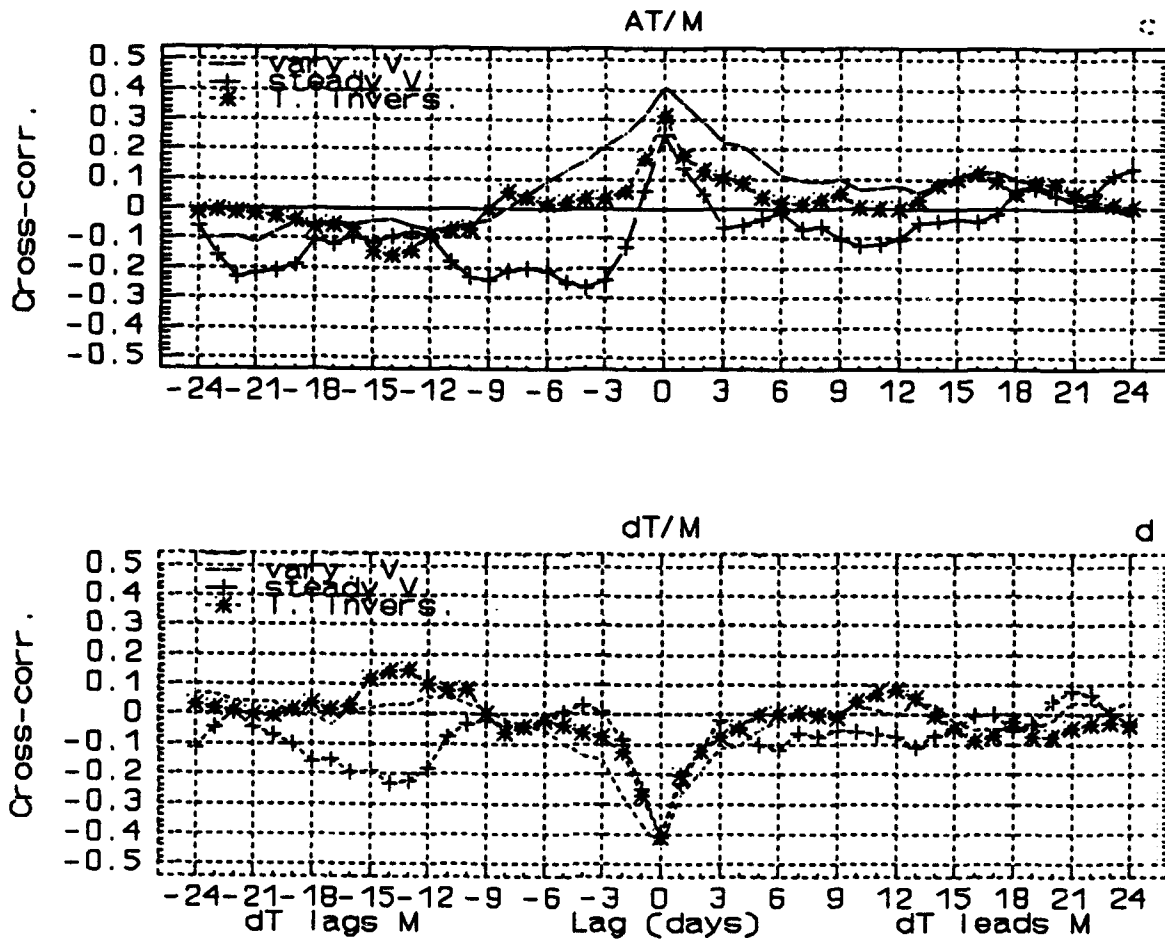


Fig. 24. (Continued) Easterly wind sub-regions cross-correlations of: a) AT/M, and b) dT/M. Each plot depicts the varying V, steady V, and ocean temperature inversion regions.

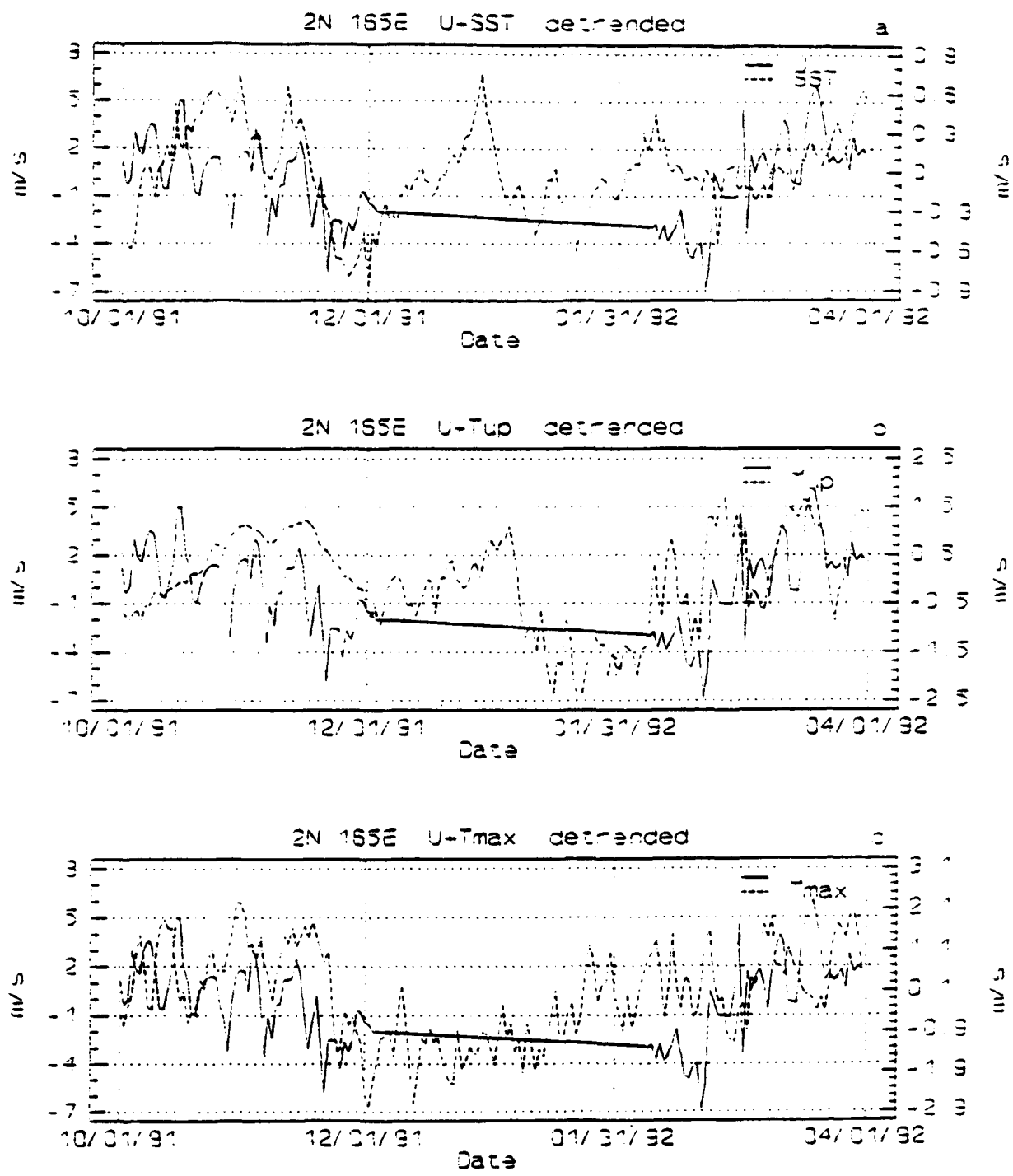


Fig. 25. U/ocean temp. relations at 2°N 165°E, within transition region. Time series of detrended U and overlaid: a) SST, b) Tup, and c) Tmax. Long straight lines are data gaps.

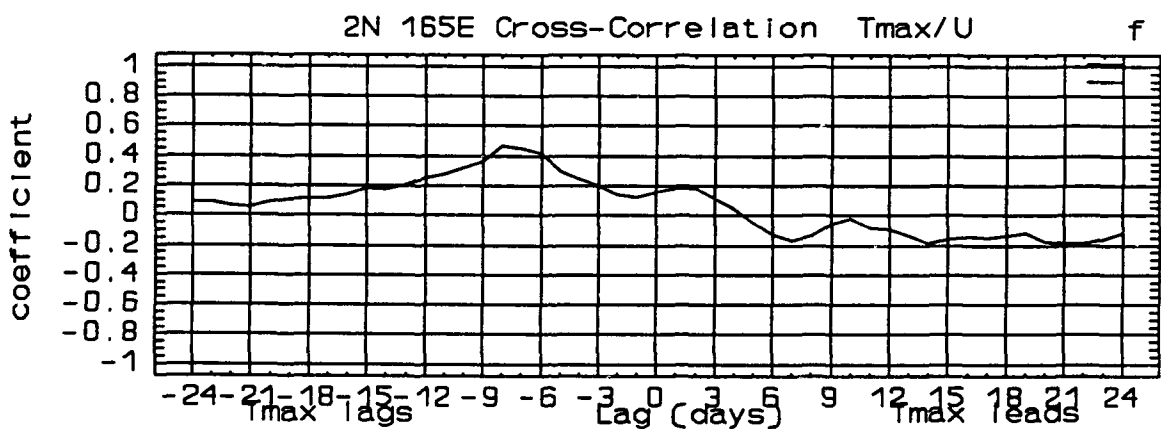
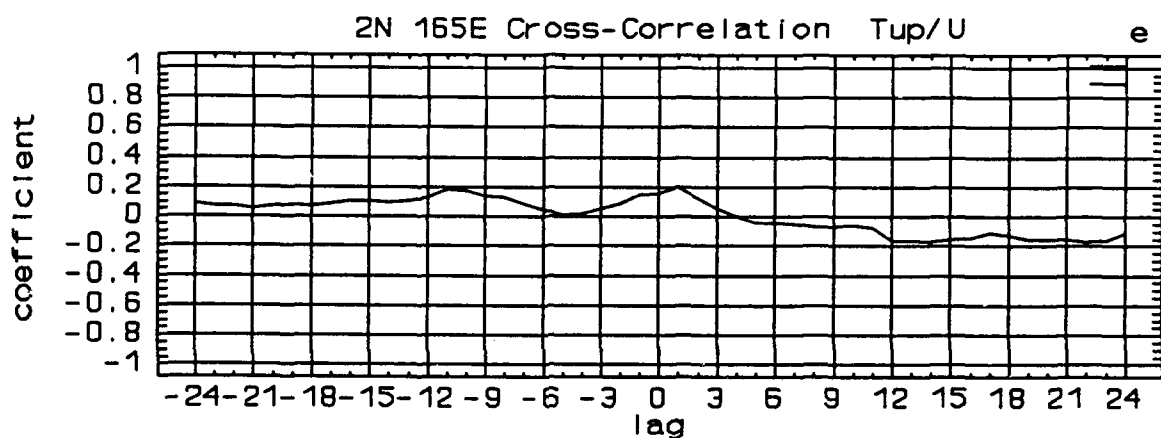
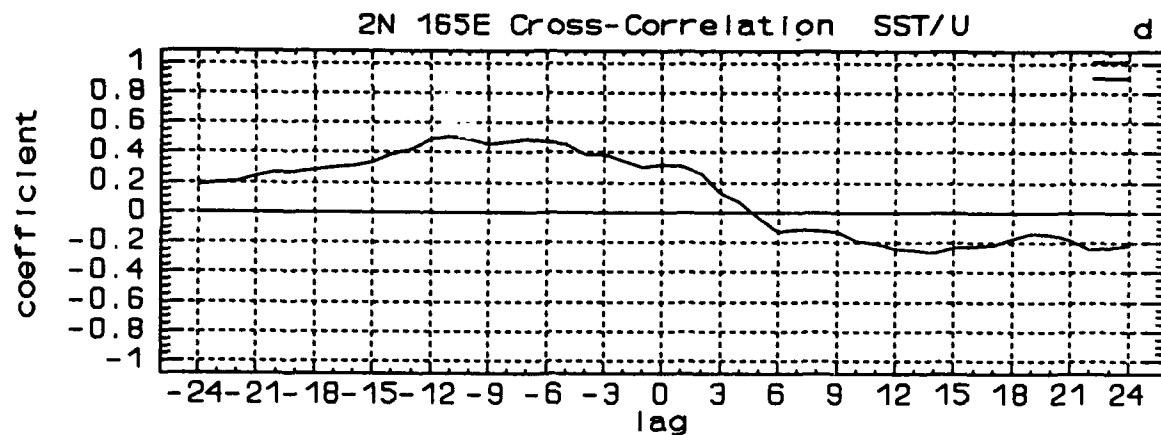


Fig. 25. (Continued) Transition region zonal wind relations at 2°N 165°W. Correlations of detrended: d) SST/U, e) T_{up}/U , and f) T_{max}/U .

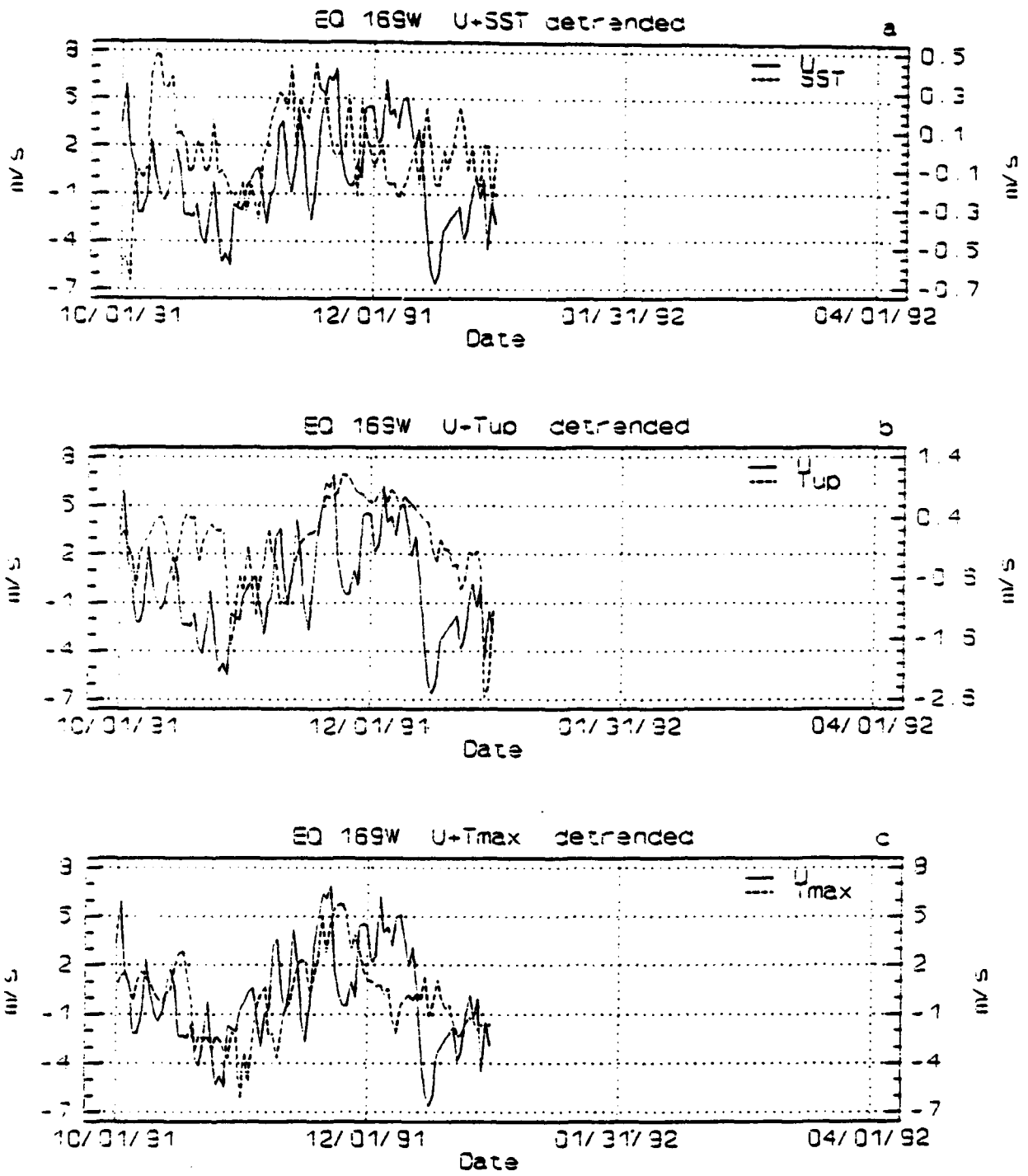


Fig. 26. U/ocean temp. relations at EQ 170°W in the transition region. Time series of detrended U and overlaid: a) SST, b) T_{up} , and c) T_{max} .

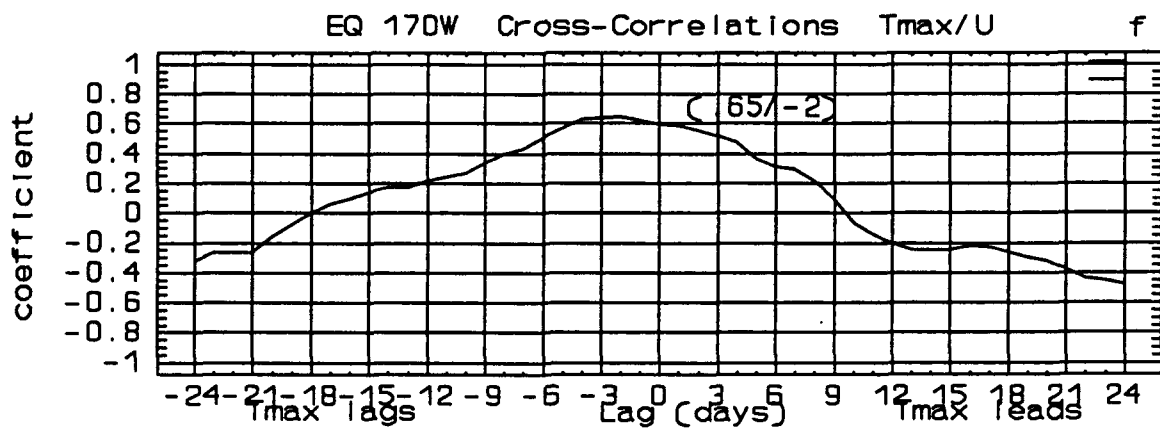
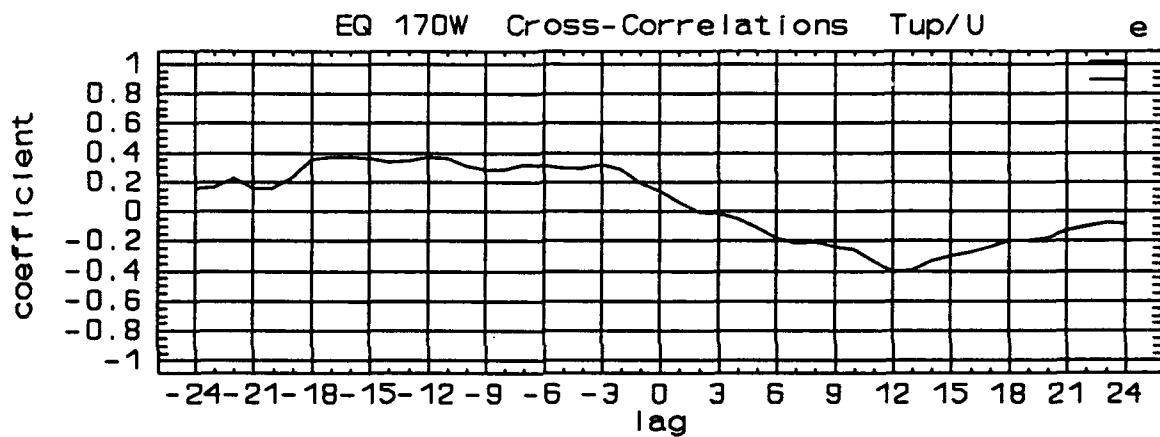
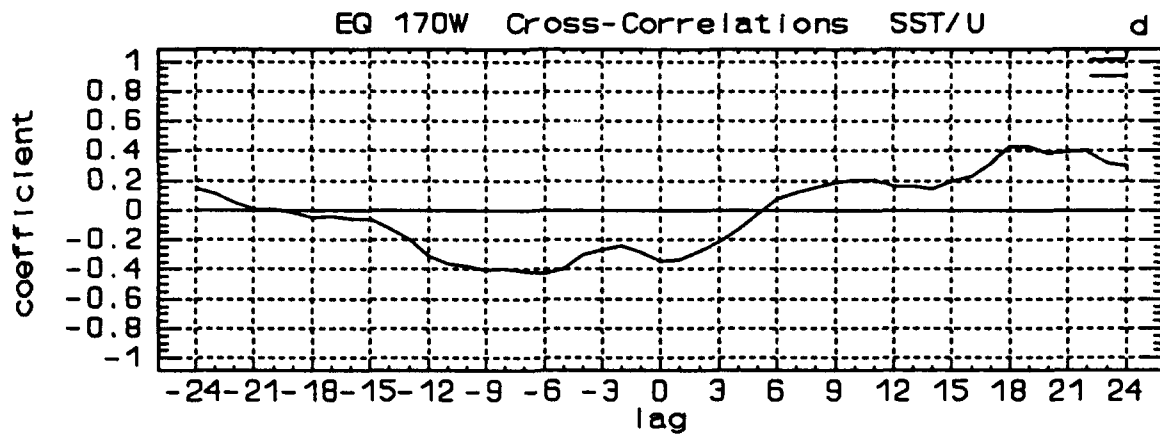


Fig. 26. (Continued) Transition region zonal wind relations at EQ 170°W. Correlations of detrended: d) SST/U, e) T_{up}/U, and f) T_{max}/U.

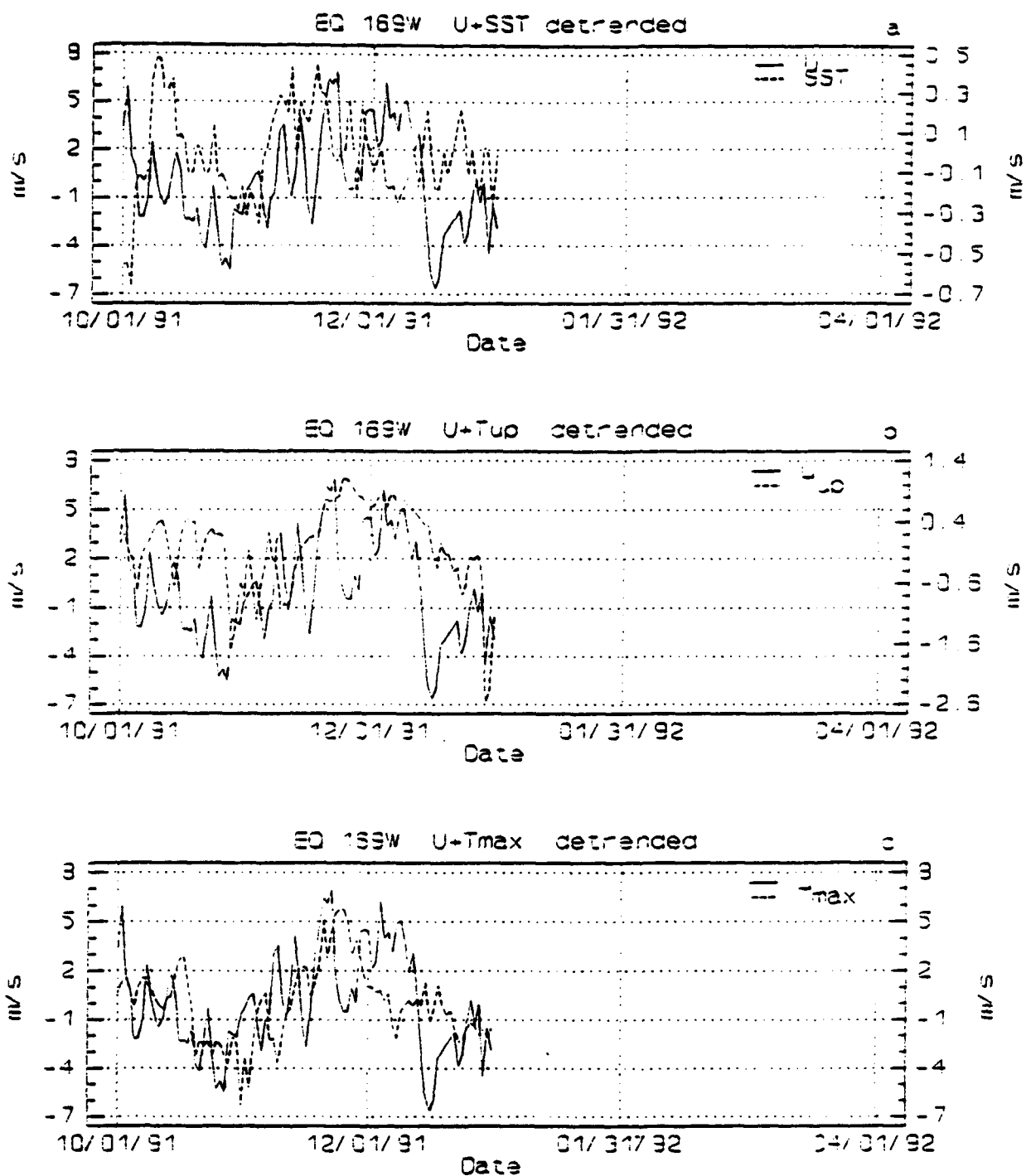


Fig. 27. U/wind relations at EQ 169°W in the transition region. Time series of detrended U and overlaid: a) SST, b) T_{up} , and c) T_{max} . Long straight lines are data gaps.

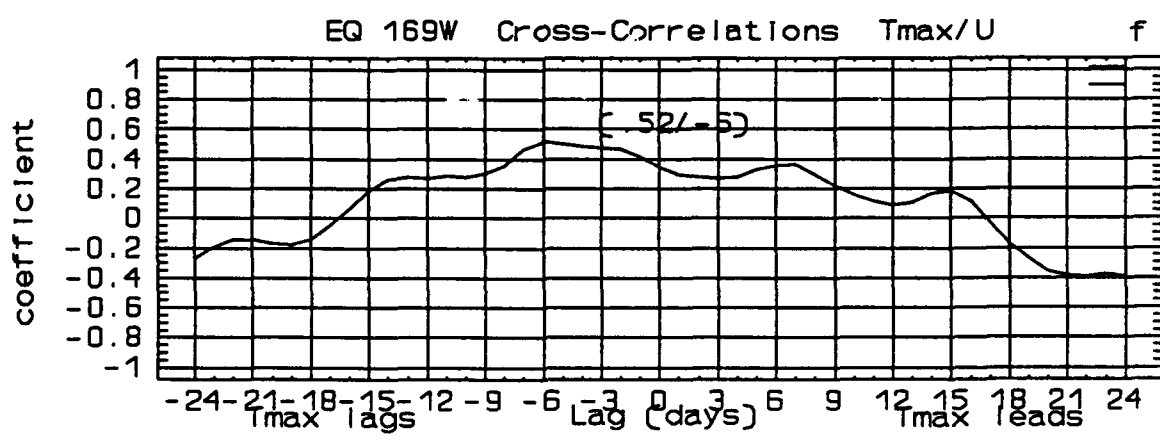
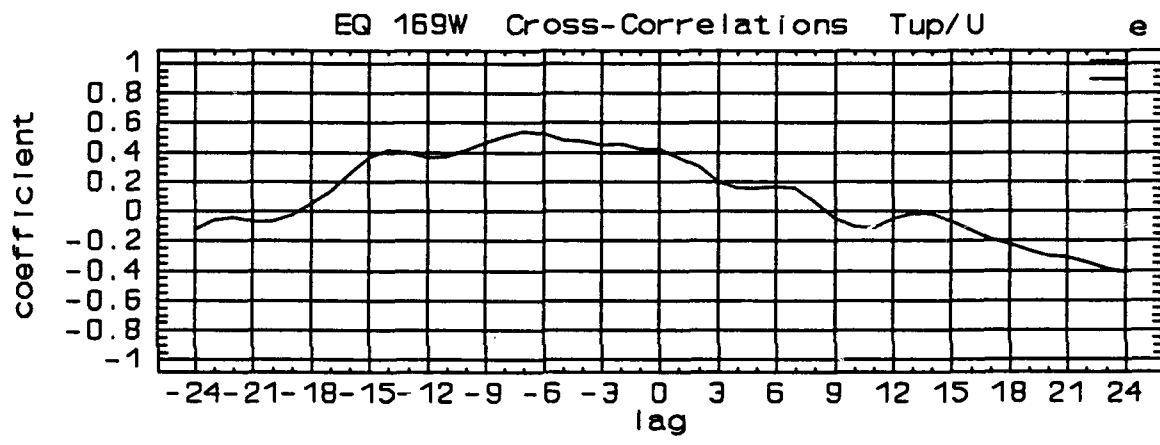
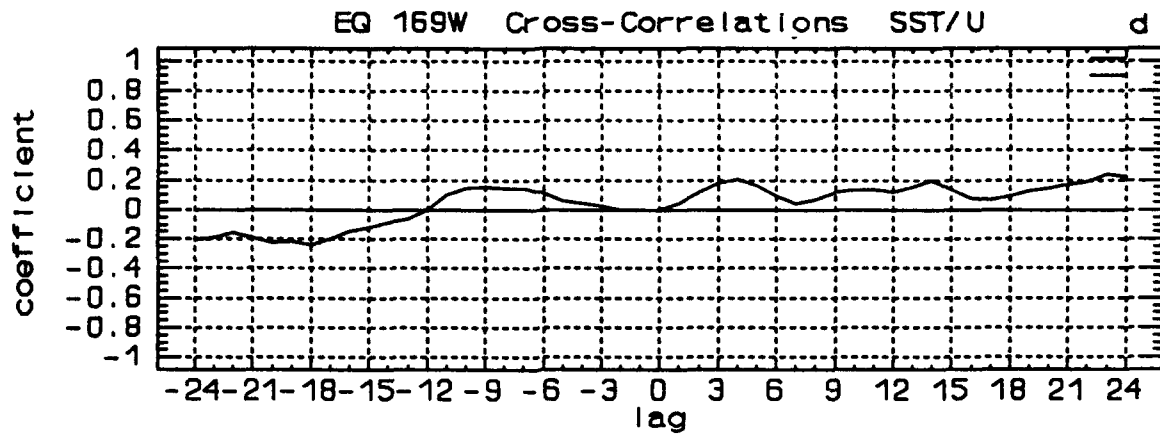


Fig. 27. (Continued) Transition region zonal wind relations at EQ 169°W. Correlations of detrended: d) SST/U, e) T_{up}/U, and f) T_{max}/U.

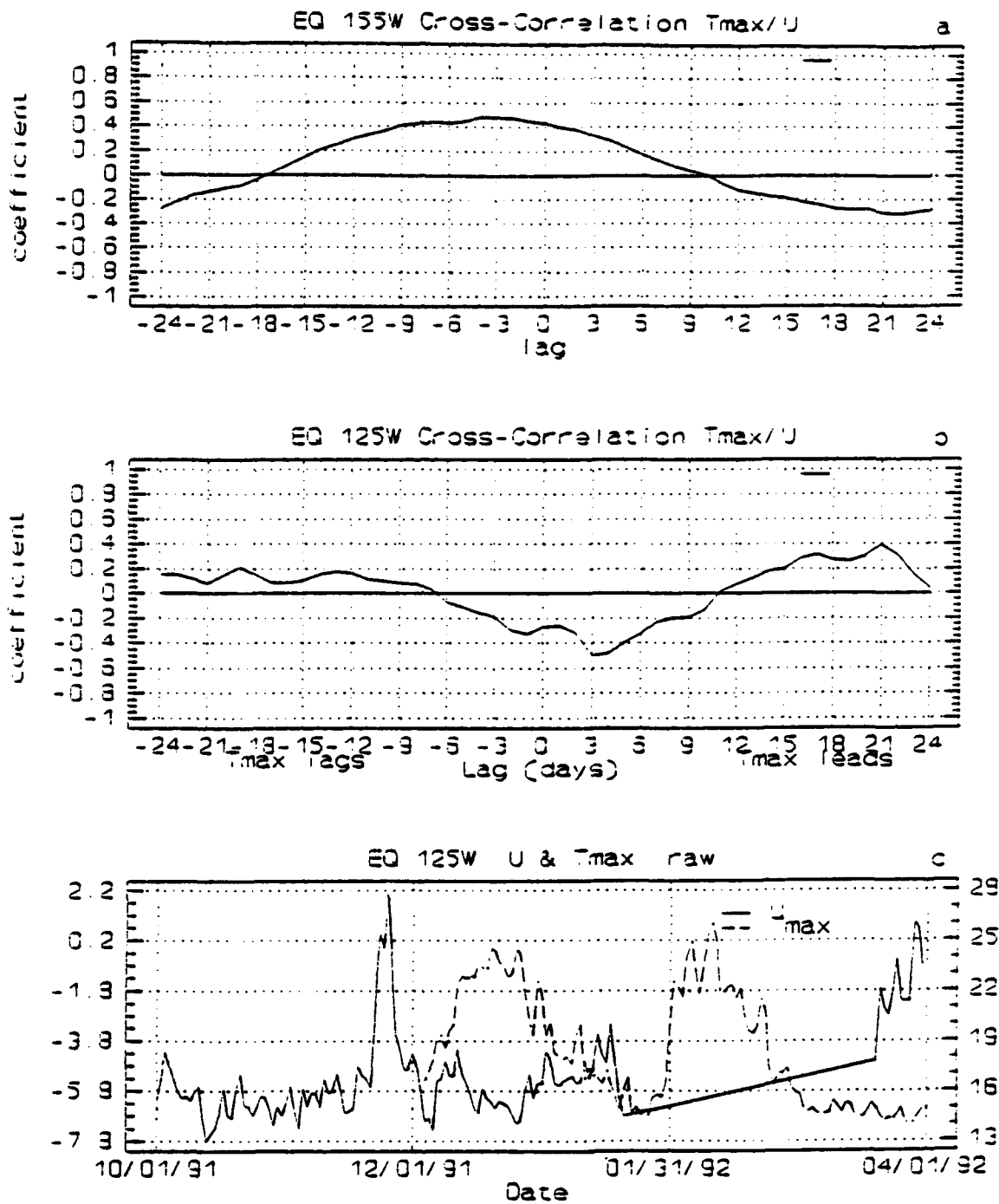


Fig. 28. Raw Tmax/U correlations for: a) EQ 155°W, and b) EQ 125°W. Panel c) is the overlaid time-series of U and Tmax for EQ 125°W. Long straight line is a data gap.

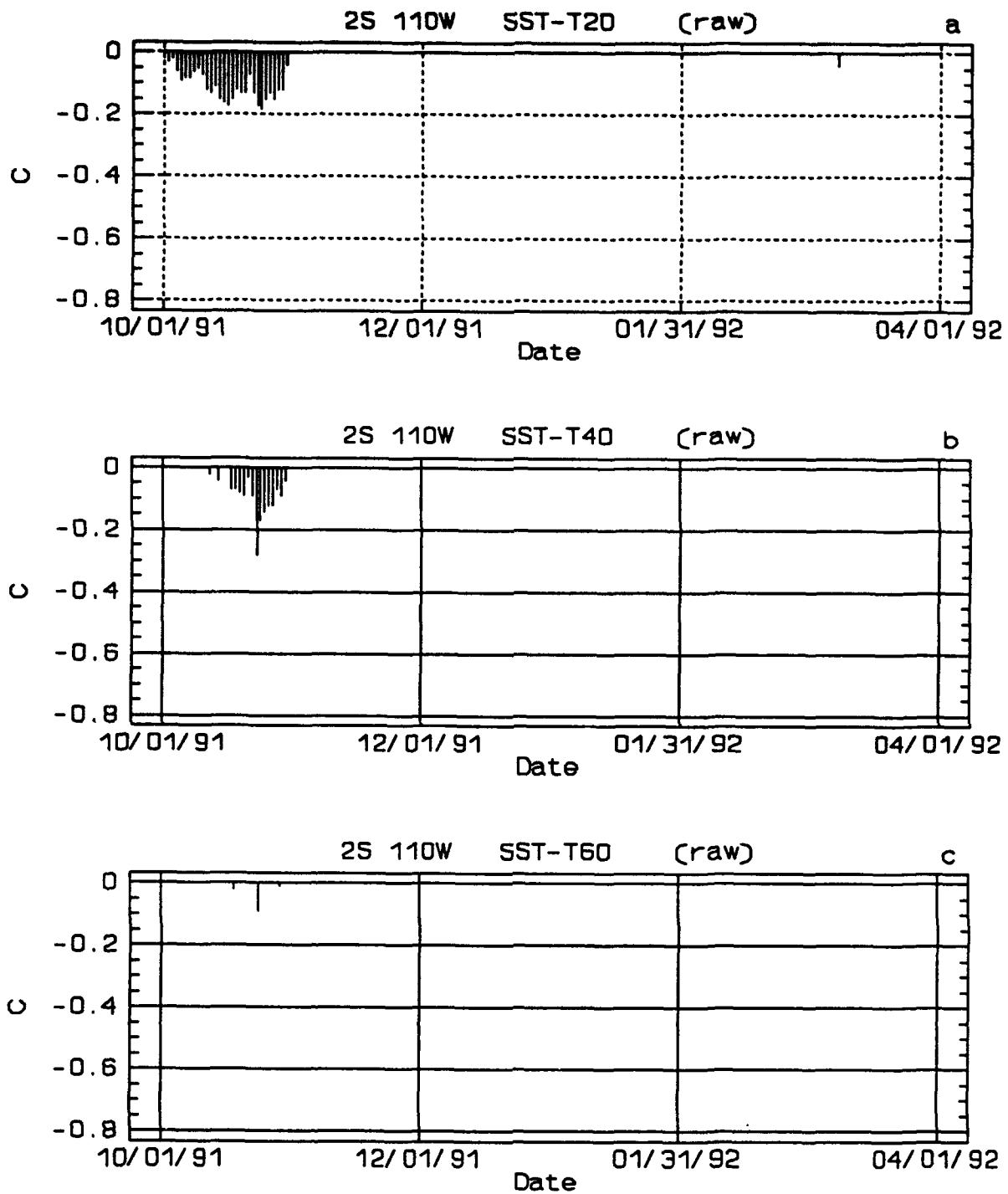


Fig. 29. Inversion at 2°N 110°W. Time series of raw SST - deeper temps.: a) T20, b) T40, and c) T60. Only negative differences, indicating an inversion, are shown.

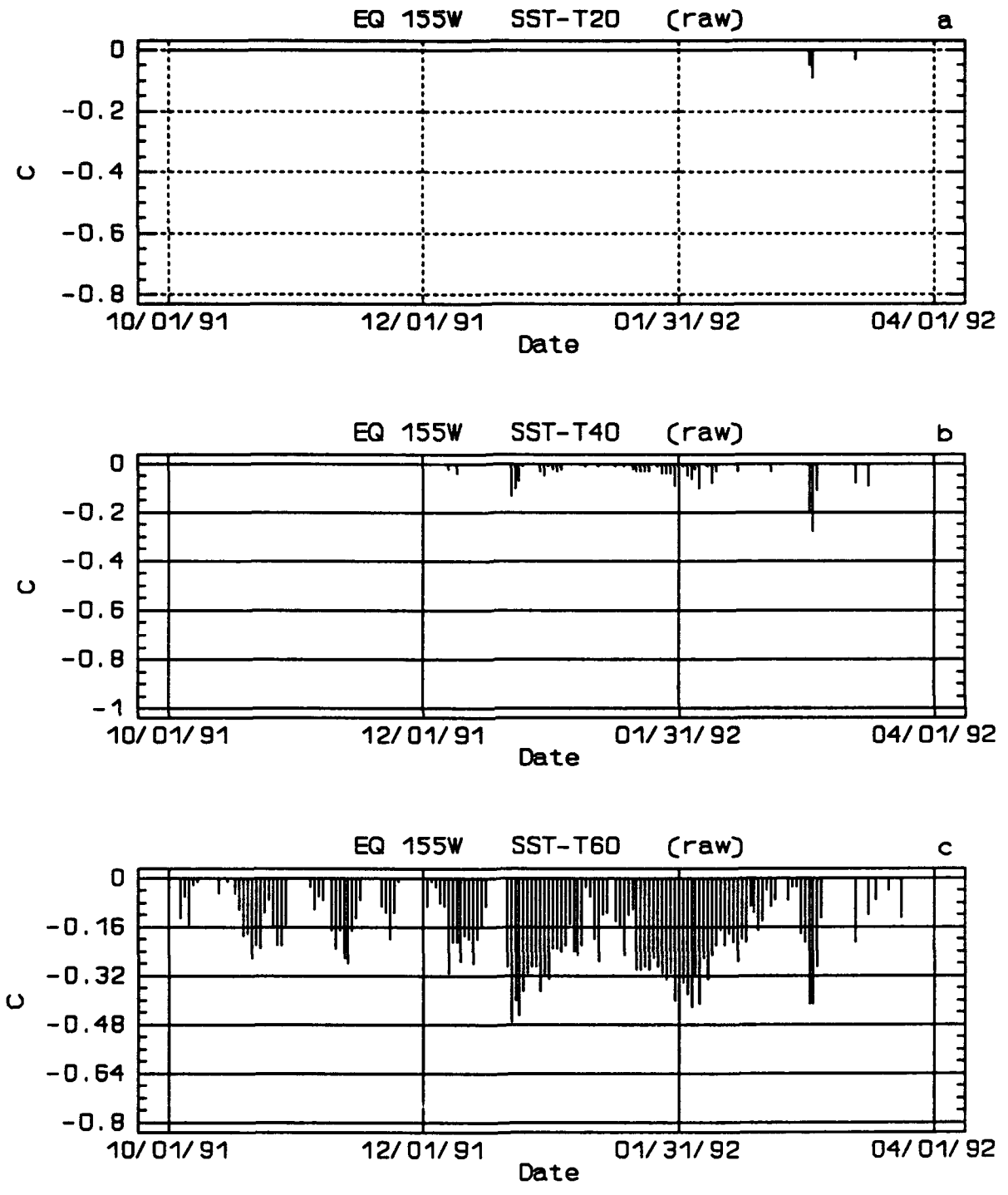


Fig. 30. Inversion at EQ 155°W. Time series of differences between raw SST and deeper temps: a) T20, b) T40, c) T60, d) T80, e) T100, f) T120, g) T140, and h) T180. Only negative differences are shown.

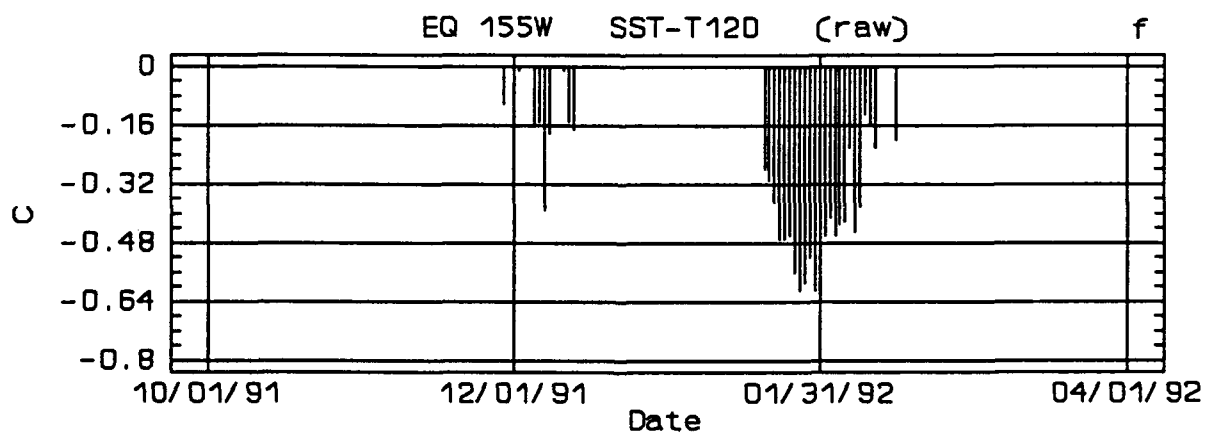
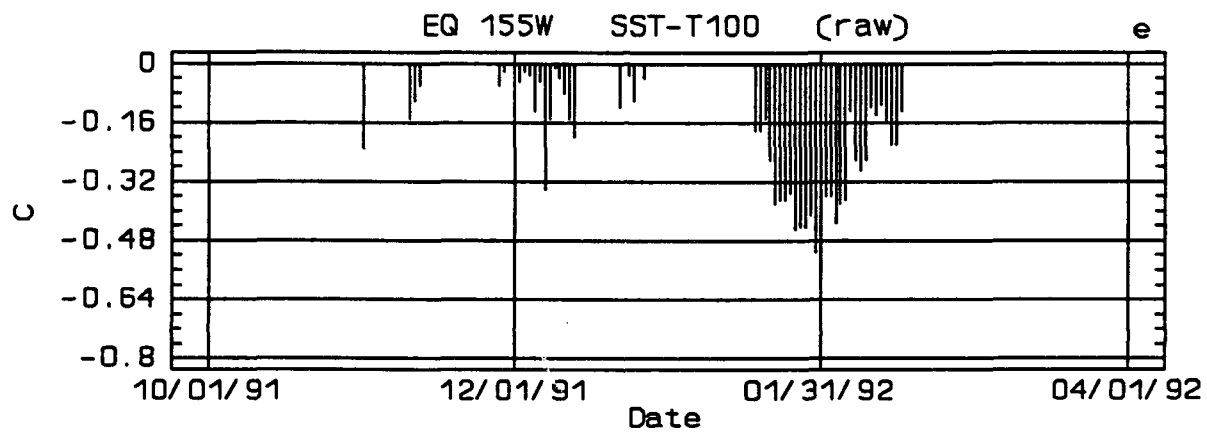
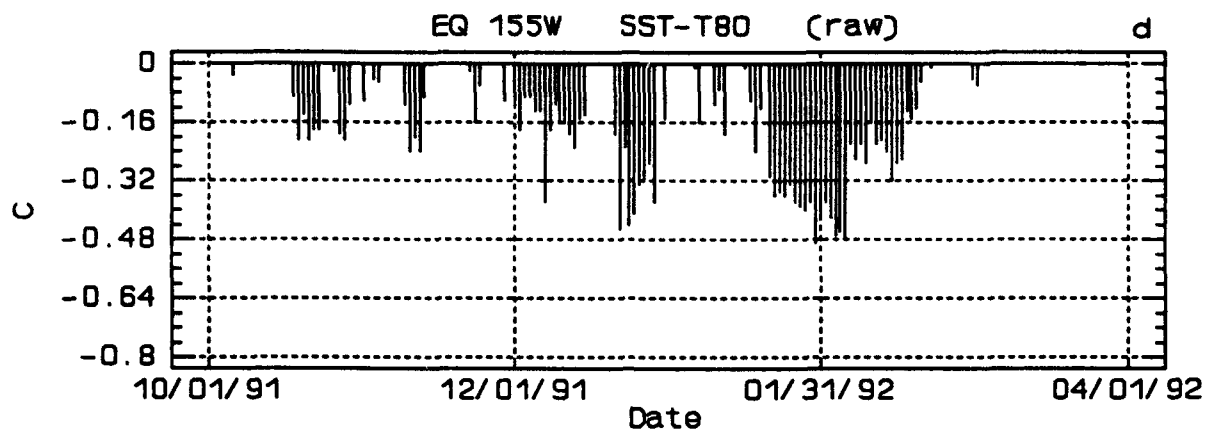


Fig. 30. (Continued)

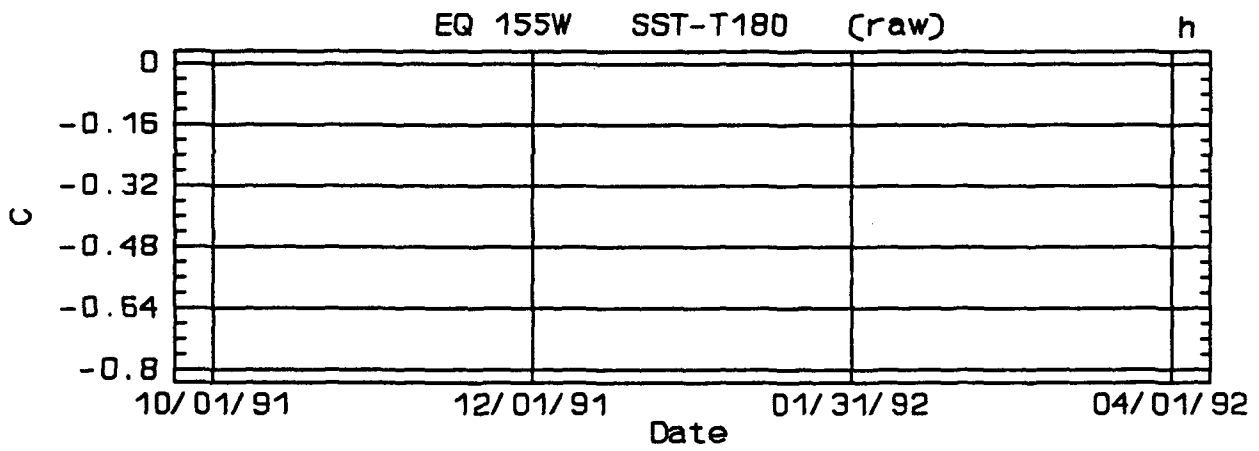
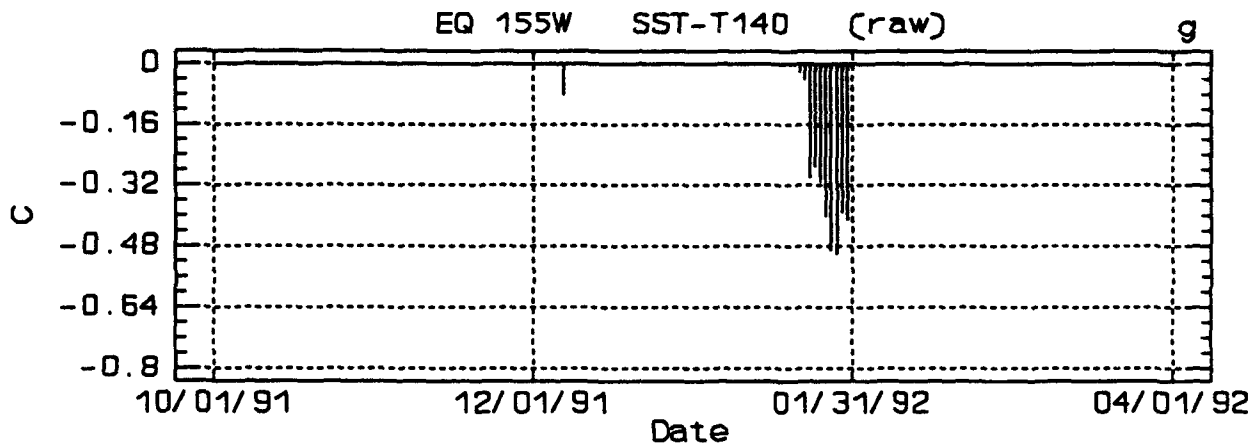


Fig. 30. (Continued)

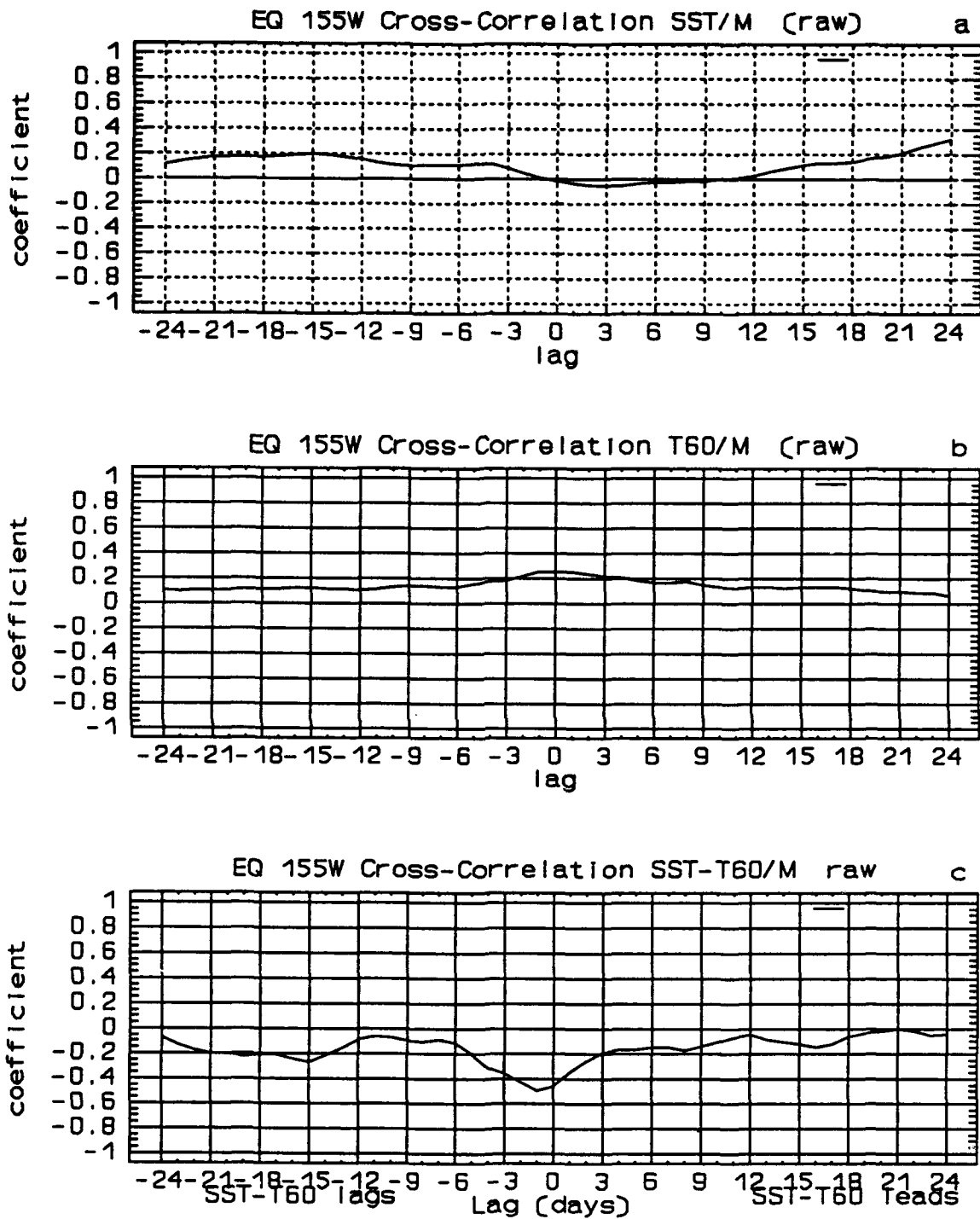


Fig. 31. Inversion related correlations at EQ 155°W. Correlations based on raw time series: a) SST/M, b) T60/M, and c) SST-T60/M.

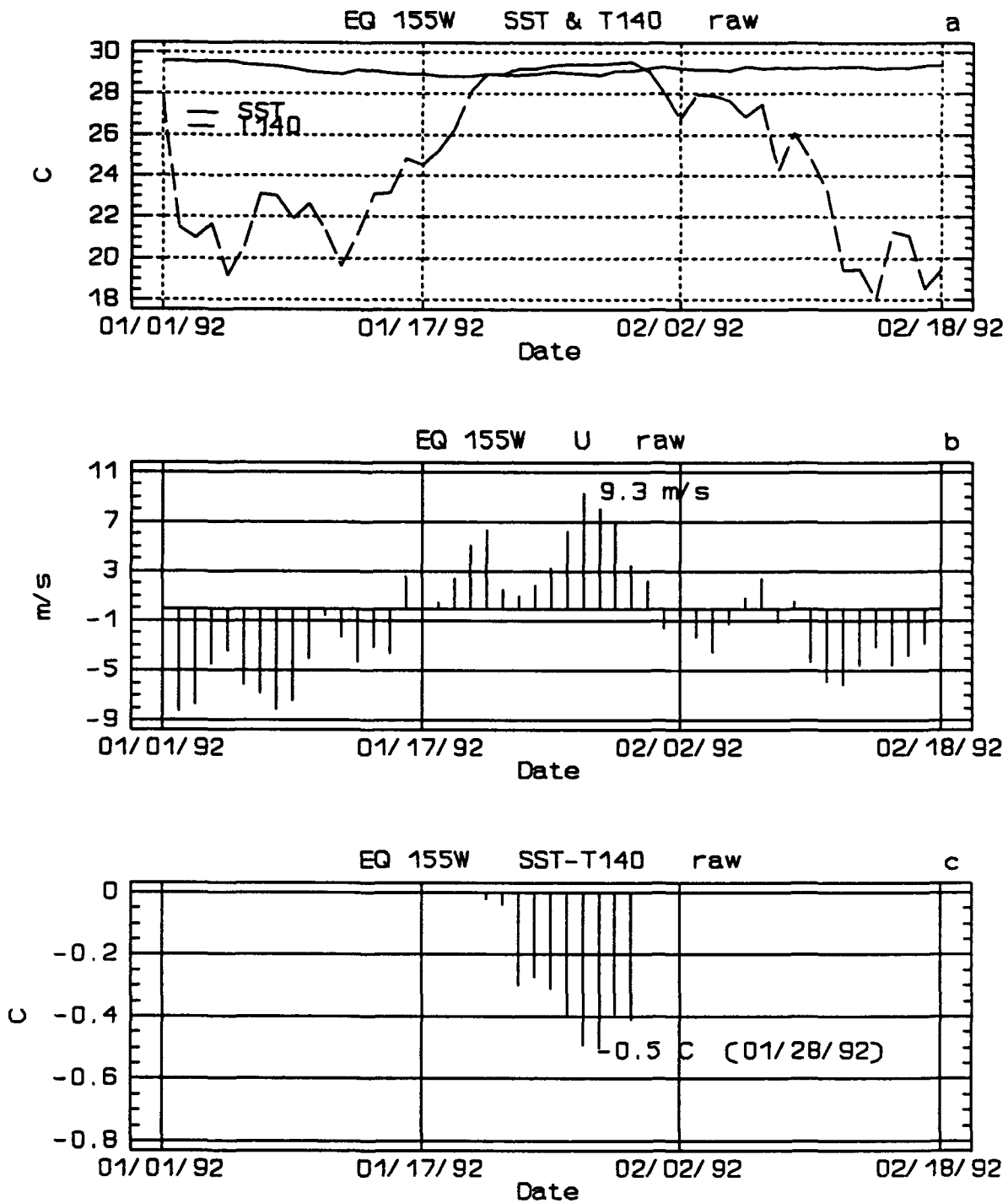


Fig. 32. Inversion related raw time series at EQ 155°W: a) SST & T140, b) U, and c) SST-T140. Note how inversion between SST and T40 was due to small SST decrease and large T140 increase.

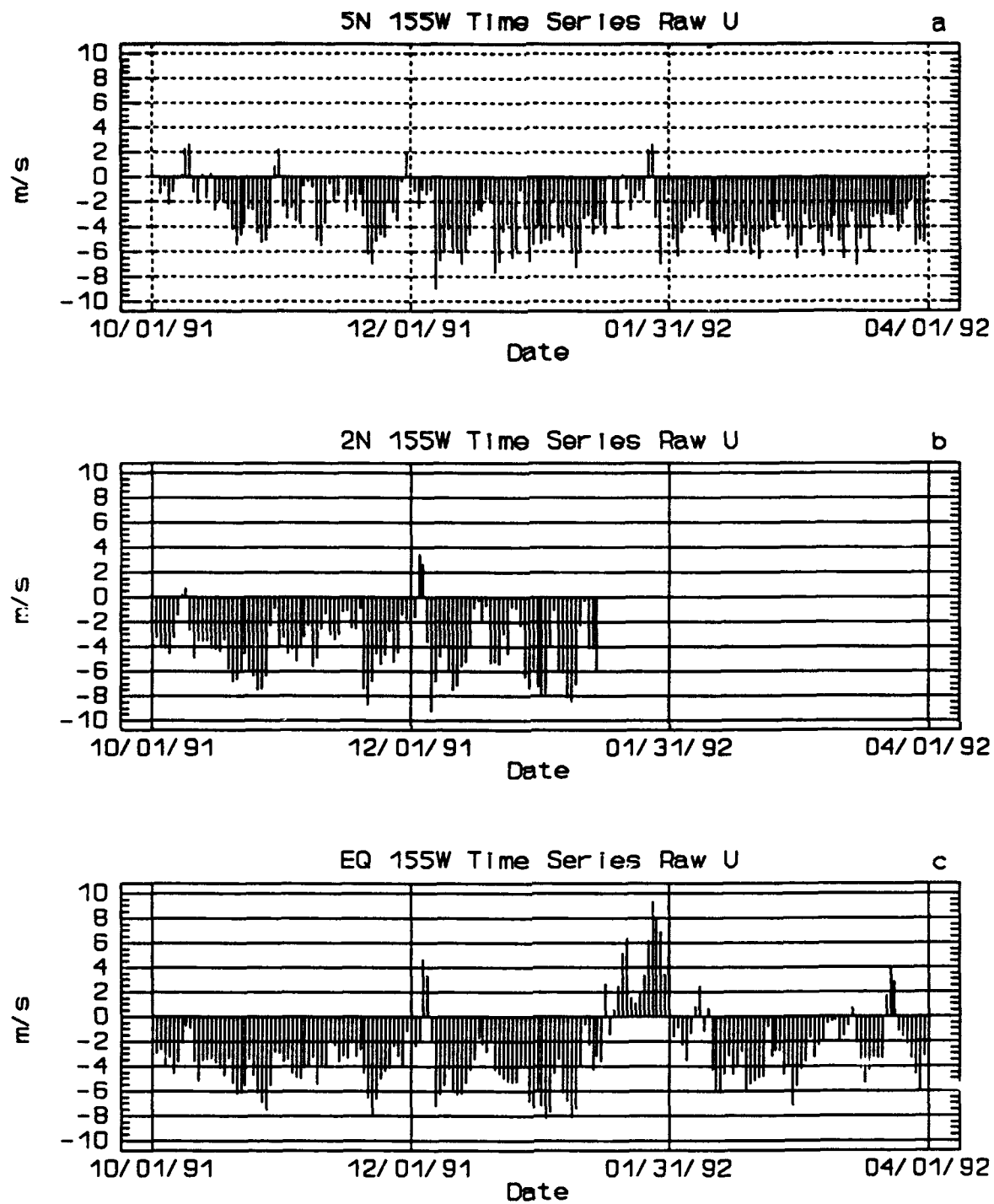


Fig. 33. Time series of raw U at: a) 5°N 155°W, b) 2°N 155°W, c) EQ 155°W. Note that wind shear around 30 Jan. created positive vorticity region north of equator.



Fig. 34. Satellite infrared (IR) image on 25 Jan. 92 of inversion region. Region is located around EQ 155°W. 155°W runs through Hawaii. Note convective activity over and north of inversion region.

↑ 16:01 27JAN92 29A-Z 0050-1640 GMT



Fig. 35. Satellite infrared (IR) image of inversion region on 27 Jan. 92, the date of the highest wind speeds recorded at EQ 155°W. 155°W runs through Hawaii.

↑ 19:01 30JA92 29A-Z 0090-1640 CD1 ↓

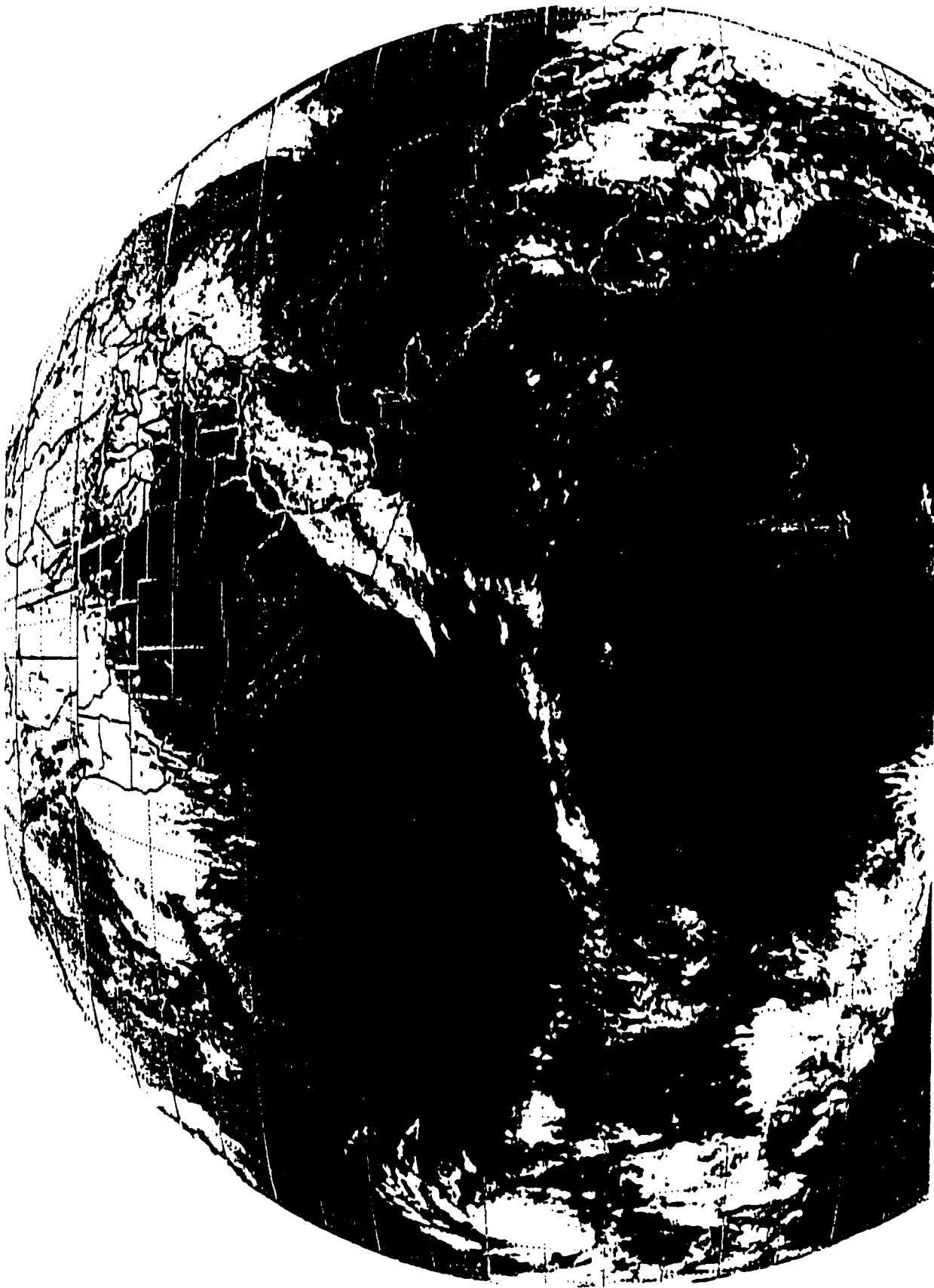


Fig. 36. Satellite infrared (IR) image of inversion region on 30 Jan. 92. Note tropical storm Ekeka at 5°N 165°W.

Remote Feedback Cycle

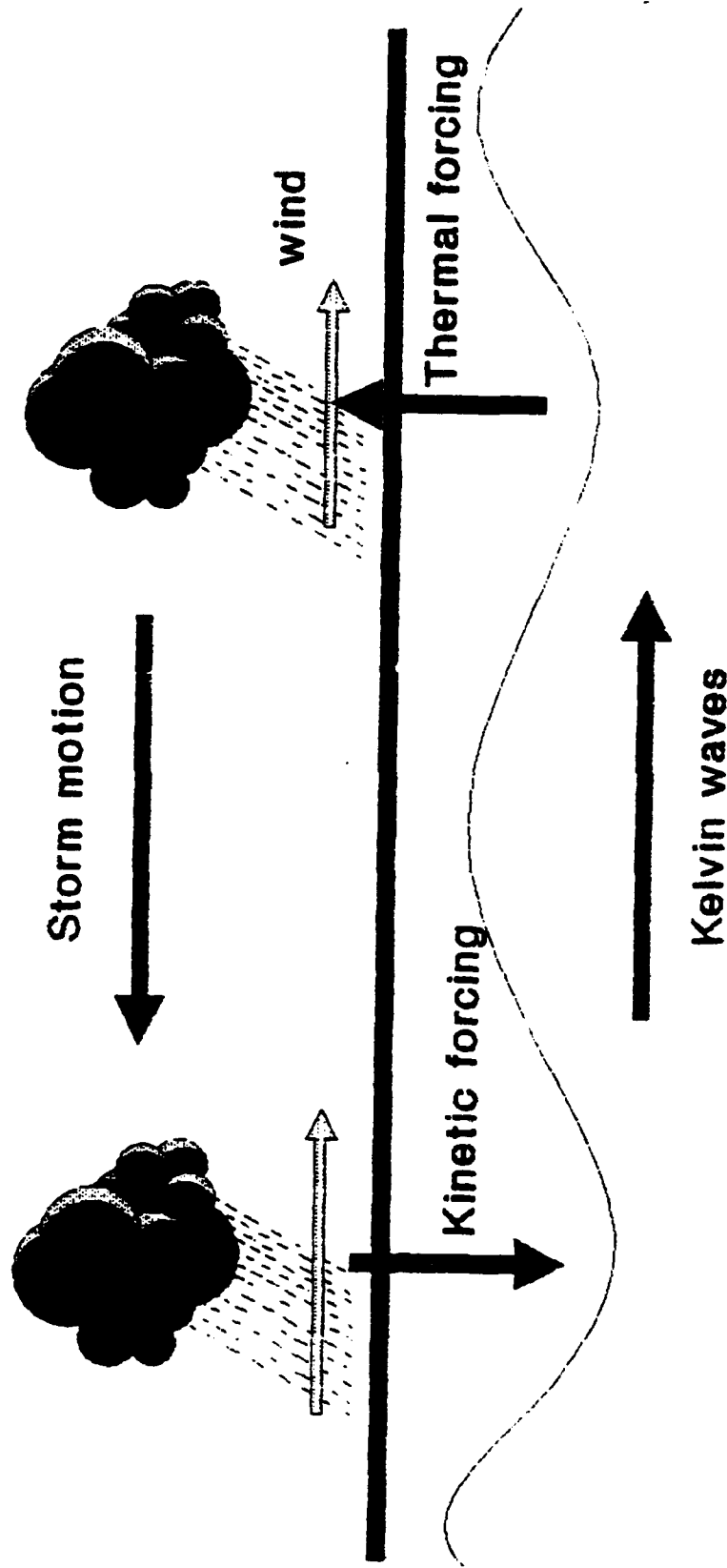
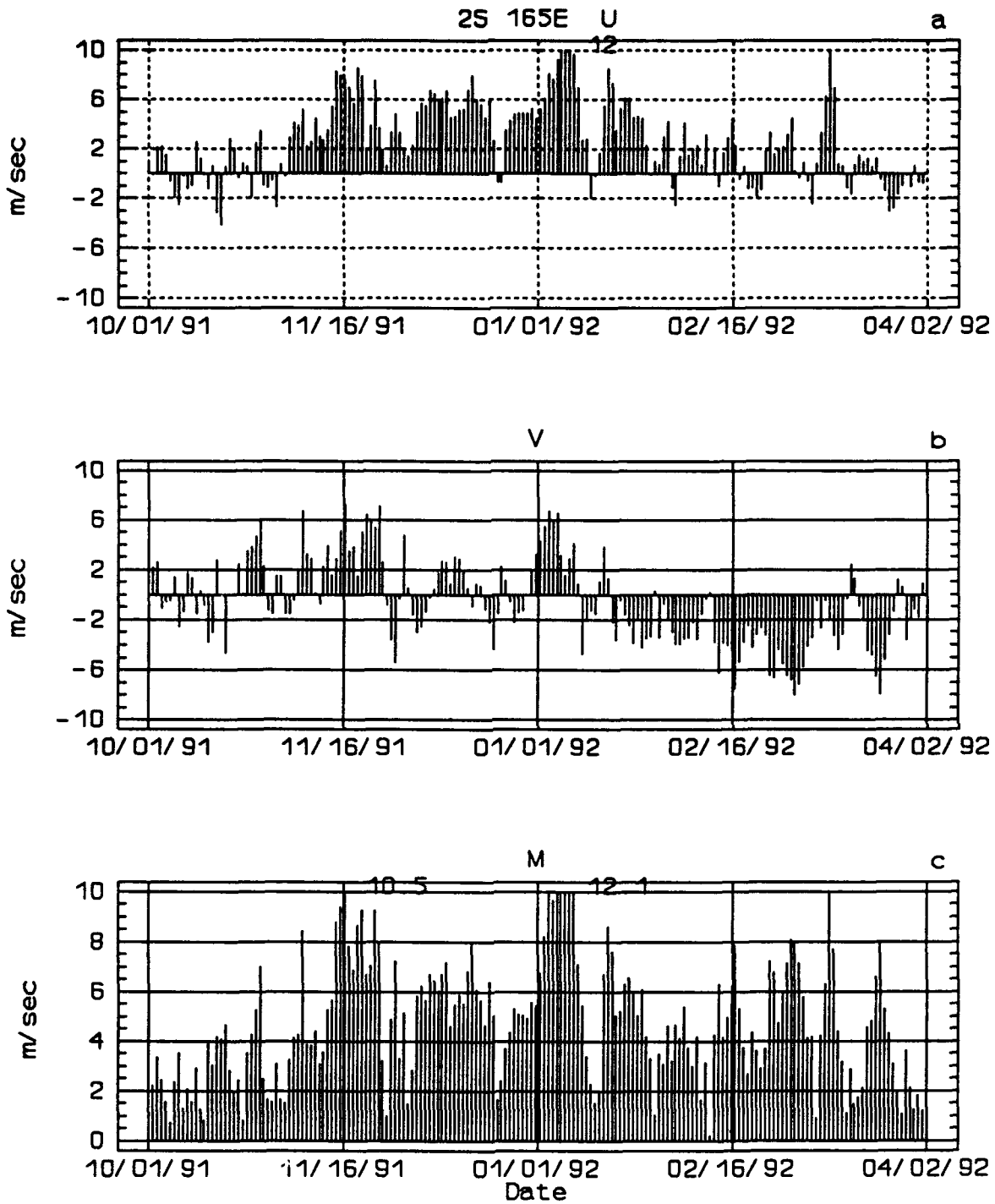
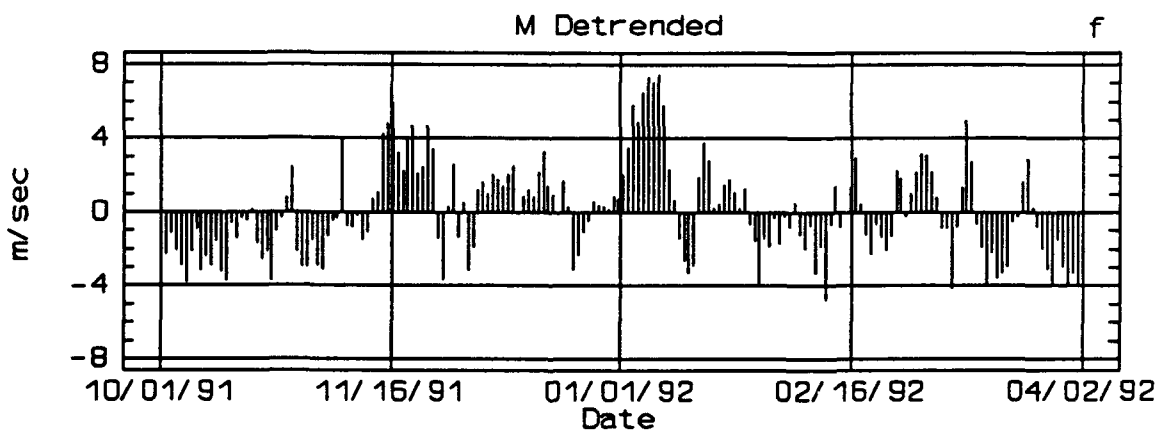
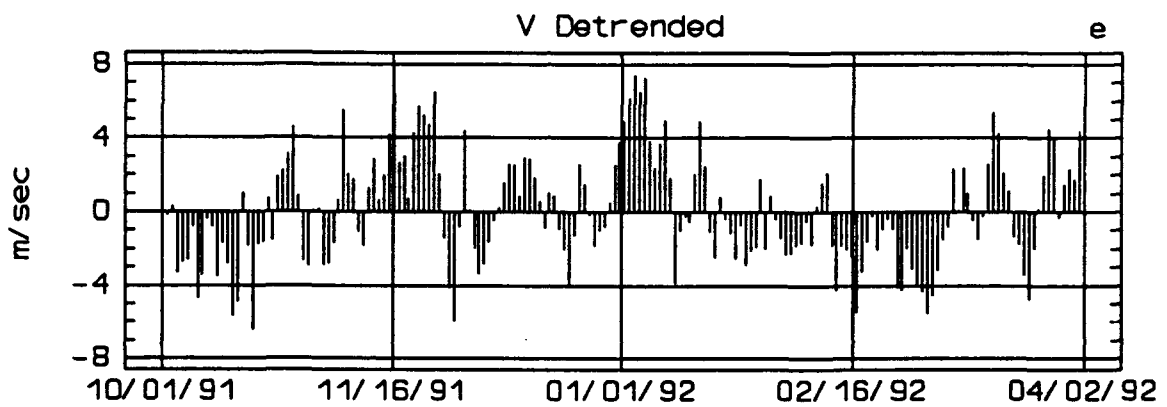
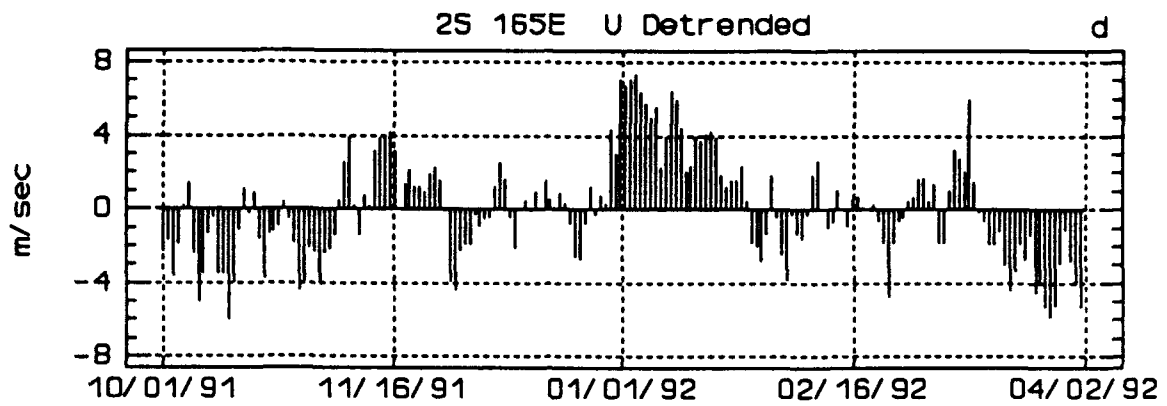


Fig. 37. Remote feedback cycle. Tropical storms in the west Pacific generate Kelvin waves (Cooper 1992). Kelvin waves travel slowly to the east, warming and thickening the mixed layer. Warm, thick, mixed layer leads to atmospheric convection and westerly winds. Westerly winds in central Pacific create positive low level atmospheric vorticity off equator. Warm ocean temperatures and positive vorticity contribute to tropical cyclone formation.

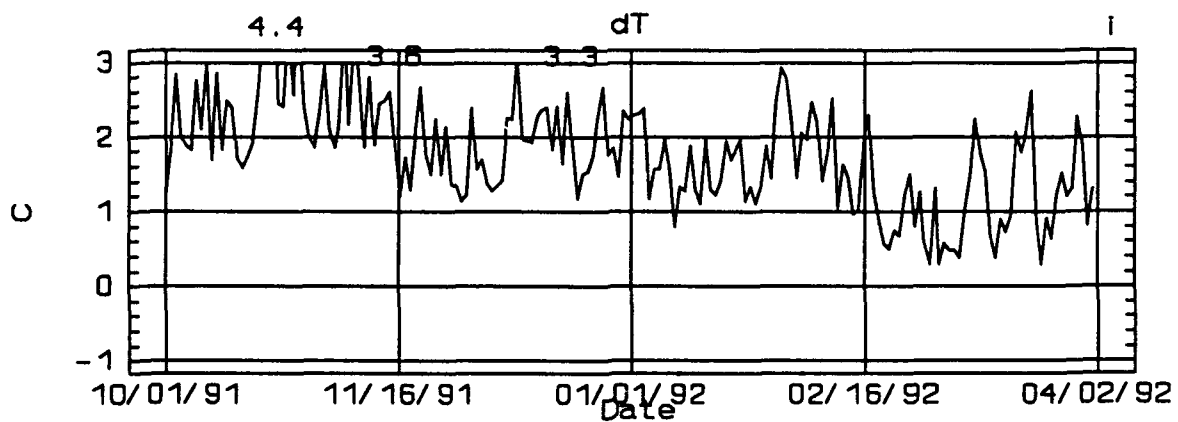
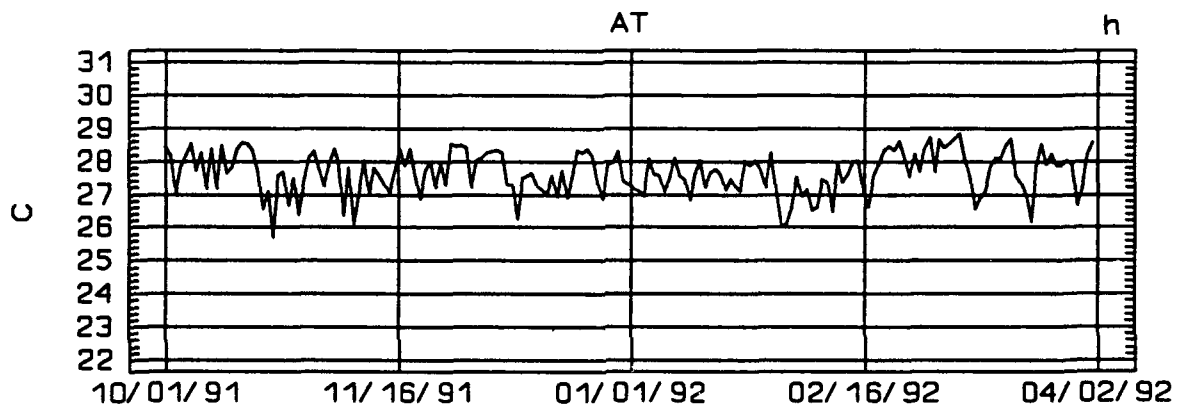
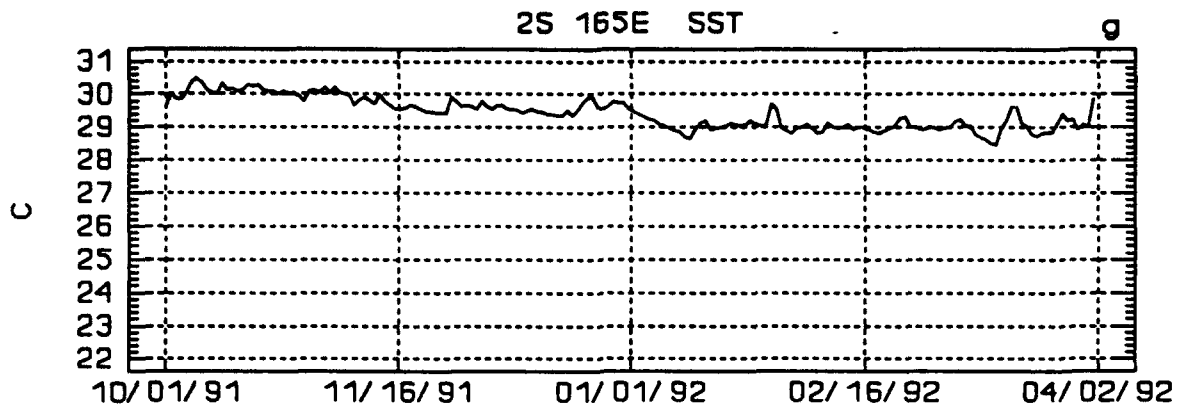
APPENDIX A. 2°S 165°E TIME SERIES



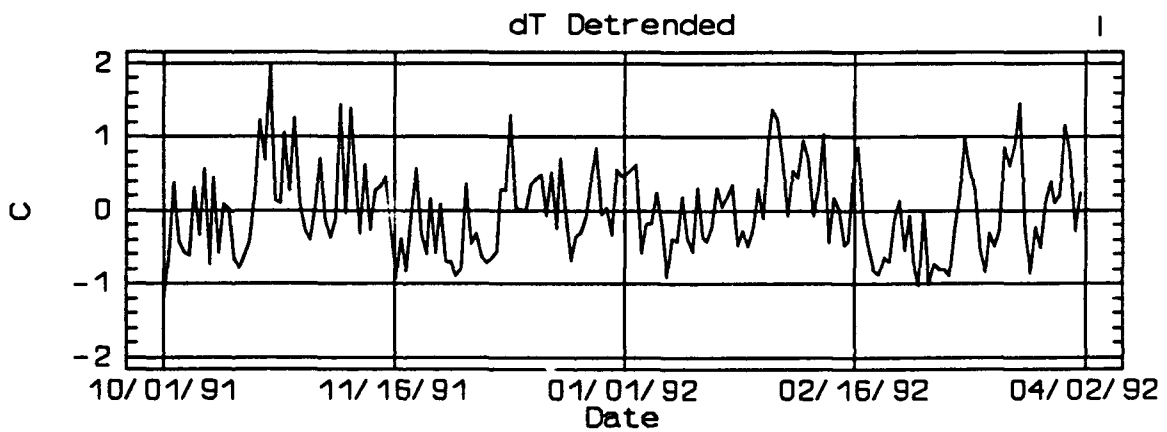
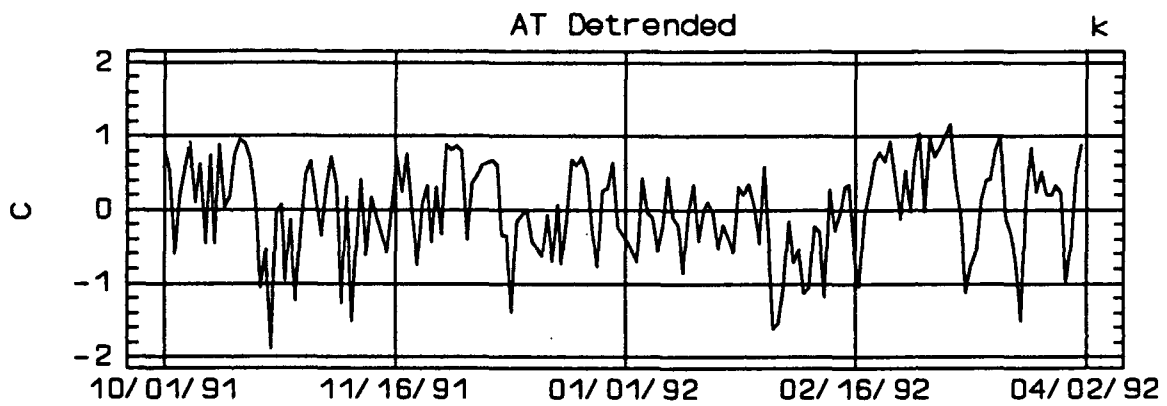
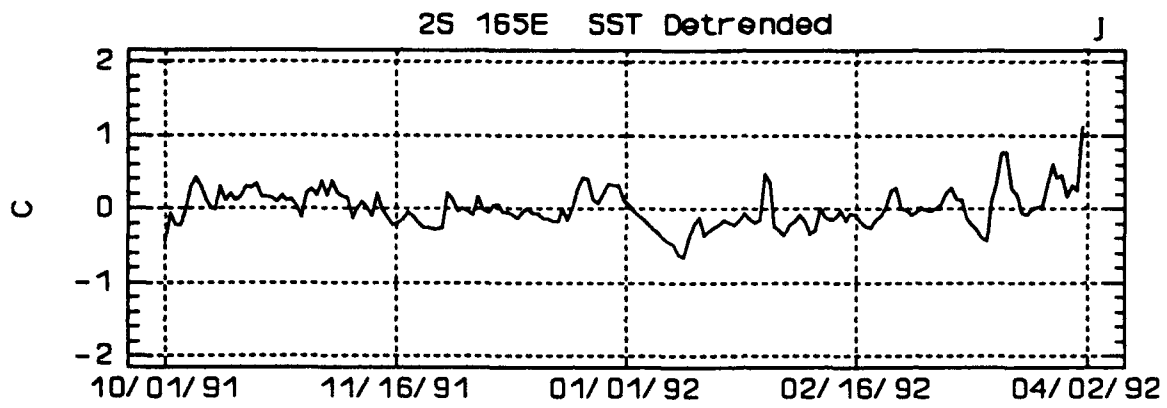
App. A. 2°S 165°E time series, representing all westerly wind region buoys. Time series are of: a) raw zonal wind (U), b) raw meridional wind (V), and c) raw horizontal wind (M).



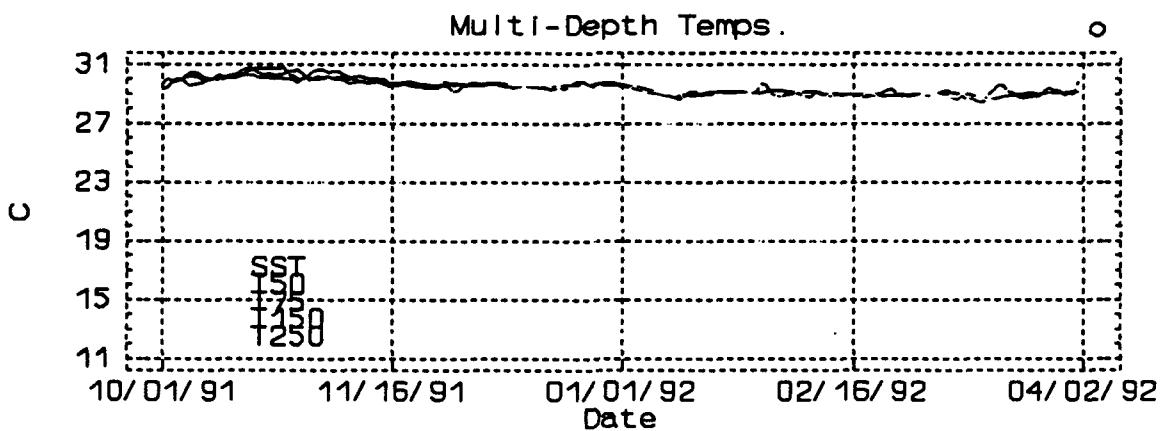
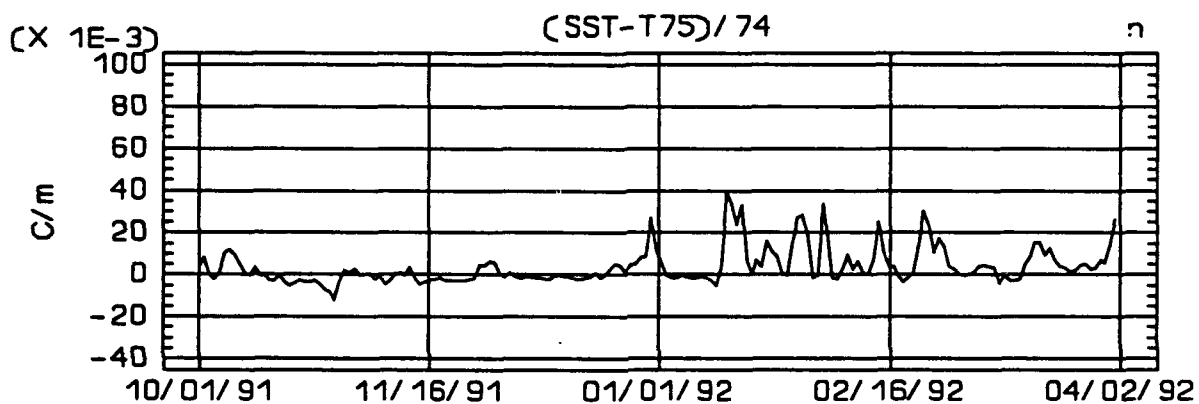
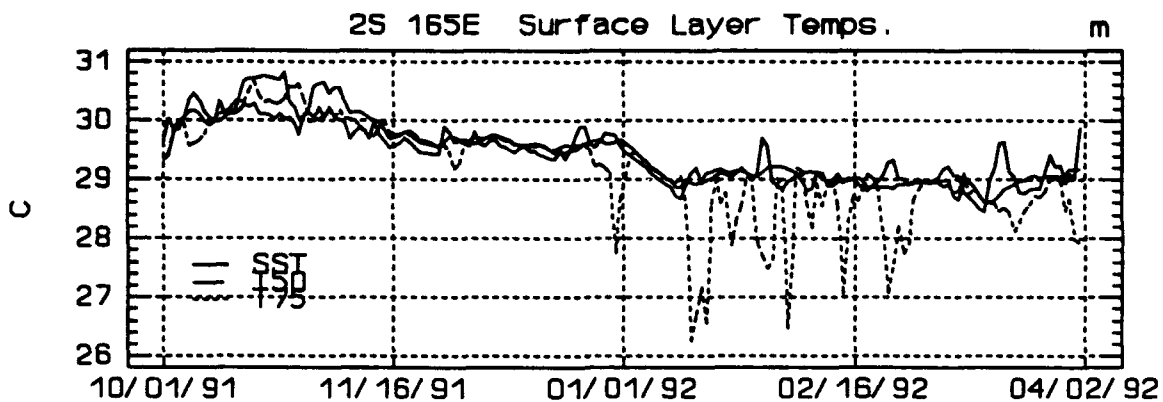
App. A. (Continued) Time series are of: d) detrended U, e) detrended V, and f) detrended M.



App. A. (Continued) Time series are of: g) raw SST, h) raw air temperature (ATFigure 37), and i) raw air-sea temp difference (dT, $dT = SST - AT$).



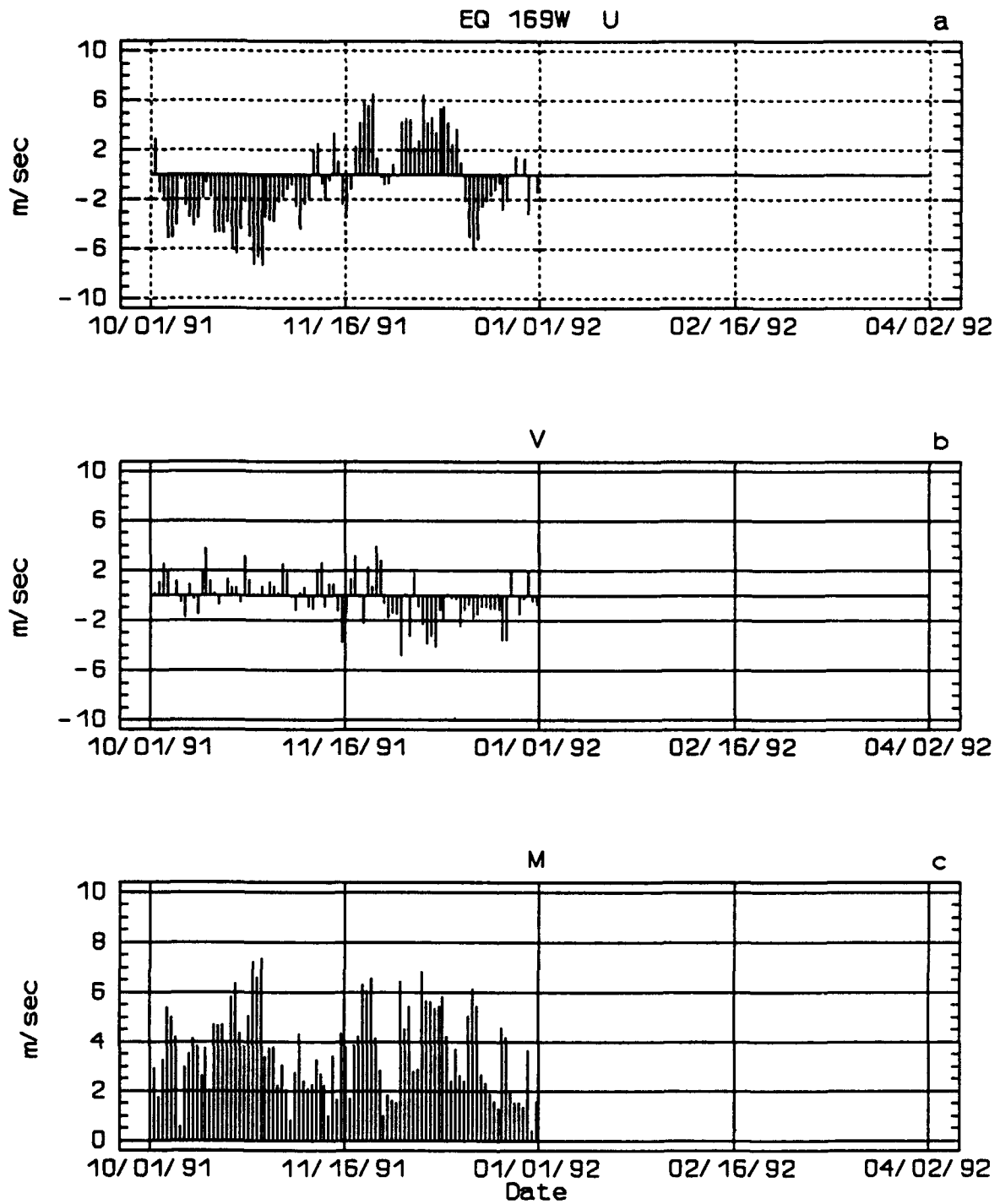
App. A. (Continued) Time series are of: j) detrended SST, k) detrended AT, and l) detrended dT.



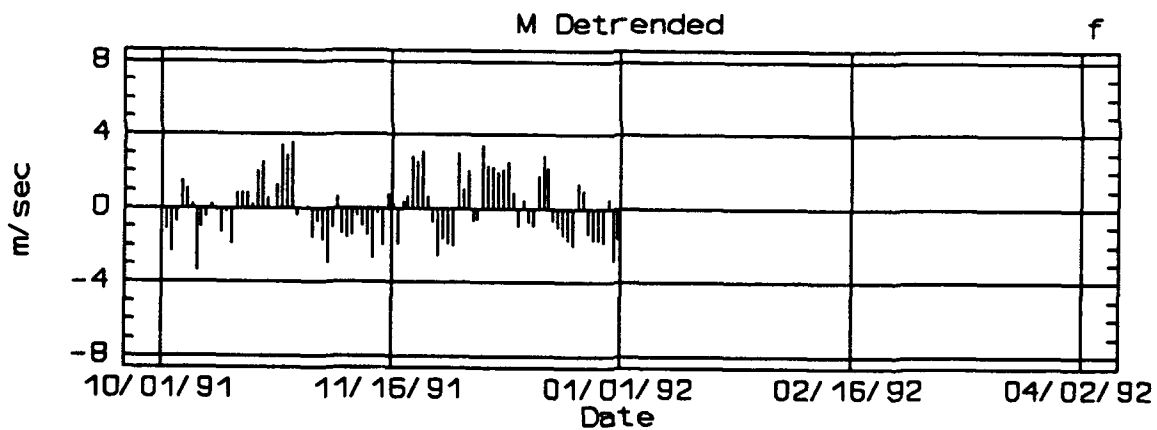
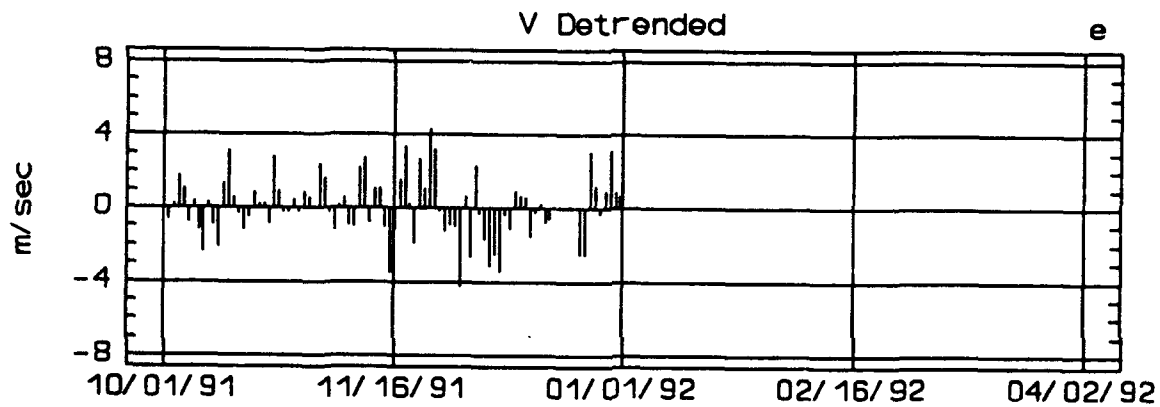
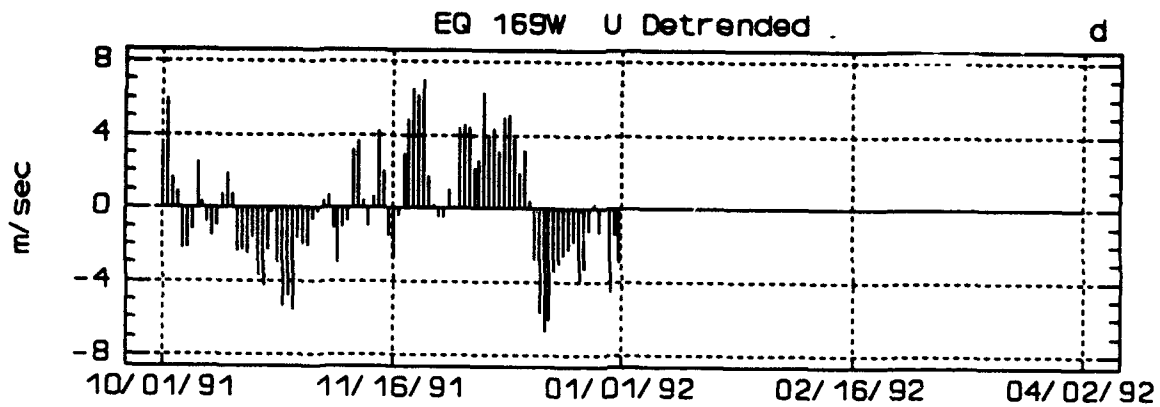
App. A. (Continued) Time series are of: m) surface layer temperatures, n) temperature gradient (TG), and o) multi-depth temperatures.

(Intentionally Blank)

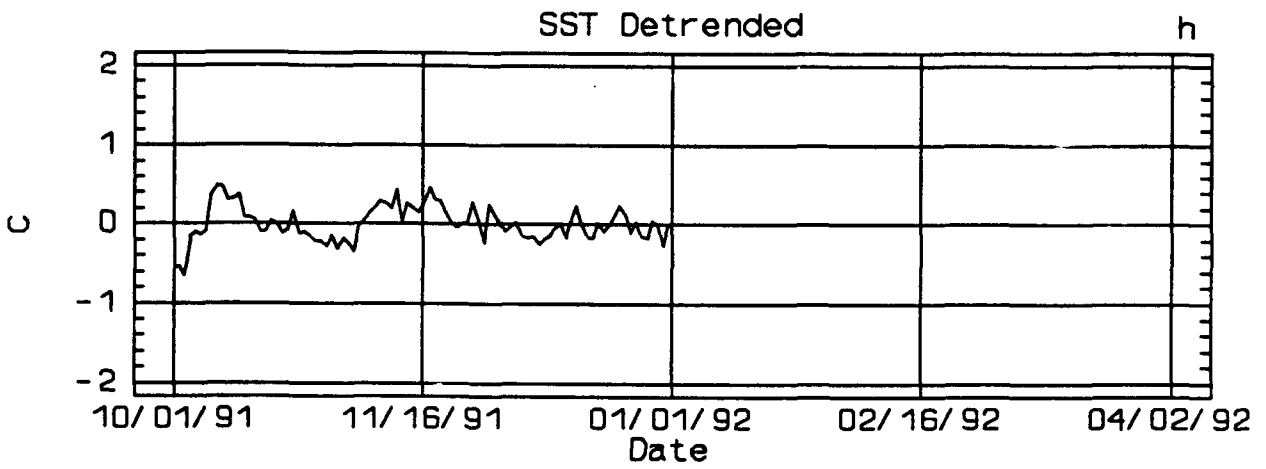
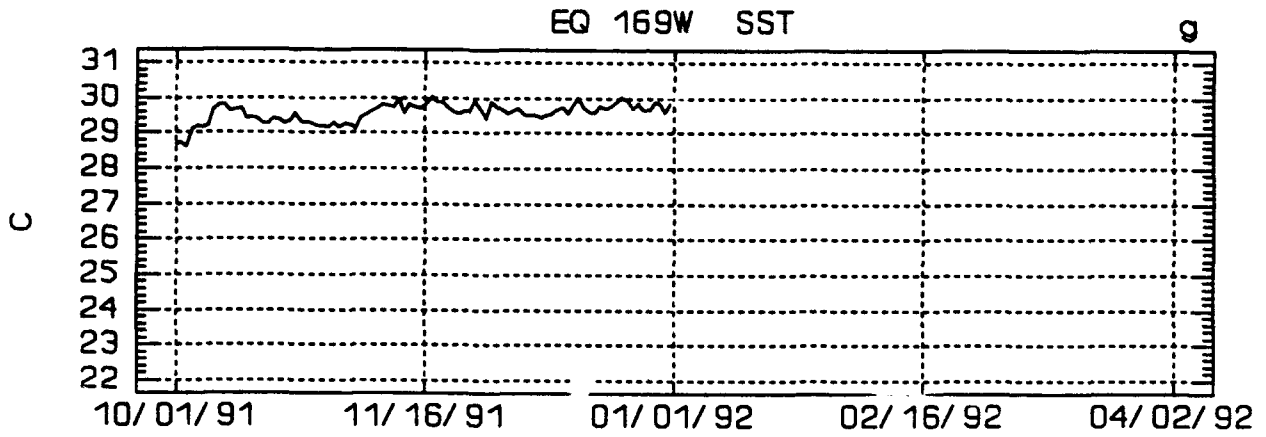
APPENDIX B. EQ 169°W TIME SERIES



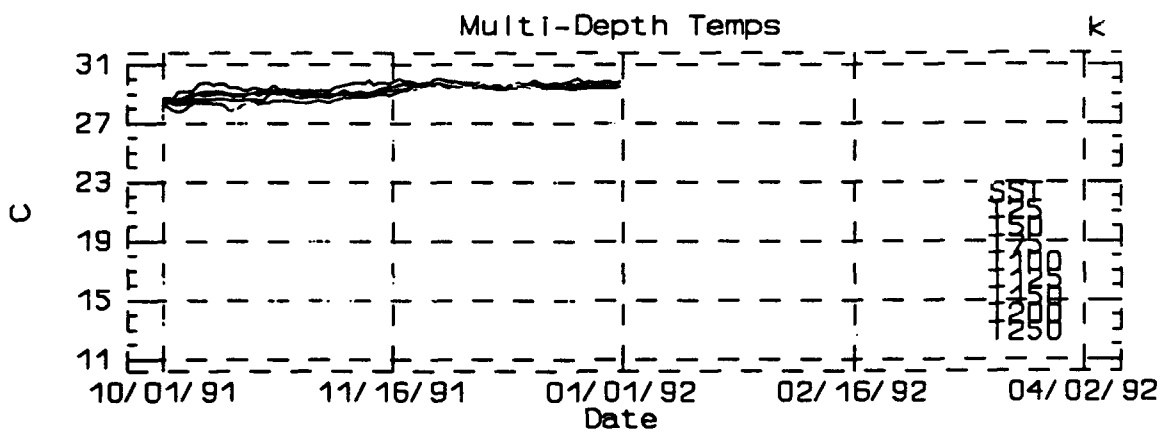
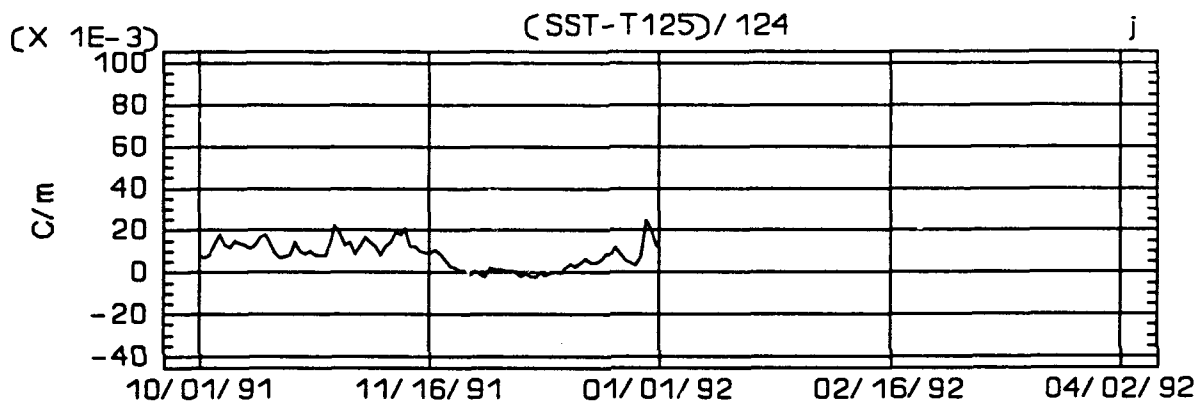
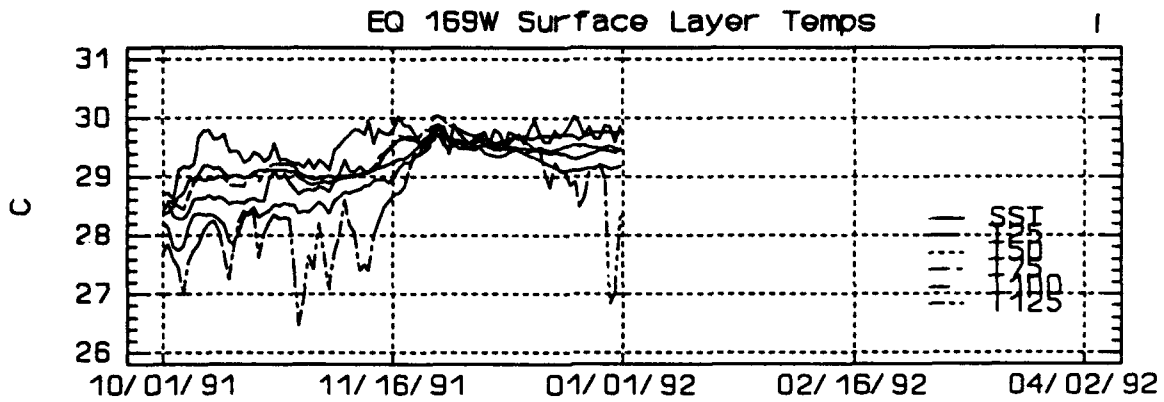
App. B. EQ 169°W time series, representing all transition region buoys. Time series are of: a) raw zonal wind (U), b) raw meridional wind (V), and c) raw horizontal wind (M).



App. B. (Continued) Time series are of: d) detrended U, e) detrended V, and f) detrended M.



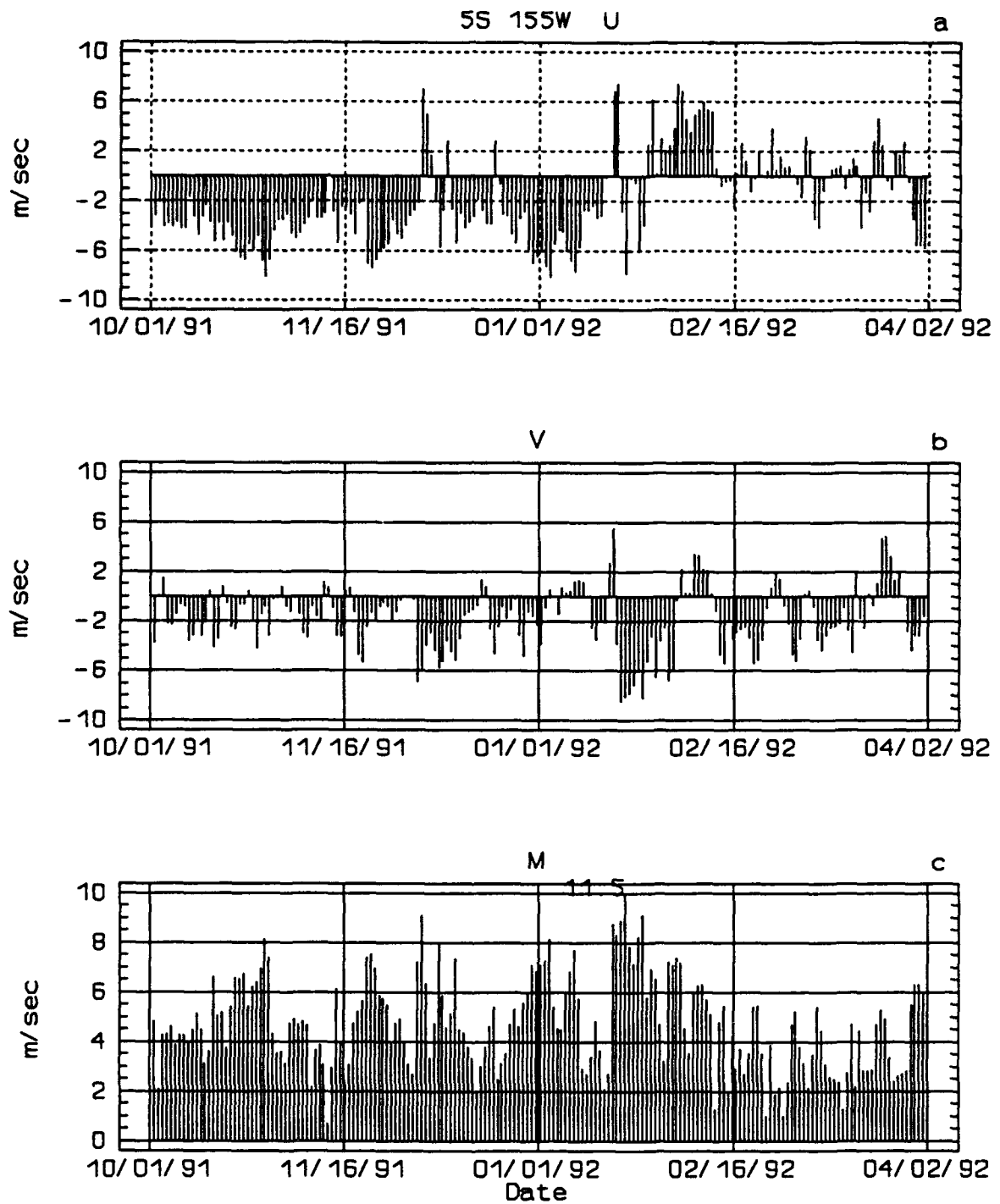
App. B. (Continued) Time series are of: g) raw SST, and h) detrended SST. This buoy was missing all AT related time series.



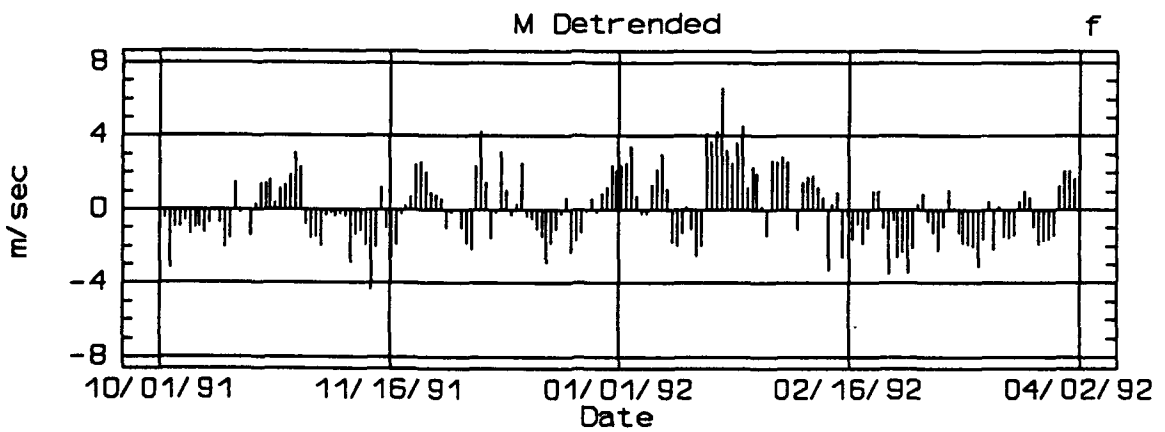
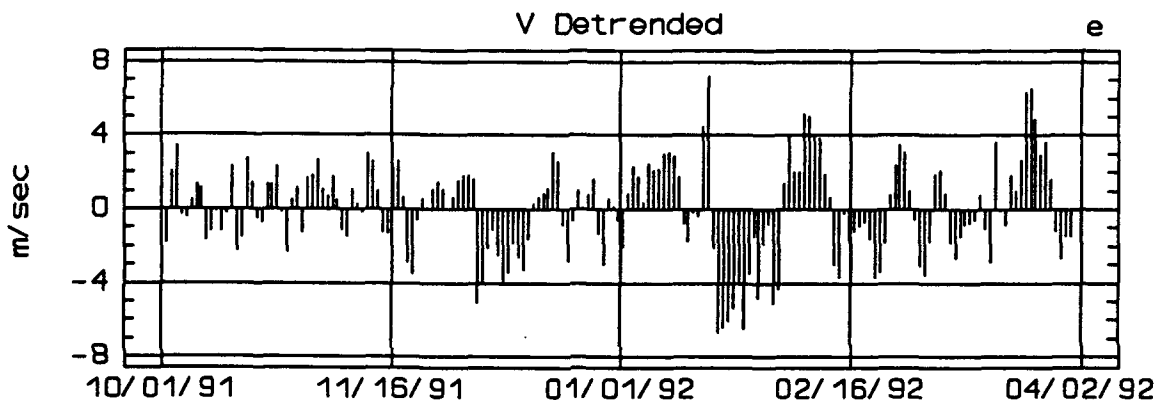
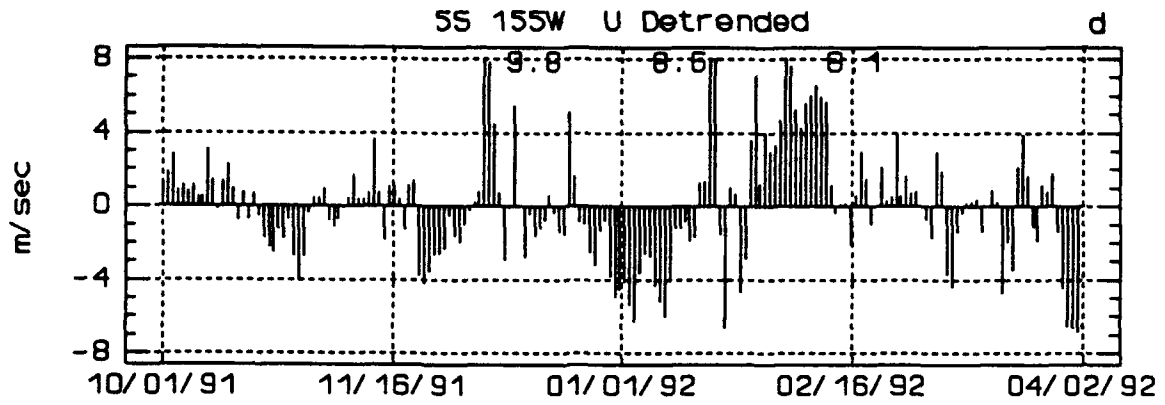
App. B. (Continued) Time series are of: i) surface layer temperatures, j) temperature gradient (TG), and k) multi-depth temperatures.

(Intentionally Blank)

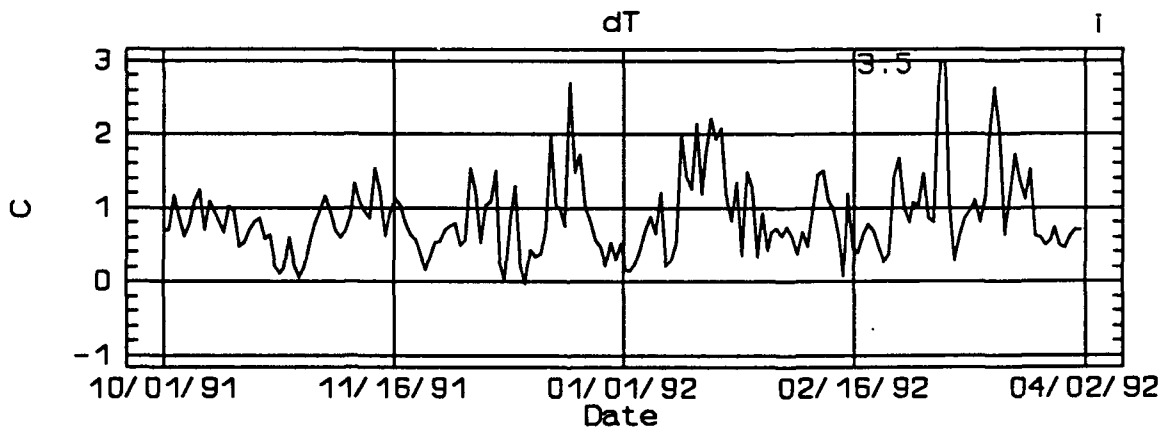
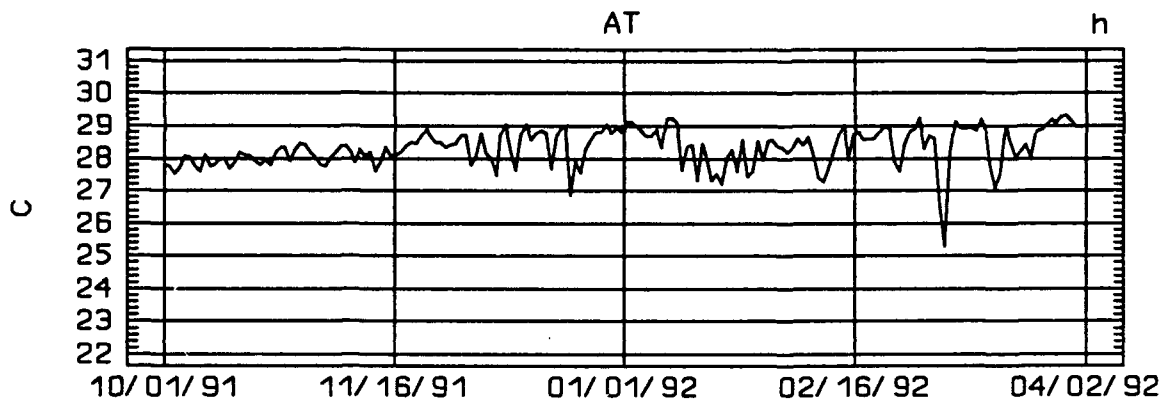
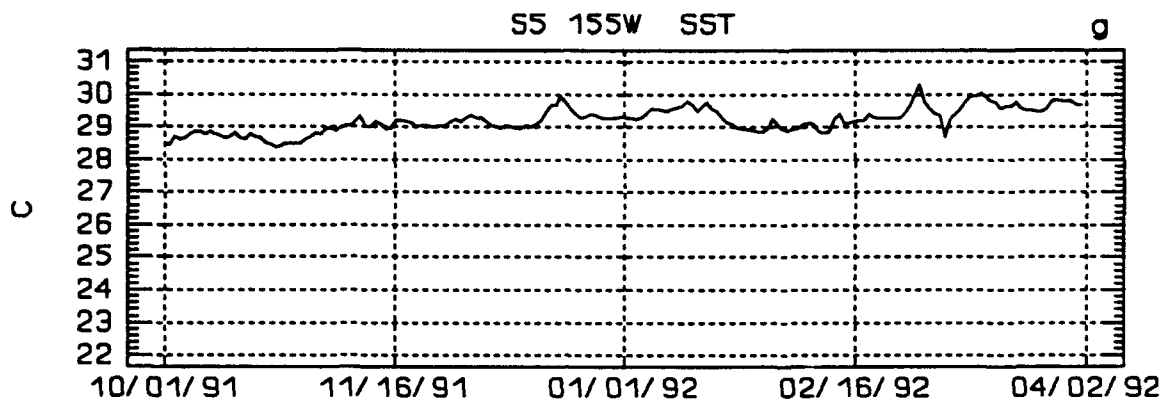
APPENDIX C. 5°N 155°W TIME SERIES



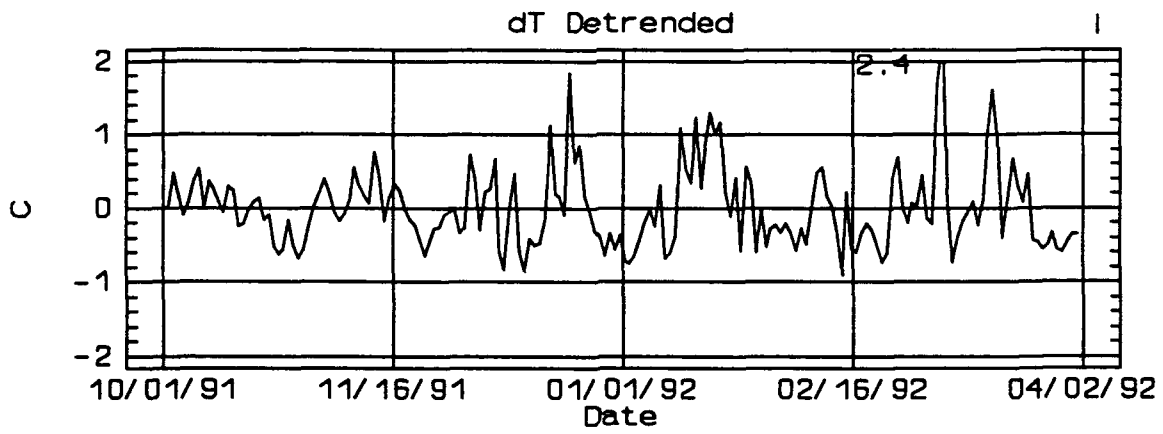
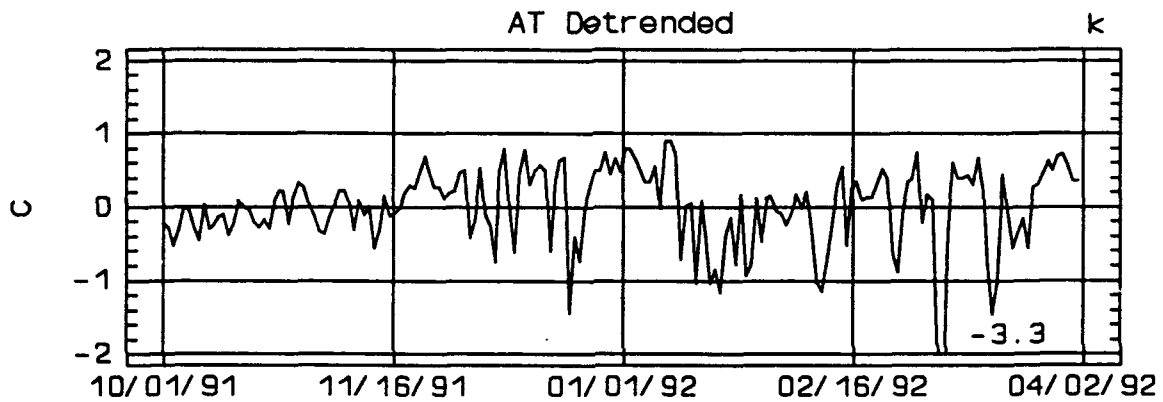
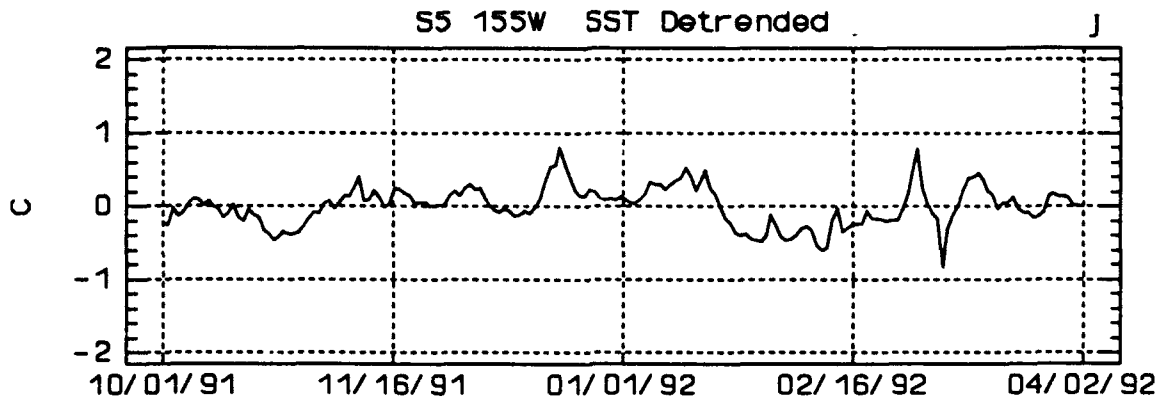
App. C. 5°S 155°W time series, representing of all easterly and varying V region buoys. Time series are of: a) raw zonal wind (U), b) raw meridional wind (V), and c) raw horizontal wind (M).



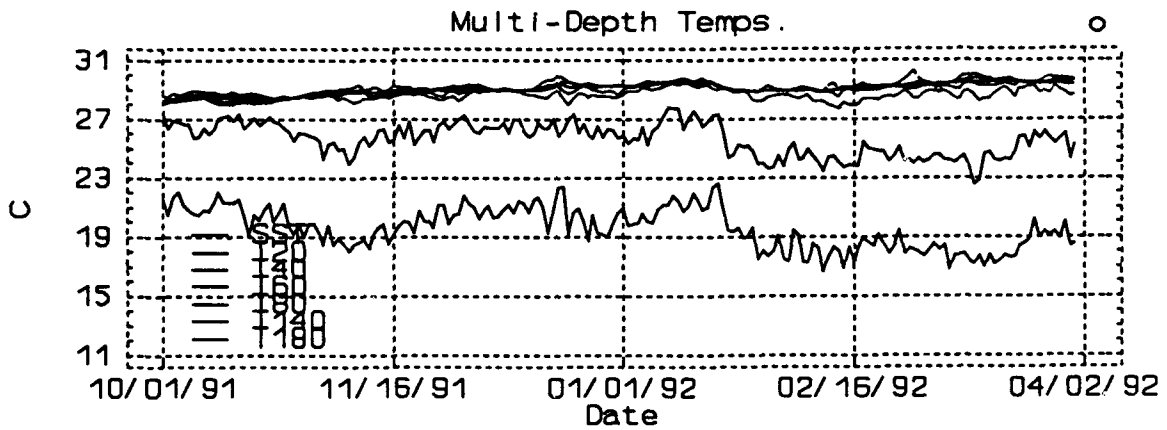
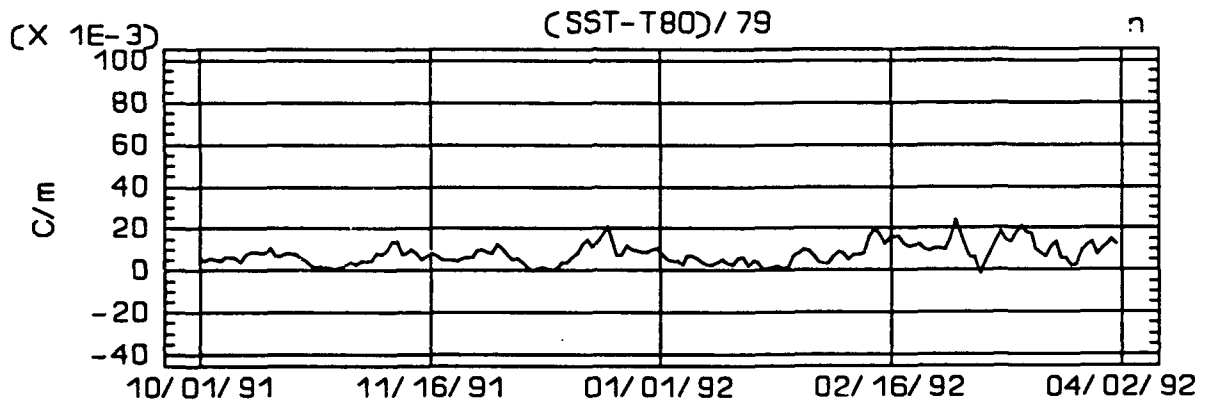
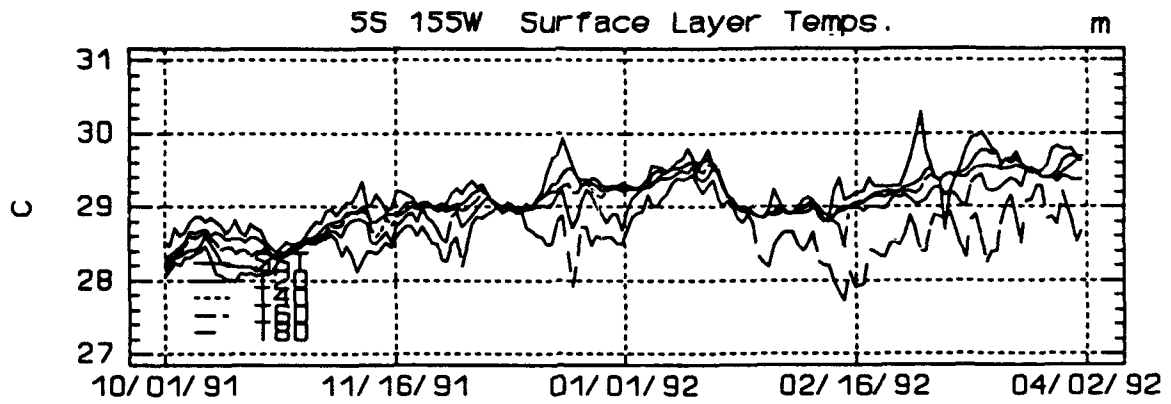
App. C. (Continued) Time series are of: d) detrended U, e) detrended V, and f) detrended M.



App. C. (Continued) Time series are of: g) raw SST, h) raw air temperature (AT), and i) raw air-sea temperature difference (dT, $dT = SST - AT$).

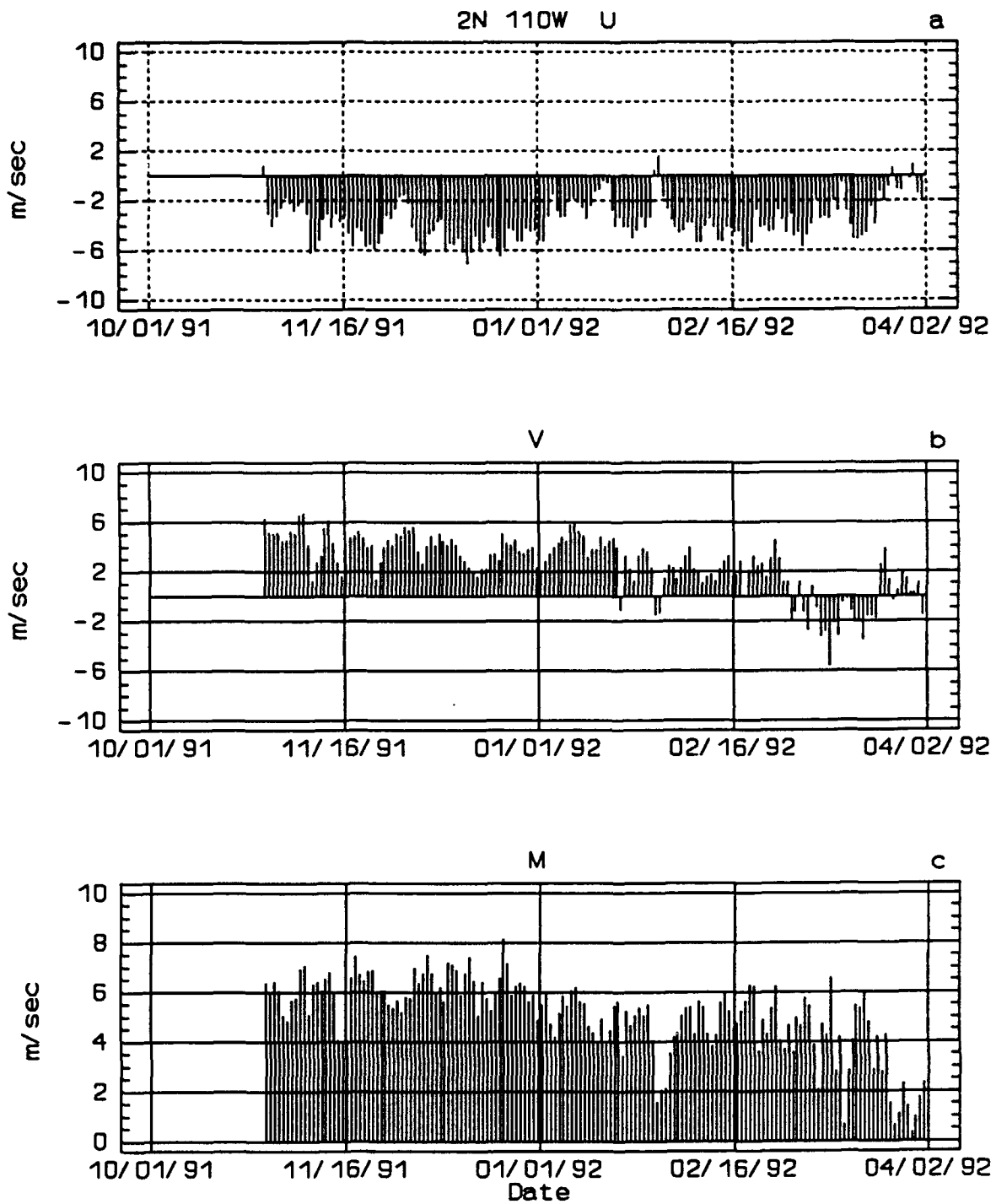


App. C. (Continued) Time series are of: j) detrended SST, k) detrended AT, and l) detrended dT.

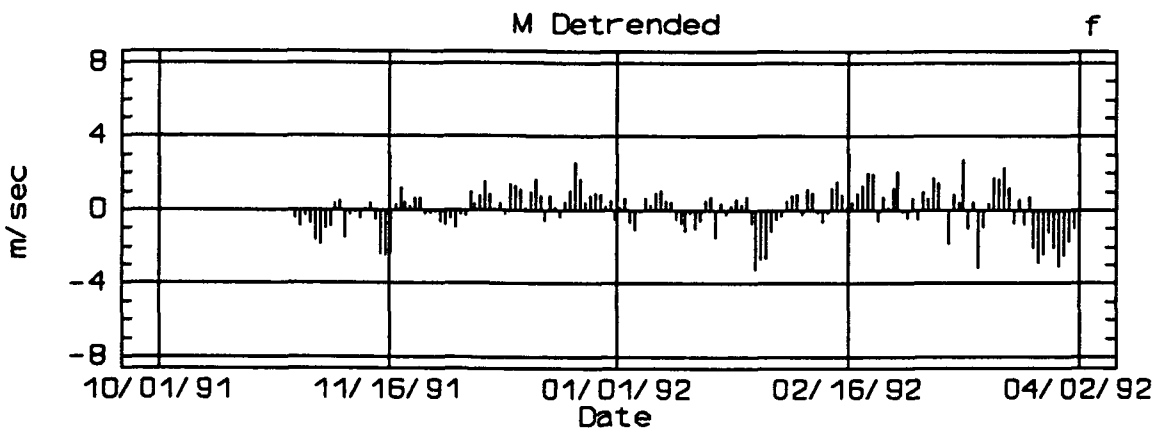
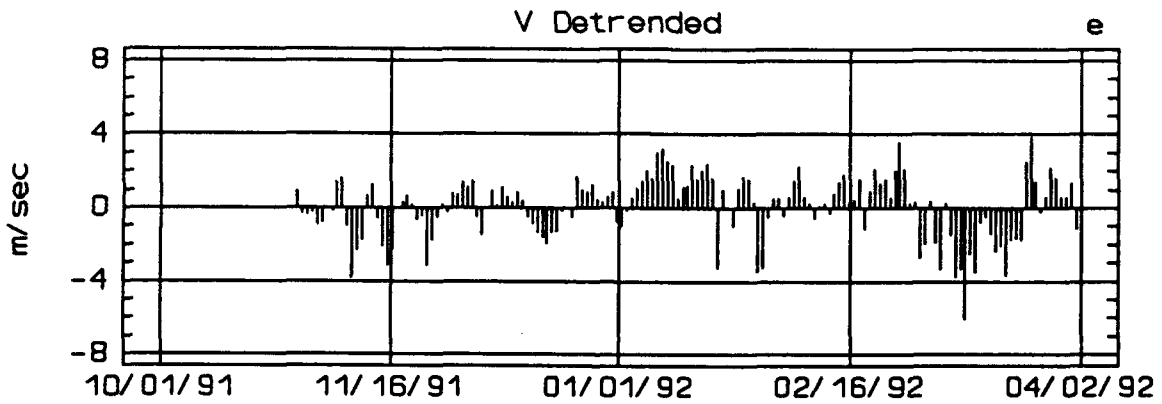
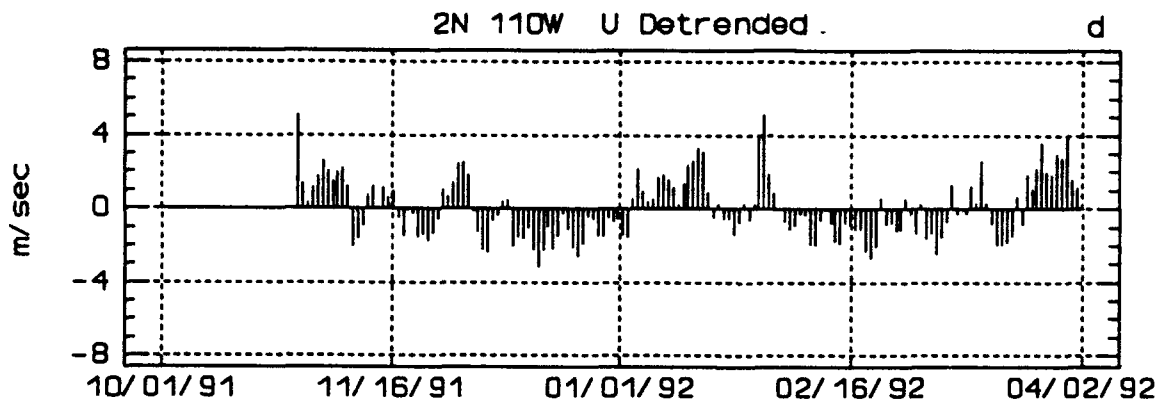


App. C. (Continued) Time series are of: m) surface layer temperatures, n) temperature gradient (TG), and o) multi-depth temperatures.

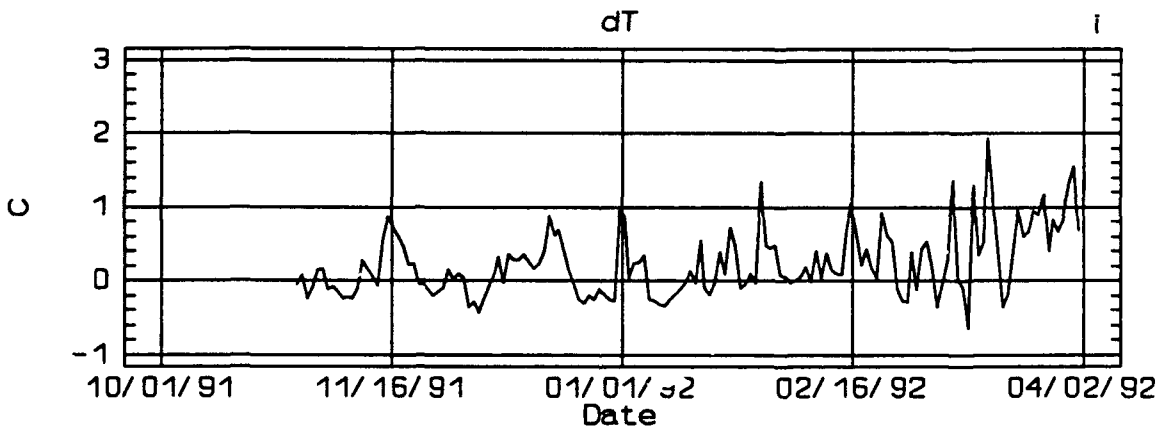
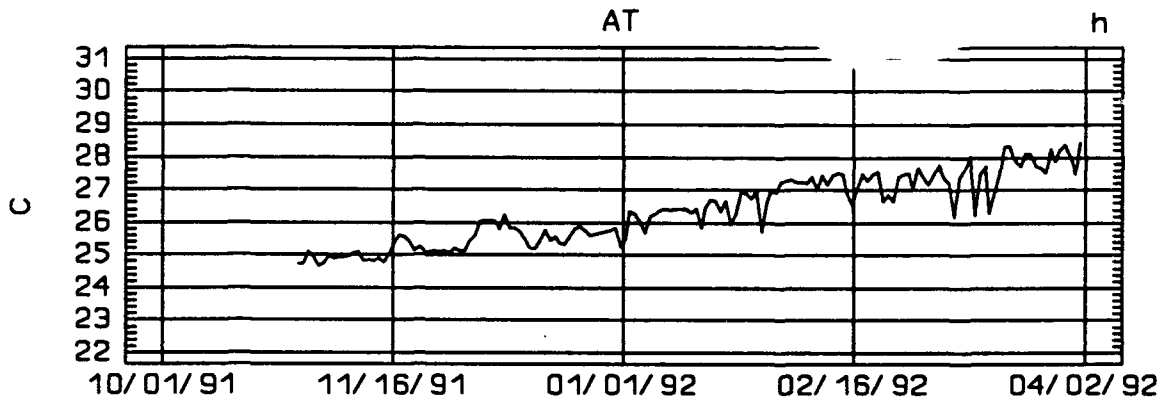
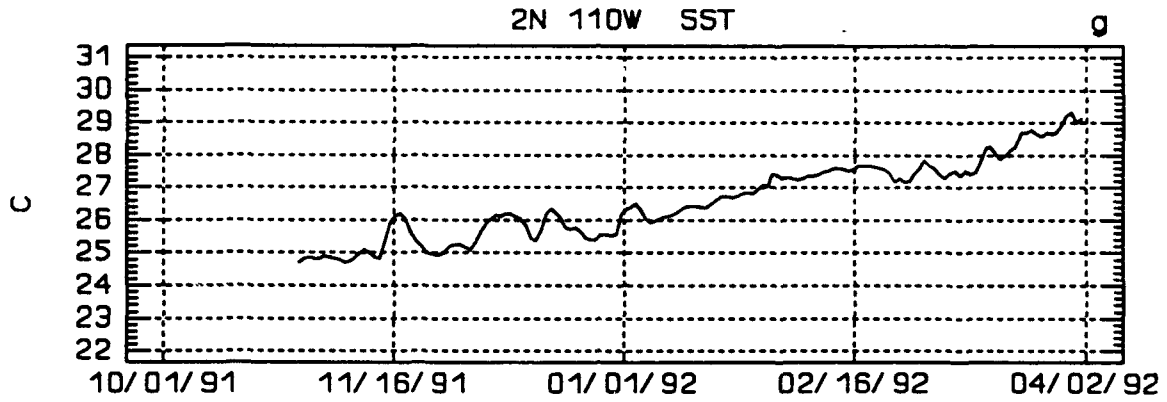
APPENDIX D. 2°N 110°W TIME SERIES



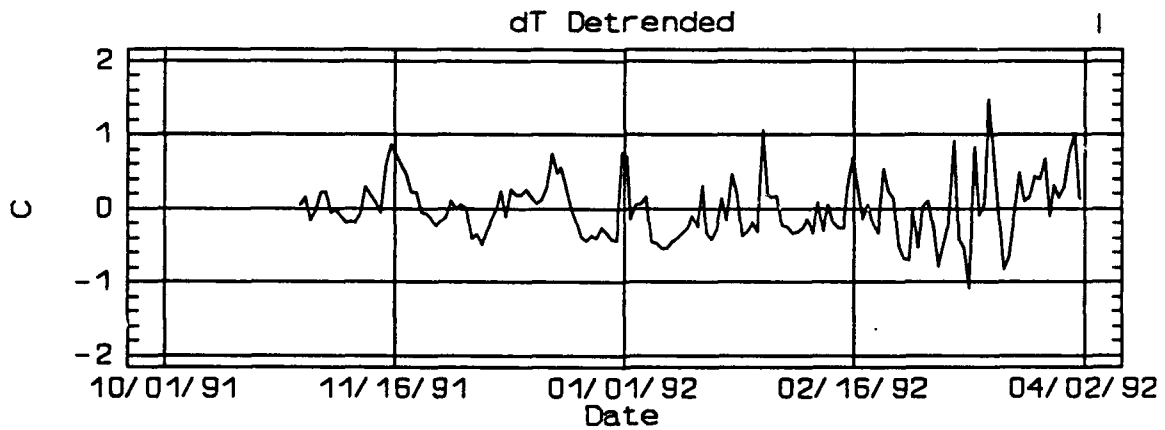
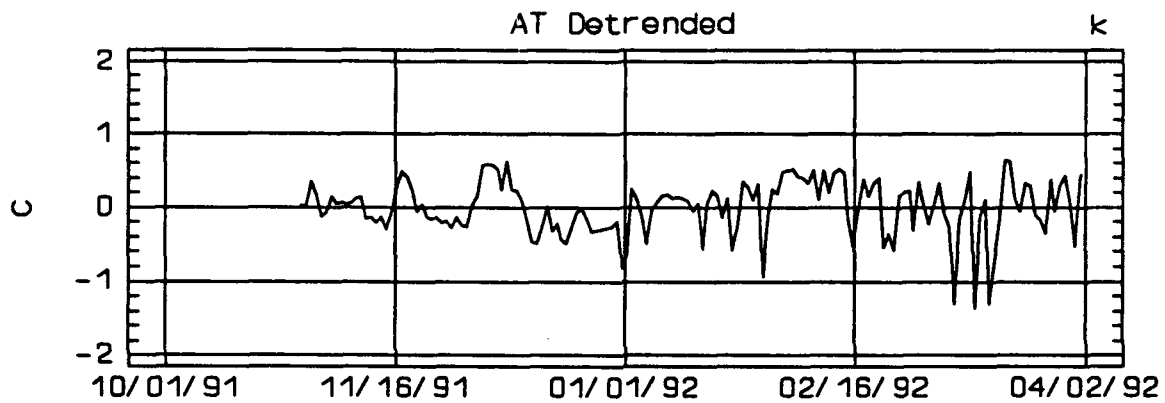
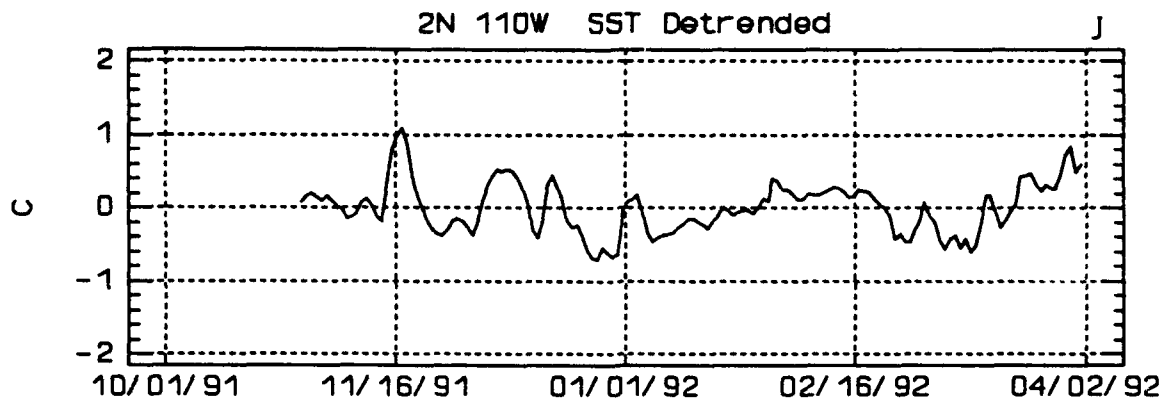
App. D. 2°N 110°W time series, representing all steady V region buoys. Time series are of: a) raw zonal wind (U), b) raw meridional wind (V), and c) raw horizontal wind (M).



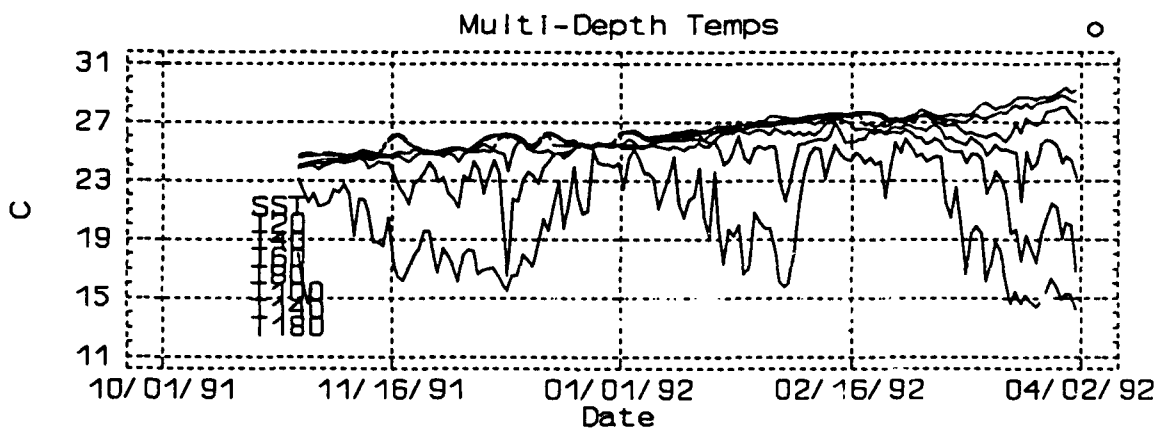
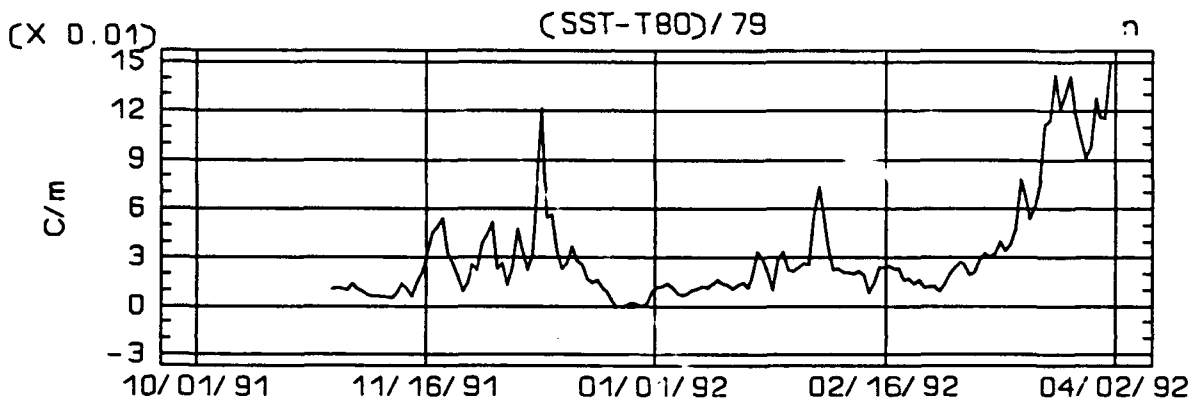
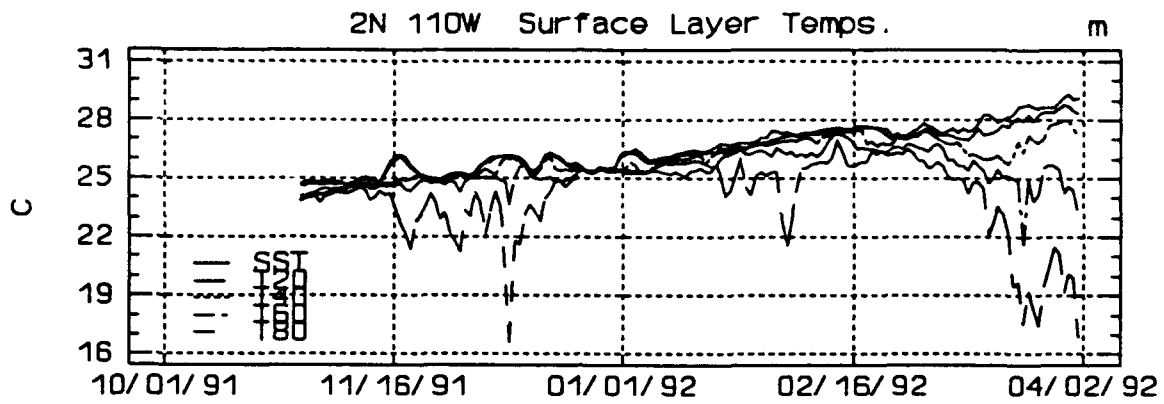
App. D. (Continued) Time series are of: d) detrended U, e) detrended V, and f) detrended M.



App. D. (Continued) Time series are of: g) raw SST, h) raw air temperature (AT), and i) raw air-sea temperature difference (dT, $dT = SST - AT$).

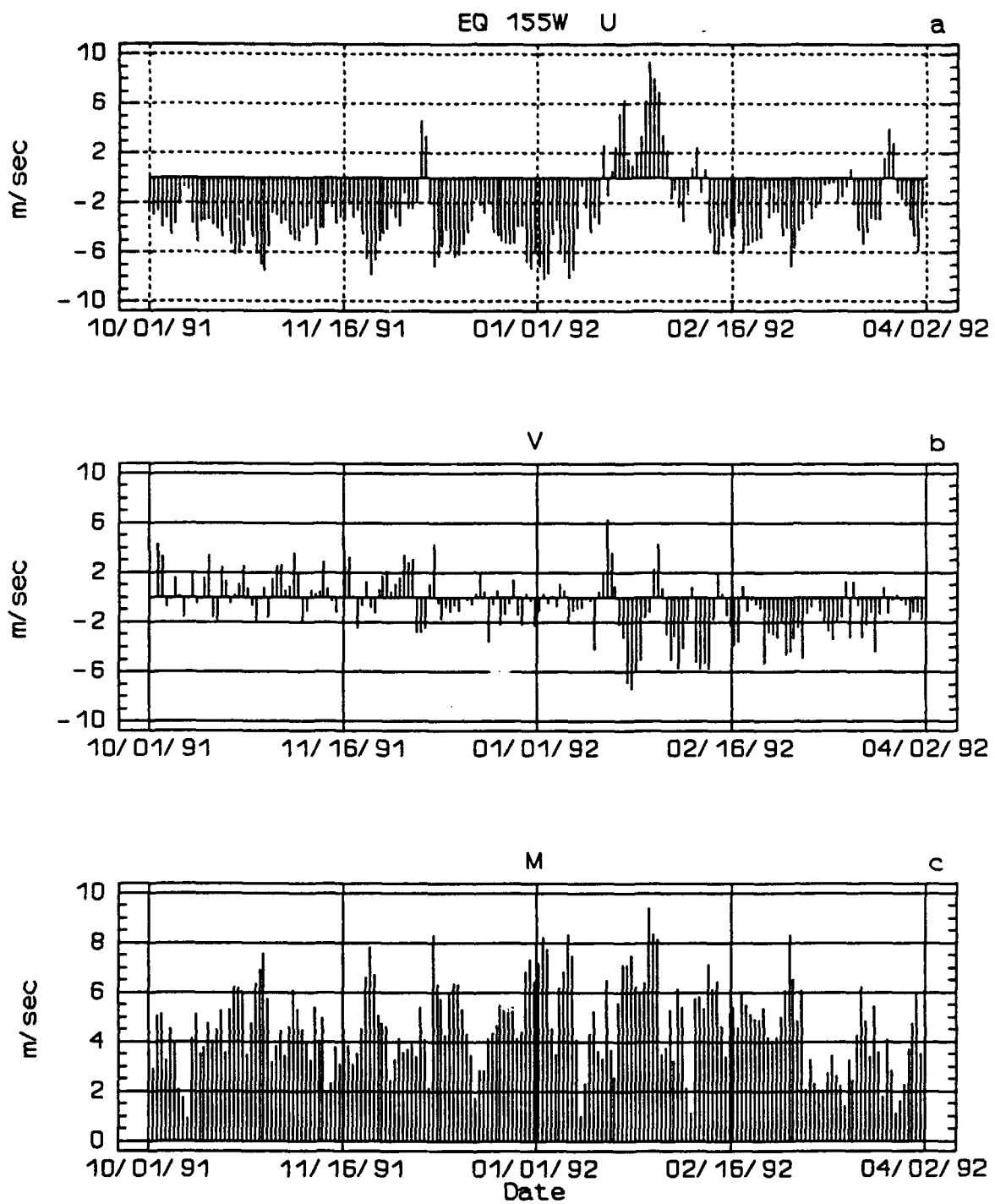


App. D. (Continued) Time series are of: j) detrended SST, k) detrended AT, and l) detrended dT.

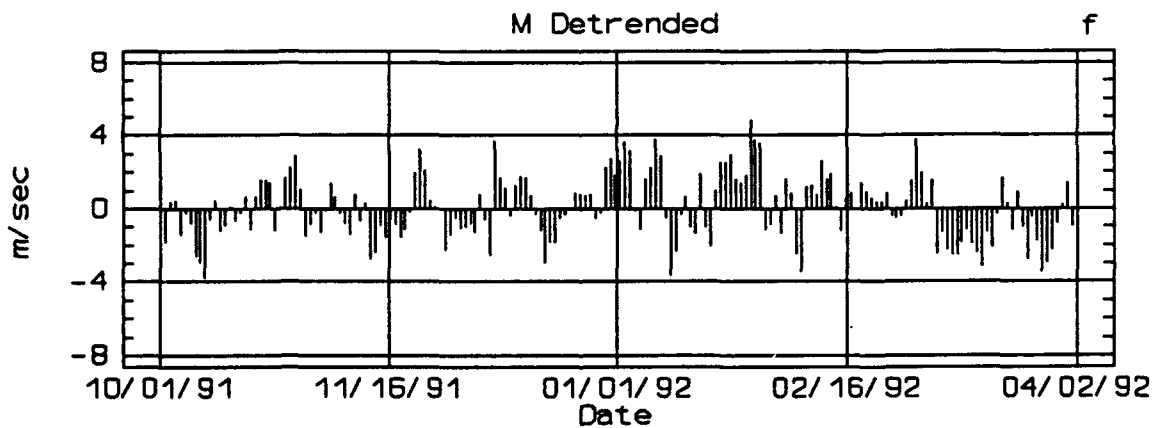
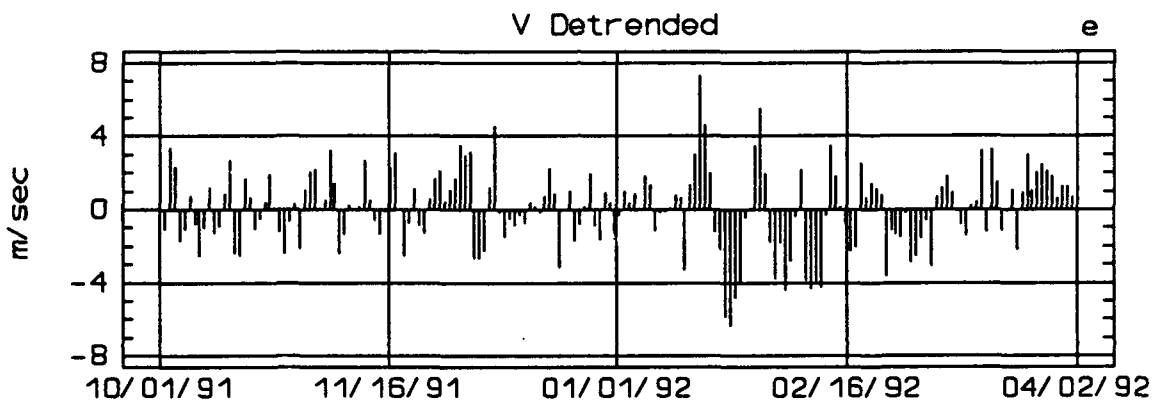
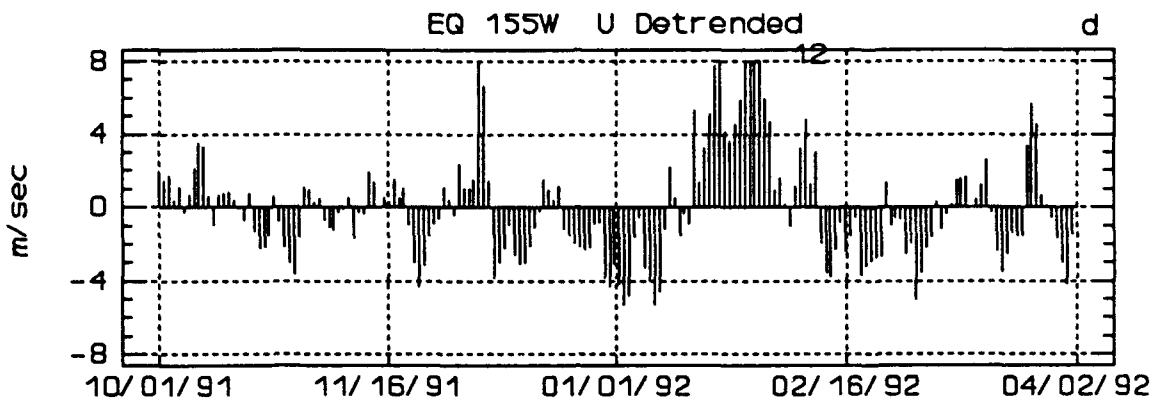


App. D. (Continued) Time series are of: m) surface layer temperatures, n) temperature gradient (TG), and o) multi-depth temperatures.

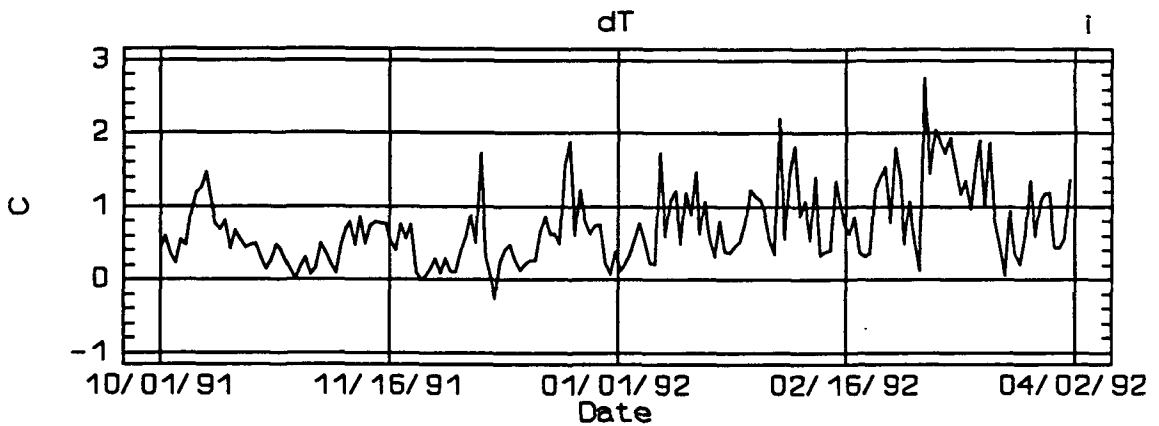
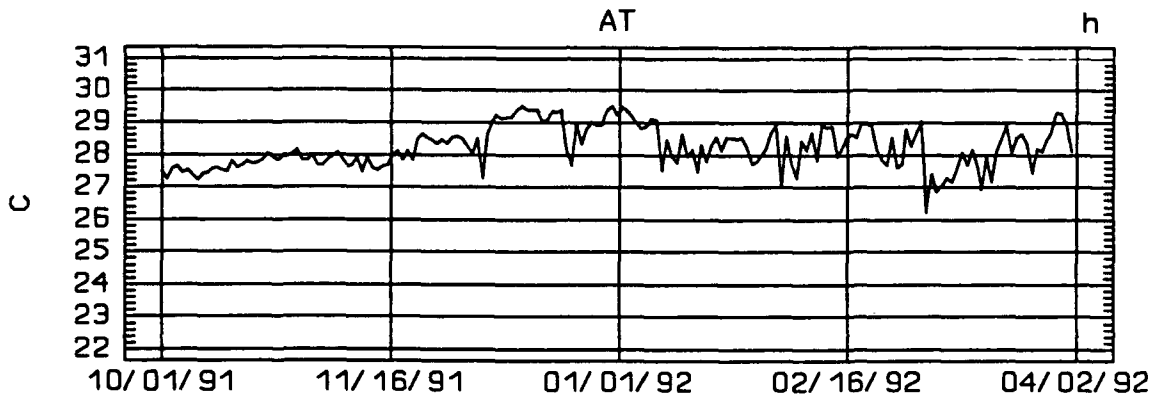
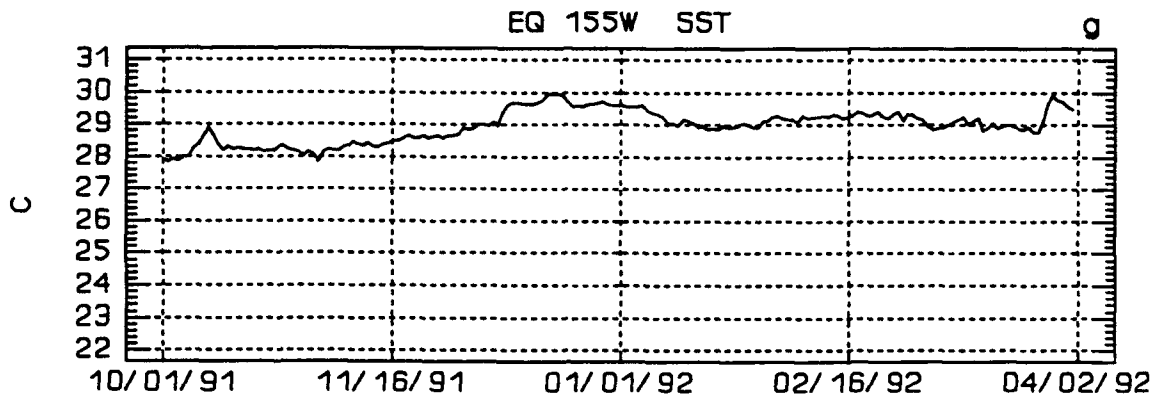
APPENDIX E. EQ 155°W TIME SERIES



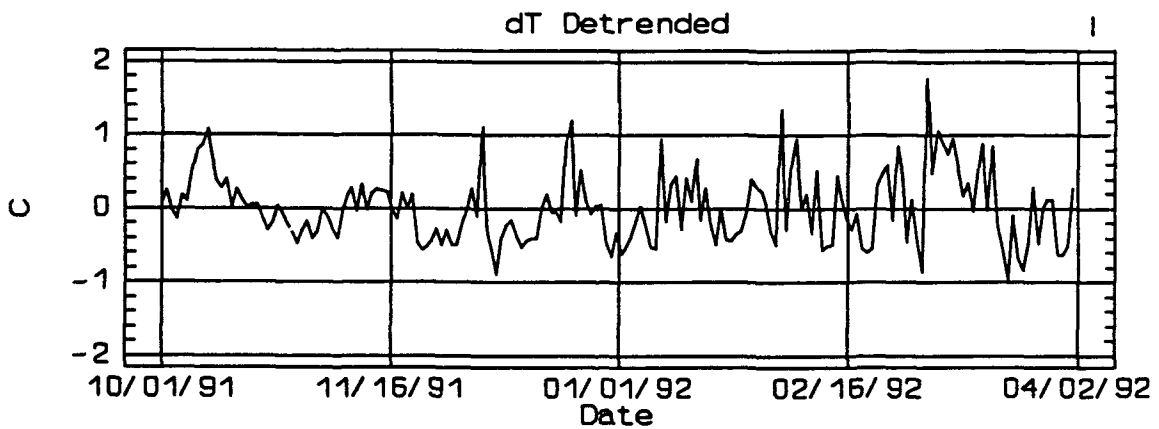
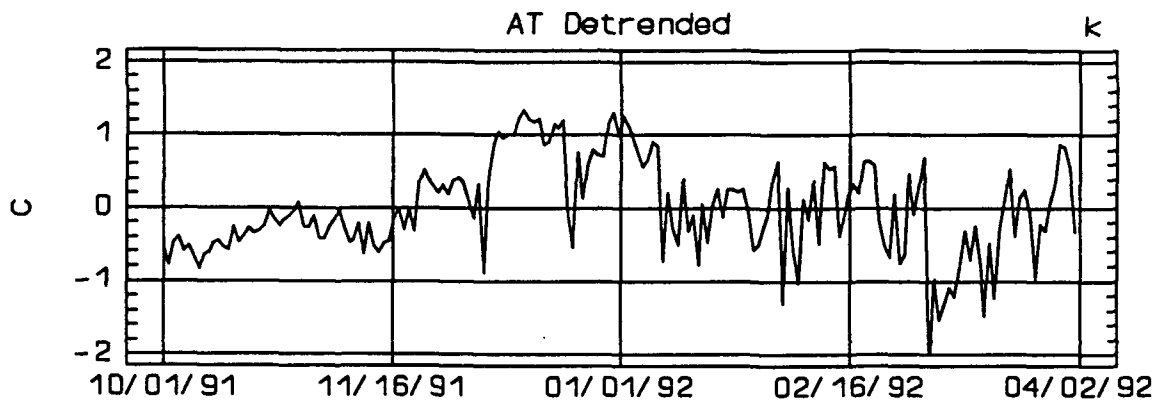
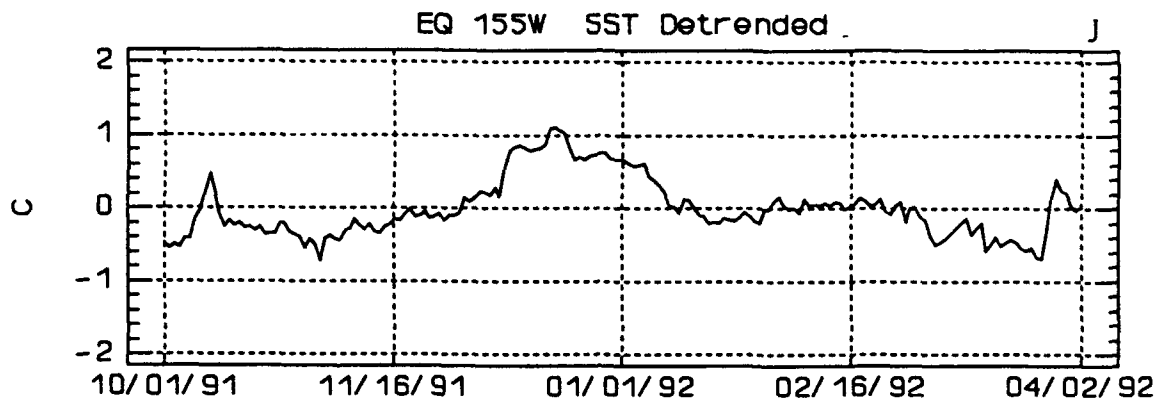
App. E. EQ 155°W time series, representing all inversion region buoys. Time series are of: a) raw zonal wind, U; b) raw meridional wind, V; and c) raw horizontal wind, M.



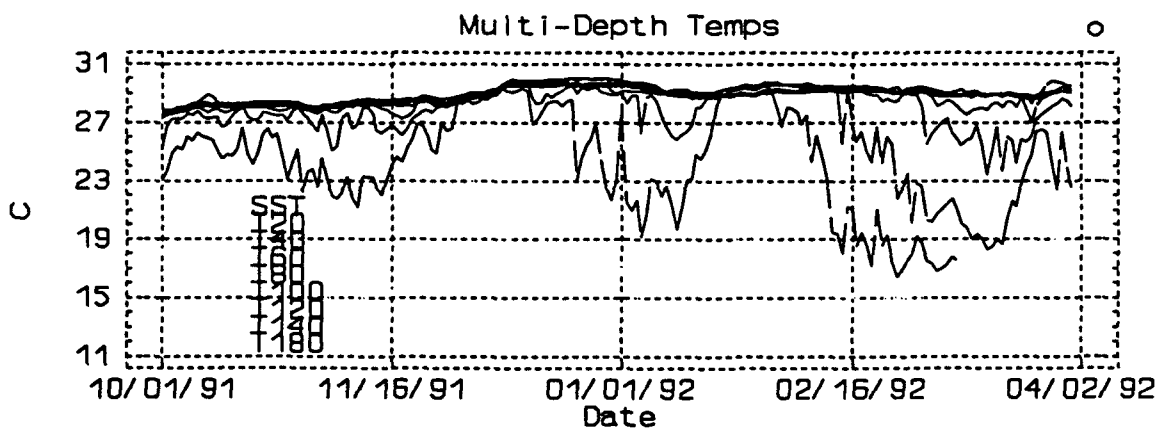
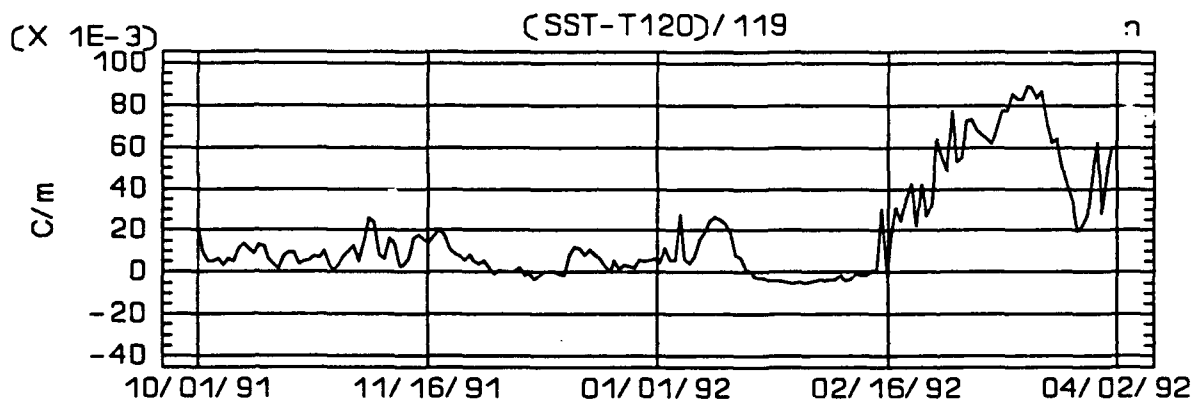
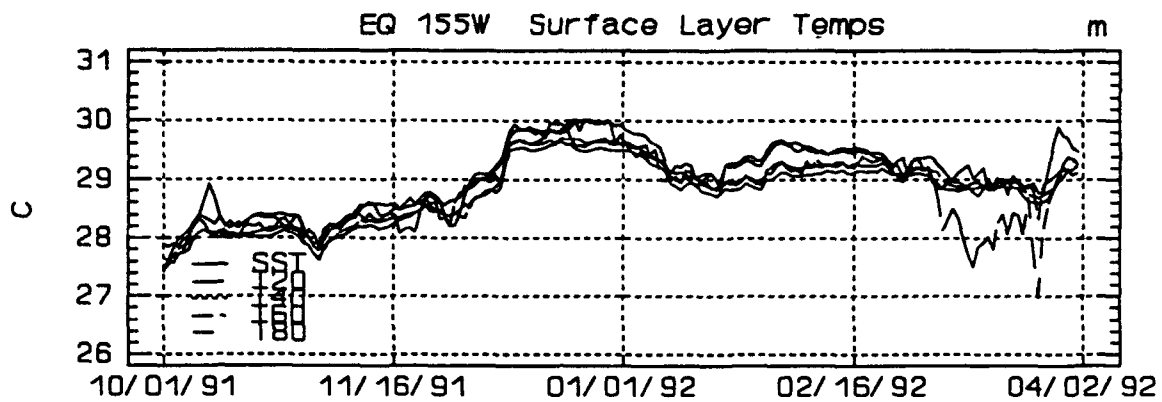
App. E. (Continued) Time series are of: (d) detrended U; (e) detrended V; and (f) detrended M.



App. E. (Continued) Time series are of: g) raw SST, h) raw air temperature (AT), and i) raw air-sea temperature difference dT , $dT = SST - AT$.



App. E. (Continued) Time series are of: (j) detrended SST; (k) detrended AT; and (l) detrended dT.



App. E. (Continued) Time series are of: (m) surface layer temperatures; (n) temperature gradient, TG; and (o) multi-depth temperatures.

(Intentionally Blank)

INITIAL DISTRIBUTION LIST

	No. Copies
1. Defense Technical Information Center Cameron Station Alexandria VA 22304-6145	2
2. Library, Code 052 Naval Postgraduate School Monterey CA 93943-5002	2
3. Chairman (Code OC/Co) Department of Oceanography Naval Postgraduate School Monterey, CA 93943-5000	1
4. Chairman (Code MR/Hy) Department of Meteorology Naval Postgraduate School Monterey, CA 93943-5000	1
5. James T. Murphree (Code MR/Me) Department of Meteorology Naval Postgraduate School Monterey, CA 93943-5000	1
6. Peter C. Chu (Code OCCu) Department of Oceanography Naval Postgraduate School Monterey, CA 93943-5000	1
7. LCDR John E. Kent 1108 Leahy Rd Monterey, CA 93940	1
8. Commander Naval Oceanography Command Stennis Space Center MS 39529-5000	1
9. Commanding Officer Naval Oceanographic Office Stennis Space Center MS 39529-5001	1

- | | | |
|-----|--|---|
| 10. | Associate Director of Research
for Ocean and Atmospheric
Science and Technology
Naval Research Laboratory
4555 Overlook Avenue, S.W.,
Washington, DC 20375-5320 | 1 |
| 11. | Director
Naval Research Laboratory
7 Grace Hopper Ave. STOP 2
Monterey, CA 93943-5502 | 1 |
| 12. | Ron Gelaro
Naval Research Laboratory
7 Grace Hopper Ave. STOP 2
Monterey, CA 93943-5502 | 1 |
| 13. | Pat Phoebus
Naval Research Laboratory
7 Grace Hopper Ave. STOP 2
Monterey, CA 93943-5502 | 1 |